Utilising Omics Approaches to Understand Kaposi's Sarcoma-associated Herpesvirus

Christopher Bradley Owen

Submitted in accordance with the requirements for the degree of Doctor of Philosophy

The University of Leeds

Faculty of Biological Sciences

School of Molecular and Cellular Biology

September 2015

The candidate confirms that the work submitted is his own and that appropriate credit has been given where reference has been made to the work of others.

Acknowledgements

I would like to express my gratitude to my supervisor Professor Adrian Whitehouse for his guidance, support and trust throughout my thesis. He has been a pleasure to work for.

My colleagues and friends from the Whitehouse and Hewitt groups, past and present, have been incredibly helpful, great fun and have created a fantastic working environment.

In addition, I am grateful to Dr. Kate Heesom, Dr. Sally Harrison, Dr. Catherine Daly, Dr. Ian Carr, Dr, Alastair Droop, Dr. Lucy Stead, Dr. Gareth Howell, Dr. Brian Jackson and Dr. Sally Boxall for technical support. I also thank Dr. Sophie Schumann for proofreading sections of this work.

I would also like to thank the BBSRC for funding this work, as well as paying my stipend for the last 4 years.

Many thanks also go to my family, who have been extremely supportive. There has always been somebody there to help with difficult situations, or to celebrate good times.

Last but not least, I would like to thank Jess for being an amazing companion, putting up with me, and making outrageously good food (seriously…).

Abstract

Kaposi's sarcoma-associated herpesvirus (KSHV) is an oncogenic human virus associated with a number of malignancies, including Kaposi's sarcoma. Similar to all herpesviruses, KSHV establishes either latent or lytic infections in host cells. The latent stage involves minimal viral gene expression, enabling the virus to remain dormant, maintaining genome integrity and enabling viral persistence. Conversely, lytic replication is characterised by the expression of a highly regulated and coordinated cascade of viral gene expression, ultimately resulting in the production of new mature, infectious virions. Importantly, lytic replication is necessary for the development and spread of Kaposi's sarcoma.

State of the art high throughput, high resolution "omics" approaches, such as mass spectrometry-based quantitative proteomics and next generation sequencing-based transcriptomics, are rapidly becoming the techniques of choice for discovering novel biological phenomena due, in part, to their sensitivity and the ability to repeatedly ask new questions of an existing dataset.

Herein, three high throughput, high resolution approaches, namely SILAC-based quantitative proteomics, miRNA sequencing and mRNA sequencing are employed in an attempt to identify and characterise novel interactions between KSHV and the host cell.

Utilising quantitative proteomics, the essential host cell splicing factor Prp19 is identified as a novel interacting partner of the lytic KSHV ORF57 protein in subnuclear bodies. This interaction, surprisingly, does not contribute to viral mRNA maturation, but instead has implications for the cellular DNA damage response, appearing to limit the effectiveness of this important pathway, possibly to reduce any negative effects on viral replication.

Proteomic analyses also highlighted a link between KSHV lytic replication and host miRNA biogenesis pathways. Through the application of miRNA sequencing, two host miRNAs, namely miR-151a-5p and miR-365a-3p, were found to be dysregulated during KSHV infection. Importantly, neither of these miRNAs appear to represent a host

antiviral response. Instead, cellular target mRNAs are identified for miR-365a-3p, through the use of mRNA sequencing. These targets, termed DOCK5 and PRUNE2 are rapidly degraded during KSHV lytic replication via the viral-mediated upregulation of miR-365a-3p expression. Subsequent analysis of DOCK5 function during lytic replication suggests this interaction may promote viral egress.

The data presented herein sheds light on previously unidentified mechanisms employed by KSHV to hijack the host cell, and may aid in the development of novel therapeutics against this important pathogen.

Contents

List of figures

List of tables

Abbreviations

%	percentage
<	less than
^{o}C	degrees Celsius
α	alpha
β	beta
γ	gamma
κ	kappa
µg	microgram
µl	microliter
µm	micrometre
µM	micromolar
γH2A.X	phosphorylated histone H2A.X
53BP1	p53-binding protein 1
aa	amino acid
Abl	Abelson tyrosine-protein kinase
AGO	argonaute
AIDS	acquired immune deficiency syndrome
AKT	RAC-alpha serine/threonine protein kinase
Aly	THO complex subunit 4
AP	adaptor protein
ATM	Ataxia telangiectasia mutated
ATP	adenosine triphosphate
ATR	Ataxia telangiectasia and Rad3-related protein
ATRIP	ATR-interacting protein

B cell	B lymphocyte
BART	Bam HI A rightward transcript
BBC3	Bcl-2 binding component 3
BCBL	body cavity based lymphoma
BCR	breakpoint cluster region
BGLF	serine/threonine-protein kinase BGLF4
BHRF1	Bam HI fragment H rightward open reading frame 1
Bim	Bcl2-interacting mediator of cell death
BoHV	bovine herpesvirus
bp	base pair
BRCA1	breast cancer type 1 susceptibility protein
BRCA2	breast cancer type 2 susceptibility protein
BSA	bovine serum albumin
bZIP	basic leucine zipper domain
C/EBPα	CCAAT/enhancer-binding protein alpha
CDC5L	Cell division cycle 5-like protein
Cdc25	M-phase inducer phosphatase
cDNA	complementary DNA
CeHV	cercopithecine herpesvirus
CF	cleavage factor
Chk	checkpoint kinase
CHPK	conserved herpesviral protein kinase
CID	collision induced dissociation
CPSF	cleavage and polyadenylation specificity factor
CPT	camptothecin
CstF	cleavage stimulation factor

CTD	carboxy-terminal domain
C-terminus	carboxy-terminus
CXCR4	C-X-C chemokine receptor type 4
DAPI	4’, 6-diamidino-2-phenylindole
DE	delayed early
DGCR8	microprocessor complex subunit DGCR8
dH_2O	distilled water
DMEM	Dulbecco’s modified Eagle’s medium
DMSO	dimethyl sulphoxide
DNA	deoxyribonucleic acid
DNA-PK	DNA-dependent protein kinase
DNA-PKcs	DNA-dependent protein kinase catalytic subunit
DNase	deoxyribonuclease
dNTP	deoxyribonucleoside (5’-) triphosphate
DOCK5	Dedicator of cytokinesis protein 5
dox	doxycycline hyclate
ds	double stranded
DSB	double strand break
dsRNA	double stranded RNA
dT	deoxythymidine
DTT	dithiothreitol
E	early
E2F-1	transcription factor E2F-1
EBER	Epstein-Barr virus-encoded small RNA
EBNA	Epstein-Barr virus nuclear antigen
EBNALP	Epstein-Barr virus nuclear antigen leader protein

EBV	Epstein-Barr virus
ECL	enhanced chemiluminescence
EGFP	enhanced green fluorescent protein
eIF	eukaryotic initiation factor
EJC	exon junction complex
ESE	exonic splicing enhancer
ESI	electrospray ionization
ESS	exonic splicing silencer
EST	expressed sequence tag
ETS1	protein-C ETS-1
ETS2	protein-C ETS-2
FAT4	protocadherin Fat 4
FCS	foetal calf serum
g	gram
g	gravitational force
G1	growth/gap 1 phase
G2	growth/gap 2 phase
GaHV	gallid herpesvirus
GAPDH	glyceraldehyde 3-phosphate dehydrogenase
gB	glycoprotein B
GDP	guanosine diphosphate
GEF	guanine exchange factor
GFP	green fluorescent protein
gH	glycoprotein H
gL	glycoprotein L
GMP	guanosine monophosphate

h	hours
H2A.X	histone H2A.X
HBV	hepatitis B virus
HCl	hydrochloric acid
HCMV	human cytomegalovirus
HCV	hepatitis C virus
HEK	human embryonic kidney
HHV	human herpesvirus
HIPK2	homeodomain-interacting protein kinase 2
HIV	human immunodeficiency virus
hnRNP	heterogeneous nuclear RNP
hpi	hours post induction
HPV	human papillomavirus
HR	homologous recombination
HRP	horseradish peroxidase
hsa	*Homo sapiens*
HSV-1/2	herpes simplex virus 1/2
HTLV-1	human T lymphotropic virus type 1
hTREX	human transcription/export
HUS1	checkpoint protein HUS1
HVS	herpesvirus saimiri
IAV	influenza A virus
ICAT	isotope-coded affinity tags
ICP0	E3 ubiquitin-protein ligase ICP0
ICTV	International Committee on Taxonomy of Viruses
IE	immediate early

IF	immunofluorescence
IFN	interferon
IgG	immunoglobulin G
IL-6	interleukin-6
IP	immunoprecipitation
IR	internal repeat
IRAK1	interleukin-1 receptor-associated kinase 1
ISS	intronic splicing silencer
iTRAQ	isobaric tags for relative and absolute quantification
kb	kilobase
kbp	kilobase pair
KCl	potassium chloride
kDa	kiloDalton
KLAR	KSHV latency-associated region
K-RBP	KSHV RTA binding protein
KS	Kaposi's sarcoma
KSHV	Kaposi's sarcoma-associated herpesvirus
ku70	X-ray repair cross-complementing protein 6
ku80	X-ray repair cross-complementing protein 5
L	late
LANA	latency-associated nuclear antigen
LAT	latency-associated transcript
LB	lysogeny broth
LC	liquid chromatography
LCL	lymphoblastoid cell line
LIBACS	Leeds Institute of Biomedical and Clinical Sciences

LMP	latency-associated membrane protein
lncRNA	long non-coding RNA
M	molar
M (gene)	matrix
m^7G	7-methyl-guanine
MALDI	matrix-assisted laser desorption/ionization
MCD	multicentric Castleman's disease
MCMV	murine cytomegalovirus
mCP	minor capsid protein
MDC1	mediator of DNA damage checkpoint protein 1
$MgCl_2$	magnesium chloride
MHC	major histocompatibility complex
MHV-68	murine gammaherpesvirus 68
miRNA	microRNA
ml	millilitre
mM	millimolar
MMR	mismatch repair
MRN	MRE11-RAD50-NBS1 complex
mRNA	messenger RNA
mRNP	messenger ribonucleoprotein particle
MS	mass spectrometry
MS/MS	tandem mass spectrometry
MTA	mRNA transcript accumulation
myoVa	myosin Va
m/z	mass to charge ratio
n	sample size

NaBu	sodium butyrate
NaCl	sodium chloride
NaOH	sodium hydroxide
NBS1	Nijmegen breakage syndrome protein 1
ncRNA	non-coding RNA
ND10	nuclear domain 10
Nef	negative factor
NER	nucleotide excision repair
NES	nuclear export signal
NF- κB	nuclear factor kappaB
ng	nanogram
NHEJ	non-homologous end joining
NIH	National Institutes of Health
NK cell	natural killer cell
NLS	nuclear localisation signal
nm	nanometre
NMD	nonsense-mediated decay
NOR	nucleolar oragnizing region
NP40	tergitol-type NP-40
NPC	nuclear pore complex
NS	non-structural
N-terminus	amino-terminus
Nup	nucleoporin
Nxf1	nuclear RNA export factor 1
Nxt1	nuclear transport factor 2-like export factor 1
ORF	open reading frame

p	p-value/phosphate
p53	cellular tumour antigen p53
PABP	polyadenylate binding protein
PABPC1	polyadenylate binding protein cytoplasmic 1
PAGE	polyacrylamide gel electrophoresis
PAN	polyadenylated nuclear
PAP	polyadenylate polymerase
PBS	phosphate buffered saline
PCR	polymerase chain reaction
PEL	primary effusion lymphoma
piRNA	PIWI interacting RNA
PML	promyelocytic leukaemia protein
pol.	polymerase
poly(A)	polyadenylated
poly(U)	polyuridylated
pre-miRNA	precursor-microRNA
pre-mRNA	precursor-messenger RNA
pri-miRNA	primary-microRNA
Prp19	Pre-mRNA-processing factor 19
PRUNE2	Protein prune homolog 2
P-TEFb	positive transcription elongation factor b
PTL	post-transplant lymphoma
qPCR	quantitative PCR
qRT-PCR	quantitative reverse transcriptase PCR
RAD1	cell cycle checkpoint protein RAD1
RAD9	cell cycle checkpoint control protein RAD9

Rad51	DNA repair protein Rad51 homolog 1
Ran	GTP-binding nuclear protein Ran
Rb	retinoblastoma
RBM14	RNA binding protein 14
RBP-Jκ	recombination signal-binding protein 1 for J-kappa
Rev	regulator of expression of viral proteins
RIPA	radioimmunoprecipitation assay
RISC	RNA-induced silencing complex
RNA	ribonucleic acid
RNAi	RNA interference
RNase	ribonuclease
RNP	ribonucleoprotein particle
RPA	replication protein A
RPMI	Roswell Park Memorial Institute medium
RRE	RTA response element/Rev response element
rRNA	ribosomal RNA
RT	reverse transcriptase
RTA	replication and transcription activator
S	synthesis phase
SD	standard deviation
SDS	sodium dodecyl sulphate
SILAC	stable isotope labelling with amino acids in cell culture
siRNA	small interfering RNA
SKP2	S-phase kinase-associated protein 2
snoRNA	small nucleolar RNA
snRNA	small nuclear RNA

SOX	shutoff and exonuclease
SR	serine/arginine rich
SSB	single strand break
ssDNA	single stranded DNA
ssRNA	single stranded RNA
SuHV	suid herpesvirus
SV40	Simian vacuolating virus 40
TBS	tris buffered saline
T cell	T-lymphocyte
Tat	trans-activator of transcription
TCL1	T-cell leukaemia gene 1
TEMED	N-N-N’-N’-tetramethylethylenediamine
Thoc5	THO complex subunit 5 homolog
TIP60	60 kDa Tat-interactive protein
TLR	toll-like receptor
TMT	tandem mass tags
TOPBP1	topoisomerase-2 binding protein 1
TPA	12-*O*-tetradecanoylphorbol-13-acetate
TR	terminal repeat
TRAF6	TNF receptor-associated factor 6
TREX	transcription/export
Tris	tris(hydroxymethyl)aminoethane
tRNA	transfer RNA
U	unit
U2AF1	U2 auxiliary factor 1
UAP56	spliceosome RNA helicase DDX39B

UIF	UAP56-interacting factor
U_L	unique long region
uORF	upstream open reading frame
UPL	universal probe library
U_S	unique short region
U snRNP	uridine-rich snRNP
UTR	untranslated region
UV	ultraviolet
V	volts
v/v	volume per volume
v-cyclin	viral cyclin
VEGF	vascular endothelial growth factor
vFLIP	viral FLICE inhibitory protein
vGPCR	viral G protein-coupled receptor
vIL-6	viral interleukin-6
vRNA	virion RNA
vRNP	viral ribonucleoprotein particle
VSV	vesicular stomatitis virus
VZV	varicella-zoster virus
w/v	weight per volume
Wee1	Wee1-like protein kinase
XLF	Non-homologous end joining factor 1
XRCC4	DNA repair protein XRCC4

Bases

A	adenine
C	cytosine
G	guanine
T	thymine

Amino acids

Alanine	Ala	A
Arginine	Arg	R
Asparagine	Asn	N
Aspartate	Asp	D
Cysteine	Cys	C
Glutamate	Glu	E
Glutamine	Gln	Q
Glycine	Gly	G
Histidine	His	H
Isoleucine	Ile	I
Leucine	Leu	L
Lysine	Lys	K
Methionine	Met	M
Phenylalanine	Phe	F
Proline	Pro	P
Serine	Ser	S
Threonine	Thr	T
Tryptophan	Trp	W
Tyrosine	Tyr	Y
Valine	Val	V

CHAPTER 1

~

Introduction

1 Introduction

1.1 Herpesviridae

1.1.1 Classification of herpesviruses

The *Herpesvirales* are an order of enveloped viruses roughly ~200 nm in diameter with large double stranded DNA genomes between 125 and 240 kb in length (Davison, 2007b). Herpesviruses are known to infect a wide range of animal hosts, and they have been classified according to their architectural and morphological properties (Davison et al., 2009). There are three distinct families within the *Herpesvirales* order: *Herpesviridae*, which infect mammals, birds and reptiles, *Alloherpesviridae*, pathogens of fish and amphibians, and *Malacoherpesviridae*, which consist of just two bivalve viruses (Davison et al., 2009; Davison et al., 2005; Savin et al., 2010). The *Herpesviridae* family was further divided in 1979, resulting in three subfamilies: the alpha-, beta- and gammaherpesvirinae (Matthews, 1979). Whilst the classifications of these three subfamilies were initially based on infectious properties, such as the temporal length of the lytic cycle and infection of specific tissue types, the distinctions have since been further strengthened due to developments in genome sequencing (Roizmann et al., 1992; Davison, 2010). **Figure 1.1** shows the evolutionary relationship between the *Herpesviridae* in the form of a phylogenetic tree.

1.1.1.1 Alphaherpesvirinae

The alphaherpesviruses exhibit a broad host range, a short lytic cycle and spread rapidly in cell culture (Roizmann et al., 1992). Latent alphaherpesvirus infections are usually established in neuronal cells, particularly sensory ganglia. Lytic alphaherpesvirus infection usually affects epidermal cells and leads to the destruction of the infected cell. This class contains five genera, including *Varicellovirus*, which contains the human herpesvirus varicella zoster virus (VZV), and *Simplexvirus*, which contains the human herpesviruses herpes simplex virus type 1 and 2 (HSV-1/2). The

class also contains a number of important animal herpesviruses including suid herpesvirus 1 (SuHV-1), a porcine pathogen that causes pseudorabies, gallid herpesvirus 2 (GaHV-2), the aetiological agent of Marek's disease in chicken, and bovine herpesvirus 1 (BoHV-1), known to cause a number of diseases in cattle (Chang, 1984). Furthermore, cercopithecine herpesvirus 1 (CeHV-1), an infectious agent of macaque monkeys, which may cause zoonotic infections in human hosts (Huff and Barry, 2003; Tischer and Osterrieder, 2010).

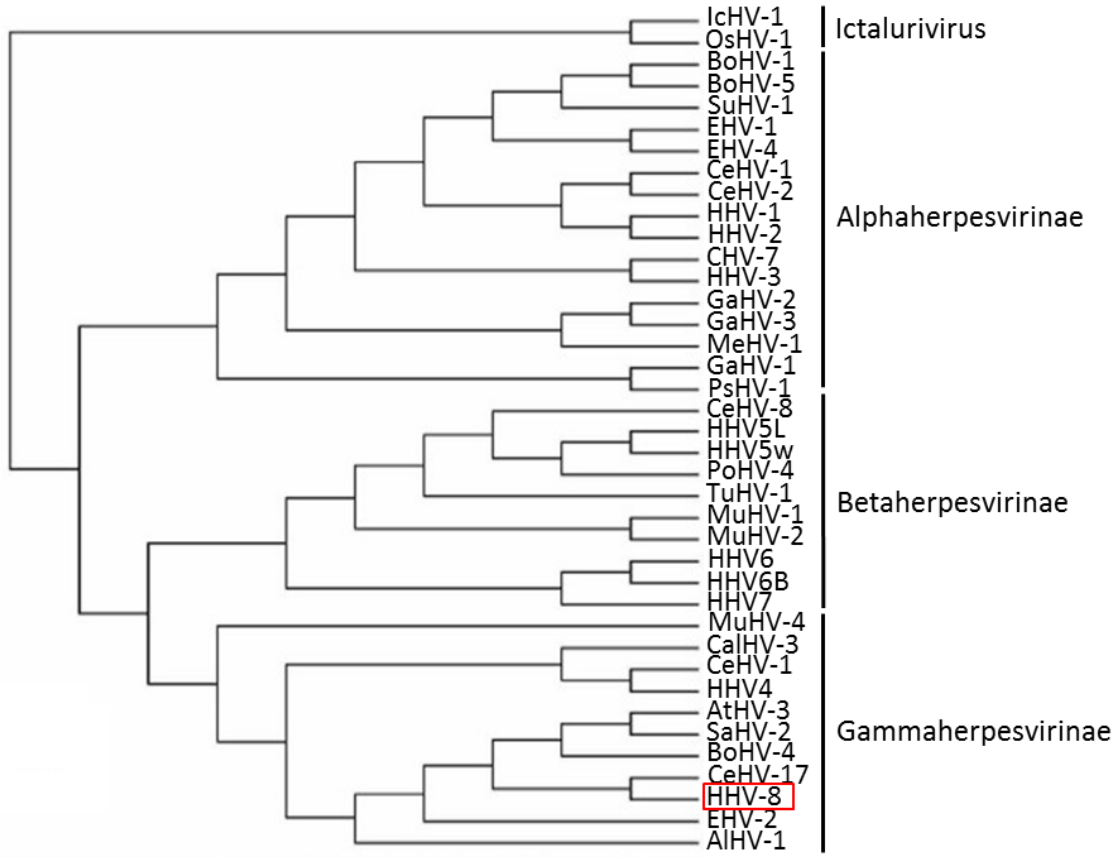

Figure 1.1: Phylogenetic tree of *Herpesviridae*.
Phylogenetic tree showing the evolutionary relationship between members of the *Herpesviridae*. KSHV (HHV-8) is highlighted by a red box. Adapted from (Gao and Qi, 2007).

1.1.1.2 Betaherpesvirinae

Defining characteristics of betaherpesviruses include a long lytic cycle, restricted host range and slow proliferation in cell culture (Roizmann et al., 1992). Furthermore,

infected cells typically exhibit a distinctive enlargement of the cell, known as cytomegaly. Latent betaherpesvirus infections usually persist in lymphoreticular cells, secretory glands and kidneys. This class consists of four genera, including *Cytomegalovirus*, which contains human cytomegalovirus (HCMV), *Roseolovirus*, containing human herpesviruses 6A, 6B and 7 (HHV6A/6B/7), *Muromegalovirus*, containing two murine herpesviruses and *Proboscivirus*, consisting of four animal herpesviruses.

1.1.1.3 Gammaherpesvirinae

Gammaherpesviruses have a narrow host range and a variable lytic cycle (Roizmann et al., 1992). Latent infection usually affects lymphoid tissue, with different viruses normally exhibiting T- or B-lymphocyte specificity. Some lytic gammaherpesvirus infections can take place in epithelial cells and fibroblasts. This class contains four genera including *Lymphocryptovirus*, containing the human herpesvirus Epstein-Barr virus (EBV) and *Rhadinovirus*, containing Kaposi's sarcoma-associated herpesvirus. These are the only two human herpesviruses in the gammaherpesvirus class, and also the only known oncogenic human herpesviruses (Davison, 2010). The remainder of the gammaherpesviruses comprise the *Macavirus* and *Percavirus* genera. Interestingly, the murine gammaherpesvirus MHV-68 (MuHV-4) has been observed to cause zoonotic infection in human hosts (Hricová and Mistríková, 2007).

1.1.2 Virion architecture

The *Herpesvirales* were originally classified together according to their unique morphology. All herpesvirus genomes consist of a single large, linear double stranded DNA molecule, which is contained within an icosahedral capsid **(Fig. 1.2)**. The capsid itself is assembled from 162 capsomeres and is around 125-130 nm in diameter when fully formed (Davison, 2007b). In the mature virion, one capsomere is replaced by the portal vertex, which is vital for both the packaging and release of the viral genome (White et al., 2003; Cardone et al., 2007; Rochat et al., 2011). Surrounding the capsid is

an amorphous layer of multiple proteins, known as the tegument. The tegument consists of at least 16 different viral and cellular proteins that are required for proper envelopment (Mettenleiter, 2004). Many tegument proteins are also involved in other processes upon entry of the virus into a host cell, including capsid transport, immune system evasion, activation of the lytic cycle and activation of the host shutoff response (Kelly et al., 2009; Penkert and Kalejta, 2011). A lipid envelope forms the final layer of the virion, and holds a number of viral membrane proteins that enable host cell binding and fusion with the membrane (Mettenleiter et al., 2009). A full herpesvirus virion ranges from 120-300 nm in diameter, mainly due to differences in the composition of the tegument (Roizmann et al., 1992).

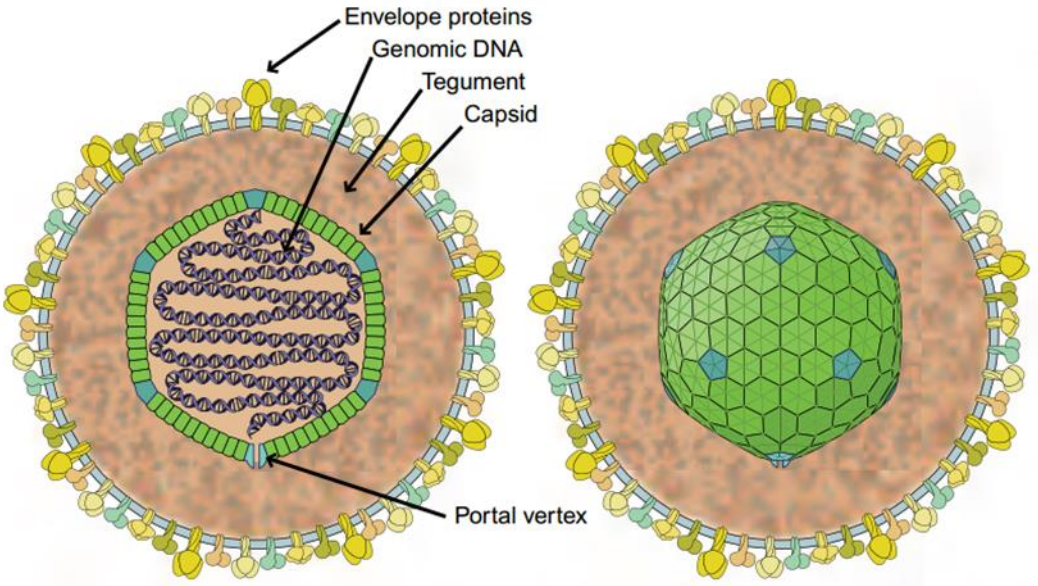

Figure 1.2: Mature Herpesvirus virion architecture.
Cartoon shows a schematic of a HSV-1 virion. A mature herpesvirus virion consists of a large, linear, double stranded DNA genome packaged within an icosahedral capsid. An amorphous layer of proteins known as the tegument sits between the capsid and a lipid envelope studded with envelope proteins. Adapted from Viral structures and antibodies (Abcam®).

1.1.3 Genomic structure

Herpesvirus genomes consist of linear, double stranded DNA, comprising 125 – 291 kbp in length, encoding between 70 and 200 genes (McGeoch et al., 2006). The ends of the genome contain unpaired nucleotides that are neither covalently closed or linked to proteins. Herpesviruses exhibit considerable differences in their nucleotide sequences, even between different strains of the same species. Most of the genome

content is made up of unique sequences, the vast majority of which is coding, however there are non-coding, repeated sequence elements in most of the different genomes, which can account for up to 30% of the total genome (Davison, 2007a). These repeat sequences can be situated at the ends of the genome as well as intragenomically, allowing for six different configurations of herpesvirus genome **(Fig. 1.3)**. Interestingly, these genome configurations do not correlate with evolutionary relations between different herpesviruses, and viruses within each class may differ in their genome configuration (Davison, 2007a).

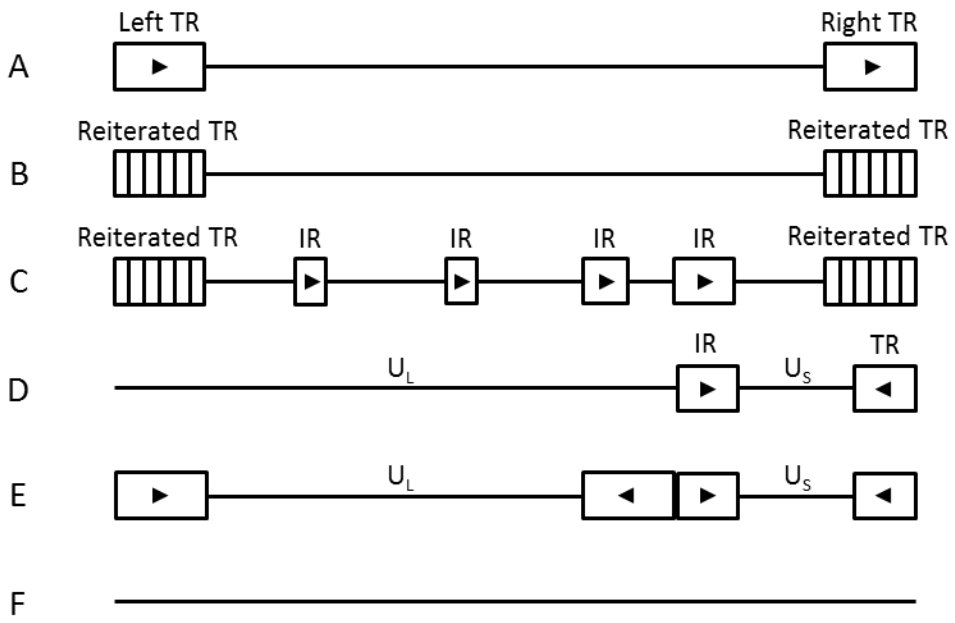

Figure 1.3: Herpesvirus genome configurations.
Schematic representations of the six different genome configurations found within the *Herpesvirales*. Lines represent unique regions and boxes represent various types of repeat sequence. Arrowheads indicate the orientation of the repeated element. TR - terminal repeat; IR – internal repeat; U_L – unique long region; U_S – unique short region. Adapted from (Domingo et al., 2008).

The divergence of the Herpesvirales into *Allo-*, *Malaco-* and *Herpesviridae* is estimated to have occurred between 180 and 400 million years ago (Davison, 2007b). Due to this, there is very little conservation between genes of the different classes. Indeed, only three genes can be clearly identified across all members of the *Herpesvirales* (McGeoch et al., 2006). Between the *Herpesviridae*, gene conservation is more apparent, and these viruses have retained a common set of 43 core genes, including those encoding the structural proteins, as well as essential genes for viral replication (Davison, 2007a). Important non-coding regions, such as those involved in genome

packaging and the origin of lytic replication are also conserved. Many herpesviruses also encode homologues of cellular genes. These genes, which regulate processes such as immune evasion and apoptosis, are less common in the alphaherpesvirinae, suggesting they are non-essential for successful viral replication during the shorter lytic cycle (Davison, 2007a). Many herpesviruses also produce non-coding transcripts such as microRNAs and untranslated latency associated RNAs (Tang et al., 2011; Lei et al., 2010; Guo et al., 2014; Cazalla et al., 2010; da Silva and Jones, 2013; Amen and Griffiths, 2011).

1.1.4 Life cycle

The herpesvirus life cycle begins upon contact between a mature, infectious virion and the surface of a host cell. The conserved glycoproteins gB, gH and gL, among other non-conserved envelope proteins studded in the viral envelope, contact and bind to cellular receptors, such as the proteoglycan heparan sulphate, which is bound by HSV-1 and KSHV (Akhtar and Shukla, 2009). Some of these receptors are utilised in order to concentrate virions on the cell surface, whilst others are used to facilitate membrane fusion, allowing viral ingress (Spear and Longnecker, 2003). In contrast, some members of the *Herpesvirales* do not enter the cell by membrane fusion, but by endocytosis, followed by acidification of the endosomal compartment leading to de-envelopment (Tortora et al., 2013). Similarly, some cell types are not permissive to membrane fusion and also require entry by endocytosis. Following de-envelopment, tegument proteins are released into the cytoplasm and begin influencing cellular processes such as capsid movement and nuclear import, host cell shutoff and immune evasion (Kelly et al., 2009). The capsid is also released and begins to traffic towards the nucleus via the microtubule network (Mabit et al., 2002; Naranatt et al., 2005). Upon reaching the nuclear membrane, the capsid releases its genome through the nuclear pore complex (Shahin, 2006; Rode et al., 2011; Labokha and Fassati, 2013). At this point, the viral DNA forms a circularised extrachromosomal episome. Here the virus can enter one of its two life cycle phases; latency or lytic replication (Mabit et al., 2002).

1.1.4.1 Latency

A characteristic of all herpesviruses is the ability to establish and maintain latent viral reservoirs for the lifetime of the host (Werner et al., 1978; Kaschka-Dierich et al., 1982). During this latent phase no mature viral progeny are produced. As different herpesviruses establish latency in different cell types, latent processes differ between viruses. HSV-1/2 and VZV establish latency in neuronal cells which do not undergo mitosis (Cohrs and Gilden, 2001). In contrast, both KSHV and EBV establish latent infections in B cells undergoing cell division, and therefore the genome is replicated by the host replication machinery, and maintained by a limited subset of latency associated genes (Lieberman et al., 2007; Damania and Pipas, 2009). Herpesviruses also encode a number of latency associated transcripts involved in immune evasion and lytic cycle regulation (Wang et al., 2005; Cliffe et al., 2009; Chentoufi et al., 2011). Indeed, some herpesviruses, such as KSHV and HSV-1, encode viral miRNAs in order to inhibit the expression of immediate early or lytic switch genes (Umbach et al., 2008; Qin et al., 2012). This repression can be overcome, however, and all herpesviruses may reactivate and undergo the lytic cycle upon an appropriate cellular stimulus (Penkert and Kalejta, 2011).

1.1.4.2 Lytic replication

The lytic cycle consists of a coordinated temporal cascade of gene expression, encompassing immediate early, delayed early and late genes (Arvin, 2007). The immediate early stage culminates in the production of viral-encoded factors which control the temporal gene cascade, as well as cellular gene expression. The delayed early stage results in the production of all proteins required for viral DNA replication, which occurs in specialised replication compartments localised around the nuclear periphery (Quinlan et al., 1984). Following viral DNA synthesis, late genes are expressed, giving rise to the structural components required for capsid assembly and packaging of viral DNA. The assembled capsid then exits the nucleus, gaining an envelope by passing through the inner nuclear membrane into the perinuclear space

(Granzow et al., 2001). Upon fusion with the outer nuclear membrane, the capsid is de-enveloped. Tegument proteins are acquired in the cytoplasm through a series of protein-protein interactions (Mettenleiter et al., 2009). The virus is then re-enveloped, forming mature viral progeny, via fusion with the membranes of a cytoplasmic organelle, the identity of which is currently debated; the prime candidates including endosomal compartments, endocytic tubules or the more commonly accepted *Trans*-Golgi network (Mocarski Jr., 2007; Mettenleiter et al., 2009; Hollinshead et al., 2012; Johns et al., 2014 p. 6). Mature viral progeny are finally released by exocytosis.

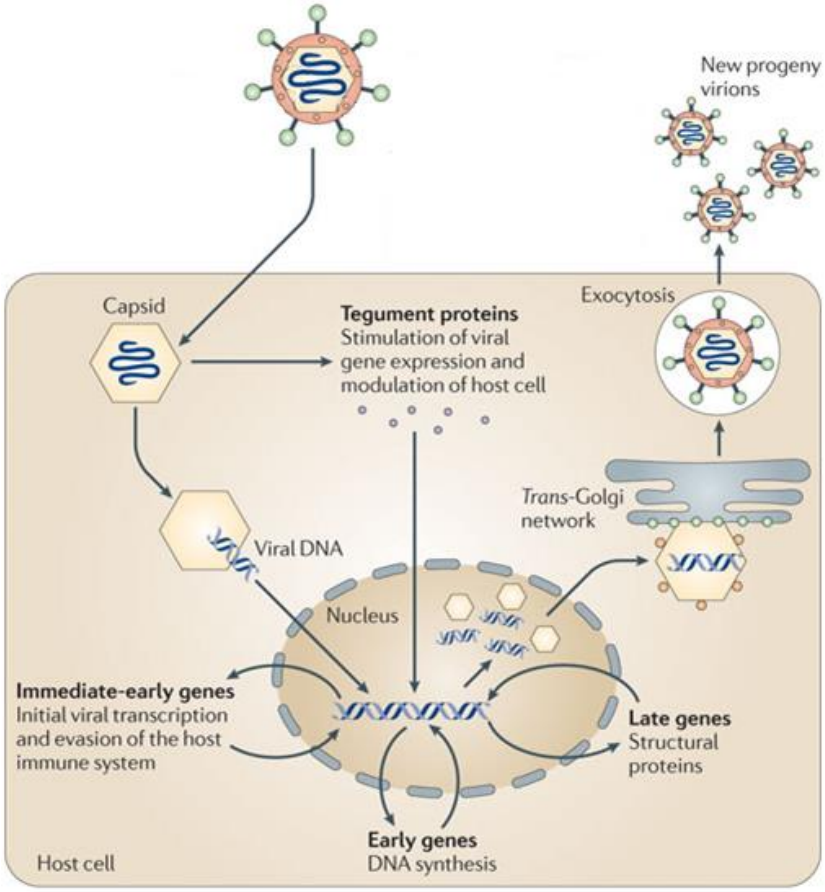

Figure 1.4: Herpesvirus lytic replication.
An infectious herpesvirus virion binds to the cytoplasmic membrane of a potential host cell, and is internalised by membrane fusion. The de-enveloped capsid is transported to the nuclear membrane and releases the viral genome into the host cell nucleus through a nuclear pore. A coordinated temporal gene cascade begins, culminating in the replication of viral DNA and the formation of a viral capsid around newly synthesised DNA. The capsid then exits the nucleus and gains an envelope through fusion with the membranes of a cellular organelle, believed to be the *Trans*-Golgi network. The mature virion is finally released from the host cell vie exocytosis. Image adapted from (Paludan et al., 2011).

1.1.5 Gammaherpesvirinae

The gammaherpesvirinae is comprised of four genera: *Lymphocryptovirus*, *Rhadinovirus*, *Macavirus* and *Percavirus* (Davison et al., 2009). Primary infection occurs in B- or T-lymphocytes, where a latent reservoir is established. An initial round of lytic infection then takes place in these lymphocytes before the shed viral progeny are able to disseminate and infect epithelial cells or fibroblasts for subsequent rounds of replication (Longnecker and Neipel, 2007; Odumade et al., 2011). The gammaherpesvirinae exhibit highly conserved genomes, particularly within a central region containing four gene blocks, separated by unique open reading frames (ORFs) (Pedro Simas and Efstathiou, 1998; Longnecker and Neipel, 2007). A variable number of terminal repeat sequences reside at either end of the central region.

Gammaherpesvirinae establish latency in dividing cells, and therefore have evolved mechanisms to ensure genome maintenance and efficient persistence in daughter cells (Cohrs and Gilden, 2001). This is accomplished through tethering of several copies of the viral episome to host mitotic chromosomes (Cotter and Robertson, 1999). Latent genes expressed by gammaherpesviruses also serve to suppress apoptosis, increase host cell survival, enhance progression of the cell cycle and subvert the immune response (Speck and Ganem, 2010). To date, EBV and KSHV are the only human herpesviruses currently known to cause cancer in infected hosts, and both are associated with multiple malignancies (Damania and Pipas, 2009).

1.1.5.1 Epstein Barr Virus

Epstein-Barr virus was discovered in primary cells from Burkitt's lymphoma tissue over 50 years ago, making it the first oncogenic human virus to be discovered (Epstein et al., 1964; Henle et al., 1967). Since then, EBV has been implicated in a range of other malignancies, including a number of B-cell associated lymphomas and carcinomas arising from epithelial infection (Damania, 2004). Over 90% of the global population are believed to be seropositive for EBV, the vast majority of infections occurring during childhood or adolescence with infected individuals remaining asymptomatic (Damania

and Pipas, 2009). Primary infection in adults, by contrast, often leads to mononucleosis and hyperproliferation of B cells. This typically manifests as fatigue and flu-like symptoms, lasting several weeks. The virus is spread by oral transmission, infecting the mucosa of the upper respiratory tract.

EBV usually establishes latency in B-lymphocytes and persists for the life of the host, with low levels of mature virus being found in the saliva (Longnecker and Neipel, 2007). Latently infected B-cells typically exhibit immortalisation, and lead to the generation of lymphoblastoid cell lines. T-cells and NK-cells are also susceptible to EBV infection, and although this is rare, this type of infection carries a much greater risk of the associated lymphomas (Jones et al., 1988). In general, a very limited number of those infected with EBV will develop the more serious malignancies associated with the virus; Burkitt's lymphoma, Hodgkin's lymphoma, immunosuppression associated lymphomas, Nasopharyngeal carcinoma and gastric carcinoma (Damania and Pipas, 2009; Levine et al., 1971; Pathmanathan et al., 1995). Often incidences of EBV associated malignancies exhibit distinct associations with geographical and ethnic groups, suggesting an important role for environmental factors in disease progression (Yu and Yuan, 2002).

At least four distinct latency gene expression profiles exist for EBV, known as type I, II, III and 0 (Young and Rickinson, 2004; Young et al., 2007). The latency I profile comprises the expression of the fewest genes, consisting of the episome maintenance and immune evasion related protein, EBNA1; a non-translated RNA implicated in reducing apoptosis, EBER; and the BART transcript, encoding up to 20 viral miRNAs, some of which have also been implicated in apoptosis avoidance. Latency I is commonly identified in Burkitt's Lymphoma tissue. Latency II consists of the expression of all genes expressed during Latency I, plus two transmembrane proteins, LMP1 and LMP2A/B, which act as constitutively active growth factors. Latency II is associated with nasopharyngeal carcinoma and Hodgkin's lymphoma. Latency III further expands on the Latency II gene repertoire, with the expression of 5 additional nuclear proteins, all associated with increased cell growth and survival, as well as transcriptional regulation. These genes are EBNA2, EBNA3A/B/C and EBNALP. Latency III is only associated with immunocompromised patients, typically those exhibiting post-

transplant lymphoma. It is not surprising, given the functions of the latency associated genes, that all EBV-associated diseases are associated with latency. A fourth latency profile also exists, termed Latency 0 in which no transcripts are produced. This profile is observed in resting memory B cells, which house the latent reservoir in immunocompetent individuals. It is believed that the Latency III profile is required for host colonisation during primary infection, in order to drive proliferation and differentiation of B-cells **(Fig. 1.5)**. In immunocompetent individuals, the virus is then thought to downregulate its own gene expression as latency becomes established and infected cells begin to exhibit phenotypes more closely associated with memory B-cells (Bollard et al., 2012).

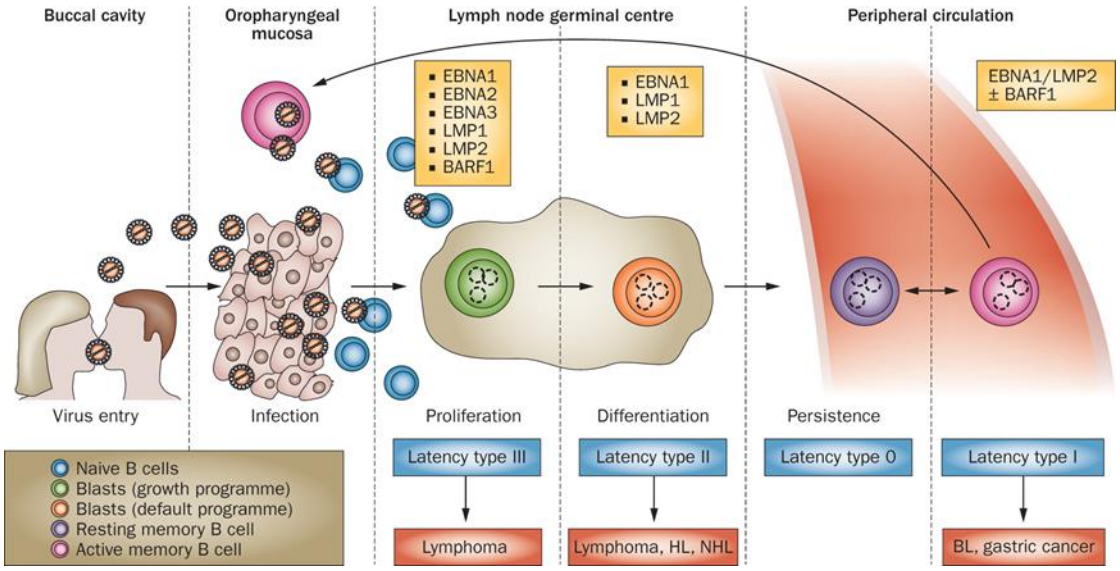

Figure 1.5: EBV primary infection and latency profiles.
EBV spreads via oral transmission and infects B-cells in the mucosa of the upper respiratory tract. The Latency III profile is established in order to facilitate host colonisation and gain access to the memory B-cell pool. Latency I or 0 is then established, with minimal need for viral maintenance or the expression of associated genes. EBV – Epstein-Barr virus; HL – Hodgkin's lymphoma; LMP – latent membrane protein; NHL – Non-Hodgkin's lymphoma. Taken from (Bollard et al., 2012)

1.1.5.2 Kaposi's Sarcoma-associated Herpesvirus

Kaposi's sarcoma (KS) is a tumour of endothelial cell origin, first described by Moritz Kaposi in 1872 (Kaposi, 1872). Over a century later in 1994, herpesvirus DNA was first isolated from KS tissue, following a surge in KS incidence associated with the AIDS epidemic (Chang et al., 1994). This virus was named Kaposi's sarcoma-associated

herpesvirus, and represents the second and most recent oncogenic human herpesvirus to be discovered. The viral genome ranges from 165-170 kb in size, containing a core of 140 kb between 25-30 kb GC rich terminal repeats (Russo et al., 1996). KSHV encodes a large number of conserved herpesvirus genes, as well as 15 open reading frames that are specific to its own species, termed K1-15. The virus also encodes 18 mature viral miRNAs, as well as a large polyadenylated nuclear RNA (PAN), widely believed to be non-coding, although a recent high resolution genomics and proteomics study contests this, suggesting that PAN may encode three small peptides of unknown function (Qin et al., 2012; Song et al., 2002; Chang et al., 2002; Arias et al., 2014).

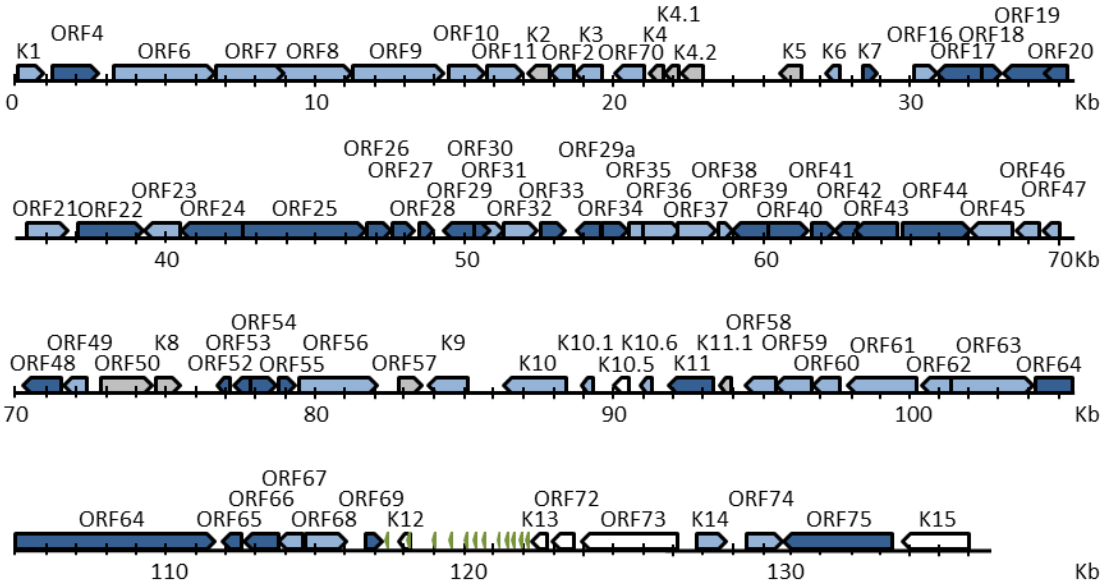

Figure 1.6: Map of open reading frames and miRNAs in the KSHV genome.
Latent KSHV genes are shown in white, immediate early lytic genes are shown in grey, early lytic genes are shown in light blue, late lytic genes are shown in dark blue, KSHV encoded pre-miRNAs are displayed as green arrowheads. Adapted from (Coscoy, 2007) following updates to gene expression classifications described in (Arias et al., 2014).

The seroprevalence of KSHV is much lower than EBV, with roughly 10% of the European, American and Asian population testing positive for the virus, compared to 50% in sub-Saharan Africa (Uldrick and Whitby, 2011). In accordance, KS is one of the most common malignancies in this region, displaying a significant association with AIDS, causing significant mortality.

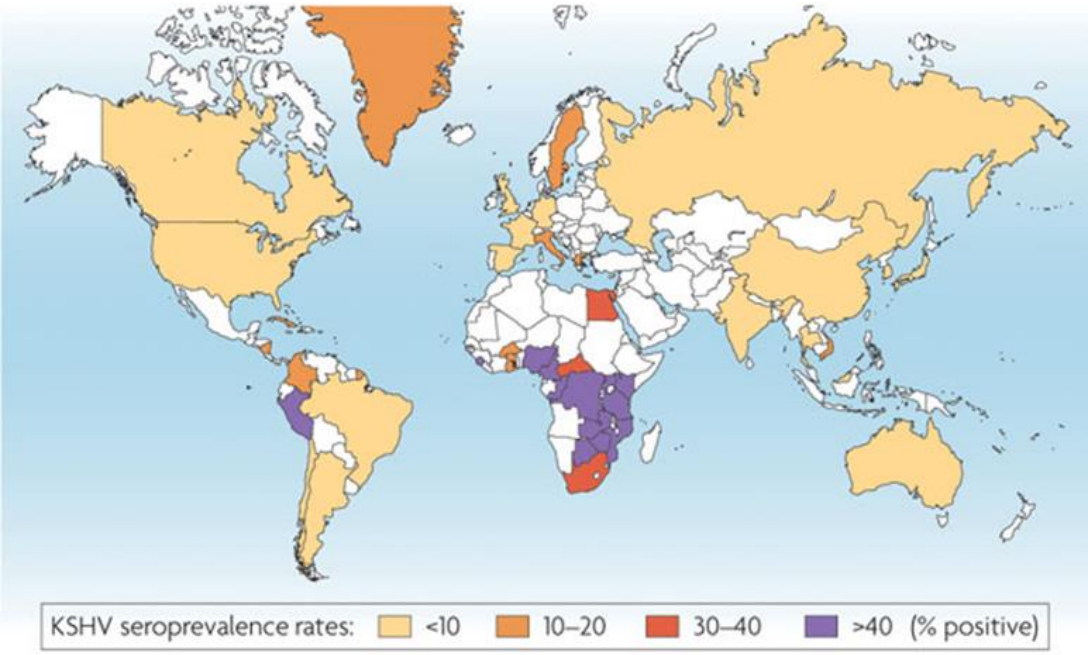

Figure 1.7: Global KSHV seroprevalence.
KSHV seroprevalence in European, Asian and American populations is typically below 10%, compared to between 20-30% in the Mediterranean and over 50% in sub-Saharan Africa. Taken from (Mesri et al., 2010)

1.1.5.3 KSHV-associated diseases

Following the identification of a close link between KSHV and AIDS-associated KS, KSHV has also been implicated in all other forms of KS, as well as Multicentric Castleman's disease and primary effusion lymphoma (Damania and Pipas, 2009).

Kaposi's sarcoma manifests as a dark red/brown skin lesion. The colour is produced due to the formation of blood-filled channels, caused by the disorganisation of the microvascular system near infected cells (Dictor and Andersson, 1988). There are four different classifications of KS; classical, endemic, AIDS-related and iatrogenic (Dourmishev et al., 2003). Classical KS is classified as a benign tumour typically presenting at the extremities and predominantly observed in elderly males of Mediterranean and Jewish descent (Boshoff and Weiss, 2001). Patients of classical KS often live with the disease for several years, commonly dying from other causes. The endemic form of KS is mainly identified in Eastern and Central Africa. It is a much more aggressive disease than classical KS, and patients, typically children or males in their thirties, usually die from this malignancy (Ziegler and Katongole-Mbidde, 1996).

Unsurprisingly, AIDS-related KS incidence increased dramatically with the AIDS pandemic in 1989 (Beral et al., 1990). KS is the most common neoplasm in AIDS patients, and exhibits a very high mortality rate (Parkin et al., 2008). AIDS-related KS initially manifests on the upper torso before rapidly and aggressively spreading to the inner organs (Ganem, 2010). Coinfection of HIV and KSHV contributes to the increased aggression of this form of the disease, primarily due to the well characterised immunosuppression of HIV+ individuals, but also due to more subtle direct and indirect mechanisms occurring in coinfected individuals (Varthakavi et al., 1999; Mercader et al., 2000). Iatrogenic KS is found in immunosuppressed patients that are not infected with HIV, such as those who have recently received a solid organ transplant. This form of KS correlates with incidence rate in the geographical area, accounting for as high as 80% of transplant related malignancies in areas of high KSHV prevalence (Qunibi et al., 1998; Duman et al., 2002).

Multicentric Castleman's disease is a rare condition in which lymphoid tissue becomes hyperproliferative (Polizzotto et al., 2013). This phenotype can spread to other organs as the disease progresses. Interleukin 6 is often observed to be upregulated in MCD, and is believed to be a major contributing factor to this condition (Yoshizaki et al., 1989). This may also explain the relation between KSHV and MCD, as KSHV encodes a viral homologue of the Interleukin 6 gene, known as vIL-6. HIV coinfection correlates strongly with KSHV involvement in MCD, with 100% of HIV-positive MCD patients exhibiting KSHV infection, compared to 40% for HIV-negative MCD (Soulier et al., 1995).

Primary effusion lymphoma is also rare and highly associated with HIV/KSHV coinfection (Chen et al., 2007; Cesarman et al., 1995). This disease is characterised by the invasion of transformed, proliferating B cells into body cavities. Survival rates are extremely low, with a median of 6 months following positive diagnosis and, to date, there is no effective therapy against this malignancy (Y.-B. Chen et al., 2007). KSHV is necessary for the onset of PEL, and PEL-derived cells are commonly used in order to study KSHV replication cycles in a laboratory setting (Damania and Pipas, 2009).

1.1.5.4 Life cycle

Upon contact with a potential host cell, KSHV envelope proteins bind to receptors on the cell surface, such as heparan sulphate, which is bound by the viral glycoproteins K8.1, gB, gH and ORF4 (Chakraborty et al., 2012). In addition, KSHV uses integrins α3β1 and αVβ3 as well as EphrinA2 for internalisation. The viral envelope proteins, gB, gH and gL, then facilitate fusion of the viral and host membranes, and the virus travels towards the nuclear membrane, depositing its genome in the host cell nucleus through a nuclear pore. Primary infection is subsequently resolved via a cytotoxic T-cell response, however, the virus persists in the host following primary infection, by establishing a latent reservoir in B-cells (Robey et al., 2010; Ganem, 2007).

Latency is associated with the expression of a limited gene repertoire including three major latency associated transcripts, the latency associated nuclear antigen (LANA), vFLIP and v-cyclin D, as well as all 18 mature viral miRNAs (Sun et al., 1999; Fakhari and Dittmer, 2002; Schulz and Chang, 2007; Qin et al., 2012). LANA acts to maintain and replicate the viral episome, a necessary process as KSHV establishes latency in dividing cells (Hu et al., 2002; Ballestas and Kaye, 2011). Furthermore, LANA acts as a regulator of viral and cellular transcription, and has also been implicated in modulating the host cell cycle and apoptosis via interactions with p53 and Rb (Garber et al., 2002; Direkze and Laman, 2004; Verma et al., 2004; An, 2004; Moore, 2007; Verma et al., 2007; Chen et al., 2010; Cai et al., 2013). vFLIP also functions to prevent apoptosis, through the inhibition of cellular caspases and an interaction with NFκB (Keller et al., 2000; Guasparri, 2004). v cyclin D interacts with and phosphorylates Rb in order to dysregulate the host cell cycle (Li et al., 1997; Verschuren, 2004). Although the latency associated expression profile of KSHV affects similar cellular processes to EBV, latency alone is not sufficient to cause any KSHV-associated malignancies (Grundhoff and Ganem, 2004).

1.1.5.5 Lytic reactivation

Latent virus is able to reactivate lytic replication upon the application of a relevant external stimulus, including HIF-1α accumulation, a typical effect of hypoxia (Cai et al., 2006). Indeed, exposure of a commonly studied KSHV positive, latently infected B-cell line to low oxygen conditions is sufficient to induce lytic reactivation, and this may explain the tendency for classical KS to affect the extremities (Davis, 2001). In addition, both B-cell differentiation and immune response factors have also been implicated in the induction of the KSHV lytic cycle (Johnson et al., 2005; Yu et al., 2007; Kati et al., 2013). Reactivation begins with expression of a viral transcription factor termed RTA, which acts as the lytic switch, driving the expression of a coordinated temporal lytic gene cascade (Lukac et al., 1998; Sun et al., 1998; Gradoville et al., 2000)). Indeed, the expression of this protein alone is sufficient to drive lytic reactivation, and numerous triggers can drive initial RTA expression, after which RTA is able to promote its own expression through a positive feedback loop (Bottero et al., 2009). RTA binds to a conserved sequence element, present in multiple viral gene promoter regions, known as the RTA response element (RRE) (Wen et al., 2009). Despite this, the RRE is not essential for RTA-mediated gene expression, and RTA also indirectly drives the expression of genes lacking this element, such as ORF57 (Liang, 2002; Chang et al., 2005). This is enhanced through the recruitment of other cellular transcription factors, such as RBP-Jκ, C/EBPα and AP-1 (Wang et al., 2003; Wang et al., 2004). RTA facilitates the recruitment of RNA polymerase II to target IE genes, driving their expression and thus beginning the lytic stage of the viral life cycle (Gwack et al., 2003). A highly co-ordinated gene cascade follows, culminating in the production of mature, infectious virions as described in Section 1.1.4.2. Prior to egress, the nuclear egress complex, composed of ORF67 and ORF69 facilitate the export of assembled capsids from the nucleus by remodelling the host nuclear membrane into transport vesicles (Luitweiler et al., 2013). Following this process, it is widely believed that, similar to other herpresviruses, KSHV utilises dynein motors to traverse the microtubule network in order to traffic assembled capsids towards the cell membrane (Lyman & Enquist, 2009).

1.2 Virus – host cell interactions

Obligate intracellular parasites such as viruses, by definition, are unable to produce adequate means for their own replication outside of a host. Therefore, all viruses interact with host cell factors in order to facilitate their own replication. Since the first virus, Tobacco mosaic virus, was discovered in 1892 by Dmitry Ivanovsky, there have been countless publications describing different interactions between viruses and their host cells. Increasing understanding of these interactions has allowed humankind to overcome some of the greatest health challenges faced. Smallpox is widely regarded as the best example, with this DNA virus responsible for the most deaths worldwide of an infectious agent (Smith and McFadden, 2002). There have also been many molecular mechanisms identified by virological studies that have greatly enhanced our collective understanding and potential in fields that are not directly associated with the study of parasites. Indeed, the interaction between Simian vacuolating virus 40 (SV40) and p53, has been essential in increasing the collective understanding of cancer, DNA damage, apoptosis and the cell cycle (Lane and Crawford, 1979; Linzer and Levine, 1979; Vousden and Prives, 2009). Furthermore, different viruses were also crucial in first identifying and describing mechanisms of mRNA splicing (Chow et al., 1977; Berget et al., 1977), capping (Muthukrishnan et al., 1975; Wei and Moss, 1975) and polyadenylation (Edmonds et al., 1971), *in vitro* DNA replication (Challberg and Kelly, 1979; Ikeda et al., 1980; Benoist and Chambon, 1981), transcription promoter sequences (Banerji et al., 1981; Fromm and Berg, 1983), transcription factors (Fromm and Berg, 1983; Payvar et al., 1983; Dynan and Tjian, 1983) and gene silencing (Fire et al., 1998; Brigneti, 1998). These discoveries represent just a fraction of the important work undertaken in the field of virology, and much of modern science would not be possible without prior knowledge of these processes. Clearly, viruses are great teachers and represent both a major health risk that must be overcome, as well as a powerful tool for the elucidation of biological phenomena.

1.2.1 mRNA maturation and virus infection

mRNA plays a central role in the gene expression of any organism, and therefore, cells have evolved complex mechanisms to ensure quality control and regulation. mRNAs undergo numerous important processing steps prior to their initial translation, and each of these steps is associated with checkpoints to ensure each mRNA produced is free of error. Intracellular pathogens, therefore, are faced with an important challenge of subverting these host checkpoints in order to efficiently facilitate the expression of their own genes.

1.2.1.1 mRNA biogenesis

The biogenesis of an mRNA begins with the transcription of a pre-mRNA from a coding genomic sequence. Large numbers of transcription factors associate with promoter sequences to mediate the expression of a gene, ultimately culminating in the recruitment of RNA polymerase II (RNA pol. II) to the site, producing an initial transcript complementary to the DNA sequence (Kornberg, 2001). The carboxy-terminal domain (CTD) of RNA pol. II then facilitates the processing of these transcripts, in a highly coordinated pathway involving the capping, splicing and polyadenylation of the mRNA (Zorio, 2004).

Capping of an mRNA involves the addition of a methylated guanine nucleotide to the 5' end of the mRNA with an unusual inverted 5' to 5' triphosphate bond (Shatkin, 1976). Capping occurs during transcription once the nascent transcript has achieved a length of between 20 and 40 nucleotides (Coppola et al., 1983; Moteki and Price, 2002). The heptameric repeat of the RNA pol. II CTD is phosphorylated at serine 5, leading to the dissociation of various transcription factors and the recruitment and activation of the capping machinery (Trigon et al., 1998; Cho et al., 2001). There are three important enzymes involved in the capping process, RNA triphosphatase, RNA guanylyltransferase and RNA-(guanine-7) methyltransferase, which act in succession (Mizumoto and Kaziro, 1987). Following cap formation, serine 5 of the CTD heptad repeat is dephosphorylated and the capping enzyme complex dissociates from RNA

pol. II and the transcript (Komarnitsky et al., 2000; Schroeder et al., 2000). Capping is important for mRNA stability, preventing the action of 5' exonuclease enzymes as well as forming an important binding site for mature mRNA circularisation following maturation (Wells et al., 1998). In addition, the cap is necessary for efficient splicing, nuclear export and translation of transcripts (Lewis et al., 1995).

Splicing involves the removal of intronic sequences from the nascent transcript. Nearly all eukaryotic genes contain introns, with an average of 9 introns per transcript, and many genes can be alternatively spliced in order to produce different protein products (Lander et al., 2001). Splicing also occurs during transcription elongation, with the phosphorylation of serine 2 of the RNA pol. II CTD by the kinase, P-TEFb (Garriga and Graña, 2004). Splicing requires interactions between five U snRNPs, U1, U2, U4, U5 and U6, as well as a large protein complex called the spliceosome, comprising as many as 200 different proteins, which can associate with the complex at different stages of the reaction (Jurica and Moore, 2003). As different introns and their splice junctions can be distant from each other, splicing components are recruited to different areas of the transcript at different times, however, the reaction begins with the recognition and binding of a GU element at the 5' splice junction by U1 and the binding of the U2 auxiliary factor (U2AF1) to the 3' splice junction (Sanford, 2004). U2 is subsequently recruited to an adenosine residue in the intron branch point, and assembly of a trimer of U4-U6-U5 shortly follows. These components then rearrange themselves to form the catalytic form of the spliceosome complex, which removes the intron sequence in a protein-assisted manner. The 5' GU of the removed intron is then ligated to the A residue in the branch point through 2 transesterification reactions catalyzed by U6 and U2, forming an intron lariat which is subsequently degraded (Reed and Maniatis, 1985). The exon junction complex (EJC) is deposited at these splice sites, and remains bound to the spliced transcript to promote important interactions during mRNA nuclear export (Le Hir, 2001; Masuda et al., 2005; Cheng et al., 2006).

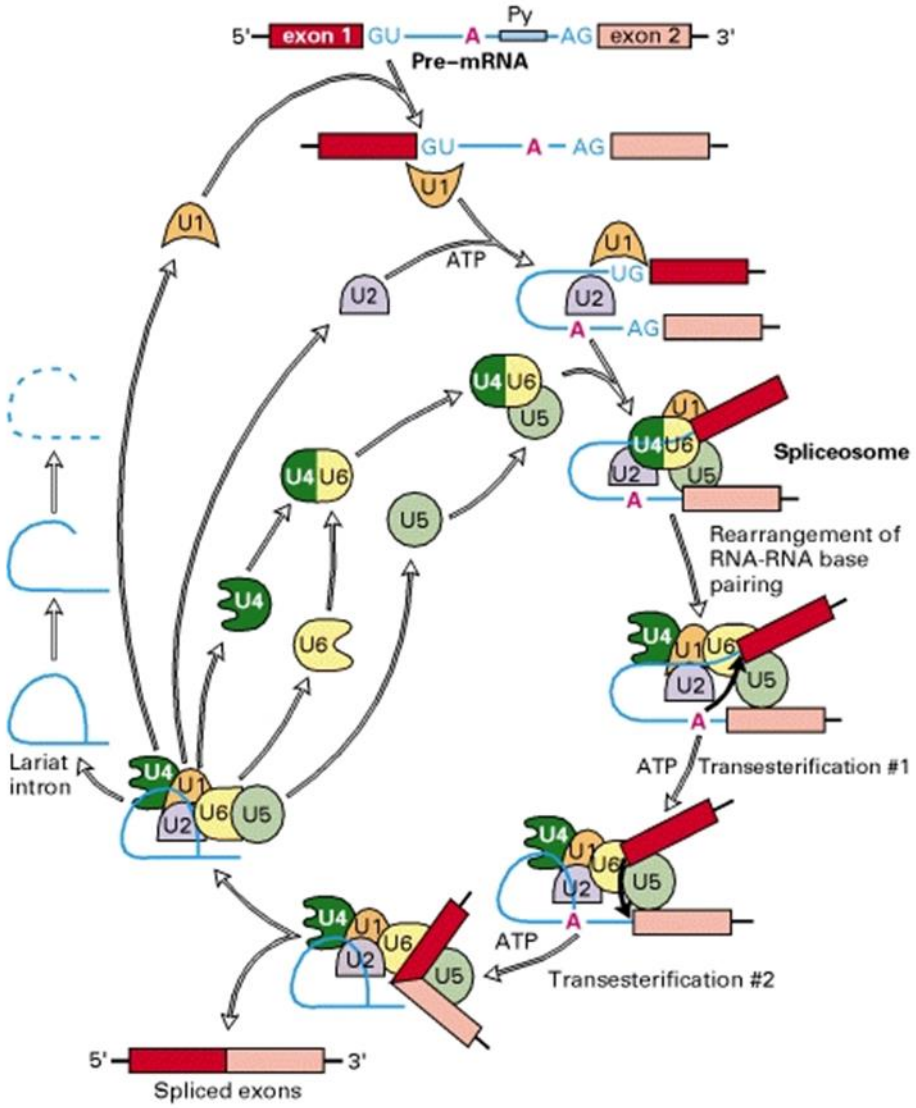

Figure 1.8: The mRNA splicing reaction.
mRNA splicing begins with the recognition of a GU element by U1 at the 5' splice junction, and an AG element by U2AF1 and U2 at the 3' splice junction. The U4-U6-U5 complex is subsequently recruited to form a catalytic complex which removes the intron and forms a lariat via two transesterification reactions. The spliced exons are ligated together, whilst the intron lariat is subsequently degraded. Taken from (Lodish, 2000).

Polyadenylation is the final stage of mRNA processing, and begins with the recognition of an AAUAAA motif, which represents the cleavage site, within 30 nucleotides of the 3' end of the transcript (Proudfoot, 1991). The cleavage and polyadenylation specificity factor (CPSF) complex, comprising CPSF-160, CPSF-100, CPSF-73 and CPSF-30, binds to the cleavage motif, and recruits both cleavage stimulation factor (CstF) and polyadenylate polymerase (PAP) to the pre-mRNA (Manley, 1995). Again, the RNA pol. II CTD is instrumental in this process, associating with both CPSF and CstF to increase polyadenylation efficiency (McCracken et al., 1997). The transcript is cleaved prior to

transcription termination, via an endonucleolytic attack by cleavage factor 1 and 2 (CF1/2) (Gilmartin and Nevins, 1989). Following cleavage, PAP begins to add adenosine residues to the 3' end of the RNA (Manley, 1995). Polyadenylate binding protein 2 (PABP2) binds to the newly formed poly(A) tail and increases the affinity between PAP and the transcript through the formation of a quaternary complex involving CPSF, PABP2, PAP and the RNA (Wahle et al., 1993; Bienroth et al., 1993). The polyadenylation reaction proceeds until the tail is ~250 nucleotides long, at which point PAP becomes too distant from CPSF and the interaction breaks down, preventing any further polyadenylation, as such this interaction determines the maximum poly(A) tail length. Polyadenylation promotes nuclear export as it is an important signal for the formation of an export-competent mRNP, and it also promotes translation via interactions with eukaryotic initiation factor 4G (eIF4G), as well as several other proteins that mediate translation (Vassalli et al., 1989; Huang and Carmichael, 1996; McKendrick et al., 2001).

Finally, nuclear export of the fully processed mRNA is also required prior to translation. This begins with the formation of an export-competent messenger ribonucleoprotein (mRNP) complex, containing various heterogeneous nuclear RNPs (hnRNPs) and the mRNA (Carmody and Wente, 2009). The ATP dependent RNA-helicase UAP56 is believed to play a major role in the formation of this complex, firstly during its recruitment to the mRNA via an interaction with the spliceosome, promoting its assembly during mRNA splicing (Zhou et al., 2000). UAP56 then recruits the export adaptor Aly, followed shortly by the recruitment and formation of the full transcription and export (TREX) complex. An interaction between Aly and cap binding protein 80 (CBP80) determines the localisation of the TREX complex at the 5' end of the mRNA (Cheng et al., 2006; Chi et al., 2013). Aly and another TREX component, Thoc5, then recruit the export receptor Nxf1, alongside its cofactor Nxt1, which are able to interact with certain FG-nucleoporins found in the nuclear pore complex (NPC) (Katahira et al., 2009). This interaction promotes the translocation of the mRNP through the nuclear pore, in a highly controlled and regulated manner.

1.2.1.2 Viral interactions with cellular mRNA processing machinery

The highly regulated and ordered processes that occur during mRNA processing represent a significant challenge for viruses to overcome. Many viruses exploit different components and mechanisms involved in all stages of the mRNA processing pathway. A common way that viruses exploit the host cell is through the acquisition of 5' m^7G caps for viral transcripts, therefore preventing the identification of uncapped nascent viral mRNAs as "non-self" by the host cell, which may lead to their degradation (Decroly et al., 2011). Viruses facilitate cap acquisition in different ways, using both conventional and unconventional capping mechanisms. For example, most DNA viruses utilise the cellular RNA polymerase II enzyme for the transcription of viral mRNAs, thereby feeding the viral transcripts into the cellular mRNA processing pathway at the earliest stage. Alternatively, some viruses, such as the Orthomyxovirus, influenza A virus (IAV), encode proteins, such as the PA and PB2 subunits of the viral heterotrimeric polymerase, that "snatch" caps and short 5' regions from cellular mRNAs via an endonucleolytic attack, subsequently using these hijacked transcripts to prime viral mRNA synthesis (Plotch et al., 1981; Guilligay et al., 2014). Alternatively, many single stranded RNA viruses encode their own capping enzymes and cofactors in order to synthesise their own capped transcripts. Vesicular stomatitis virus (VSV), for example, encodes the L protein, which adds GDP, rather than GMP, to the 5' end of VSV encoded transcripts, acting in the same manner as a canonical cap (Abraham et al., 1975).

The splicing reaction is an important part of mRNA processing, with strong links to mRNA export, whilst also representing an important cellular checkpoint to ensure mRNA quality control. Many viruses encode introns in their genes despite the fitness cost associated with a larger genome, demonstrating the importance of the cellular splicing checkpoint (Holmes, 2010). Some viruses have developed alternative splicing mechanisms in order to benefit further from their introns, for example, human immunodeficiency virus 1 (HIV-1) encodes a single primary transcript that gives rise to over 40 different mRNA species (Stoltzfus and Madsen, 2006). This 9 kb transcript serves as both the viral genome and mRNA, and so HIV-1 carefully regulates and

controls alternative splicing mechanisms. The virus encodes multiple non-canonical splice sites over the length of the polycistronic transcript, which are recognised and processed with different efficiencies by the host spliceosome (O'Reilly et al., 1995; Staffa and Cochrane, 1994). During early stages of infection, five 3' splice junctions near the centre of the transcript are used to produce the partially and fully spliced Tat, Rev and Nef mRNAs (Purcell and Martin, 1993). As Rev protein accumulates, it binds to the Rev response element (RRE) present in the transcript and mediates the nuclear export of the viral singly spliced (4 kb) and unspliced genomic RNAs. The use of suboptimal splice sites is further regulated by viral sequences, known as exonic splicing enhancers (ESE) and exonic/intronic splicing silencers (ESS/ISS), which interact with various cellular factors such as hnRNPs and SR proteins to modulate splice site usage (Caputi and Zahler, 2002; Jacquenet et al., 2001; Zahler et al., 2004). Alternative splicing is also important for IAV replication, as IAV expresses two polycistronic transcripts; NS and M (Dubois et al., 2014). Similarly to HIV-1, IAV uses suboptimal splice sites, however it regulates the use of different sites of NS using intronic sequences that are believed to inhibit spliceosome activity by folding into secondary structures (Chua et al., 2013; Dubois et al., 2014). Alternative splicing of M uses a different mechanism, with two 5' splice sites located within close proximity on the transcript. It has been suggested that the viral polymerase is able to promote the use of the proximal, rather than the distal splice site, producing more M2 mRNA (Shih et al., 1995; Tsai et al., 2013). In addition, M mRNAs all use the same 3' splice site, which is located within an ESE that binds the SR protein, SF2, to promote M2 production, suggesting a mechanism similar to that used by HIV-1 (Shih and Krug, 1996).

Viruses must also overcome the cellular mRNA checkpoint of polyadenylation, if they are to disguise their transcripts as "self" so as not to be detected by the host. IAV, which, as previously described, has mechanisms to cap and splice its mRNA, also has a mechanism to polyadenylate them, thereby completing the process of disguising its transcripts. IAV uses a host independent mechanism to transcribe polyadenylated mRNA from the virion RNA (vRNA), in which a poly(U) tract in the genome is encoded in close proximity to a base-paired region of a pan-handle structure (Plotch and Krug, 1977; Desselberger et al., 1980). It has been suggested that the viral RNA polymerase

is unable to navigate this genomic region, and therefore "slips" on to the poly(U) run, and transcribes this as a poly(A) tail (Hsu et al., 1987; Pritlove et al., 1998). VSV also produces polyadenylated transcripts, albeit by a different mechanism. VSV genes occur upstream of a consensus 5' – AUACU_7 – 3' intercistronic sequence, which acts as both a non-canonical polyadenylation signal, causing "stuttering" of the viral RNA polymerase at the U_7 residues, as well as a transcriptional stop site (Schubert et al., 1980). In addition, this sequence has been shown to be necessary for the transcription of monocistronic transcripts from the VSV genome (Hwang et al., 1998).

The mechanisms employed by KSHV to overcome the host cell mRNA quality control checkpoints are particularly interesting. KSHV encodes many intronless mRNAs which, therefore, do not undergo splicing. Splicing is closely linked with mRNA export, and so to overcome this potential problem, the KSHV encoded ORF57 protein directly binds and recruits Aly or another TREX export adaptor, UIF, to these transcripts (Malik et al., 2004; Jackson et al., 2011). Through this interaction, ORF57 is able to recruit the entire TREX complex to KSHV intronless mRNAs, forming export-competent RNPs. Interestingly, the viral mRNAs are then trafficked through the nucleolus, and disruption of nucleoli or nucleolar localisation signals within the ORF57 protein drastically reduce KSHV mRNA nuclear export (Boyne and Whitehouse, 2009; Boyne and Whitehouse, 2006). Furthermore, TREX components also colocalise with ORF57 is the nucleolus. The reason for this process is not yet understood, however this mechanism may avoid the host cell shutoff process, caused by the KSHV-encoded shutoff and exonuclease (SOX) protein. SOX interacts with multiple components of the polyadenylation machinery, including PAP2 and PABP1, inducing the hyperadenylation of cellular transcripts resulting in their increased turnover (Lee and Glaunsinger, 2009; Covarrubias et al., 2011). Interestingly, KSHV promotes polyadenylation of the viral mRNAs using two canonical polyadenylation sites at the 3' end of many of its genes, however the viral mRNAs are not hyperadenylated like their cellular counterparts (Majerciak et al., 2013). It is therefore likely that this nucleolar localisation prevents SOX activity on viral mRNAs. Following nucleolar trafficking, viral mRNAs are exported through the nuclear pore complex, via an interaction with Nxf1, which is bridged by Aly **(Fig. 1.9)** (Boyne et al., 2008).

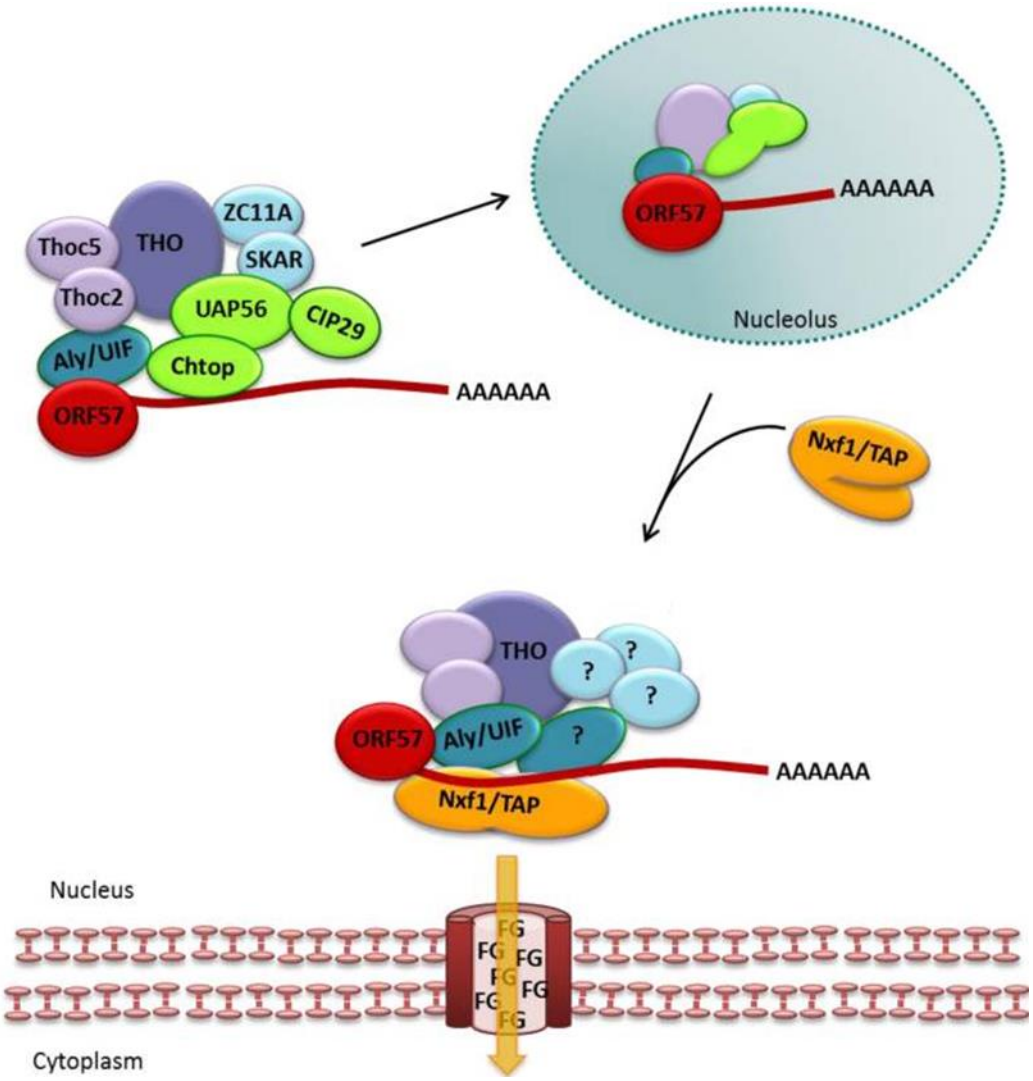

Figure 1.9: ORF57 mediated TREX recruitment, nucleolar trafficking and nuclear export of viral mRNA. ORF57 directly recruits Aly/UIF to intronless viral transcripts, leading to the subsequent recruitment of the full TREX complex. ORF57 then mediates the trafficking of the viral transcript through the nucleolus. Finally, Aly bridges an interaction between the viral mRNA and the export receptor, Nxf1, which facilitates the transit of the transcript through the nuclear pore via an interaction with FG-nucleoporins. Adapted from (Schumann et al., 2013).

1.2.2 The DNA damage response, apoptosis and virus infection

Genome integrity is vital for the correct regulation and production of new biological material. DNA is repeatedly exposed to insults and stresses that, if not adequately repaired, could lead to the formation of cancerous tissue (Branzei and Foiani, 2008). To combat this, multicellular organisms have evolved a series of defence mechanisms designed to quickly identify various forms DNA damage and then mediate DNA repair (Smith et al., 2010). Alternatively, if the damage cannot be rectified, affected cells are

forced into a programmed cell death pathway known as apoptosis, in order to preserve genome integrity (Roos and Kaina, 2006). Many of the cellular factors that contribute to the DNA damage response and trigger DNA repair or apoptosis are highly conserved between multicellular organisms, demonstrating their importance (Aravind, 1999).

1.2.2.1 DNA damage

The genome of any organism is constantly under attack from many different sources, and there are many different forms of DNA damage **(Fig. 1.10)** (Helleday et al., 2014). The most common type of DNA damage is caused by the spontaneous breaking of the N-glycosidic bond between the pentose-phosphate DNA scaffold and the nucleobase, leading to an abasic (apurinic or apyrimidinic) site (Krokan et al., 1997). This is a common phenomenon, believed to occur up to 10^4 times per cell per day, and is rectified by the activity of AP endonuclease enzymes, which cleave the DNA strand to remove the affected position (Loeb and Preston, 1986; Wilson et al., 1997). The newly formed single strand break is subsequently repaired, usually by the short patch base excision repair pathway (Helleday et al., 2014). Deamination, the removal of an amine group, is a similar spontaneous reaction most commonly associated with the conversion of cytosine to uracil by hydrolysis, forming a GU mismatch (Krokan et al., 2002). Uracil is subsequently removed by Uracil-DNA glycosylase, which promotes glycosidic bond cleavage using a “pinch-push-pull” mechanism. Other mismatches can also occur spontaneously by insertion, deletion or misincorporation, rather than by a chemical reaction affecting correctly matched bases. All mismatches are repaired by the mismatch repair (MMR) machinery, which is able to distinguish the newly synthesised daughter strand, which is likely to contain any mismatches, from the parental strand by a mechanism which is not yet fully understood (Jiricny, 2013).

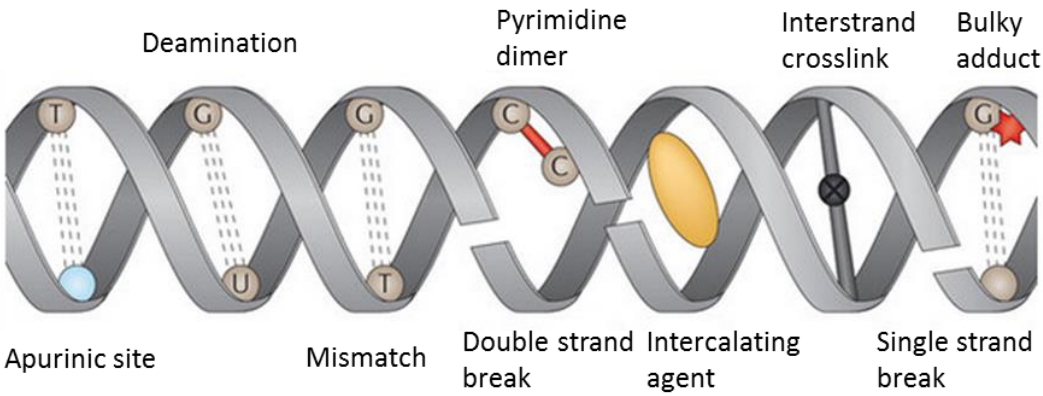

Figure 1.10: Common forms of DNA damage.
Many forms of DNA damage exist including abasic (apurinic or apyrimidinic) sites, deamination, mismatches, pyrimidine dimers, intercalating agents, interstrand crosslinks, bulky adducts, single strand breaks and double strand breaks. The thick grey bars represent a DNA double helix, dashed grey lines represent base complementarity. Adapted from (Helleday et al., 2014).

In contrast, many forms of DNA damage are induced by exogenous sources, and it has long been known that exposure to certain chemicals or energy sources dramatically increases the risk of cancer development (Poirier, 2012). Pyrimidine dimers, a form of bulky adduct, occur during excitation of two pyrimidines by UV light, resulting in C=C double bonds between the residues (Goodsell, 2001). This type of molecular lesion is most commonly repaired by the nucleotide excision repair (NER) pathway, which removes a short strand of DNA containing the adduct (Marteijn et al., 2014). The missing strand is subsequently replaced and ligated by DNA polymerase and DNA ligase. Other bulky adducts are also repaired in this manner.

Interstrand crosslinks can be formed by both exogenous and endogenous sources, and frequently cause stalled replication forks (Clauson et al., 2013). As interstrand crosslinks affect both strands, the aforementioned simple repair pathways do not suffice, and instead a more complicated repair pathway known as homologous recombination takes place **(Fig. 1.11)**. Homologous recombination at interstrand crosslink associated stalled replication forks begins with cleavage of one of the strands to form a one sided double strand break (Li and Heyer, 2008). A second cleavage event occurs on the other strand at the other side of the interstrand crosslink. This allows the affected area to “flip out”, and translesion synthesis is then able to bypass this area, generating a new strand. The double strand break is subsequently resolved by invasion of one strand into the area containing the “flipped out” lesion, displacing the newly

generated strand. The lesion is again bypassed by translesion synthesis. The replication fork is restored with the generation of the final strand and the formation of a Holliday junction, which can be resolved by a number of mechanisms, usually with the junction being cleaved in different patterns by different enzymes (Rass et al., 2010).

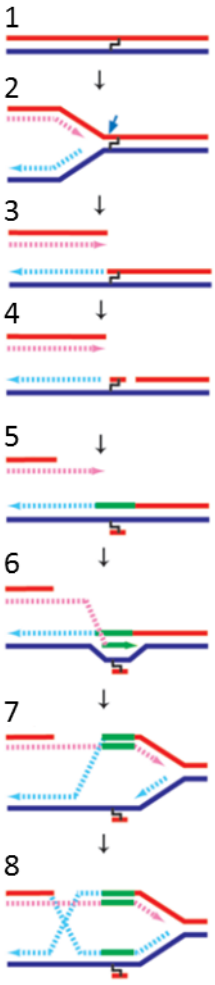

Figure 1.11: Homologous recombination repair at interstrand crosslink associated stalled replication forks.
Schematic showing the steps in interstrand crosslink associated stalled replication fork resolution by homologous recombination. 1. Interstrand crosslink formation; 2. Stalled replication fork formation; 3. Generation of a one sided double strand break; 4. Cleavage of affected strand near lesion; 5. "Flipping out" of lesion and translesion synthesis; 6. Strand invasion and translesion synthesis; 7. Restoration of replication fork past lesion; 8. Translesion synthesis and Holliday junction formation. Taken from (Li and Heyer, 2008).

Various alterations to the described method of homologous recombination can occur depending on the type of replication stress or DSB formed. However, HR cannot always be used to rectify damage, as it is only applicable during certain stages of the cell cycle (Branzei and Foiani, 2008). Similarly, sometimes translesion synthesis cannot occur as there is a loss of sequence data on both strands of the DNA, and a sister chromosome

may not have been generated for use as a template. In these scenarios, a process known as non-homologous end joining (NHEJ) takes over. NHEJ always resolves double strand breaks, although if a single strand break is generated that cannot be rectified by HR, the unbroken strand may be cleaved before the subsequent DSB is repaired by NHEJ. NHEJ acts to ligate two ends found at a DSB together with two ends of another DSB (Davis and Chen, 2013). Usually there are short homologous overlaps found at the broken ends, and in these scenarios NHEJ normally leads to the correct repair of the DSB. Occasionally, however, DSBs will generate flush ends, with no guiding homologous sequence. In this scenario, NHEJ will ligate the broken ends with any other broken ends the NHEJ machinery comes into contact with, and this often results in the generation of aberrant sequences. Indeed, this process often leads to well documented chromosome translocations at specific sites, as chromosomes occupy defined territories in the nucleus, and certain areas of each chromosome are highly prone to DSBs (Roukos and Misteli, 2014). Furthermore, although many chromosome translocations are well tolerated and do not produce an altered phenotype, some translocations can lead to alterations to gene function, occasionally generating oncogenes if a strong promoter from one gene is translocated upstream of another minimally expressed gene. This effect is frequently observed in the case of "Philadelphia chromosome" formation, a well characterised and recurring chromosome translocation between chromosome 9 and chromosome 22 that is associated with chronic myelogenous leukaemia **(Fig. 1.12)** (Koretzky, 2007; Kosior et al., 2011). Both the breakpoint cluster region (*BCR*) of chromosome 22 and the *Abl1* gene on chromosome 9 are highly prone to the generation of DSBs, and these two regions are often ligated together by NHEJ, forming the oncogenic *BCR-Abl1* fusion gene that acts as a constitutively active tyrosine kinase.

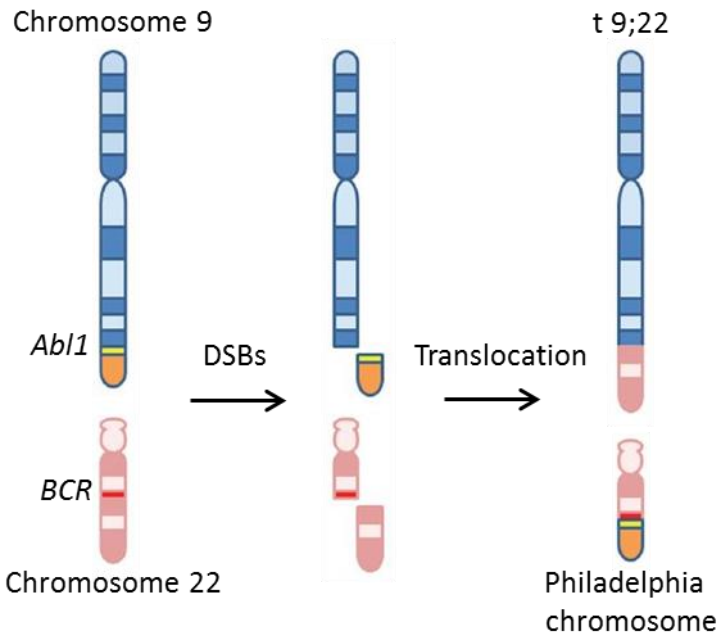

Figure 1.12: Philadelphia chromosome formation via a translocation between chromosome 9 and chromosome 22.
Schematic showing the formation of a Philadelphia chromosome. Double strand breaks occur on chromosome 9 and chromosome 22. Subsequent erroneous NHEJ forms t 9;22 and the Philadelphia chromosome, generating a fusion gene between *Abl1* and *BCR*. Yellow and red lines represent the promoter regions for *Abl1* and *BCR* respectively, orange block represents *Abl1* gene. Adapted from (Kosior et al., 2011).

The cellular DNA damage response profile is highly complex, and many proteins have been identified as signal transducers, responding to various forms of genotoxic stress and facilitating the expression of large numbers of genes which contribute to the repair or apoptosis pathways (Yang et al., 2003). What is less clear, however, is how damaged DNA is first detected and how specific signalling cascades are triggered. Recent research suggest roles for a small subset of protein kinases in this function. In particular, three kinases known as ataxia-telangectasia mutated (ATM), ATM- and Rad3 related (ATR) and DNA-dependent protein kinase catalytic subunit (DNA-PKcs) have major roles in sensing DNA damage and initiating the subsequent DDR protein kinase cascade (Yang, 2003). These kinases have been demonstrated to respond to specific forms of genotoxic stress, and each appear to be responsible for the activation of different pathways. Interestingly, however, there appears to be a degree of crosstalk between the three different pathways, and each kinase has been shown, in certain conditions, to phosphorylate targets of the other pathways.

1.2.2.2 The ATM-Chk2 DNA damage response pathway

ATM is a Serine/Threonine (Ser/Thr) protein kinase, first discovered as a mutated gene associated with the genomic instability syndrome ataxia-telangiectasia, a disease characterised by a defect in the response to DSBs (Shiloh and Ziv, 2013). It is not surprising, therefore, that the primary role of ATM and its associated protein kinase cascade is to signal the presence of DSBs and bring about their repair.

The MRE11-RAD50-NBS1 (MRN) complex is believed to be one of the first complexes to be recruited to DSBs, acting as a physical scaffold to keep the two ends of the DSB in close proximity (Uziel, 2003; Shiloh and Ziv, 2013). The MRN complex also acts as an initial sensor of DNA damage, and its localisation to DSBs is required for the activation and recruitment of ATM to DSBs **(Fig. 1.13)**. The biophysical mechanism of ATM recruitment and activation is not fully understood, however, an interaction between ATM and Nijmegen breakage syndrome protein 1 (NBS1), strengthened by breast cancer type 1 susceptibility protein (BRCA1) and tumour suppressor p53-binding protein 1 (53BP1), as well as Lys63-linked ubiquitylation of NBS1 by S-phase kinase-associated protein 2 (SKP2), is crucial to this process. ATM is found as a homodimer in its inactive form, but quickly dissociates into active monomers, which are recruited to sites of DSBs following their induction. Upon its recruitment, ATM forms a “turret” structure with other DSB associated proteins, and begins to function as a kinase of nearby proteins. One of the first phosphorylation events following DSB localisation is its auto-phosphorylation at Ser1981, which aids in the retention of active ATM at DSBs. ATM also phosphorylates components of the MRN complex, which is believed to both activate a number of subsequent ATM signalling cascades and act as a positive feedback loop to generate a sustained effort to repair the detected DSB (Shiloh and Ziv, 2013).

Other members of the turret structure also function in a similar manner to MRN complex components, such as mediator of DNA damage checkpoint protein 1 (MDC1) (Mochan et al., 2003). MDC1 associates with DSBs through an interaction with the well characterised marker of DNA damage, phosphorylated histone H2A.X (γH2A.X). Upon

ATM recruitment, ATM binds and phosphorylates MDC1, in another feedback loop, stabilising the protein turret and promoting a sustained effort to rectify the DSB. Moreover, ATM also phosphorylates additional H2A.X residues and interacts with a number of proteins associated with histone ubiquitylation, further amplifying the DNA damage markers associated with the DSB.

Downstream of the DSB-related protein turret assembly, ATM activation culminates in the phosphorylation of several other protein kinases, including a cofactor of the aforementioned DNA damage sensor, DNA-PK, demonstrating one of the ways in which the three major DDR pathways exhibit crosstalk (B.P.C. Chen et al., 2007). In addition, ATM phosphorylates RAC-alpha serine/threonine-protein kinase (AKT) (Xu et al., 2012), homeodomain-interacting protein kinase 2 (HIPK2) (Hofmann et al., 2013) and checkpoint kinase 2 (Chk2) (Smith et al., 2010), as well as a number of other, less well characterised protein kinases. Chk2 is particularly interesting, as this protein kinase is frequently defective in a range of cancers, and phosphorylates other well characterised and important cell stress associated proteins, such as cellular tumour antigen p53 (p53), BRCA1, transcription factor E2F-1 (E2F-1), M-phase inducer phosphatase 1 (Cdc25A) and M-phase inducer phosphatase 3 (Cdc25C) (Bartek et al., 2001). ATM phosphorylates Chk2 at T68, and this modification is detected by the FHA domain of other Chk2 molecules (Ahn et al., 2002). The two molecules then transiently form dimers, and the inactive form is autophosphorylated by the active form, culminating in the full activation of the Chk2 pool. Through its interaction with p53, Chk2 is then able to enhance DNA repair, initiate cell cycle blockade and, in extreme cases, force the cell into apoptosis (Shiloh and Ziv, 2013).

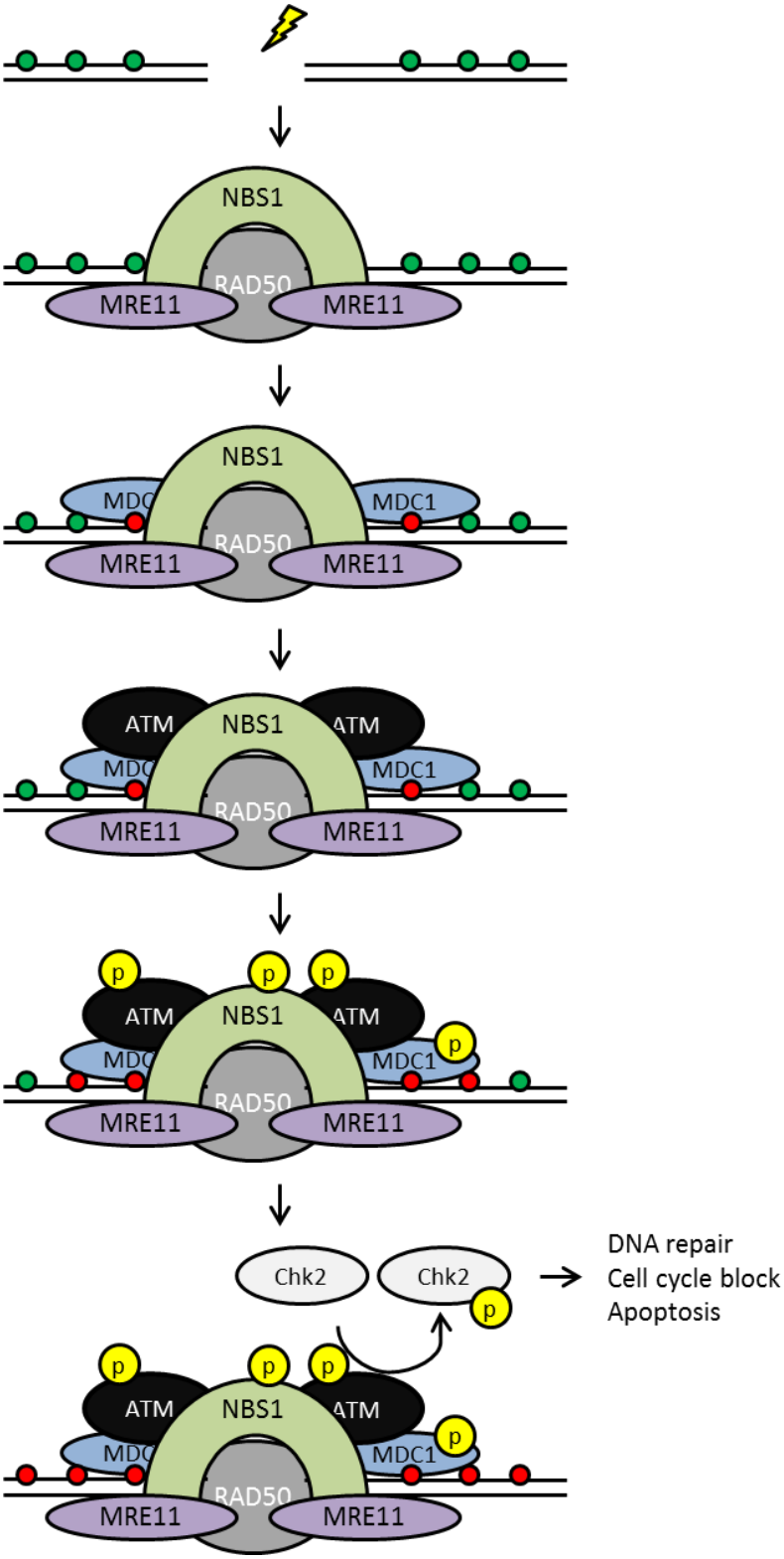

Figure 1.13: The ATM protein kinase DNA damage signalling and repair pathway.
Following the induction of a DSB, the MRN complex forms a scaffold structure holding the two broken ends in close proximity. MDC1 associates with the DSB site, binding to γH2A.X moieties. ATM is recruited to the DSB site through interactions with NBS1 and MDC1, as well as numerous other nearby proteins. ATM phosphorylates itself, as well as NBS1, MDC1 and additional H2A.X residues. Eventually ATM phosphorylates Chk2, leading to DNA repair, cell cycle block or apoptosis. Green circles - H2A.X; red circles - γH2A.X; yellow circles labelled "p" – phosphate; lightning bolt – source of DNA damage; horizontal black lines – DNA.

1.2.2.3 The ATR-Chk1 DNA damage response pathway

ATR is a protein kinase with sequence homology to members of the PIKK family, similar to ATM (Cimprich and Cortez, 2008). In contrast to ATM, ATR is typically associated with the repair of DNA single strand breaks (SSBs).

Sites of DNA SSBs generally leave a stretch of single stranded DNA, which is rapidly coated with multiple copies of replication protein A (RPA) (Zou, 2007; Smith et al., 2010). RPA subsequently becomes hyperphosphorylated and is detected by a member of the mRNA splicing machinery, known as pre-mRNA processing factor 19 (Prp19), which has only recently been demonstrated to play a role in the DNA damage response, along with a number of other mRNA splicing associated proteins (Maréchal et al., 2014). Prp19 associates with RPA at sites of SSBs, and facilitates the recruitment of ATR to these sites, through an interaction with the ATR cofactor ATR interacting protein (ATRIP). Similarly to ATM, ATR is believed to require autophosphorylation for its activation, however it also relies heavily on the actions of two other proteins; DNA topoisomerase-2 binding protein 1 (TopBP1) and Claspin (Liu et al., 2011; Smith et al., 2010). TopBP1 is recruited to sites of SSBs through an interaction with a protein "clamp" structure made up of the DNA repair protein RAD9 (RAD9), cell cycle checkpoint protein RAD1 (RAD1) and checkpoint protein HUS1 (HUS1), and is able to stimulate ATR activity through an unknown mechanism. Claspin is phosphorylated by ATR, and then subsequently acts as a scaffold, binding Chk1 and recruiting it to the SSB site in order to facilitate its phosphorylation and activation by ATR. ATR phosphorylates Chk1 at several sites including S317 and S345. Chk1 is subsequently believed to dissociate from Claspin and phosphorylates multiple targets including Cdc25A, Cdc25C, Wee1-like protein kinase (Wee1), breast cancer type 2 susceptibility protein (BRCA2) and DNA repair protein Rad51 homolog 1 (Rad51). Similarly to Chk2, activated Chk1 is able to bring about DNA repair, cell cycle arrest or apoptosis, depending on the situation, through further kinase signalling cascades. ATR is also able to phosphorylate p53 at S15 and S37 (Menon and Povirk, 2014).

1.2.2.4 The DNA-PK DNA damage response pathway

DNA-PK is a complex consisting of a catalytic subunit termed DNA-PKcs, and a targeting subunit, composed of a heterodimer of Ku70 and Ku80 (Gottlieb and Jackson, 1993). Similarly to both ATM and ATR, DNA-PKcs is a member of the PIKK family of Ser/Thr protein kinases, which acts in response to the detection of genomic instability (Durocher and Jackson, 2001). The DNA-PK associated DDR pathway typically culminates in NHEJ.

The Ku70-Ku80 heterodimer has a high affinity for DNA and forms a ring-like structure which is able to slide over the broken end of a DNA molecule containing a DSB **(Fig. 1.14)**. It binds to the DNA backbone, rather than the bases, and so binding occurs in a sequence independent manner (Rivera-Calzada et al., 2007). Once bound, the heterodimer acts as a scaffold for the recruitment of NHEJ associated proteins. The first protein to be recruited is the catalytic subunit of DNA-PK; DNA-PKcs. Binding of DNA-PKcs to the Ku70-Ku80 heterodimer drives the movement of the heterodimeric ring further along the DNA strand, and this in turn activates DNA-PKcs kinase function (Yoo, 1999). DNA-PKcs forms a scaffold structure that holds the broken ends of the DSB in close proximity, similar to the MRN complex in the ATM pathway. DNA-PKcs phosphorylates a multitude of NHEJ associated proteins, including Ku70, Ku80, DNA repair protein XRCC4 (XRCC4), DNA ligase IV and Non-homologous end-joining factor 1 (XLF) (Davis and Chen, 2013). Interestingly, however, none of these phosphorylation events are necessary for canonical NHEJ. Phosphorylation of the NHEJ protein Werner by DNA-PKcs, however, does appear to increase the efficiency of DSB repair (Kusumoto-Matsuo et al., 2014). DNA-PKcs is also able to phosphorylate p53 and H2A.X, but this is not specific to this pathway, as both phosphorylation events are also observed in the ATM-Chk2 and ATR-Chk1 pathways (Lakin and Jackson, 1999; Podhorecka et al., 2010). As such, the mechanism for DNA-PK dependent NHEJ is not fully understood, but DNA-PK binding at DSBs is able to inhibit the activities of ATM-Chk2 and ATR-Chk1 pathway proteins at these sites (Davis and Chen, 2013).

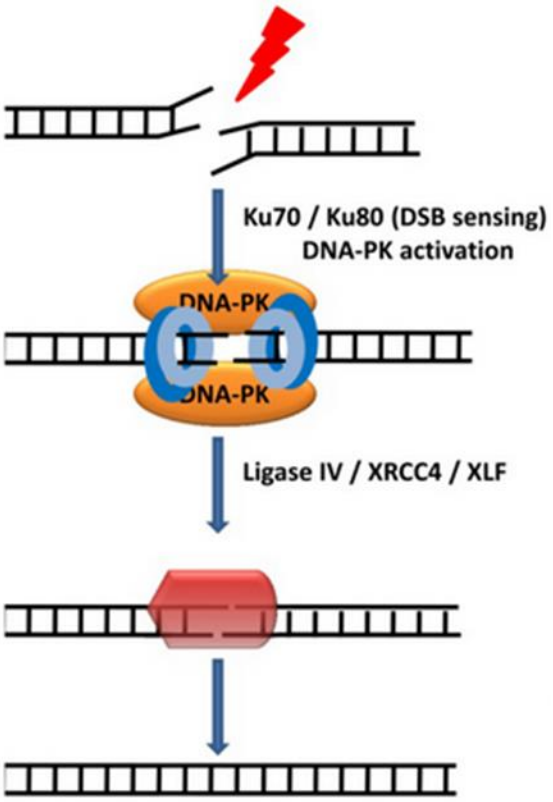

Figure 1.14: DNA-PK associated non-homologous end joining.
Following the induction of a double strand break, the Ku70-Ku80 heterodimer ring slides over the broken ends of the DNA and then bind and activate DNA-PKcs. This catalytic subunit then phosphorylates a number of non-homologous end joining associated proteins, including DNA ligase IV, XRCC4 and XLF, and the DSB is repaired by NHEJ. Taken from (Joaquin and Fernandez-Capetillo, 2012).

1.2.2.5 Viral activation of the DNA damage response

Many viruses initiate a DNA damage response during infection. Incoming or replicating viral DNA often features abnormal structures that are recognised by components of the DDR, often leading to the suppression of viral gene expression (Everett, 2006; Luftig, 2014). The phenomenon is not specific to DNA viruses, and integration of retroviral genomes can also trigger the DDR. These processes are common amongst many different classes of viruses, however, a large number of viruses also have further potential to cause a host DDR, through other common viral processes, such as cell cycle modulation or host transcriptional regulation. Activation of a host cell DDR through these means is widely regarded as being an unintentional side effect of general virus infection, which must be overcome by the virus.

Detection of foreign DNA is not the only way the DDR machinery can be activated during virus infection. During lytic replication, many DNA viruses express proteins that are able to modulate the cell cycle, as these viruses often infect dormant cells and must stimulate the generation of cellular factors that are crucial for viral replication. For example, the SV40 T-antigen, adenovirus E1A and the human papillomavirus (HPV) E7 proteins all inhibit the interaction between the cellular tumour suppressor gene Rb and the E2F transcription factor (DeCaprio et al., 1988; Ikeda and Nevins, 1993; Münger et al., 1989). Rb normally blocks the transactivation domain of E2F in order to silence E2F target genes and repress the G1/S transition (Giacinti and Giordano, 2006). By inhibiting this interaction, SV40, adenovirus and HPV force the cell into S phase, however, a side effect of this process is abnormally high E2F levels, which promote hyperproliferation, leading to an abundance of replication fork collapses and associated genome instability. The high levels of damage subsequently trigger the activation of the DDR machinery during early virus infection, as a side effect of cell cycle modulation (Luftig, 2014).

Detection of foreign DNA or abnormal structures, along with the induction of replicative stress through modulation of the cell cycle both represent ways in which a virus can trigger the DDR as a side effect of other viral replication processes. However, many viral proteins directly interact with DDR components in order to promote the viral life cycle **(Fig. 1.15)**. For example, both the HPV E7 protein and the murine gammaherpesvirus 68 (MHV-68) M2 protein are able to bind directly to ATR and force the activation of a number of ATR targets (Moody and Laimins, 2009; Liang et al., 2006). Conversely, some viruses interact with the DDR components in order to subvert the response. Human T lymphotropic virus type 1 (HTLV-1) encodes an oncoprotein called Tax, which inhibits the interaction between ATM and chromatin, allowing infected cells to progress into S phase despite potentially large amounts of DNA damage (Chandhasin et al., 2008). Furthermore, Tax forms small foci of DDR components in HTLV-1 infected cells. MDC1, BRCA1, γH2A.X, Chk2 and activated DNA-PK are all recruited to these foci, and through this mechanism it is hypothesised that Tax sequesters these proteins away from sites of viral DNA replication, allowing replication to proceed uninhibited (Belgnaoui et al., 2010).

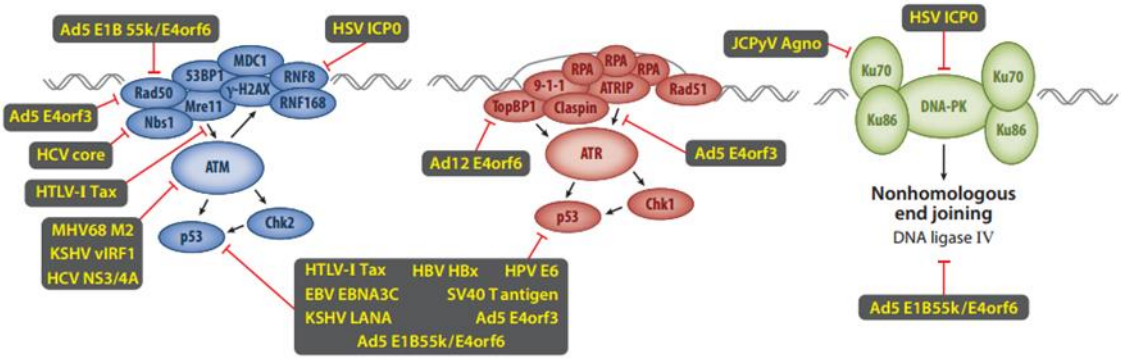

Figure 1.15: Viral protein interactions with DNA damage repair factors.
Many viral proteins interact with components of the ATR, ATM and DNA-PK DDR pathways. Ad5 – adenovirus 5; Ad12 – adenovirus 12; HCV – hepatitis C virus; HBV – hepatitis B virus; JCPyV – JC polyomavirus. Taken from (Luftig, 2014).

Herpesviruses, in particular, interact with components of the DDR in multiple ways. Firstly, herpesvirus infections are associated with an activation of the DDR, at least in part due to the detection of incoming viral DNA, leading to the repression of the viral genomes at nuclear domain 10 (ND10) bodies (Everett et al., 2006; Glass and Everett, 2013). HSV-1 overcomes this host cell response via expression of the viral protein ICP0, which is able to mediate the degradation of the core ND10 protein, PML, thereby dispersing any ND10 bodies associated with the viral genome (Everett et al., 2006). Despite this, herpesviruses also hijack the DDR machinery to promote lytic replication. Indeed, a well conserved family of proteins exist in all of the *Herpesviridae*, known as conserved herpesviral protein kinases (CHPKs) that are vital for viral replication and spread (Gershburg and Pagano, 2008). The BGLF4 kinase encoded by EBV promotes the switch between the latent and lytic phases via the activation of the histone acetyltransferase, TIP60 (Li et al., 2011). The histone acetyltransferase function of TIP60 has also been implicated in events during the ATM and DNA-PK DDR signalling pathways, as well as transcriptional activation of p53 (Squatrito et al., 2006). Unsurprisingly, activation of TIP60 by BGLF4 coincides with a DDR in EBV infected cells (Li et al., 2011). Although the full mechanisms are not understood, it appears that an activated DNA damage response is necessary for the replication of many herpesviruses (Xie and Scully, 2007; E et al., 2011; Hollingworth et al., 2015).

1.2.3 Viral and cellular microRNAs

Regulation of gene expression represents a fundamental area of biological studies. There are many dynamics in the expression of a gene, working on multiple levels. For instance, at the DNA level there are factors such as promoter and enhancer sequences. At the mRNA level, turnover rates of transcripts, mRNA processing and nonsense mediated decay can affect the expression of a gene. Considering proteins, transcription factor availability and binding, protein turnover rate, and even factors such as protein-protein interactions can affect the expression of whole subsets of genes. The discovery of miRNAs in 1993 revealed another player in the gene expression and regulation field. Since then, thousands of miRNAs have been identified and characterised, and the vast majority are able to regulate multiple genes at the mRNA stage.

1.2.3.1 miRNA biogenesis and function

The biogenesis of a miRNA begins with the transcription of a long primary transcript known as a pri-miRNA (Lee et al., 2002). Pri-miRNAs exist in a number of genomic contexts, most commonly being located in intronic sequences of other, longer transcripts, however they can also be found in exons. The pri-miRNA is released from the longer transcripts by the ribonuclease Drosha and its cofactor DGCR8, which form a complex known as Microprocessor (Denli et al., 2004). Upon complex formation, Drosha cleaves a 60-110 nucleotide region out of the pri-miRNA ~11 bp away from the basal junction, where the ssRNA becomes dsRNA, which is ~22 bp away from the apical junction at the terminal loop **(Fig. 1.16)** (Zeng et al., 2005**;** Han, 2004). This cleaved product is known as a pre-miRNA, and forms a tertiary structure generally consisting of a stem loop with a number of other loops residing down the length of the stem at the sites of non-complementary bases (Ha and Kim, 2014). The pre-miRNA is subsequently exported into the cytoplasm via the nuclear pore by a protein complex consisting of Exportin-5 and Ran-GTP (Bohnsack et al., 2004; Yi et al., 2003). Once in the cytoplasm, the complex dissociates following GTP hydrolysis, releasing the pre-miRNA, which is

subsequently cleaved in the cytoplasm, just after the terminal loop, by the endonuclease Dicer **(Fig. 1.16)** (Bohnsack et al., 2004**;** Yang and Lai, 2011). Dicer binds at a 2 nucleotide 3' overhang, previously generated during Drosha cleavage of the pri-miRNA, and cleaves the pre-miRNA 22 nucleotides away from the 5' end of the molecule (Park et al., 2011). This produces a ~22 nucleotide double stranded RNA, known as a miRNA:miRNA* duplex. One of these strands is typically more prevalent or biologically active than the other, and is distinguished as the miRNA, whilst the less active strand is referred to as miRNA* (Chiang et al., 2010; Ha and Kim, 2014).

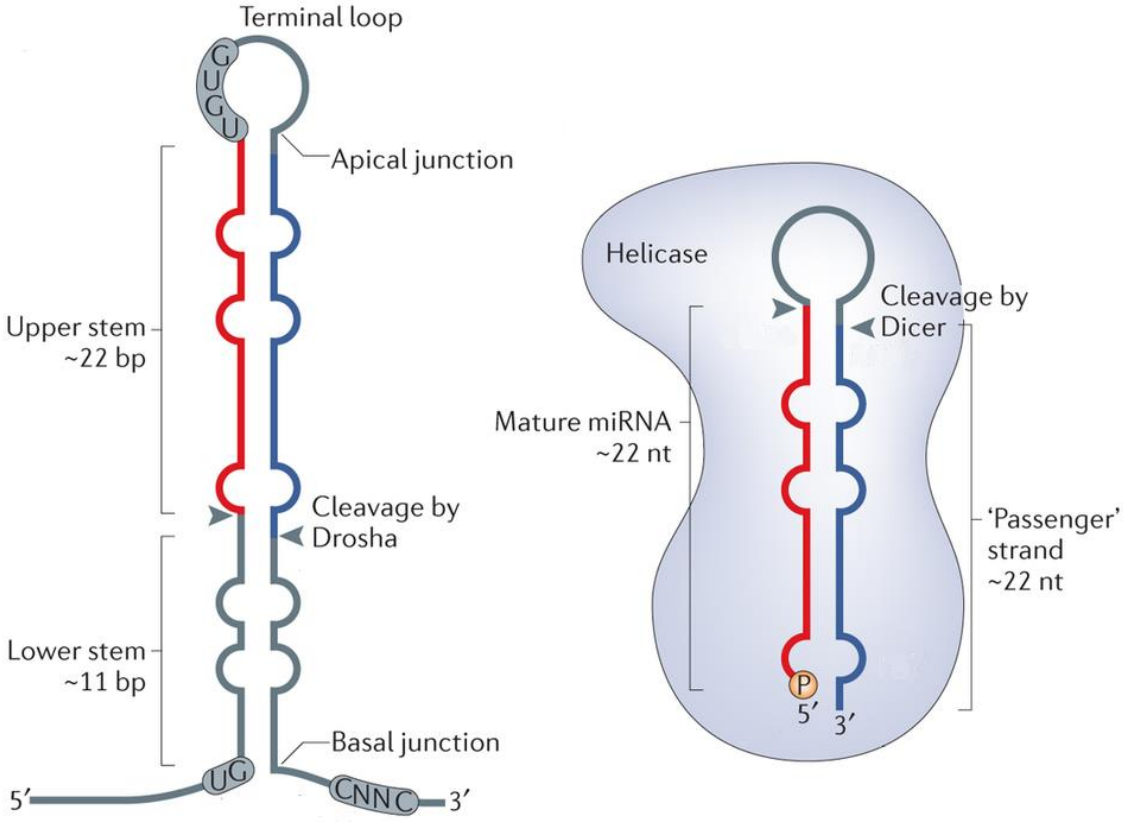

Figure 1.16: Sites of pri-miRNA and pre-miRNA cleavage.
Pri-miRNAs are cleaved ~11bp from the basal junction and ~22nt from the apical junction by the ribonuclease Drosha, generating a pre-miRNA. Pre-miRNAs are subsequently cleaved near the terminal loop by Dicer, generating a miRNA:miRNA* duplex. Adapted from (Ha and Kim, 2014).

The Dicer-generated miRNA:miRNA* duplex is bound by an Argonaute (AGO) protein, forming the RNA-induced silencing complex (RISC). RISC activation is thought to be completed via the dissociation of the duplex, either by passenger strand cleavage or through a more complex process guided by mismatches in the dsRNA (Kawamata and Tomari, 2010). Often, both strands of the duplex can be recruited to functional RISC

complexes, and strand selection involves sensing of RNA stability, with more unstable 5' ends generally indicating the guide strand, or miRNA (Khvorova et al., 2003). The active RISC then acts to degrade or repress transcription of a subset of mRNAs containing complementary sequences to the miRNA, usually found within the 3' UTR of target mRNAs **(Fig. 1.17)** (Lewis et al., 2005). There is also evidence of miRNA binding at the 5' UTR or coding regions of mRNAs, which again leads to inhibitory effects on gene expression, ultimately reducing protein synthesis (Tay et al., 2008; Lytle et al., 2007). One important factor guiding miRNA activity is the complementarity between the mRNA target region and the miRNA "seed" sequence, located between positions 2 and 8 (Lewis et al., 2003; Brennecke et al., 2005). However, recent evidence suggests this may be an oversimplified model, as nucleotide alterations at various positions of the seed region of miHDS1 have been demonstrated to produce similar mRNA silencing as the unmodified miRNA (Monteys et al., 2014). Therefore, more recent models suggest that ~60% of the gene regulation controlled by a given miRNA is due to perfect seed sequence binding (Zisoulis et al., 2010).

Interestingly, the view that miRNAs generally inhibit protein synthesis of target genes has recently been challenged with the discovery that some miRNAs are able to increase protein output. This has been demonstrated to occur through a number of mechanisms, including de-repression of mRNAs by interfering with repressor protein-target mRNA binding, or through the recruitment of protein complexes to AU rich regions (Vasudevan et al., 2007; Eiring et al., 2010). Clearly, despite large amounts of work into their function, there are still many dynamics in the regulation of miRNA gene silencing that are not fully understood.

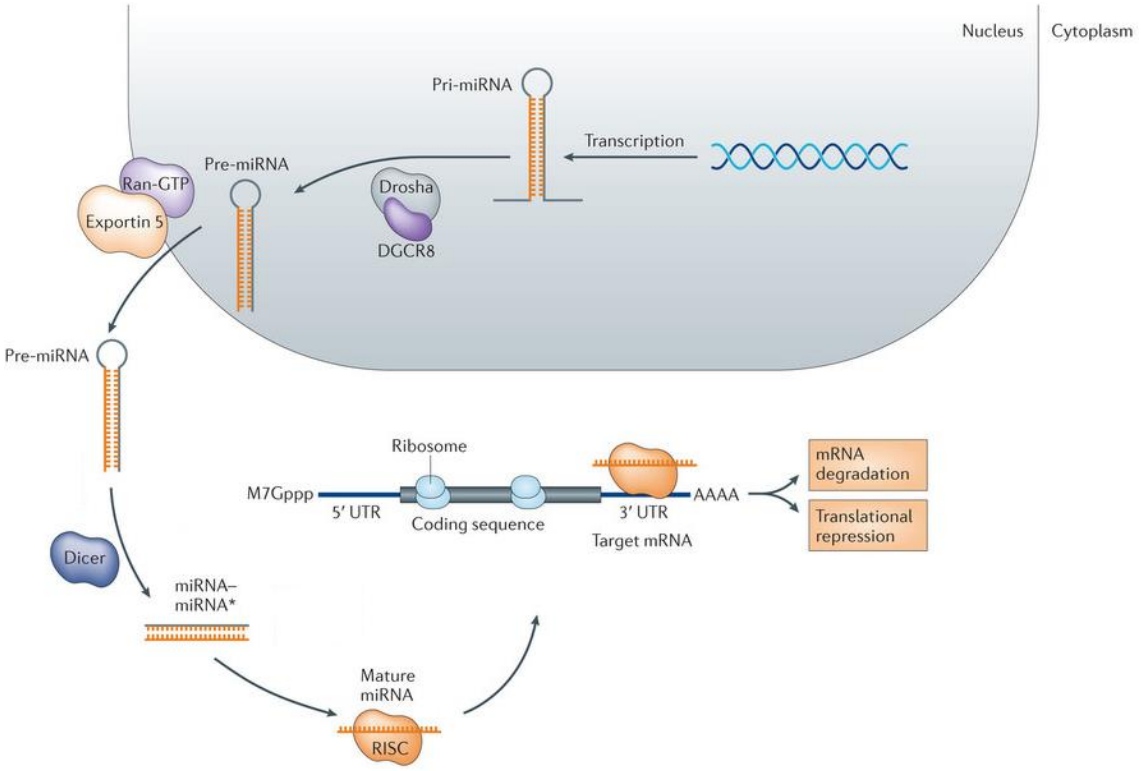

Figure 1.17: miRNA biogenesis, RISC complex formation and RISC-mediated degradation or repression of target mRNAs.
Pri-miRNAs are transcribed by RNA polymerase II and cleaved into pre-miRNAs by Drosha and DGCR8 in the nucleus. Pre-miRNAs are then exported into the cytoplasm by Exportin-5 and Ran-GTP, where they are cleaved into miRNA:miRNA* duplexes by Dicer. A guide strand is then selected by Argonaute, forming a functional RISC complex, which binds target mRNAs at complementary sites in the 3' UTR, mediating degradation or translational repression of the target mRNA. Adapted from (Ling et al., 2013).

1.2.3.2 Viral miRNAs

It is generally believed that RNAi evolved as a defense mechanism against harmful genetic species, such as viruses. However, if this model is correct, viruses have been able to subvert this defense, and have hijacked miRNAs for their own purposes. miRNAs represent important tools for viruses, as they can modulate host cell function whilst being less detectable than foreign proteins by the host immune system. Over the last decade, more than 500 viral miRNAs have been discovered (miRbase.org; July 2015) and, interestingly, nearly half of these miRNAs are encoded by members of the *Herpesvirales* **(Fig. 1.18)**. Epstein-Barr virus was the first human virus demonstrated to encode miRNAs, 5 of which were initially identified in the BHRF1 and BART genomic regions (Pfeffer et al., 2004). An additional 39 EBV miRNAs have subsequently been

identified, and show varying levels of expression in different EBV infected cell lines and latency profiles (Pratt et al., 2009). These miRNAs have been demonstrated to regulate numerous viral and cellular mRNAs, and modulate the host cell immune response and apoptosis pathways in order to maximise viral replication (Barth et al., 2011). For example, miR-BART5 targets the host cell Bcl-2-binding component 3 (BBC3) mRNA, whilst other BART miRNAs target the pro-apoptotic Bim transcript (Choy et al., 2008; Marquitz et al., 2011). Indeed, it appears that most characterised viral miRNAs play roles in the persistence of the virus within the host cell, regulating host or viral genes and limiting the effectiveness of the host immune response, in order to expand the longevity of infected cells. This, therefore, explains the high numbers of viral miRNAs found within herpesviruses, all of which exhibit a latent phase and persistence in the infected host.

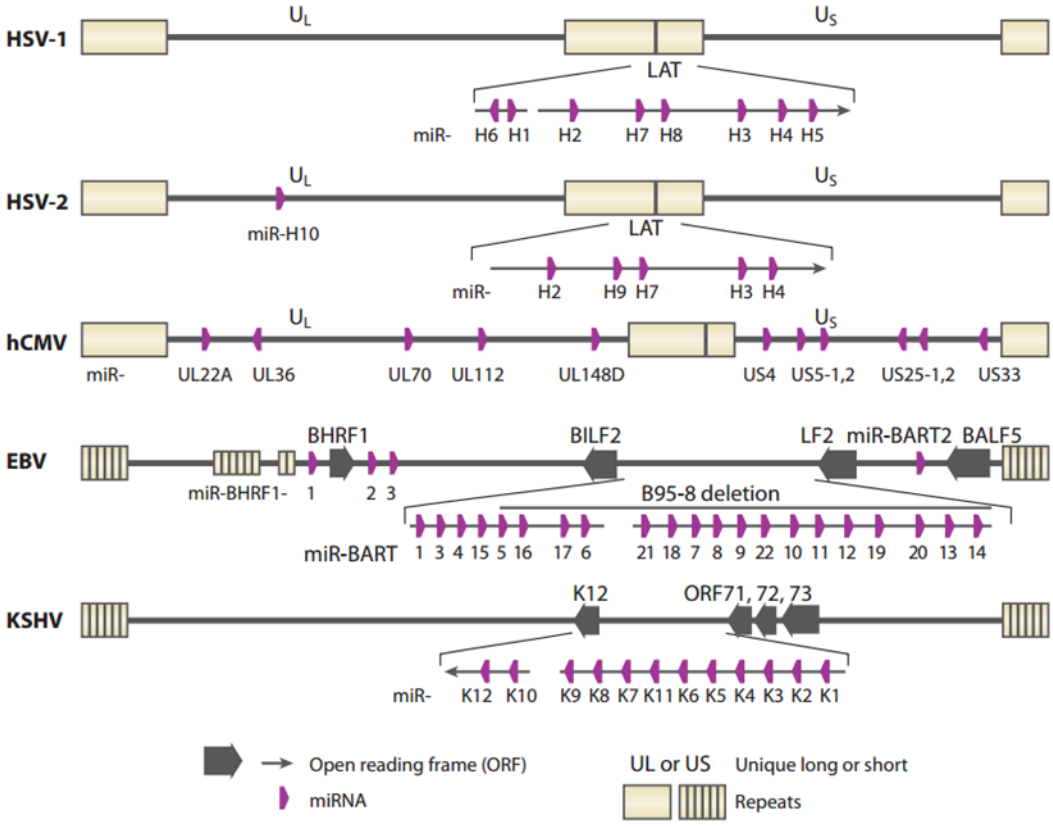

Figure 1.18: Herpesvirus-encoded pre-miRNAs and their positions within the viral genomes.
Schematic showing the position of pre-miRNAs within the genomes of the *Herpesviridae*. Pre-miRNAs may produce more than one mature miRNA. Taken from (Skalsky and Cullen, 2010).

KSHV encodes at least 18 mature viral miRNAs, all of which are expressed during latency and encoded within the latency-associated region (KLAR) of the genome (Qin

et al., 2012). Of these, KSHV encodes at least two miRNA orthologs of a cellular miRNAs, miR-K12-11 and miR-K10a, analogs of miR-155 and miR-142-3p respectively, and has retained both the complete seed sequences as well as many of the mRNA targets are thought to be cellular transcripts (Gottwein et al., 2007; Gottwein et al., 2011). Overexpression of miR-155, as with many cellular miRNAs, has been implicated in cancer formation, affecting a number of processes including haematopoiesis and tumorigenesis (Faraoni et al., 2009). The KSHV ortholog has been demonstrated to affect these processes in similar ways, highlighting one of the ways latently infected cells contribute to KSHV associated pathogenesis (Gottwein et al., 2007; Ganem, 2010; Qin et al., 2012). KSHV also encodes a number of miRNAs which do not appear to have cellular counterparts, and therefore may target non-cellular genes. For example, both miR-K12-9-5p and miR-K12-7-5p inhibit reactivation of the lytic cycle by repressing expression of the viral RTA transcript (Bellare and Ganem, 2009; Lin et al., 2011). Other KSHV miRNAs target distinct subsets of cellular genes, also showing limited relation to host miRNAs, such as miR-K12-1-5p, which represses the IκBα transcript, repressing activation of the NFκB pathway, which also drives lytic reactivation (Lei, Bai, et al., 2010).

1.2.3.3 Viral dysregulation of cellular miRNAs

In addition to encoding their own miRNAs, many viruses are also able to alter the expression or function of host miRNAs for pro-viral processes. Often, these interactions occur during viral latency to evade the host immune response, similarly to a number of previously described examples of viral encoded miRNAs. For example, during latency III, the EBV latent membrane protein 1 (LMP1) stimulates upregulation of both miR-146a and miR-29b during B cell infection (Cameron et al., 2008; Anastasiadou et al., 2010). miR-146a subsequently targets at least two members of the toll-like receptor (TLR) signalling pathway, TNF receptor-associated factor 6 (TRAF6) and interleukin-1 receptor-associated kinase 1 (IRAK1), limiting the host innate immune response (Cameron et al., 2008; Xiao and Rajewsky, 2009). Meanwhile, miR-

29b targets T-cell leukaemia gene 1 (TCL1) to modulate cell survival and proliferation (Anastasiadou et al., 2010).

Interestingly, a number of RNA viruses have also evolved mechanisms of promoting viral replication by utilising host miRNAs. The RNA genomes of enteroviruses lack a cap structure and therefore depend on internal ribosome entry sites for their translation (Thompson and Sarnow, 2003). During enterovirus infection, miR-141 expression is strongly upregulated, as this miRNA targets the eukaryotic translation initiation factor 4E (eIF4E), a protein which promotes the translation of capped RNAs. This limits the cells ability to translate its own mRNAs, ultimately contributing to a host shutoff response and allowing the enterovirus genome to be replicated much more efficiently (Ho et al., 2011). Hepatitis C virus also utilises host miRNAs for processes associated with the viral RNA genome. HCV infects hepatocytes which express the liver specific miR-122, and HCV is able to interact with miR-122 in a number of unique ways. It was first discovered that miR-122 acts as a shield for the viral genome, binding to the 5' UTR and protecting it from the actions of exonuclease enzymes, such as Xrn1 (Jopling et al., 2005; Y. Li et al., 2013). It was subsequently demonstrated that through this mechanism, HCV also acts as a miRNA sponge to de-repress a number of miR-122 target mRNAs **(Fig. 1.19)** (Luna et al., 2015). The effects of the dysregulation of miR-122 target genes has not been further examined, however, it is believed that miR-122 acts as a tumour suppressor, necessary for long term liver homeostasis. By interrupting this function, it is likely that HCV promotes its own replication while also increasing its oncogenic potential.

KSHV has also been shown to dysregulate the expression of host miRNAs, causing increased oncogenic potential. Expression of the miR-221-222 cluster is downregulated by LANA and Kaposin B during KSHV latent infection, while miR-31 levels are increased by K15 via its SH2-binding motif (Wu et al., 2011; Tsai et al., 2009). Downregulation of miR-221 and miR-222 is predicted to cause an increase in their target mRNAs, namely protein-C ETS-1 and -2 (ETS1/ETS2), both enhancers of endothelial cell migration. Downregulation of the known miR-31 target, Protocadherin Fat 4 (FAT4), also contributes to this phenotype, and it is believed that this process enhances the oncogenic potential of KSHV by spreading malignant KS progenitor cells. Furthermore,

the KSHV-encoded viral FLICE inhibitory protein (vFLIP) interacts with NFκB, and this interaction promotes the upregulation of miR-146a, which, in turn, targets mRNAs encoding the C-X-C chemokine receptor type 4 (CXCR4) (Punj et al., 2010). The associated downregulation of CXCR4 is associated with release of KSHV infected endothelial progenitor cells into the circulation, which is also believed to increase the potential for KS development and spread.

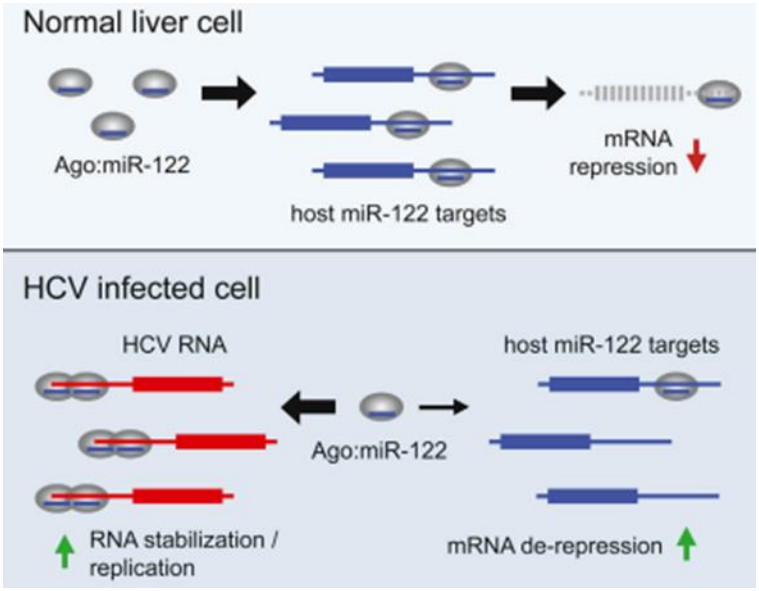

Figure 1.19: Recruitment of miR-122 to HCV genomes causes de-repression of miR-122 targets. Schematic showing the functions of miR-122 in normal vs HCV infected hepatocytes. In uninfected hepatocytes, miR-122 binds to target mRNAs, causing mRNA repression. In HCV infected cells, miR-122 is recruited to the 5' UTR of the HCV RNA genome, and is therefore sequestered away from cellular target mRNAs, causing their de-repression. Taken from (Luna et al., 2015).

1.3 Omics approaches

Over decades of studies into biology at a molecular level, countless interactions between different biological materials have been described, and chief amongst these materials are those that, together, form the central dogma of molecular biology; DNA, RNA and protein. Despite the extraordinary amount of work undertaken during this time, it appears there are still millions of undiscovered and uncharacterised interactions occurring in each and every cell. However, with the invention of new scientific technologies comes the promise of greater and greater understanding, and nowhere is this more apparent than in the recent developments in "omic" approaches. Genome sequencing represents the most widely cited aspect of these developments, and has reduced the average time required to sequence a sample to just a few hours (Greninger et al., 2015). Compare this to the effort undertaken by Ray Wu to produce the first published sequence data in 1972 using a location-specific primer extension technique and it becomes apparent that the power of modern sequencers cannot be overstated (Wu, 1972). Furthermore, the cost of sequencing continues to decrease, to the point where now laboratories all over the world routinely sequence samples. Similarly, advances in high throughput, high resolution proteomics and transcriptomics have greatly aided investigative potential, and their power continues to increase with novel experimental designs, even without the invention of new hardware. Indeed, the large datasets produced by these technologies are now frequently published and shared in online databases, allowing large scale biological association studies to be undertaken without access to a laboratory, just a computer and a hypothesis.

1.3.1 Proteomics

Early attempts to analyse the cellular proteome began in 1970, with the advent of polyacrylamide gel electrophoresis (PAGE) (Laemmli, 1970). This technique is still commonly used in laboratories around the world for the separation of proteins as an important part of the Western blotting protocol. PAGE has numerous limitations, however, and it is often difficult to detect individual proteins in a complex mixture, requiring successful antibody binding which can prove problematic. Despite a number

of improvements to the initial PAGE technique in both detection limits and sample separation, its power is still limited, mainly due to the complexity of the samples being analysed (O'Farrell, 1975)(Klose and Kobalz, 1995; Görg et al., 2004; Patton, 2002). Fortunately, subsequent developments in proteomics now allow protein samples to be further characterised by mass spectrometry (MS).

Mass spectrometry can be used to identify and quantify the protein composition of protein samples of differing complexities, however samples can be separated using PAGE or liquid chromatography (LC) in order to reduce highly complex mixtures into more manageable samples for better detection rates and subsequent analysis (Owen et al., 2014). Other methods may also be used to reduce sample complexity, such as subcellular fractionation. Despite this, MS-based proteomics will generally only achieve coverage of ~10% of the proteome, while quantifying even less (Michalski et al., 2011). Although this still represents an important step forward in the power of proteomics, improving this coverage rate remains an important technical challenge. Following any separation protocol, proteins are digested into peptides, typically using trypsin, before being separated further by LC. Either electrospray ionization (ESI) or matrix-assisted laser desorption/ionization (MALDI) is then used to charge the peptides, before they are analysed by tandem MS/MS. In the first round of MS, known as MS1, the mass to charge ratio (m/z) of the ionized peptides in the sample are measured, generating a precursor ion spectrum. Individual peptide populations are subsequently taken forward for collision induced dissociation (CID), prior to the second round of MS, MS2, which again measures the m/z generates a final CID spectrum via detection of the peptide fragments produced **(Fig. 1.20)**. These spectra are then compared to theoretical databases in order to assign protein identification to the samples, and their peak intensities are used to quantify these proteins (Washburn et al., 2001; Yates et al., 1995). This technique is usually applied to multiple samples simultaneously to compare protein composition across multiple conditions. Samples can be differentiated using a number of peptide tagging protocols, such as stable isotope labelling with amino acids in cell culture (SILAC) or with the addition of pre-made isotopic tags, such as tandem mass tags (TMT), isobaric tags for relative and absolute quantification (iTRAQ) or isotope-coded affinity tags (ICAT)(Ong et al., 2002; Wiese et

al., 2007; Shiio and Aebersold, 2006; Gygi et al., 1999). Alternatively, label free approaches have also been recently developed in order to overcome some limitations of the tagging procedures (Griffin et al., 2010; Wong and Cagney, 2010).

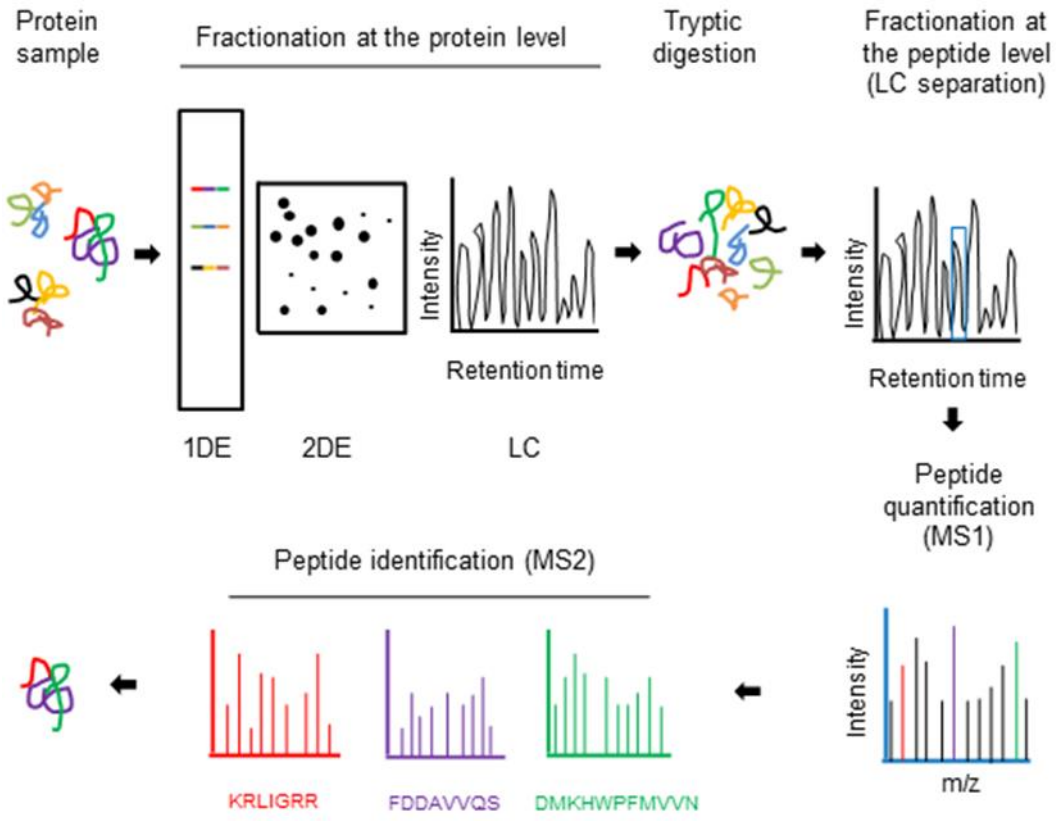

Figure 1.20: Separation of protein samples by PAGE/LC and identification and quantification by MS/MS.
Complex protein samples are separated by 1D or 2D PAGE or LC. Separated samples are then digested into peptides and subjected to LC coupled to ESI. Ionized peptides are then subjected to MS1, generating a precursor ion spectrum that is used for peptide quantification. Peptides are then identified using CID and a second round of MS. The CID spectrum generated by this procedure is compared to a theoretical database in order to assign a protein identity to the analysed peptides. Adapted from (Owen et al., 2014).

1.3.1.1 SILAC

SILAC makes use of the different stable (non-radioactive) isotopes of carbon (C^{12} and C^{13}) and nitrogen (N^{14} and N^{15}) to create amino acids of different masses (Ong et al., 2002). By growing cells in the presence of differentially weighted amino acids, these residues are incorporated into all proteins synthesised by that cell. This normally requires several days of growth due to differential protein turnover rates, and 6 to 8

cell doublings are usually recommended when analysing cell culture systems by SILAC, normally generating over 90% isotopic incorporation. Interestingly, SILAC has also been demonstrated to be effective when using simple organisms such as *D. melanogaster* or *C. elegans*, and this technique has even been applied to mice using diets containing specific labelled amino acids (Krijgsveld et al., 2003; Krüger et al., 2008). Most commonly arginine and lysine are labelled, as these residues are cleaved at the C-terminus by trypsin, which is typically used to generate peptide fragments from the proteins for analysis (Ong and Mann, 2007). This means that all peptides generated will contain one labelled amino acid, excluding the C terminal peptide, allowing maximum sample differentiation. Following labelling, cells/organisms are subjected to the treatment being investigated, for example, virus infection, and protein samples are harvested. Samples are then normalised and mixed at equal ratios before being subjected to LC-MS/MS. As the amino acids incorporated into the different samples have different masses, they are easily detected and differentiated during analysis by MS.

SILAC has a number of advantages over other MS-based proteomics techniques, as samples are mixed into one pooled sample which is then processed at once, reducing errors arising from differential handling of samples. In addition, as tagging occurs during protein synthesis, the vast majority of proteins in the final sample are labelled, reducing biases that may be introduced during tagging reactions using pre-made tags. However, SILAC can only be used to analyse live material, due to the requirement for incorporation of isotopically labelled amino acids into the proteins at the point of synthesis. Furthermore, certain cell lines may not be compatible with SILAC, due to cell sensitivity to changes in medium composition.

1.3.1.2 TMT/iTRAQ/ICAT

Isotopic tags have been used in MS-based quantitative proteomics since 1999, with the advent of ICAT (Gygi et al., 1999). Tags are created with variable masses, but otherwise identical physical properties, and make use of the ability to covalently link additional

material to one end of a peptide sequence. TMT, iTRAQ and ICAT tags differ in their composition, but work in the same manner.

ICAT tags comprise a biotin molecule for streptavidin-mediated peptide purification, a linker group containing different stable isotopes for differential masses between tags, and a reactive iodoacetyl group which can be covalently linked to free thiols on cysteine residues. This introduces a heavy bias for peptides containing cysteine residues, however, a variation on the ICAT method has been developed in order to overcome this limitation, in which isotopic tags are bound to free amino groups of any amino acid, therefore improving coverage (Schmidt et al., 2005).

TMT and iTRAQ tags differ from ICAT tags in that they are all of the same mass (Thompson et al., 2003; Ross et al., 2004). This is achieved through the use of variable mass reporter groups, containing different isotopes, at one end of the tag, with variable mass carbonyl balance groups in the middle of the tag to normalise the weight. A reactive group makes up the rest of the tag. An advantage of using these tags over ICAT tags is that the identical masses allow the proteins to behave in exactly the same way during separation by LC and the first round of MS. Differential quantification of peptides between samples is achieved during MS2, when the tags are cleaved from the peptide during CID, generating different peaks on the CID spectrum relative to the amounts present in each sample. TMT and iTRAQ allow the simultaneous analysis of up to 8 different protein samples, a significant increase over other methods.

MS-based proteomics using isotopic tags carries the advantage that any sample containing protein can be used, as the tags are added following protein synthesis.

1.3.1.3 Label free proteomics

Due to various issues with labelling of protein samples prior to analysis by MS, two label free proteomics techniques have recently been developed. The first of these approaches makes use of spectral counting, based on the principle that more

concentrated peptides will take longer to elute into the ionisation chamber following LC, and therefore more fragment-ion spectra will be acquired from highly concentrated peptides than less concentrated peptides (Liu et al., 2004; Ryu et al., 2008). This technique has been modified in recent years to include analysis of peptide count and physical properties, protein length and fragment-ion intensity, in an attempt to reduce sample to sample variation that was previously associated with the technique (Griffin et al., 2010). This technique is controversial, however, as it relies on simple counting of the acquired spectra rather than any tangible physical measurements.

The second approach is less controversial, and utilises the measurement of chromatographic peak areas of peptide precursor ions, as each peptide of a particular m/z ratio generates a mono-isotopic mass peak in the acquired spectra. The retention time of this mass peak has been demonstrated to directly correlate with peptide abundance in a linear fashion over a wide range, allowing protein abundances to be directly calculated from this measurement (Bondarenko et al., 2002; Chelius and Bondarenko, 2002). Label free proteomics are associated with greater proteome coverage, however there are also issues associated with the quantification accuracy and reproducibility using these methods (Megger et al., 2013).

1.3.2 Transcriptomics

The first attempt to profile a mammalian transcriptome was undertaken in 1991 by a large group at the NIH, led by Craig Venter. Using cDNA clones to generate expressed sequence tags (ESTs), this group was able to sequence 609 different genes, 337 of which were newly identified (Adams et al., 1991). However, the success of this technique was relatively short lived due to the announcement of microarray technology in subsequent years (Schena et al., 1995). Using picomoles of complementary probes spotted on a small chip, it was possible to quantify the expression of thousands of genes or other expressed sequences simultaneously and with minimal effort. Microarrays represented a leap forward in the power of transcriptomics, and were widely used for the following decade, prior to the

development of next generation sequencing platforms that are more commonly used today. Modern sequencing technologies again make use of ESTs, and eliminate the false positive signals that were associated with microarrays due to non-specific binding, whilst also not requiring prior knowledge of the sequences to be examined, allowing the identification of novel sequence expression. Furthermore, next generation sequencing introduces less bias for specific sequences, and allows the processing of large numbers of samples simultaneously by tagging different samples with a unique sequence code.

1.3.2.1 mRNA sequencing

The most commonly investigated transcripts are mRNAs, due to their central role in gene expression and regulation. The first investigation into mRNA expression using next generation sequencing was published in 2006, making use of Roche 454 sequencing technology (Bainbridge et al., 2006). This approach utilised the sequencing-by-synthesis principle of the previously developed Sanger sequencing, where nucleotide incorporation could be detected due to the release of pyrophosphate. This pyrophosphate is first converted into ATP by ATP sulfurylase, and then used as a substrate for a chemiluminescent enzyme such as luciferase, which emits a detectable light signal. Single cDNA fragments were bound to beads, which were then individually settled into wells on a slide where a DNA synthesis reaction could begin using these fragments as a template. By sequentially flowing pools of individual bases over these samples, the incorporation of specific bases could be recorded for large numbers of different sequences simultaneously. This approach demonstrated the potential of next generation sequencing technologies, however it was limited in its power and struggled to compete with microarrays.

Short read technology was first described in three separate studies published in 2008, using approaches developed by Solexa (Mortazavi et al., 2008; Sultan et al., 2008; Wilhelm et al., 2008). Different adaptor sequences are added to both ends of cDNA fragments, and one end of the molecule is stuck to a flow cell at a random position, while the other uses a complementary sequence, also positioned at various locations

on the flow cell, as a primer for the sequencing reaction. These adaptor sequences also contain unique sequence codes to allow multiple samples to be sequenced on the same flow cell while still allowing differentiation during the analysis stage. During the sequencing-by-synthesis reaction, clusters are generated from a single cDNA at any position on the flow cell, ultimately generating ~1 million copies **(Fig. 1.21)**. This method also makes use of light emission following nucleotide incorporation, however nucleotides do not need to be applied sequentially, as each contains a fluorescent label specific to that base. The newly incorporated nucleotide contains a 3'-OH chemical blocking element, that prevents further synthesis, meaning that each nucleotide incorporation is a single event. After each incorporation, this block is removed by chemical treatment, allowing the next incorporation to take place. This process repeats for a user-defined period, usually between 25 and 35 times. Poor quality sequences are removed and sequenced fragments can then be analysed.

Solexa/Illumina sequencing allows much higher throughput than 454 sequencing as, all four bases are incorporated on different fragments during one flow cycle, and the fragments sequenced are much shorter. Short read sequencing has also been demonstrated to give much better coverage than 454 sequencing (Li et al., 2014 p. 454). There are now multiple competitors to the Solexa/Illumina platform, achieving short read sequencing through modified mechanisms and each providing different advantages. In addition, 454 sequencing is still useful in certain experimental contexts, for instance, short read sequencing may fail to differentiate between different closely related species or strains of microorganism due to perfect homology over short stretches of the genomes (Luo et al., 2012).

Next generation sequencing of mRNA is now widely used in various scientific studies. Interestingly, however, it has been revealed that mRNA abundance does not always directly correlate with expression at the protein level, and so analyses of gene expression should be carefully considered and validated in a wet laboratory setting (Evans et al., 2012). Nevertheless, combining mRNA sequencing with other high throughput omics technologies can produce interesting results and begin to answer questions that no individual approach can achieve. For instance proteomics informed by transcriptomics allows novel protein discovery using reference transcriptomes. This

is particularly useful when attempting to characterise genes of poorly annotated genomes or of multiple species simultaneously (Evans et al., 2012). Transcriptomics has also been used in combination with both metabolomics and lipidomics to characterise metabolites and gene expression influencing lipogenesis (Batushansky et al., 2014; Caesar et al., 2010).

1.3.2.2 Small RNA sequencing

In recent years, transcriptomics has become increasingly useful in the investigation of small, noncoding RNAs, such as miRNAs, PIWI interacting RNAs (piRNAs) and small nucleolar RNAs (snoRNAs), as modified library preparation protocols have been developed to allow the specific sequencing of small RNAs. Small RNA sequencing was first described in two studies published in 2006, using pyrosequencing technology (Rajagopalan et al., 2006; Ruby et al., 2006). In the first of these investigations, 340,114 unique small RNA sequences were found in *Arabidopsis thaliana*, most of which had high similarity to siRNA sequences found in other organisms, as indicated by their presence in intergenic regions and their ~22 nt length (Rajagopalan et al., 2006). In addition, 38 confirmed novel *A. thaliana* miRNAs were discovered, with many more candidate miRNAs also observed. In the second study, a set of novel nematode specific small RNAs known as 21U-RNAs were discovered in *Caenorhabditis elegans*, as well as 18 novel miRNAs and numerous uncharacterised siRNAs (Ruby et al., 2006). More recently, the development of short read sequencing platforms with higher throughput has aided the discovery of ever increasing numbers of small RNAs and small RNA classifications. It is important to note, however, that small RNA sequencing is unable to provide absolute expression data, and this is believed to be due to biases during sample preparation or during the sequencing reaction (Kawaji and Hayashizaki, 2008; Linsen et al., 2009).

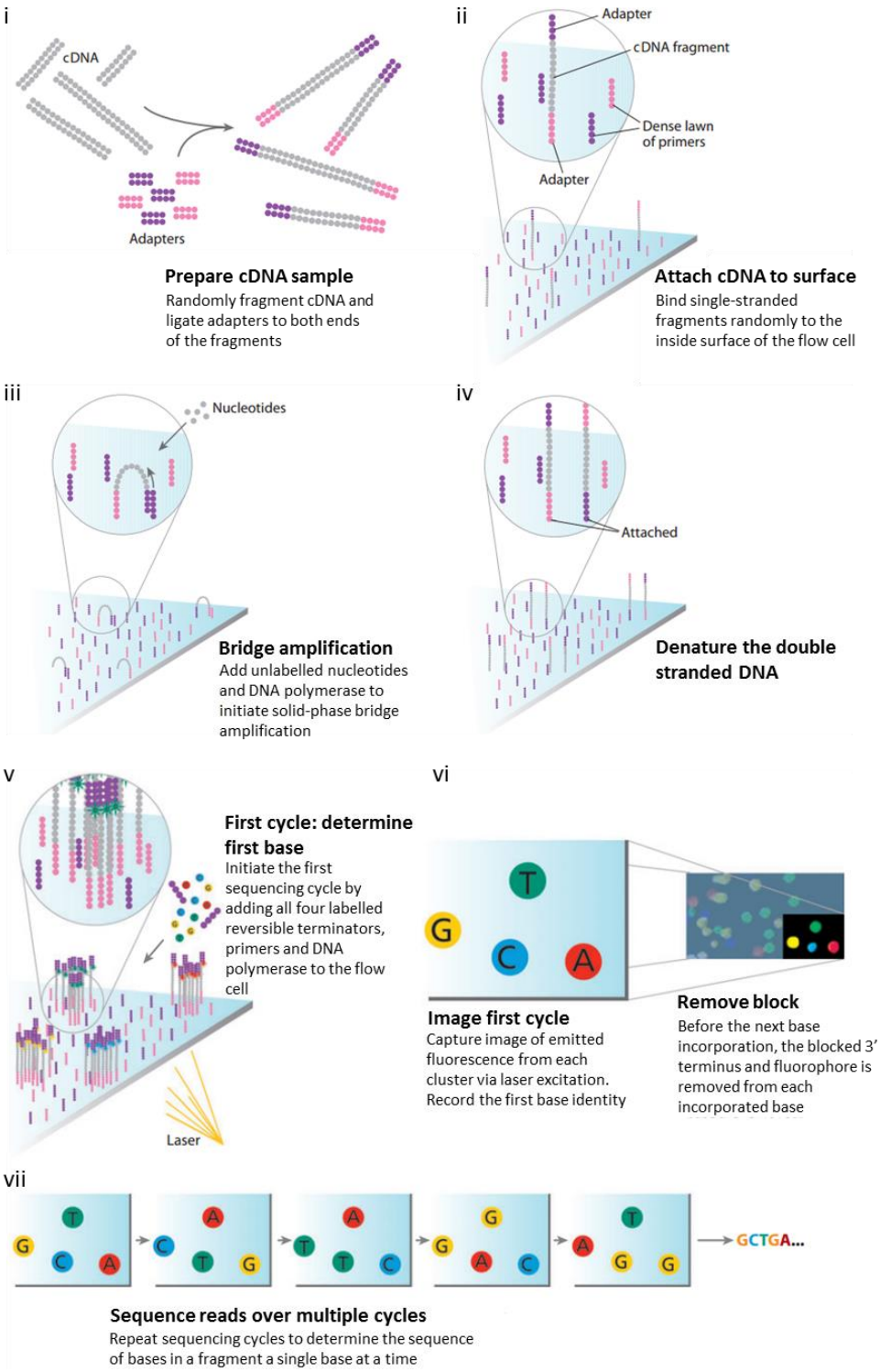

Figure 1.21: Mechanism of Solexa/Illumina short read sequencing platforms.
i. cDNA samples are generated and different adaptor sequences are bound at both ends of each cDNA. ii. Adaptor ligated cDNAs are then randomly attached to the surface of a flow cell, which presents numerous complementary adaptor sequences. iii. The unbound adaptor associates with its complementary sequence on the flow cell, and the bound adaptor acts as a primer for DNA synthesis across the newly formed bridge. iv. Following full strand synthesis, the double stranded DNA product is denatured. v. Sequencing begins by flowing primers, labelled bases and DNA polymerase across the flow cell. vi. The identity of the first base is recorded and the block and fluorophore are removed from the base. vii. This process is repeated until the full fragment sequence has been recorded. Adapted from (Mardis, 2008).

1.4 Thesis aims

Previous work in the Whitehouse laboratory and many other laboratories around the world has shown that high throughput, high resolution "omics" techniques can uncover novel interactions between viruses and the host cell. Proteomics and mRNA/miRNA sequencing based transcriptomics have all been used to great effect individually, and especially when used in combination with each other.

The initial aim of this thesis was to use a combination of subcellular fractionation and SILAC based proteomics to uncover novel interactions between KSHV and host cell proteins, occurring in subnuclear organelles. Chapter 3 identifies a novel interaction between KSHV ORF57 and the cellular mRNA processing/DNA damage factor, Prp19. Interestingly, this interaction does not appear to directly contribute to the previously observed interactions between KSHV proteins and the mRNA processing pathway. Instead, ORF57 limits the effectiveness of the ATR-Chk1 driven DNA damage response pathway, colocalising with numerous proteins involved in this pathway, including Prp19, at probable sites of DNA damage, ultimately preventing downstream pathway activation via an unknown mechanism.

Chapter 4 investigates host miRNA dysregulation during KSHV lytic replication using miRNA sequencing. 19 differentially expressed miRNAs are detected at different times post lytic reactivation in KSHV-infected cells. Upregulation of miR-151a-5p and miR-365a-3p occurs in multiple KSHV infected cell lines, at different times during lytic replication, but does not appear to reflect a host driven response against the virus, as neither viral RNA or protein production are targeted by either of these miRNAs. Instead, it seems more likely that the virus promotes the upregulation of these miRNAs for pro-viral mechanisms, as inhibition of miRNA activity, particularly that of miR-365a-3p, corresponds with a block in a viral process prior to viral egress.

Finally, chapter 5 described the identification of host mRNAs targeted by the upregulated miR-365a-3p late in the KSHV lytic cycle. Utilising a combination of mRNA sequencing and open source host miRNA target prediction software, numerous cellular transcripts were identified as potential targets of miR-151a-5p or miR-365a-3p and

observed to decrease in abundance over the course of KSHV lytic replication. Transcripts of both DOCK5 and PRUNE2, predicted miR-365a-3p targets, are observed to be stabilised at 18 hours into KSHV lytic replication in the presence of a miR-365a-3p inhibitor. The overexpression of DOCK5 is subsequently investigated, ultimately demonstrating a similar effect as miR-365a-3p inhibition on a viral process following DNA replication but prior to viral egress.

In summary, these findings shed light on multiple cellular pathways exploited by KSHV during lytic replication. The increased understanding of these interactions may present novel drug targets for the prevention of KSHV associated malignancies, as well as other herpesviruses. In addition, research into oncogenic pathogens may concomitantly help in the understanding of mechanisms associated with other cancers. Moreover, the datasets generated by the three high throughput, high resolution technologies used in this thesis will become an invaluable resource for future investigations into interactions between KSHV and the host cell.

CHAPTER 2

~

Materials and methods

2 Materials and methods

2.1 Materials

2.1.1 Chemicals

Unless stated otherwise, chemicals were obtained from Sigma Aldrich®, Invitrogen™, VWR International Inc., or Merck Chemicals Ltd. Sterilisation was achieved by autoclaving (121°c, 30 minutes, 15 psi) or sterile filtration (0.22 µm filters, Millipore).

2.1.2 Enzymes

Enzymes were obtained as indicated in Table 2.1.

Table 2.1: List of enzymes and suppliers.

Enzyme	**Supplier**
Taq DNA Polymerase	Invitrogen™
RNase A	Fermentas
DNase I	Invitrogen™
Protoscript II Reverse Transcriptase	Invitrogen™

2.1.3 Antibodies

Specific antibodies were obtained from sources indicated in Table 2.2. Secondary Goat antibodies specifically targeting Mouse or Rabbit primary antibodies, conjugated with Horse Radish Peroxidase for immunoblotting were obtained from DAKO. Secondary Rabbit antibody specifically targeting Sheep primary antibody, conjugated with Horse Radish Peroxidase for immunoblotting was obtained from Santa Cruz Biotech®. Secondary antibodies for immunofluorescence microscopy conjugated to Alexa488, Alexa546 and Alexa633 were obtained from Invitrogen™.

Table 2.2: List of antibodies and suppliers.

Target	Catalogue #	Species	Supplier
B23	sc-47725	Mouse	Santa Cruz Biotech®
C23	sc-55486	Mouse	Santa Cruz Biotech®
CDC5L	A301-682A	Rabbit	Bethyl Laboratories, Inc.
ORF57	sc-135746	Mouse	Santa Cruz Biotech®
p53 (phos.S15)	#9284P	Rabbit	Cell Signaling Technology, Inc.
GFP	632381	Mouse	Clontech Laboratories, Inc.
HA	H9658	Mouse	Sigma-Aldrich®
SC-35	S4045	Mouse	Sigma-Aldrich®
GAPDH	ab8245	Mouse	Abam®
LaminB1	ab16048	Rabbit	Abcam®
Prp19	A300-101A	Rabbit	Bethyl Laboratories, Inc.
Minor Capsid Protein	F110P	Sheep	2B Scientific Ltd.
RPA p34	R1280	Mouse	Sigma-Aldrich®
RPA (phos.T21)	ab109394	Rabbit	Abcam®
ATRIP	A300-095A	Rabbit	Bethyl Laboratories, Inc.
Nup414	ab24609	Mouse	Abcam®

2.1.4 Oligonucleotides

Oligonucleotides were purchased from IDT, Universal Probe Library Probe 21 was purchased from Roche. Oligonucleotides used in this work are listed in Table 2.3.

Table 2.3: List of primer names and sequences.

Primer name	Sequence (5'-3')
GAPDH Fw	AGGGTCATCATCTCTGCCCCCTC
GAPDH Rv	TGTGGTCATGAGTCCTTCCACGAT
K8 Fw	CCACCAAGAGGACCACACATTC
K8 Rv	CACACAAAGTCTGGCATGGTTCTC
ORF47 Fw	CGCGGTCGTTCGAAGATTGGG
ORF47 Rv	CGAGTCTGACTTCCGCTAACA
ORF57 Fw	GCCATAATCAAGCGTACTGG
ORF57 Rv	GCAGACAAATATTGCGGTGT
ABI3 Fw	GCATATGGAGAAGGTGGCCC
ABI3 Rv	GGTAGGTTCTCTGGGGCGAT
5s rRNA Fw	TACGGCCATACCACCCTGAA
5s rRNA Rv	GCGGTCTCCCATCCAAGTAC
18s rRNA Fw	GTAACCCGTTGAACCCCATT
18s rRNA Rv	CCATCCAATCGGTAGTAGCG
DSP Fw	GCTGGCAAAGGTAAGAAACCAC

DSP Rv	TGCATGGATATCTCCTTGATGGTG
FAM9C Fw	GGACAGTCCGTGAGGGGGAG
FAM9C Rv	CTCGCTGATTGGTCGGCCC
SPINK2 Fw	GTTACTGGCGGTTCCCCAGAG
SPINK2 Rv	CTGAGAGCAGTTTGGCGTTCTAT
HSPA8 Fw	GCTGGTGGGAGAAGTAGGCT
HSPA8 Rv	ACAATGCTCTGAAGGGCAACT
SLC15A4 Fw	GCGCCGACCAGGTTAAAGAT
SLC15A4 Rv	GGCAATGCCACCTAACGACA
HOXA3 Fw	CAGCTCATGAAACGGTCTGCG
HOXA3 Rv	AGGGGTTTGACACCCGTGA
ZNF512 Fw	TCTTCCAGACTCGGTGCTGT
ZNF512 Rv	CAGTGCAAAGGCGGGTAACA
DOCK5 Fw	ATCGGCTATCACCATTTCACGG
DOCK5 Rv	AACGATGGGGAGCTTAGGGT
PRUNE2 Fw	GACAACCGGCTTTGGAGGAC
PRUNE2 Rv	CCTCCGTGAGAAATGACTCTCC
FMN2 Fw	ACAGGCTCGAGGATGCTGAA

FMN2 Rv	TCAACAACTTCCTTCTGGACAGC
SGK1 Fw	ACGGTGAAAACTGAGGCTGC
SGK1 Rv	TCAGACCCATCCTCCTCTGC
vIL-6 Fw	GGCATCTGCAAGGGTATTCT
vIL-6 Rv	AAATCCTATTAACCCGCAGTGAT
IL-6 Fw	TCTGCGCAGCTTTAAGGAGT
IL-6 Rv	GACCAGAAGAAGGAATGCCCA
ORF74 Fw	ATATGAGCGGATATGACTACTCTGG
ORF74 Rv	TCATCTCACACACGCTCACTT
PAN Fw	TTTTCCAGTGTAAGCAAGTCGATTT
PAN Rv	TGTTCTTACACGACTTTGAAACTTCTG
K12 Fw	AACAGACAAACGAGTGGTGGTATC
K12 Rv	CAGTTCATGTCCCGGATGTG
hsa-miR-151a-5p RT Stem Loop	GTTGGCTCTGGTGCAGGGTCCGAGGTATTCGCACCAGAGCCAACACTAGA
hsa-miR-151a-5p Fw	GTGTGGAGTGTGACAATGG
Universal Reverse	GTGCAGGGTCCGAGGT
hsa-miR-365a-3p RT Stem Loop	GTTGGCTCTGGTGCAGGGTCCGAGGTATTCGCACCAGAGCCAACATAAGG

hsa-miR-365a-3p Fw	GTTGGGTAATGCCCCTAAAAAT
Universal Probe Library Probe 21	TGGCTCTG

2.1.5 Mammalian cell culture reagents

Tissue culture media, FCS, Glutamate and Lipofectamine® 2000 were purchased from Invitrogen®. SILAC labelling media and FCS were obtained from Dundee Cell Products.

2.1.6 Plasmid constructs

pPRP19-HA expressing PRP19 as a HA fusion protein and pPRP19-Myc expressing PRP19 as a Myc fusion protein were kindly provided by Dr. Marko Noerenberg (Whitehouse Laboratory).

pORF57-EGFP expressing ORF57 as an EGFP fusion protein, pEGFP-N1 and pORF47 expression constructs were kindly provided by Dr. Brian Jackson (Whitehouse Laboratory).

pDOCK5-GFP expressing DOCK5 as a GFP fusion protein was kindly provided by Dr. Matthew Sanders (Wayne State University).

2.1.7 siRNAs and miRIDIAN miRNA Hairpin Inhibitors

All siRNAs and miRIDIANs were purchased from Dharmacon (GE Life Sciences). siRNAs and miRIDIANs used in this work are listed in Table 2.4.

Table 2.4: List of siRNAs and miRIDIAN microRNA inhibitors.

siRNA/miRIDIAN	Catalogue #
CDC5L	M-011237-00-0005
Prp19	M-004688-02-0005
hsa-mir-151a-5p	IH-301086-02-0002
hsa-mir-365a-3p	IH-300666-05-0002

2.2 Methods

2.2.1 Mammalian cell culture

2.2.1.1 Routine maintenance

Cells were grown in a humidified atmosphere with 5% CO_2. HEK 293T, 293T rKSHV.219 and iSLK.219 cells were cultured in DMEM high glucose supplemented with 10% heat inactivated FCS. Prior to use, FCS was heat inactivated for 30 minutes at 50^{o}C. HEK 293T and 293T rKSHV.219 cells were usually split 1:20 every 3 days. HEK 293 derived cells were split by "shake off" method and an aliquot diluted into fresh media. KSHV lytic cycle was induced in 293T rKSHV.219 cells by supplementing media with 3 mM sodium butyrate and 20 ng/ml TPA (12-O-tetradecanoylphorbol-13-acetate). TREx BCBL1-Rta cells were cultured in RPMI1640 supplemented with 10% heat inactivated FCS. TREx BCBL1-Rta cells are grown as a suspension culture and were diluted into fresh media for passaging. KSHV lytic cycle was induced in TREx BCBL1-Rta cells by supplementing media with 2 µg/ml doxycycline hyclate.

2.2.1.2 Transient transfection

Cells were transfected using Lipofectamine® 2000, according to manufacturer's recommendation. In short, 100 µl Opti-MEM was mixed with 3 µl Lipofectamine 2000 and 100 µl Opti-MEM was mixed with 1 µg plasmid DNA per 35mm dish (10 cm^2) for 15 minutes. The solutions were then combined for 15 minutes, after which they were pipetted into the 35mm dish containing cells to be transfected, and mixed by gentle agitation. Transfection media was replaced 4 hours post transfection. Experiments were conducted 24 hours post transfection unless otherwise stated.

2.2.1.3 Long term storage of mammalian cells

Approximately 2 x 10^6 cells were harvested before reaching confluency, washed in PBS and resuspended in freeze down media (10% DMSO, 20% FCS, 70% DMEM). Cells were frozen in cryotube vials inside a 5100 Cryo 1^oC freezing container (NALGENE®) at -80^oc overnight, before being transferred to liquid nitrogen for long term storage.

2.2.1.4 Immunofluorescence confocal microscopy analysis

HEK 293Tor 293T rKSHV.219 cells were grown on poly-L-lysine coated coverslips for 24 hours before transfection. Transfections were performed as described in Section 2.2.1.2. Cells were fixed for 15 minutes with 4% paraformaldehyde in PBS. Cells were then washed three times with PBS, permeabilised with 1% Triton X-100 in PBS, washed three times with PBS, blocked with 10% BSA in PBS and incubated with primary antibodies diluted 1:100 in 10% BSA in PBS for 1 hour at 37^oc. Cells were then washed five times in PBS and then incubated with secondary antibodies conjugated with fluorophores diluted 1:500 in 10% BSA in PBS for 1 hour at 37^oc. Cells were mounted on to slides with VectaShield mounting media containing DAPI (Vector). Images were taken with an Upright Zeiss LSM 510 (Carl Zeiss Ltd, Welwyn Garden City; UK) and analysed with Zen 2011 image browser.

2.2.1.5 siRNA/miRIDIAN transfection

Cells were transfected using Lipofectamine 2000, according to manufacturer's recommendation, with the following modifications: a 100 nM final concentration siRNA/miRIDIAN was used, and transfection was performed whilst cells were 30-50% confluent. Transfection media was replaced 4 hours post transfection. Cells were then transfected again 24 hours post initial transfection. Transfection media was replaced 4 hours post transfection. Experiments were conducted 48 hours post second transfection unless otherwise stated.

2.2.2 Protein analysis

2.2.2.1 SDS-Polyacrylamide gel electrophoresis

Protein samples were separated by migration through a Sodium dodecyl sulphate polyacrylamide gel. Protein samples were mixed 1:1 in 2 x Laemmli loading buffer (50 mM Tris-HCl [pH 6.8], 2% [w/v] SDS, 20% [v/v] Glycerol, 50 µg/ml bromophenol blue, 10 mM DTT) and subsequently incubated at 95^{o}C for 5 minutes. Typically, 10% polyacrylamide gels were cast containing 10% (v/v) Acrylamide/bis-acrylamide 37:5:1 (Severn Biotech Ltd.), 375 mM Tris-HCl (pH 8.8), 0.1% (w/v) SDS, 0.1% (w/v) APS, 0.1% (v/v) TEMED, overlaid with 5% stacking gels containing 5% (v/v) Acrylamide/bis-acrylamide 37:5:1, 125 mM Tris-HCl (pH 6.8), 0.1% (w/v) SDS, 0.1% (w/v) APS, 0.1% (v/v) TEMED. Gels were placed in 1x Tris-Glycine buffer (5 mM Tris, 250mM Glycine, 0.1% [w/v] SDS) and protein samples were separated by electrophoresis at 180 V until sufficient separation was achieved. Following electrophoresis, gels were either used for immunoblotting, silver stain or Coomassie stain analysis.

2.2.2.2 Immunoblot analysis

Protein samples were separated by SDS-PAGE and blotted onto Hybond™-C (Amersham – GE Healthcare). Blots were blocked with 3% non-fat Marvel milk in TBS-T

(150 mM NaCl, 50 mM Tris-HCl [pH 7.5], 1% Tween 20) for 1 hour and incubated with primary antibodies diluted 1:500-1:10,000 in 3% non-fat Marvel milk TBS-T for 1 hour at room temperature. Blots were washed five times in TBS-T for 10 minutes and incubated with HRP conjugated secondary antibodies diluted 1:500 in 3% non-fat Marvel milk TBS-T for 1 hour at room temperature. Blots were then washed five times in TBS-T for 10 minutes, and then incubated with EZ-ECL substrate (Geneflow) and visualised on Hyperfilm® ECL (Amersham).

2.2.2.3 Coomassie staining of SDS-Polyacrylamide gels

Following SDS-PAGE separation, proteins were visualised by incubating the polyacrylamide gel in Coomassie staining solution (30% [v/v] methanol, 10% [v/v] acetic acid, 0.2% [w/v] Coomassie blue G) for 30 minutes. Stained gels were then incubated in destaining solution (25% [v/v] methanol, 10% [v/v] acetic acid) until a sufficient signal to background ratio was achieved.

2.2.2.4 Silver staining of SDS-Polyacrylamide gels

Following SDS-PAGE separation, proteins were visualised by fixing the polyacrylamide gel in buffer A (50% [v/v] ethanol, 10% [v/v] acetic acid) for 30 minutes and then incubating the fixed gel in buffer B (5% [v/v] ethanol, 1% [v/v] acetic acid for 15 minutes. Gel was then washed three times in dH_2O and incubated in buffer C (0.02% [w/v] $Na_2S_2O_3$) for 2 minutes. Gels were then washed 3 x in dH_2O and incubated in buffer D (0.2% [w/v] $AgNO_3$, 0.075% [v/v] formaldehyde) for 20 minutes in the absence of light. Gels were then washed three times in dH_2O before being developed in buffer E (6% [w/v] Na_2CO_3, 0.05% Formaldehyde, 0.0004% [w/v] $Na_2S_2O_3$). When bands were sufficiently visible, developing was stopped by the addition of buffer F (5% [v/v] acetic acid).

2.2.2.5 Preparation of subnuclear fractions for SILAC analysis

TREx BCBL1-Rta cells were grown in either light media (DMEM-14, Dundee Cell Products) or media containing the heavy isotopes of arginine and lysine (DMEM-16, Dundee Cell Products) supplemented with 10% SILAC dialysed FCS (DS1003, Dundee Cell Products) for 5 passages prior to experiments to ensure complete labelling of proteins. Roughly 2 x 10^8 cells per condition were used as starting material. Cells grown in heavy media were induced for KSHV lytic cycle by the addition of doxycycline (2 µg/ml) for 8, 16 or 24 hours prior to fractionation. Cells grown in light media were not induced for KSHV lytic cycle, and served as a latent KSHV control. Cellular fractionation was performed according to a protocol published by the Lamond laboratory (Lam et al., 2010), with minor modifications of the removal of $MgCl_2$ in buffers S2 and S3, as well as increased sonication cycles as described below. Cells were pelleted by centrifugation and washed with PBS, then pelleted and resuspended in 5ml ice cold swelling buffer (buffer A: 10 mM HEPES, 1.5 mM $MgCl_2$, 10 mM KCl, 0.5 mM DTT, 1 x Complete Protease Inhibitor cocktail) and incubated for 20 minutes on ice. All steps from this point were carried out on ice and samples examined under a light microscope after each step. Cells were lysed by 25 strokes with a Dounce homogeniser using a tight pestle. Lysate was clarified by centrifugation at 230 x *g* at 4^{o}C for 5 minutes. Supernatant was retained as the cytoplasmic fraction for subsequent immunoblot and silver stain analysis. The nuclear pellet was resuspended in 3ml buffer S1 (0.25 mM Sucrose, 1 x Complete Protease Inhibitor cocktail, 1.5 mM $MgCl_2$) and layered over buffer S2 (0.35 mM Sucrose, 1 x Complete Protease Inhibitor cocktail) prior to centrifugation at 1,400 x *g* at 4^{o}C. The pellet was resuspended in buffer S2 and sonicated for 25 cycles with a Soniprep 150 (MSE) at an amplitude of 10 µm for 10 seconds with 10 seconds pause to prevent overheating of the sample. In addition, samples were returned to ice for 5 minutes after every 5 cycles to prevent overheating. The sonicated samples were layered over a cushion of buffer S3 (0.88 mM Sucrose, 1 x Complete Protease Inhibitor cocktail) and subnuclear fractions were pelleted by centrifugation at 2,800 x *g* for 10 minutes at 4^{o}C. The pellet was further enriched by resuspension in buffer S2 and a second centrifugation through a cushion of buffer S3. Fractions were aliquoted to prevent repeated freeze-thaw cycles and

stored at -80^{o}C. Successful fractionation was confirmed by SDS-PAGE and subsequent silver stain or immunoblot using antibodies specific to cytoplasmic, nucleoplasmic and nucleolar marker proteins.

2.2.2.6 GFP-Trap® immunoprecipitation assays

GFP and GFP fusion ORF57 proteins were expressed by transient transfection in HEK 293T cells, as described in Section 2.2.1.2. 24 hours post transfection cells were washed in PBS and lysed by resuspension in ice cold modified RIPA buffer (150 mM NaCl, 50 mM Tris-HCl [pH 7.5], 1% NP-40 Alternative) for 20 minutes on ice with frequent gentle agitation. Lysates were clarified by centrifugation at 12,000 x *g* at 4^{o}C for 10 minutes and pellets were discarded. An aliquot of the supernatant was retained and mixed 1:1 with 2 x Laemmli loading buffer as an input sample. The supernatant was precleared by incubation with 20 µl bab20 blank beads (Chromotek, GmbH) which were washed three times before use in PBS, prior to use, for 1 hour at 4^{o}c with gentle agitation. Beads were then removed by centrifugation at 12,000 x *g* for 5 minutes at 4^{o}C. The supernatant was then incubated with 1 x RNase A (Fermentas) and 20 µl GFP-TRAP beads (Chromotek, GmbH) which were washed three times in PBS, prior to use, for 1 hour at 4^{o}C with gentle agitation. Beads were pelleted by centrifugation at 500 x *g* for 10 minutes at 4^{o}C and washed 3 x in PBS and once in modified RIPA buffer. Pelleted beads were then mixed with 50 µl Laemmli loading buffer. Resuspended beads and associated proteins, as well as input samples were analysed by SDS-PAGE and immunoblotting as described in Sections 2.2.2.1 and 2.2.2.2.

2.2.3 RNA analysis

2.2.3.1 RNA isolation

1 x 10^{6} cells were washed once with PBS before RNA isolation was performed using TRIzol (Invitrogen™) reagent according to manufacturer's instructions. In short, 500 µl TRIzol was added to the cell pellets and incubated for 5 minutes at room temperature.

100 µl chloroform was then added to the samples and vortexed. Phase separation was achieved by centrifugation at 4^{o}C for 15 minutes at 12,000 x *g*. The upper aqueous phase was then removed and mixed with 250 µl isopropanol to precipitate RNA, which was pelleted by centrifugation at 4^{o}C for 10 minutes at 12,000 x *g*. Pelleted RNA was washed with 75% ethanol and allowed to air dry, before being solubilised in 50 µl nuclease free water (Sigma-Aldrich®).

2.2.3.2 Preparation of miRNA sequencing library

Changes in abundance of cellular miRNAs were analysed using miRNA sequencing. KSHV lytic replication was induced in 1 x 10^7 TREx BCBL1-Rta cells with for 8 or 18 hours, or left uninduced (latent KSHV control) prior to RNA isolation (as described in Section 2.2.3.1). Total RNA was then treated with DNA-free (Ambion™), run on an Agilent Technologies 2100 Bioanalyzer to calculate a RIN number for each sample and 5 µg of total RNA from each sample was used to generate miRNA sequencing libraries using NEBNext Multiplex Small RNA Library Prep Set for Illumina (New England Biolabs, Inc.) according to manufacturer's instructions. In short, 3' SR adaptors were ligated onto RNA molecules present in the samples using T4 RNA Ligase 1 before excess 3' SR adaptors were hybridised to SR RT primer to prevent adaptor-dimer formation. 5' SR adaptors were then ligated on to the RNA molecules present in the samples and adaptor ligated RNAs were reverse transcribed using an adaptor specific primer. PCR amplification was then performed for 12 cycles using LongAmp *Taq* polymerase with an SR primer, as well as a different index primer for each sample to ensure that samples could be differentiated after sequencing. Samples were checked using an Agilent Bioanalyzer to assess whether adaptor-dimers (represented by a 127 bp peak) or excess primers (represented by a 70-80 bp peak) were present in the sample. AMPure XP beads were then used to specifically select and purify small RNAs from the samples. Final libraries were analysed using an Agilent Technologies 2100 Bioanalyzer to assess the purity of adaptor ligated small RNAs (represented by a 150 bp peak). Small RNA libraries were subsequently sequenced using a HiSeq (Illumina, Inc.)

sequencing platform. Reads were aligned to known *Homo sapiens* miRNA sequences and read counts were normalised using SeqEM and edgeR bioinformatic algorithms.

2.2.3.3 Preparation of mRNA sequencing library

Changes in abundance of cellular mRNAs were analysed using mRNA sequencing. 1 x 10^7 TREx BCBL1-Rta cells were induced for KSHV lytic cycle with doxycycline hyclate (2 µg/ml) for 8 or 18 hours, or left uninduced (latent KSHV control) prior to RNA isolation using Trizol reagent as described in Section 2.2.3.1. Total RNA was then treated with DNA free (Ambion), run on an Agilent Technologies 2100 Bioanalyzer to calculate a RIN number for each sample and 2 µg of total RNA from each sample was used to generate mRNA sequencing libraries using an Illumina TruSeq Stranded mRNA Sample Prep Kit (Illumina) according to manufacturer's instructions. In short, polyadenylated mRNAs were purified from total RNA samples with poly-T oligomers conjugated to magnetic beads during 2 rounds of purification. mRNAs were then fragmented and first strand cDNA was synthesised by SuperScript II Reverse transcriptase (using random hexamers). Actinomycin D was added to prevent spurious DNA dependent DNA synthesis, while allowing RNA dependent synthesis to occur, improving strand specificity. Blunt ended cDNA was then generated with the synthesis of the second strand using dUTP in place of dTTP in order to quench the second strand during amplification, as the polymerase does not incorporate past this nucleotide. A single Adenine residue was then ligated to the 3' ends of the blunt ended cDNA molecules to prevent them ligating together during adaptor ligation. 3' adaptors containing multiple index sequences for each sample were then ligated on to the cDNA molecules using a single Thymine overhang. 5' adaptors were also ligated during this step. 15 cycles of PCR were then performed to specifically enrich the DNA fragments ligated to adaptors at both ends, by using primers specific to the adaptors. Libraries were then analysed using an Agilent Technologies 2100 Bioanalyzer to assess the purity of adaptor ligated cDNAs generated from mRNAs in the original sample (represented by a peak at approximately 260 bp). Libraries were sequenced using a HiSeq (Illumina, Inc.)

sequencing platform. Reads were aligned to the *Homo sapiens* genome using the Burrows-Wheeler Transform method.

2.2.3.4 Reverse transcription

1 x 10^6 cells were washed once with PBS before RNA isolation was performed using TRIzol reagent as described in Section 2.2.3.1. For this, total RNA was then treated with DNA-free™ (Ambion®) according to the manufacturer's instructions. In short, 16 µl RNA sample was mixed with 1 µl DNase I and 2 µl reaction buffer and incubated at 37^{o}C for 30 minutes. The reaction was then stopped using the supplied stop beads at room temperature for 2 minutes before the sample was separated by centrifugation at 10,000 x g for 2 minutes and 20 µl supernatant was removed. 250 ng (measured by NanoDrop ND-1000 [NanoDrop Technologies] spectrophotometer) of this RNA was reverse transcribed with Protoscript II Reverse Transcriptase (Invitrogen™) according to the manufacturer's instructions. In short, 10 µl RNA (0.5 µg total amount) was mixed with 1 µl oligo-dT primer and 1 µl 10mM dNTP mix and incubated at 65^{o}C for 5 minutes, then placed on ice. A reaction mixture consisting of 4 µl reaction buffer, 2 µl DTT, 1 µl RNase OUT (Invitrogen ™) and 1 µl Protoscript II reverse transcriptase was then added to each sample, mixed and incubated at 42^{o}C for 50 minutes. The reaction was then stopped by incubating at 70^{o}C for 15 minutes. Changes in transcript abundance of either endogenous mRNAs or transfected constructs were analysed using qPCR.

2.2.3.5 ORF57 mRNA export activity assay

Export assays were performed as described previously (Boyne et al., 2008). HEK 293T cells were transfected without DNA (mock) or with a Prp19-HA expression construct as described in Section 2.2.1.2. Alternatively, cells were transfected with scramble siRNA (control), Prp19 specific siRNA or CDC5L siRNA or cotransfected with a mixture of both Prp19 and CDC5L specific siRNAs as described in Section 2.2.1.5. HEK 293T cells were then cotransfected with 1 µg ORF47 expression construct and 1 µg ORF57-EGFP or

EGFP-N1 expression constructs per 35mm dish (10 cm^2). 24 hours post transfection cells were washed in PBS and incubated in 1% Triton X-100 in PBS supplemented with 40 U/ml RNaseOUT (Invitrogen™) for 10 minutes on ice. Fractions were separated by centrifugation at 500 x *g* for 5 minutes at 4^oC. RNA extraction was then performed on both cytoplasmic and nuclear fractions as described in Section 2.2.3.1. RT and qPCR were performed as described in Sections 2.2.3.4 and 2.2.4.1, using primers specific to GAPDH and ORF47.

2.2.3.6 Splicing assay

293T rKSHV.219 cells were transfected with plasmid DNA as described in Section 2.2.1.2 or with siRNA as described in Section 2.2.1.5. 24 hours following transfection, cells were washed in PBS and pelleted by centrifugation. The pellet was resuspended in TRIzol reagent and total RNA was extracted as described in Section 2.2.3.1. Total RNA was then DNase treated and reverse transcribed as described in section 2.2.3.4. PCR was then performed using *Taq* DNA Polymerase (Invitrogen™) according to manufacturer's instructions using primers flanking the inner exons of KSHV K8, as well as primers specific to GAPDH. PCR products were mixed 1:10 with 10x loading dye (0.25% (w/v) Orange G, 30% (v/v) glycerol) and were separated by size using horizontal gel electrophoresis in a gel containing 1% Agarose in 1 x TBE buffer (90 mM Tris-base, 2 mM EDTA, 80 mM boric acid) prestained with 0.5 µg/ml ethidium bromide. Gel electrophoresis was performed at 100 V until sufficient separation was achieved. Invitrogen™ 1Kb Plus DNA Ladder was used to estimate product size. DNA bands were visualised in a GeneGenius bio-imaging system (Syngene) under ultra-violet light.

2.2.3.7 miRNA stem loop based qRT-PCR

Changes in abundance of either endogenous cellular miRNAs were analysed using Stem Loop based qRT-PCR. 1 x 10^6 cells were washed once with PBS before RNA isolation was performed as described in Section 2.2.3.1. Total RNA was then treated with DNase as described in Section 2.2.3.4 and 10 ng RNA was reverse transcribed

using miRNA specific Stem Loop RT primers and TaqMan MicroRNA Reverse Transcription Kit (Applied Biosystems) according to the manufacturer's instructions. Briefly, 3 µl 5 x stem loop RT primer was added to each 5 µl RNA sample and incubated at 85^{o}C for 5 minutes, followed by 60^{o}C for 5 minutes, then placed on ice. 7 µl reaction mix consisting of 0.15 µl 100 mM dNTP mix, 1 µl MultiScribe™ Reverse Transcriptase, 1.5 µl 10 x reverse transcription buffer, 0.19 µl (final concentration of 20 U/µl) RNase inhibitor and 4.16 µl nuclease free water was then added to each sample. The reaction was incubated at 16^{o}C for 30 minutes, followed by 42^{o}C for 30 minutes, and was then stopped by incubation at 85^{o}C for 5 minutes. qPCR was then performed using 2 ng cDNA (in 5 µl) with 10 µl LightCycler 480 Probes Master Mix (Roche), 0.4 µl Universal Probe Library Probe #21 (Roche), 1.2 µl 10 µM miRNA and stem loop specific primer mix and 3.4 µl nuclease free water on a Corbett Rotor Gene 6000 5 Plex with a 3 step PCR (15 seconds denaturation at 95^{o}C, 55 seconds annealing at 60^{o}C, 5 seconds elongation at 72^{o}C). Data were analysed with RotorGene 6000 series software version 1.7, exported into Microsoft Excel and relative changes of the samples calculated.

2.2.4 DNA analysis

2.2.4.1 qPCR

qPCR was performed using 10 ng cDNA or DNA (in a volume of 4 µl) with a reaction mix of 10 µl SensiMix™ Plus (Bioline), 1 µl 5mM gene specific primer mix and 5 µl nuclease free water on a Corbett Rotor Gene 6000 5 Plex (QIAGEN) with a 3 step PCR (15 seconds denaturation at 95^{o}C, 30 seconds annealing at 60^{o}C, 20 seconds elongation at 72^{o}C). Data were analysed with Rotor-Gene 6000 series software version 1.7, exported into Microsoft Excel and relative changes of the samples calculated using the ΔΔCT method. For this, all samples were normalised against the housekeeping gene GAPDH and quantified using comparative CT analysis unless otherwise stated.

2.2.4.2 Virus replication assay

Changes in viral load were analysed using qPCR. 1 x 10^6 293T rKSHV.219 cells were transfected with miRIDIAN miRNA inhibitors as described in section 2.2.1.5 or plasmid DNA as described in section 2.2.1.2. Following transfection, cells were either treated with sodium butyrate and TPA to induce KSHV lytic replication or left untreated as latent controls. After 7 days, cells were harvested by centrifugation at 500 x *g* for 5 minutes and DNA was extracted using a QIAGEN QIAamp DNA mini kit, according to manufacturer's instructions. In short, cell pellets were resuspended in 200 µl PBS and 20 µl Proteinase K was added to each sample. 200 µl buffer AL is then added to the samples, mixed and incubated at 56^{o}C for 10 minutes to ensure cell lysis. 200 µl 100% ethanol was then added to each sample, mixed and each sample was added to a QIAamp Mini spin column and centrifugated at 6,000 x *g*. Flow through was discarded and DNA bound to each column was then washed with 500 µl buffer AW1 at 6,000 x *g* and flow through was discarded. A second wash step was performed with buffer AW2, followed by centrifugation at 6,000 x *g* and the flow through was discarded. Each spin column was then placed inside a 1.5 ml microcentrifuge tube and 150 µl nuclease free water (Sigma-Aldrich®) was added to each spin column and incubated for 2 minutes. The spin column was then centrifugated at 6,000 x *g* for 2 minutes to elute the DNA. qPCR was then performed as described in Section 2.2.4.1 using primers specific to ORF47 and GAPDH.

2.2.4.3 Virus reinfection assay

Changes in viral reinfection were analysed using qPCR. 1 x 10^6 293T rKSHV.219 cells were transfected with miRIDIAN miRNA inhibitors as described in section 2.2.1.5 or plasmid DNA as described in section 2.2.1.2. Following transfection, cells were either treated with sodium butyrate and TPA to induce KSHV lytic replication or untreated as latent controls. 7 days later, cells and media were harvested by centrifugation at 500 x *g* for 5 minutes. 1 ml supernatant containing mature virions was then used to infect 1 x 10^6 naïve HEK 293T cells. DNA was extracted from these HEK 293T cells after 24 hours

using a QIAGEN QIAamp DNA mini kit, as described in Section 2.2.4.2. qPCR was then performed as described in Section 2.2.4.1 using primers specific to ORF47 and GAPDH.

2.2.5 Molecular cloning

2.2.5.1 Bacterial transformation

Chemically competent *E. coli* DH5α were incubated with 1 ng plasmid DNA for 15 minutes on ice and then "heat shocked" at 42^{o}C for 45 seconds, before again being incubated on ice for 2 minutes. Cells were then precultured for 1 hour at 37^{o}C in S.O.C. medium (0.5% [w/v] yeast extract, 2% [w/v] Tryptone, 10 mM NaCl, 2.5 mM KCl, 10 mM $MgCl_2$, 10 mM $MgSO_4$, 20 mM Glucose) with gentle agitation before plating onto lysogeny broth (LB)-agar (1.5% [w/v] microagar in LB medium) plates with an appropriate antibiotic for selection (50 µg Ampicillin or Kanamycin). Single colonies were picked after 16 hours at 37^{o}c for the subsequent inoculation of liquid culture.

2.2.5.2 Large scale plasmid DNA purification

Large scale purifications of plasmid DNA were performed with a QIAGEN Plasmid Maxi Kit according to the manufacturer's recommendations. In brief, 100 ml overnight cultures of bacteria were grown at 37^{o}C in LB media containing an appropriate antibiotic, pelleted by centrifugation and resuspended in 10 ml buffer P1. 10 ml lysis buffer P2 was then added and gently mixed by inversion of the sample tube. The solution was then incubated at room temperature for 5 minutes to allow alkaline lysis to occur. 10 ml buffer P3 was subsequently added, mixed and incubated on ice for 20 minutes. The precipitate was removed by centrifugation at 4,500 x *g* for 30 minutes and the supernatant was allowed to flow through a pre-equilibrated QIAGEN-tip 500 column by gravity flow. Columns were washed twice with 30 ml of wash buffer QC, and DNA was eluted with 15 ml elution buffer QF. Plasmid DNA was precipitated by the addition of 10.5 ml isopropanol and pelleted at 4,500 x *g* at 4^{o}C for 30 minutes. The pelleted DNA was washed with 70% ethanol and allowed to air dry. DNA was

resuspended in 200 µl sterile, nuclease free water and the DNA concentration determined by absorption at λ=260 nm in a NanoDrop ND-1000 (NanoDrop Technologies) spectrophotometer.

CHAPTER 3

~

ORF57 interacts with Prp19 to interrupt the cellular DNA damage response

3 ORF57 interacts with Prp19 to interrupt the cellular DNA damage response

3.1 Introduction

The KSHV lytic replication cycle, as with many herpesviruses, can be categorised by three stages of gene expression: immediate early, early and late (Sun et al., 1999). Immediately after gaining entry to the host cell nucleus, the KSHV RTA (ORF50) protein is able to drive the expression of its own gene and a number of viral genes such as ORF57 (MTA) (Sun et al., 1998; Lukac et al., 1998; Gradoville et al., 2000). These immediate early proteins then begin a cascade of gene activation, culminating in the production of viral proteins involved in DNA replication and viral structural proteins which subsequently lead to the biogenesis of mature viral progeny (Sun et al., 1999).

ORF57 has been well characterised and associates with a large number of host cell proteins belonging to many distinct cellular biochemical pathways (Jackson et al., 2012; Majerciak and Zheng, 2015). The most widely characterised interactions are between ORF57 and the host cell post-transcriptional mRNA processing machinery, of which there are three distinct subsets: capping, splicing and polyadenylation-associated proteins (Rodríguez-Navarro and Hurt, 2011; Boyne et al., 2008; Majerciak et al., 2008; Jackson et al., 2012). As such, ORF57 has been shown to enhance nuclear stability, export and translation of viral intronless mRNAs, and to facilitate splicing of viral intron-containing mRNAs (Sahin et al., 2010; Boyne et al., 2008; Boyne et al., 2010; Majerciak et al., 2008). Furthermore, ORF57 has been shown to interact with the nucleolar protein B23 and appears to localise primarily in the nucleolus using fluorescence microscopy analysis (Boyne and Whitehouse, 2006; Boyne and Whitehouse, 2009).

The nucleolus is a tripartite, subnuclear structure that forms around ribosomal DNA loci, known as nucleolar organizing regions (NORs). It is involved in a number of host cell processes including ribosome biogenesis, cell cycle progression and regulation of the response to various types of cellular stress (Paniagua et al., 1986; Wachtler et al., 1986; Boisvert et al., 2007). There are many examples of viruses from various

Baltimore classes, including viruses that replicate in the cytoplasm, which interact with the nucleolus in order to promote their own replication. This suggests that this subnuclear organelle is of particular importance during many viral replication cycles (Hiscox, 2002; Hiscox, 2007; Salvetti and Greco, 2014). The nucleolus can be purified from cells using a relatively straightforward fractionation protocol, enabling the use of modern mass spectrometry-based proteomic approaches to examine the nucleolar proteome at various stages of virus infection in an unbiased manner (Andersen et al., 2002; Emmott et al., 2008; Lam et al., 2010).

One such method is SILAC (stable isotope labelling with amino acids in cell culture), which can be coupled to LC-MS/MS in order to detect a large number of proteins present in multiple samples at the same time, and compare the relative amounts of these proteins between samples (Ong et al., 2002; Owen et al., 2014). This approach first requires the incorporation of different stable isotopes of amino acids into both the host cell and viral proteins. This is achieved by culturing cells in medium containing either the naturally occurring isotopes of these amino acids containing ^{12}C and ^{1}H (light medium), or amino acids containing heavy stable isotopes of these amino acids containing ^{13}C and ^{2}H. Arginine and lysine are the most commonly used amino acids for this labelling, ensuring each peptide fragment generated by tryptic digest before LC-MS/MS will contain at least one labelled amino acid, allowing the identification of each peptide, and subsequent assignment of the protein. Two populations are split from an initial culture of cells and then grown for at least five passages in the presence of each medium. These two populations are then treated differently, for example either mock infected or infected with a virus. Proteins are then harvested from each population of cells using the same extraction protocol, before the samples are mixed in a 1:1 ratio and analysed by LC-MS/MS. Peptides from each sample may then be distinguished by the mass shift caused by the presence of the differentially weighted isotopes, and the relative quantities of each present in the initial sample will be directly correlated with the m/z peak intensity. This approach represents a reliable, quantifiable and unbiased method for the detection of changes in the abundance of a large number of proteins between any two proteomes. This approach and similar variants are now widely used in molecular biology-based studies, clearly demonstrating the potential to uncover

large numbers of protein alterations and interactions that had previously been unidentified and uncharacterised.

In this chapter, SILAC-based quantitative proteomic approaches are employed to discover an interaction between the cellular mRNA splicing factor Prp19 and the viral ORF57 protein. Interestingly, this interaction does not appear to play a role in viral mRNA maturation or translation, but instead has implications for the ATR-Chk1 cellular DNA damage response pathway, of which Prp19 is an important early signalling factor. ORF57 limits the Prp19-mediated activation of the ATR-Chk1 pathway, and associates with Prp19, as well as ATRIP, another important factor in this pathway, in discrete nuclear foci, believed to be sites of damaged euchromatin.

3.2 Subnuclear fractionation of differentially labelled cell populations

In order to examine the interactions between KSHV and the proteomes of subnuclear organelles of infected host cells over the full course of the lytic replication cycle, four populations of TREx BCBL1-Rta cells harbouring a latent KSHV genome capable of being induced to initiate the lytic replication cascade with the addition of doxycycline hyclate (dox) were labelled with light or heavy SILAC medium for five passages (Nakamura et al., 2003). Cells grown in heavy medium were then reactivated for 8, 16 or 24 hours, whilst cells grown in light medium were kept under latent KSHV conditions (uninduced) **(Fig. 3.1A)**. Subnuclear fractionation was then performed using a previously described protocol with modifications **(Fig. 3.1B)** (Andersen et al., 2002).

Harvested proteins from each of the lytically infected populations were individually mixed at a 1:1 ratio with proteins from the latently infected control cells (protein ratios were judged using a combination of Coomassie/silver stain/immunoblot analysis **(Fig. 3.2)** and Bio-Rad Bradford reagent based protein assay). Mixed samples were then sent for LC-MS/MS analysis at the University of Bristol Proteomics Facility.

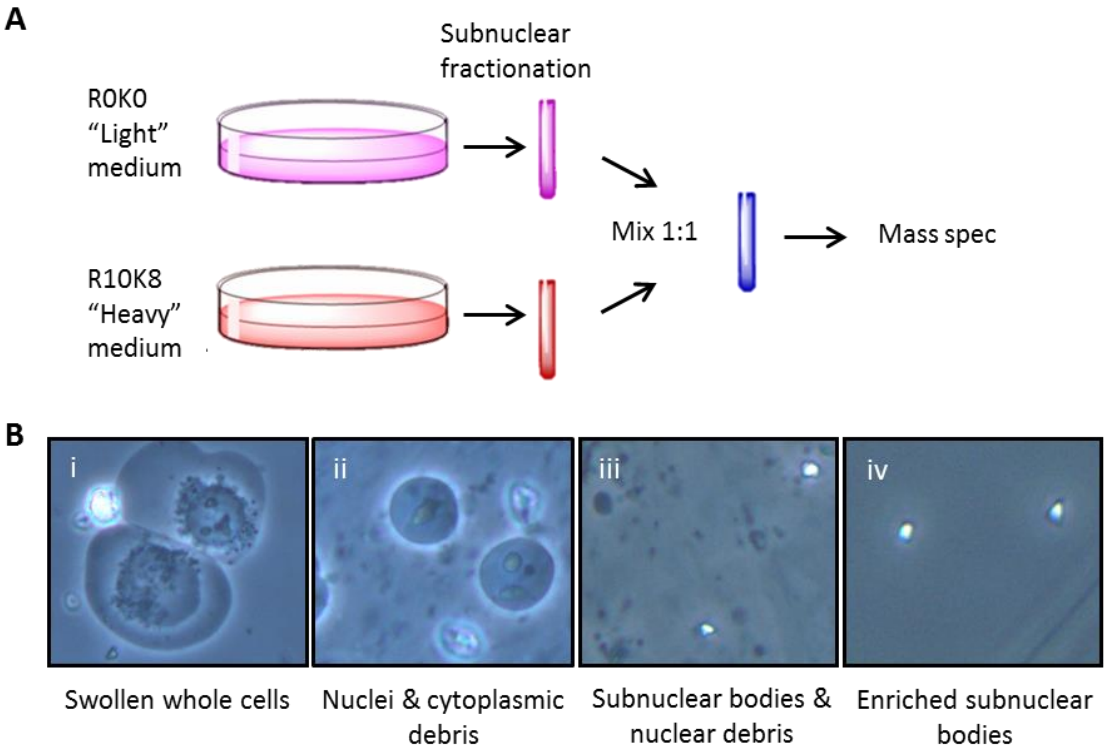

Figure 3.1: Subnuclear fractionation of TREx BCBL 1-Rta cells.
(a) Four populations of TREx BCBL1-Rta cells were split from a single population and each then grown in SILAC media containing different isotopes of the amino acids Arginine (R) and Lysine (K) (3 populations were grown in R10K8 media, one population was grown in R0K0 media). Each population was allowed to grow to ~90% of their maximum capacity before being passaged 5 times. KSHV lytic reactivation was then induced in cells grown in R10K8 media for 8, 16 or 24 hours, and all cells were then pelleted and individual populations were subjected to a fractionation procedure resulting in the isolation of enriched subnuclear body proteins. Reactivated samples were then mixed in a one to one protein ratio with the latent control sample, resulting in three samples; 0h + 8h, 0h + 16h and 0h + 24h. These samples were then sent for mass spectrometry analysis at the University of Bristol. (b) Microscope images taken during subnuclear fractionation of TREx BCBL1-Rta cells clearly showing cells at different stages of the protocol. (i) Cells were swollen in hypotonic buffer. (ii) Cells were passed through a dounce homogeniser, causing the swollen membrane to burst and releasing cytoplasmic debris and intact nuclei. Enriched nuclei were then obtained by centrifuging this material through a sucrose cushion. (iii) Enriched nuclear material was sonicated, bursting the nuclear membrane and releasing subnuclear bodies (nucleoli are clearly seen as bright puncta). (iv) Enrichment of subnuclear bodies was achieved by centrifugation of sonicate through a sucrose cushion.

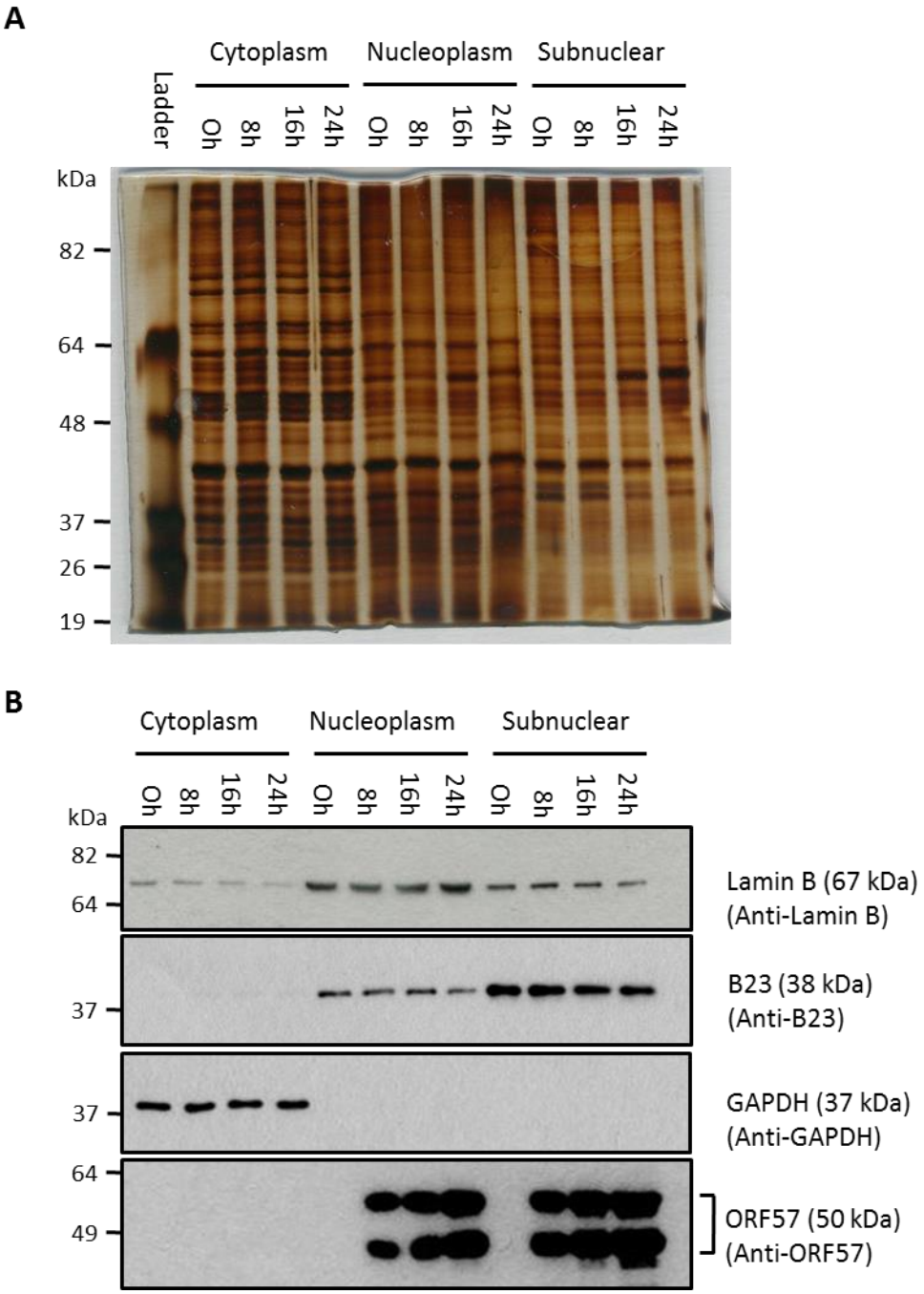

Figure 3.2: Generation of SILAC enriched subnuclear body protein samples.
(a) Cytoplasmic, nuclear and subnuclear fractions obtained from subnuclear fractionation were separated by SDS-PAGE and then analysed by silver stain to assess different protein band profiles. (b) Fractions were also analysed by SDS-PAGE and immunoblots for protein markers for the cytoplasm (GAPDH), nuclear envelope (Lamin B), nucleolus (B23) and KSHV lytic infection (ORF57).

3.3 Bioinformatic analysis of proteomics data

Metadata generated by LC-MS/MS analysis of subnuclear fractionation/SILAC samples, as well as previously generated data from subcellular fractionation (cytoplasmic, nuclear and nucleolar fractions)/SILAC and SILAC based immunoprecipitation of ORF57-GFP using GFP (additional SILAC experiments performed by Dr. Marko Noerenberg) as a control were analysed using DAVID bioinformatics (Huang et al., 2007). This metadata approach, combining several datasets was used to increase the likelihood of discovering genuine KSHV/host cell protein interactions and also aiming to reduce the possibility of attempting to validate false positive results due to the imperfect nature of the fractionation protocol employed. As anticipated, bioinformatic analysis revealed a large number of proteins involved in mRNA maturation, as well as a previously characterised interaction between KSHV and the mRNA decay protein, Xrn1 **(Fig. 3.3A)** (Covarrubias et al., 2011). On closer inspection, a large proportion of splicing-related proteins could be seen to associate with subnuclear structures and ORF57 over the course of KSHV lytic infection, including proteins from major spliceosome subunits, the Prp19 complex and the hTREX complex **(Fig. 3.3B)**. As the interaction between the hTREX complex and KSHV ORF57 has been well characterised, we elected to further analyse the involvement of the Prp19 complex in KSHV lytic infection. Initially, we focused on the Prp19 protein, which was shown to interact with ORF57 in both the ORF57 SILAC IP analysis and also to increase in abundance in the nucleolus in the ORF57 subcellular fractionation SILAC analysis **(Fig. 3.3C)**.

A

Process	Protein	Fold change
Splicing	FUBP2	7.6
	DDX38	4.13
	ABS	3.94
	SF1	3.87
	SAP155	3.45
	SKAR	3.2
	SAP145	3.17
	CDC5L	3.07
	SAP49	2.94
	PRP19	2.84
	KIAA0017	2.61
	SF3B10	2.06
Polyadenylation	CPSF1	3.2
	CPSF100	2.7
	CPSF3	2.47
mRNA Decay	XRN1	83

B

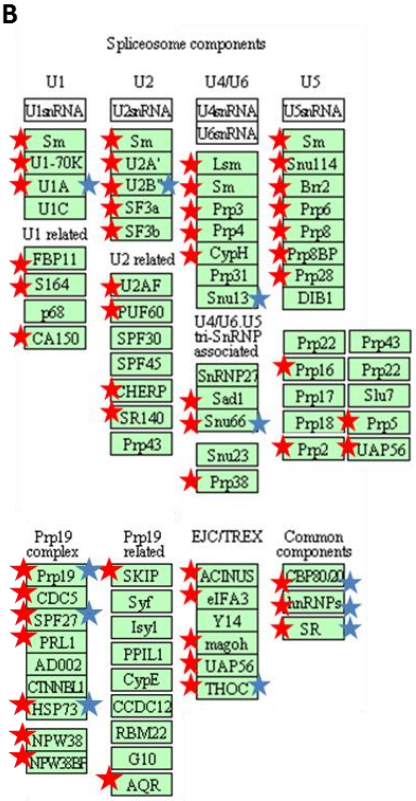

C

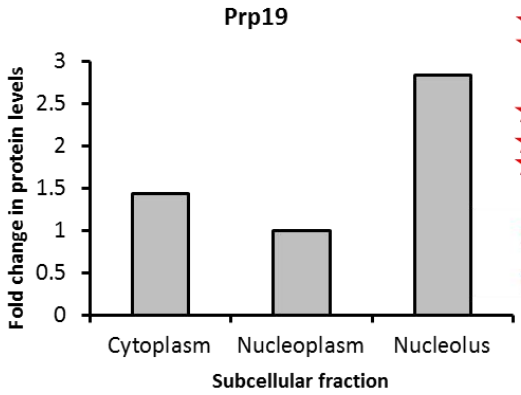

Figure 3.3: Bioinformatic analysis of SILAC results.
(a) Table displaying a subset of mRNA processing related proteins found at increased levels in the subnuclear fractions of lytically infected TREx BCBL1-Rta cells. Numbers shown are maximum increase over latently infected (unreactivated) cells. (b) DAVID bioinformatics analysis output showing all of the splicing related proteins identified at increased levels in both lytic KSHV subnuclear fractionation SILAC and KSHV ORF57 SILAC-IP experiments. (c) Fold change increase of Prp19 protein levels in subcellular fractions of ORF57 SILAC samples compared to control cells.

3.4 Prp19 interacts with ORF57 in an RNA independent manner

To initially validate whether Prp19 functioned in the KSHV lytic infection cycle, confocal microscopy analysis was performed using an HA tagged Prp19 fusion protein cotransfected in the presence of GFP (control) or ORF57-GFP **(Fig. 3.4A)**. Prp19-HA colocalised with a portion of ORF57-GFP protein in discrete subnuclear structures believed to be the nuclear speckles. Interestingly, overexpression of Prp19-HA appeared to modulate the normal localisation of ORF57-GFP, which is usually observed mainly localising to the nucleolus with only a diffuse presence in other regions of the

nucleus. This experiment was repeated to examine the localisation of ORF57 and endogenous Prp19 using ORF57- and Prp19-specific antibodies in TREx BCBL1-Rta cells **(Fig 3.4B)**. Prp19 exhibited diffuse nuclear localisation, clearly excluded from the nucleolus in control cells transfected with GFP, in contrast, Prp19 was seen to accumulate at high levels in the nucleolus upon overexpression of ORF57-GFP. These results suggest that Prp19 interacts with ORF57 and the levels of either protein can regulate the subcellular localisation of the other protein.

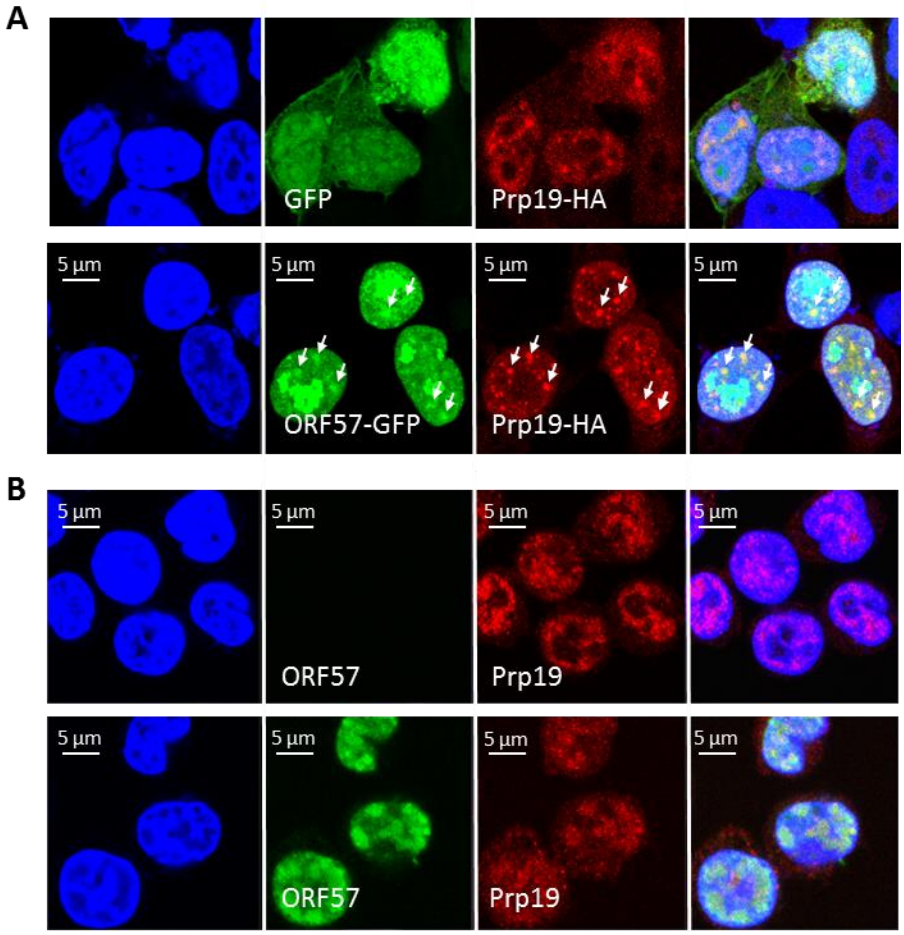

Figure 3.4: ORF57 co-localises with Prp19-HA in nuclear speckles.
(a) HEK 293T cells transfected with pEGFP-N1/pORF57-EGFP and Prp19-HA or (b) Unreactivated/reactivated TREx BCBL1-Rta were fixed with paraformaldehyde and stained using primary antibodies specific to (a) HA and (b) Prp19 and ORF57 and secondary antibodies conjugated to Alexa-Fluor 488 and 548 fluorophores. Stained cells were then mounted on slides with mounting media containing DAPI. Slides were analysed using a Zeiss LSM 510 confocal laser scanning microscope.

In order to examine the potential for a direct protein-protein interaction between Prp19 and ORF57, co-immunoprecipitation experiments were performed using cells transfected with GFP or ORF57-GFP **(Fig. 3.5)**. Input and IP samples were examined for the presence of GFP/ORF57-GFP and endogenous Prp19 in the presence of RNase A to

prevent the identification of RNA bridged interactions. Prp19 was shown to interact with ORF57-GFP but not the GFP control or unconjugated agarose beads. As both ORF57 and Prp19 proteins are known to interact with mRNA, the identification of an unbridged protein-protein interaction, in the presence of RNase A, suggests KSHV has evolved to exploit the cellular protein Prp19 to enhance viral replication.

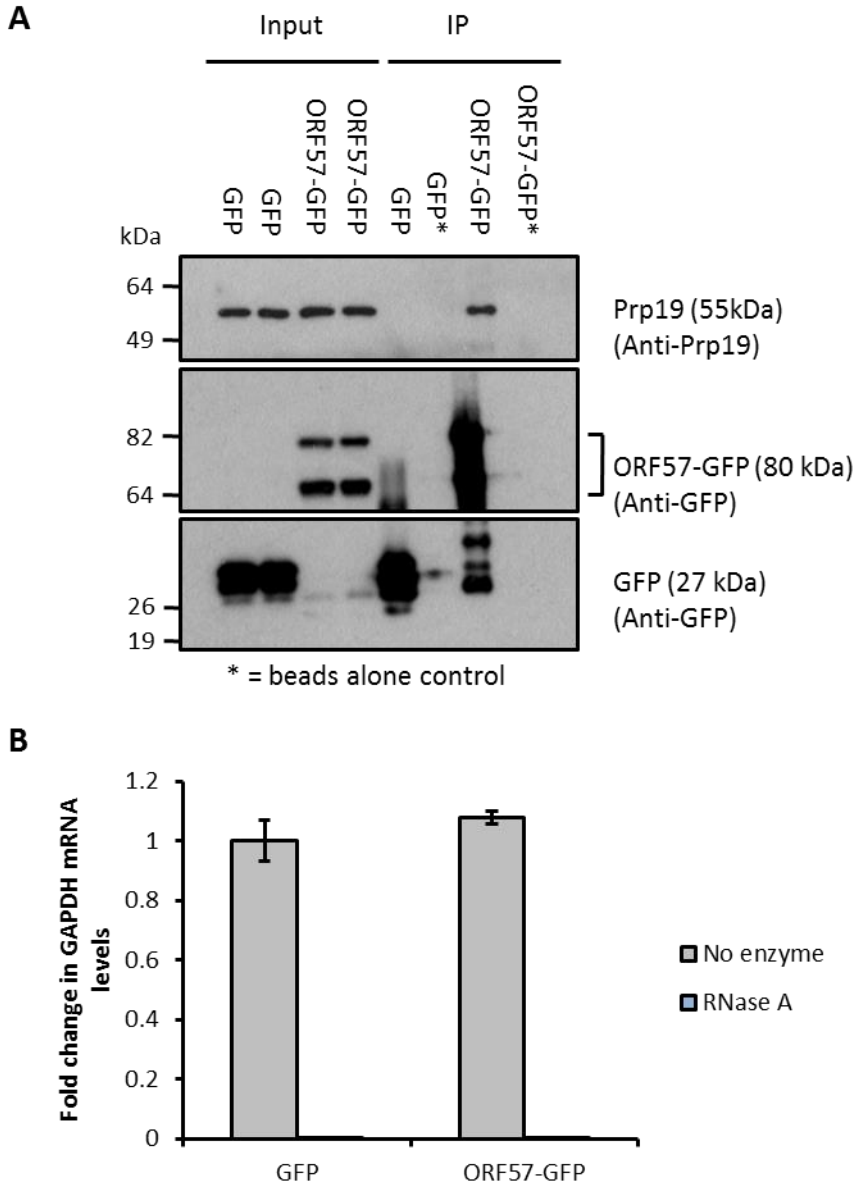

Figure 3.5: ORF57 interacts with Prp19.
HEK 293T cells were transfected with pEGFP-N1 or pORF57-EGFP. After 24 hours lysates were harvested, (a) treated with RNase A and immunoprecipitation with GFP-trap beads was performed. Input and Co-IP samples were separated by SDS-PAGE and immunoblots were performed using antibodies specific for Prp19 and GFP (b) RNA levels were equalised, and either treated with RNase A or left untreated. Samples were then DNase treated and reverse transcribed, before GAPDH levels were analysed by qPCR. Ct values were not compared against GAPDH control for ΔΔCT normalisation, and instead inverse Ct values were used to quantify RNA levels (b - performed by Dr. Anja Berndt).

3.5 Prp19 overexpression does not affect nuclear stability or export of viral intronless mRNAs or splicing of viral intron containing mRNAs.

As Prp19 has previously been characterised as an important factor in the splicing and export of cellular mRNA (Grote et al., 2010), it was hypothesised that KSHV ORF57 may be hijacking this cellular protein in order to facilitate the export of KSHV mRNAs. Previous work has already shown that the cellular hTREX complex to be of vital importance in this process, and occupancy of Prp19 at maturing mRNAs has previously been demonstrated to be an essential factor in the recruitment of the hTREX complex to both intron containing and intronless mRNAs (Masuda et al., 2005; Katahira, 2012; Chanarat et al., 2011). As the majority of KSHV encoded transcripts are intronless (Arias et al., 2014), the effect of overexpressing Prp19-HA on the nuclear export of the viral intronless reporter mRNA, ORF47, was examined using a well characterised viral mRNA nuclear export assay (Boyne et al., 2008). It was hypothesised that if Prp19 was involved in the nuclear export of viral intronless mRNAs, its overexpression should increase the amount of viral mRNA found in the cytoplasmic fraction, relative to the nuclear fraction. However, surprisingly results showed that overexpression of Prp19-HA appeared to have no effect. Expression of ORF57 did significantly enhance the amount of viral intronless mRNA exported to the cytoplasm, as well as their nuclear stability, as has been shown previously **(Fig. 3.6)** (Boyne and Whitehouse, 2009).

As overexpression of Prp19-HA did not appear to enhance the export of viral intronless transcripts, it was hypothesised that Prp19 may be utilised by ORF57 to promote the splicing of viral intron-containing mRNAs. ORF57 has previously been shown to be a vital component in the splicing of the final intron of the KSHV K8β transcript resulting in the fully spliced K8α transcript (Majerciak et al., 2008). Therefore, the efficiency of KSHV K8β splicing was assessed in the presence of Prp19 overexpression, as it was hypothesised that if ORF57 is hijacking Prp19 to promote the splicing of this important viral transcript, overexpression of Prp19-HA would further enhance this effect. Results again showed that overexpression of Prp19 has no effect on the levels of viral splicing during KSHV lytic replication (Unpaired T-test: p=0.1621) **(Fig. 3.7)**. This suggests that KSHV is able to use other cellular or viral machinery to facilitate the splicing of viral

intron-containing mRNAs, or that endogenous Prp19 is present in high enough abundance to maximise splicing efficiency of KSHV intron-containing mRNA.

3.6 Depletion of endogenous Prp19 does not affect nuclear stability, export of intronless viral mRNAs, splicing of viral intron containing mRNAs or production of late viral protein.

As the overexpression of Prp19-HA did not appear to enhance the export of intronless viral mRNAs or the splicing of viral intron-containing transcripts, it was hypothesised that endogenous levels of Prp19 were probably sufficient to achieve maximum levels of either or both of these processes. Therefore, reducing endogenous levels of Prp19 using siRNA appeared a more appropriate way to examine the effect of Prp19 on the splicing and export of viral transcripts. siRNA-mediated depletion of endogenous Prp19 was tested in both HEK 293T cells and in a HEK 293T based cell line harbouring a latent viral genome; 293T rKSHV.219 cells (Vieira and O'Hearn, 2004). Prp19 directed siRNA had a clear inhibitory effect on cellular Prp19 levels in both cell lines after 24 hours, with a greater reduction at 48 and 72 hours, when compared with untransfected cells or cell transfected with a scramble siRNA control **(Fig. 3.8)**.

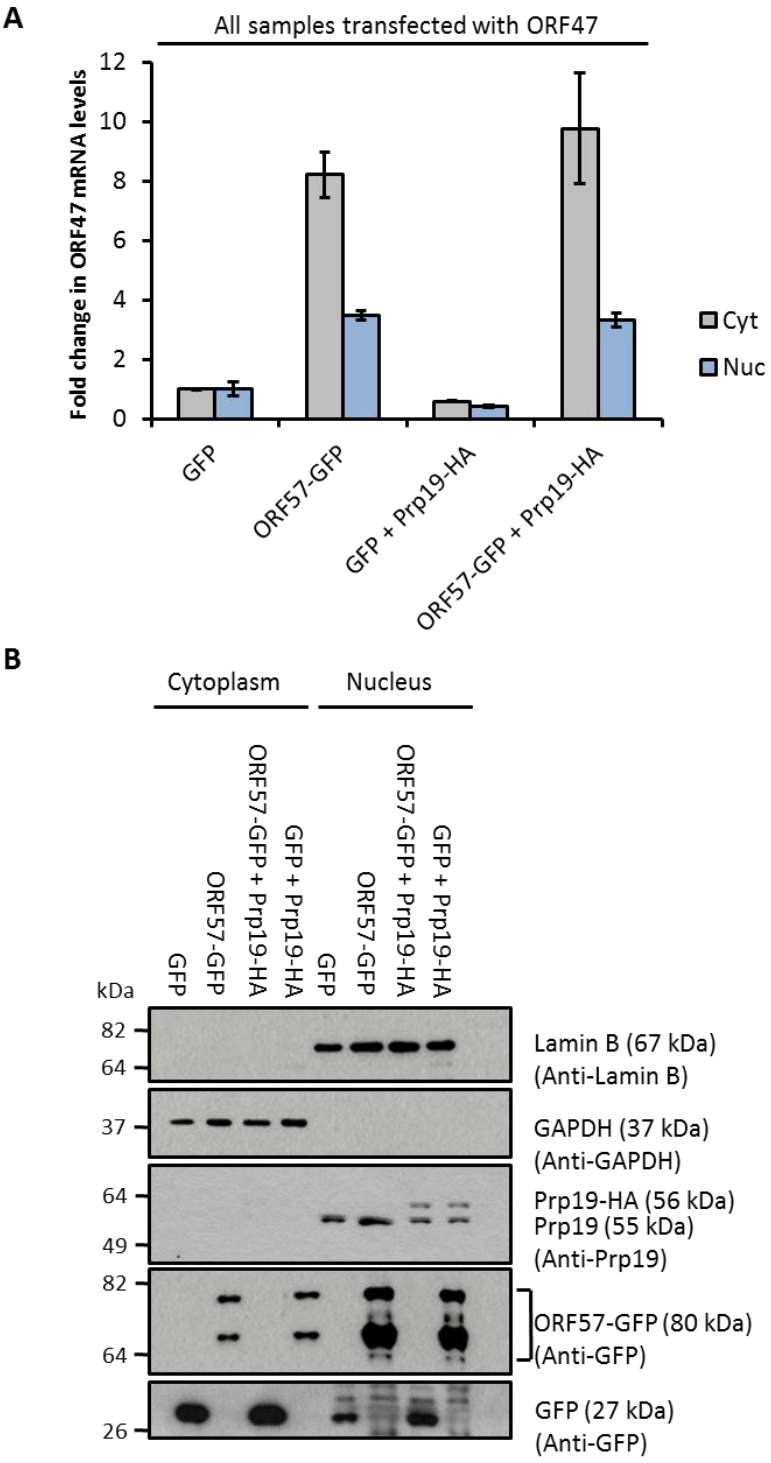

Figure 3.6: Prp19-HA overexpression does not affect nuclear stability or ORF57 mediated export of intronless KSHV mRNAs.

(a) HEK 293T cells were transfected with pEGFP-N1/pORF57-EGFP and pORF47 ± pPrp19-HA. 24 hours post transfection cells were separated into cytoplasmic and nuclear fractions. RNA was extracted from each fraction and extracted RNA was subjected to DNase treatment. RNA was then reverse transcribed into cDNA using an oligo dT primer and qPCR was performed using primers specific to ORF47. 3 biological replicates were combined, the relative values were displayed on a graph and the standard deviation was calculated. Error bars = SD, $p<0.01$ = **, $p<0.05$ = * compared with same fraction from GFP/ORF57-GFP control samples (b) Fractionation samples were separated by SDS-PAGE and immunoblots were performed using antibodies specific for Lamin B, GAPDH, Prp19 and GFP.

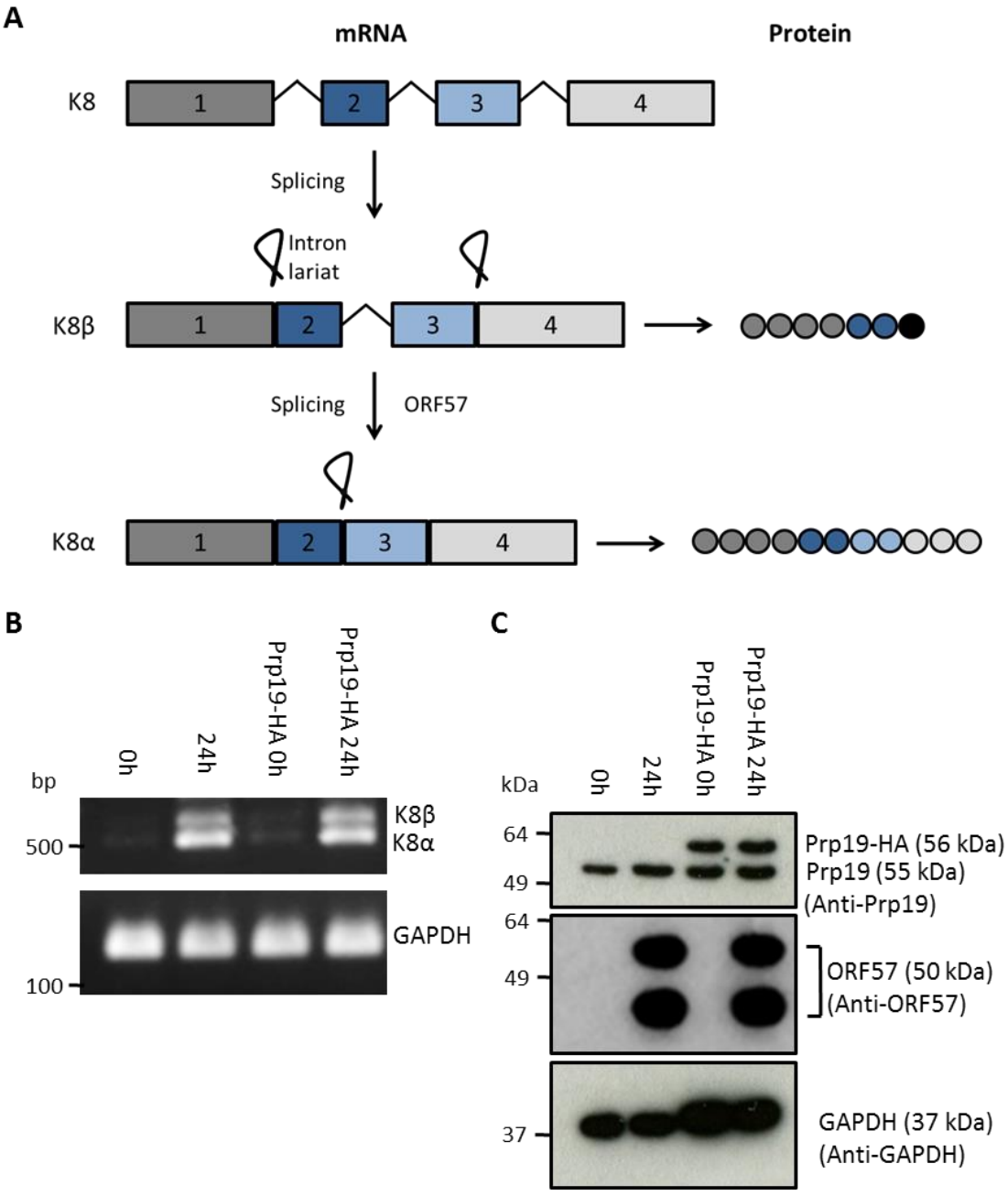

Figure 3.7: Prp19-HA overexpression does not affect ORF57 mediated splicing of KSHV K8 mRNA.
(a) Schematic of the alternative splicing of the KSHV K8 mRNA and the proteins that result from each spliceoform. Image adapted from Majerciak *et al.* (2007) (b, c) 293T rKSHV.219 cells were transfected without DNA (mock) or with pPrp19-HA. 48 hours after transfection cells were either reactivated with NaBu and TPA for 24 hours (lytic infection) or left unreactivated (latent - control). (b) RNA was then extracted from cells, samples were treated with DNase and reverse transcription was performed. PCR was then performed on the resulting cDNA using primers specific for KSHV K8. GAPDH was used as a loading control. (c) Lysates were harvested at 0 and 48 hours post viral reactivation. Samples were separated by SDS-PAGE and immunoblots were performed using antibodies specific to Prp19, ORF57 and GAPDH.

The effect of Prp19 depletion on the export of the intronless viral mRNA ORF47 was then examined, and it was hypothesised that if ORF57 was hijacking Prp19 to enhance

the export of KSHV intronless transcripts, depletion of Prp19 would dramatically reduce or ablate this process. The mRNA export assay described in Section 3.5 was employed using siRNAs directed against Prp19 or scramble (control) in cells cotransfected with ORF47 and ORF57-GFP or GFP (control). Results show that depletion of Prp19 did not affect viral intronless mRNA nuclear export (Unpaired T-test: p=0.5629), surprisingly, however, Prp19 depletion did cause a minor disruptive effect on the nuclear stability of viral intronless mRNAs (Unpaired T-test: p=0.0183). ORF57 was again observed to increase the nuclear stability and export of the intronless ORF47 transcript, as previously described, demonstrating that the assay was working correctly **(Fig 3.9)**.

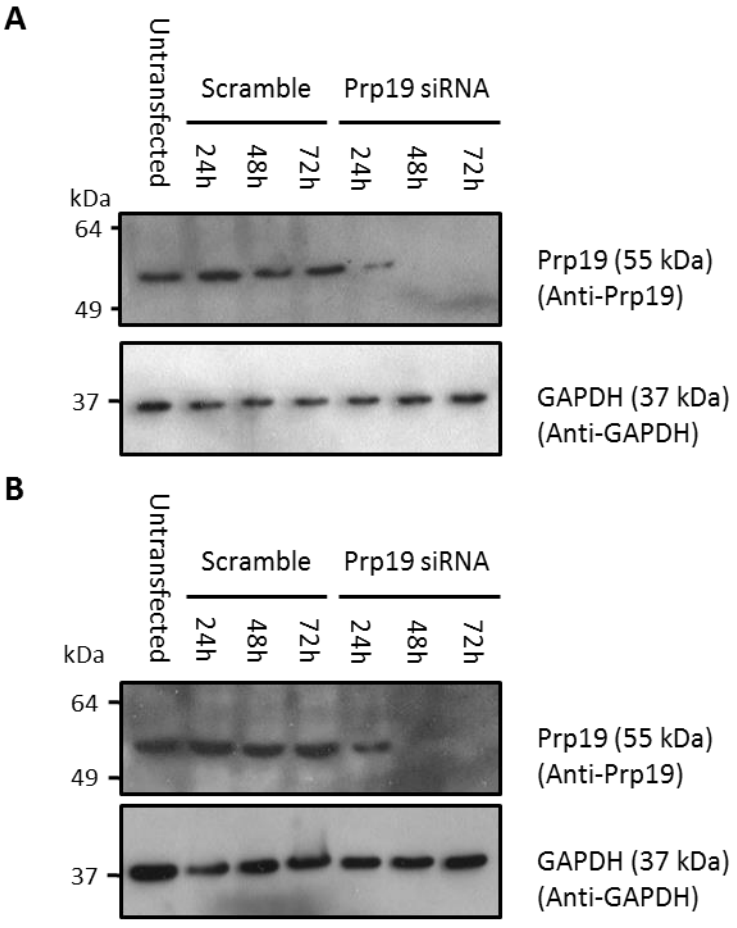

Figure 3.8: Prp19 is efficiently depleted using siRNAs in HEK 293T and 293T rKSHV.219 cells .
(a) HEK 293T cells and (b) 293T rKSHV.219 cells were transfected with siRNA specific to Prp19 or scramble siRNA. Lysates were harvested at 24, 48 and 72 hours post transfection. Samples were separated by SDS-PAGE and immunoblots were performed using antibodies specific to Prp19 and GAPDH.

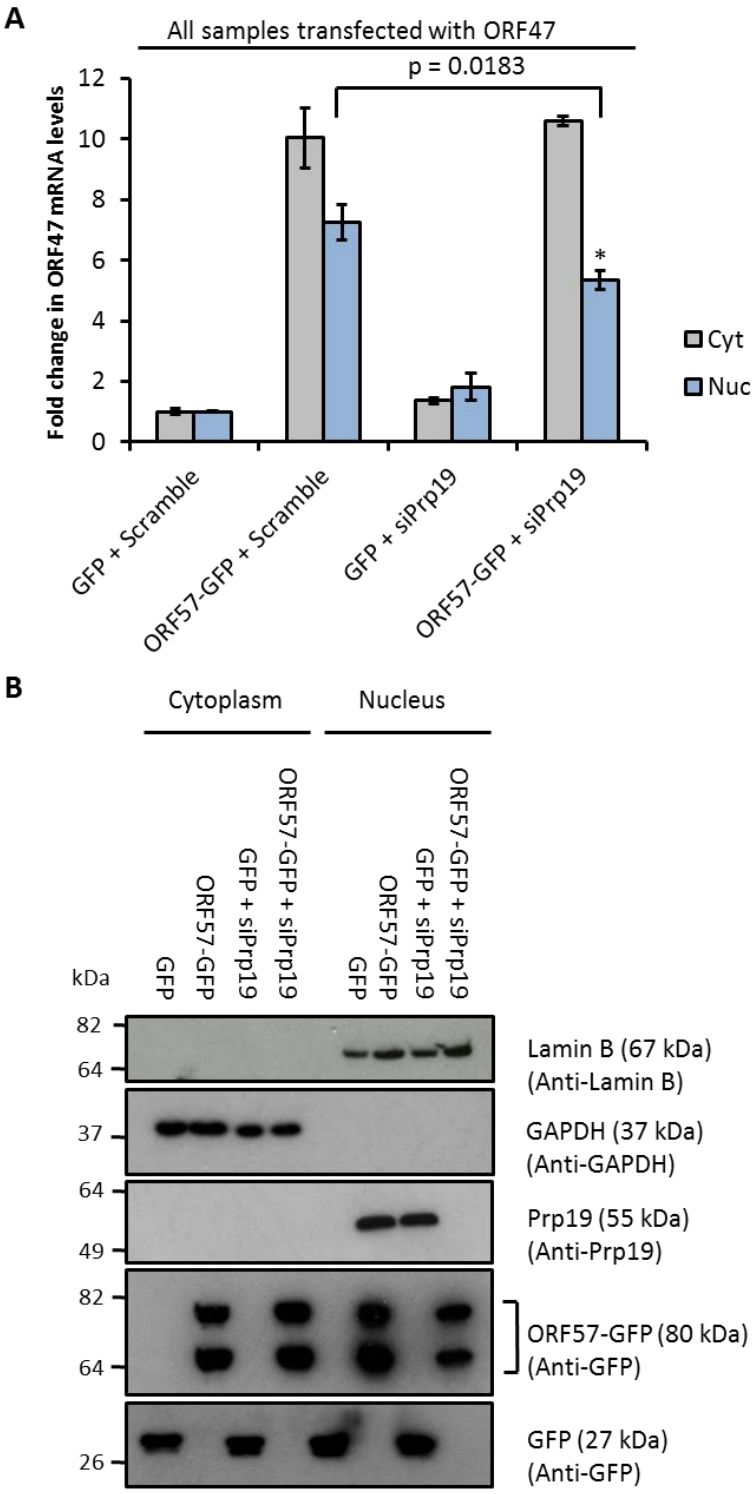

Figure 3.9: Prp19 knockdown does not affect nuclear stability or ORF57 mediated export of intronless KSHV mRNAs.

(a) HEK 293T cells were transfected with pEGFP-N1/pORF57-EGFP and pORF47 ± Prp19 specific siRNA. 24 hours post transfection cells were separated into cytoplasmic and nuclear. RNA was extracted from each fraction and subjected to DNase treatment. RNA was then reverse transcribed into cDNA using an oligo dT primer and qRT-PCR was performed using primers specific to ORF47. 3 biological replicates were combined, the relative values were displayed on a graph and the standard deviation was calculated. Error bars = SD, $p<0.01$ = **, $p<0.05$ = * compared with same fraction from GFP/ORF57-GFP + scramble control samples (b) Fractionation samples were separated by SDS-PAGE and immunoblots were performed using antibodies specific for Lamin B, GAPDH, Prp19 and GFP.

Secondly, the effect of Prp19 depletion on the ORF57-mediated splicing of the K8β transcript was subsequently examined as previously described in Section 3.5. Again, it was hypothesised that if ORF57 was hijacking Prp19 in order to promote the production of the K8α transcript, this effect would be severely reduced or ablated with the depletion of Prp19. Results show that Prp19 depletion appeared to have no effect on this process, as cells undergoing lytic reactivation were able to produce similar levels of both the K8β and K8α transcripts when transfected with siRNAs directed against Prp19 or scramble siRNA (control) **(Fig 3.10)**.

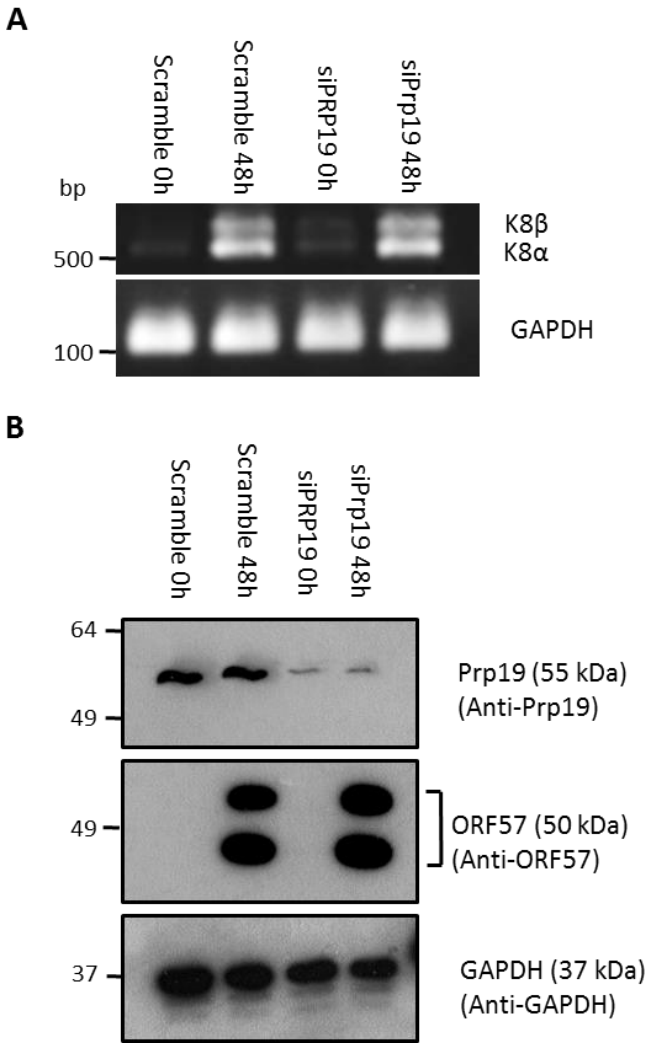

Figure 3.10: Prp19 knockdown does not affect ORF57 mediated splicing of KSHV K8 mRNA.
293T rKSHV.219 cells were transfected with Prp19 specific siRNA or scramble siRNA. 48 hours after transfection cells were either reactivated with NaBu and TPA for 24 hours (lytic infection) or left unreactivated (latent - control). (a) RNA was then extracted from cells, samples were treated with DNase and reverse transcription was performed. PCR was then performed on the resulting cDNA using primers specific for KSHV K8. GAPDH was used as a loading control. (b) Lysates were harvested at 0 and 48 hours post viral reactivation. Samples were separated by SDS-PAGE and immunoblots were performed using antibodies specific to Prp19, ORF57 and GAPDH.

In order to determine whether depletion of Prp19 had any effect on the lytic replication cycle, the effect of Prp19-HA overexpression or depletion of endogenous Prp19 on production of the late viral protein, minor capsid protein, was examined. It was hypothesised that if Prp19 has a role at immediate early, early, or late stages during KSHV lytic infection, this would be most evident at a late time point due to a magnification effect further along the lytic gene cascade. Therefore, levels of the KSHV minor capsid protein (mCP) were examined as a working antibody was available for this protein and other late KSHV protein antibodies tested were ineffective. 293T rKSHV.219 cells were transfected with either Prp19-HA, siRNAs directed against endogenous Prp19, scramble siRNA (control) or left untransfected (control). Following transfection for 24 hours (plasmid DNA) or 72 hours (siRNA) cells were either induced for the KSHV lytic cycle using sodium butyrate and TPA, or left uninduced (control). After a further 72 hours cell lysates were harvested and examined by immunoblot. Data indicated that neither Prp19-HA overexpression nor endogenous Prp19 depletion had any discernible effect on the production of KSHV minor capsid protein (Unpaired T-test: $p>0.05$) **(Fig. 3.11)**.

3.7 Assessing the role of other Prp19 complex components in ORF57 function

Previous results have demonstrated that overexpression or depletion of Prp19 displayed no effects on any of the viral pathways examined. It was therefore hypothesised that this could be due to potential redundancy in the Prp19/CDC5L complex. The predicted architecture of the Prp19/CDC5L complex shows Prp19 to be present as 4 molecules on one side of the complex, only interacting with SPF27 **(Fig. 3.12)** (Grote et al., 2010). However, CDC5L was also shown to interact with ORF57 in the SILAC immunoprecipitation experiment **(Fig. 3.3B)**. Furthermore, SILAC analysis showed a similar increase in the nucleolar levels of CDC5L as Prp19 **(Fig 3.13A)**. Therefore, CDC5L represented another potential option for depletion in order to further examine the effects of the Prp19 complex on the KSHV lytic cycle.

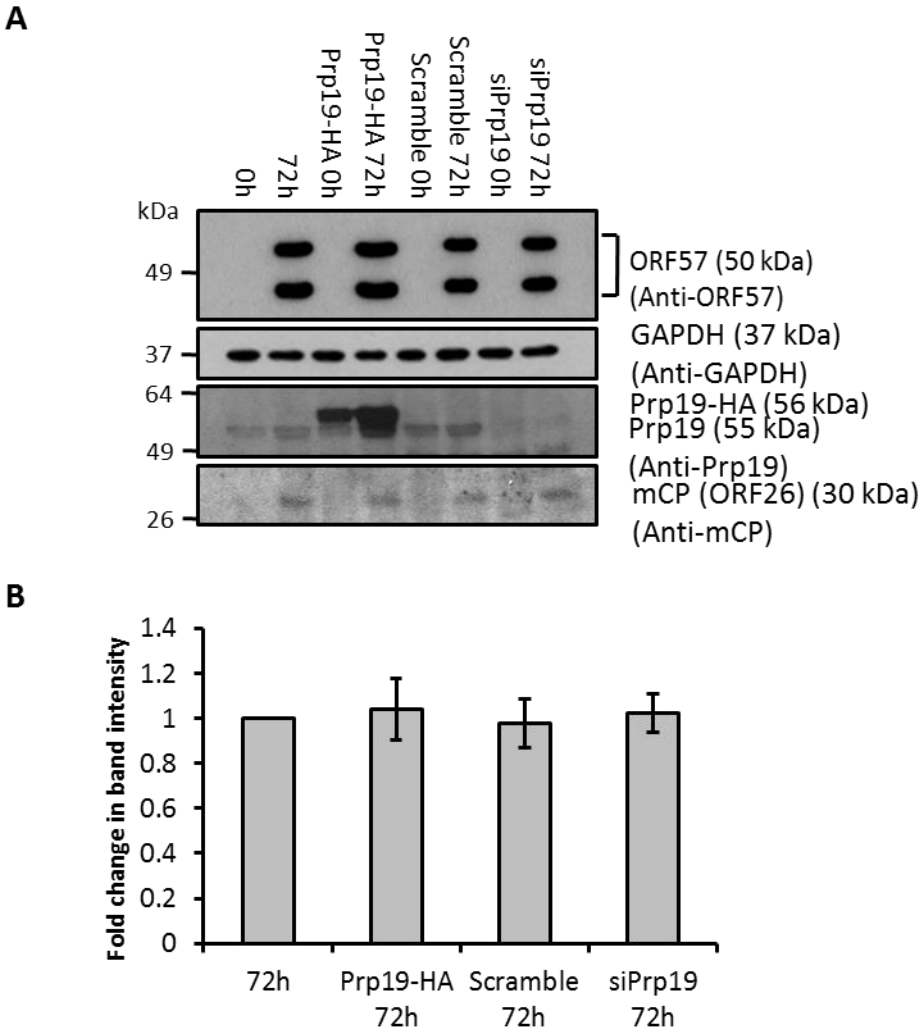

Figure 3.11: Prp19 overexpression/knockdown has no effect on KSHV minor capsid protein (mCP) ORF26 expression.

(a) 293T rKSHV.219 cells were transfected without DNA (mock), pPrp19-HA, Prp19 specific siRNA or scramble siRNA. 48 hours after transfection cells were either reactivated with NaBu and TPA for 72 hours (lytic infection) or left unreactivated (latent - control). Lysates were then harvested and proteins were separated by SDS-PAGE. Immunoblots were performed with antibodies specific to KSHV ORF57, GAPDH, Prp19 and KSHV mCP ORF26. GAPDH specific antibody was used to control for equal loading. (b) The fold change in mCP levels was calculated for each reactivated sample when compared with mock transfected reactivated 293T rKSHV.219 cells. Immunoblots were analysed using ImageJ software. Values are average of 3 independent immunoblots. Error bars = SD, $p<0.01$ = **, $p<0.05$ = * compared with 72h control sample.

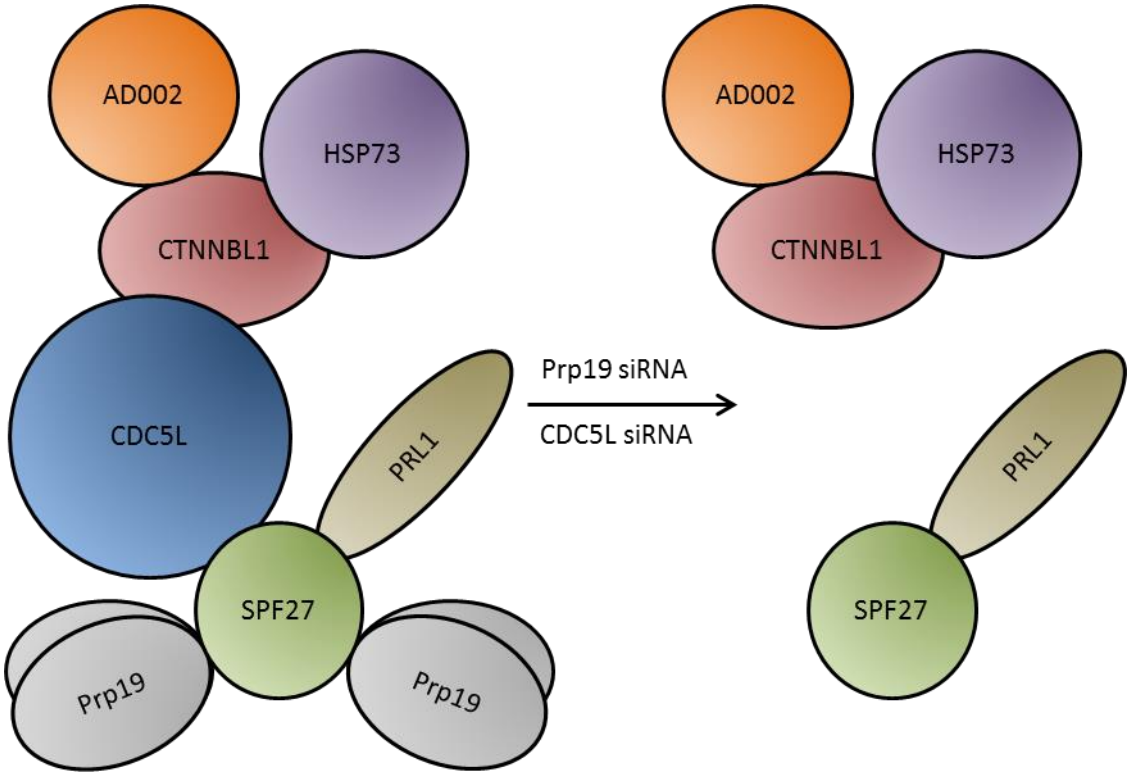

Figure 3.12: Predicted Prp19/CDC5L complex architecture and predicted effects of depletion of both Prp19 and CDC5L.
The predicted architecture of the Prp19/CDC5L complex based on numerous protein-protein interaction assays (Grote et al., 2010) and a predicted model of how this architecture would be altered by the depletion of Prp19 and CDC5L proteins by siRNA.

To examine whether ORF57 interacted with CDC5L, a co-immunoprecipitation assay was performed **(Fig 3.13B)**. Results show that CDC5L was able to interact with ORF57, in contrast to GFP control or unconjugated beads. This immunoprecipitation was performed in the presence of RNase A, suggesting this interaction is not bridged by RNA and is a direct protein-protein interaction.

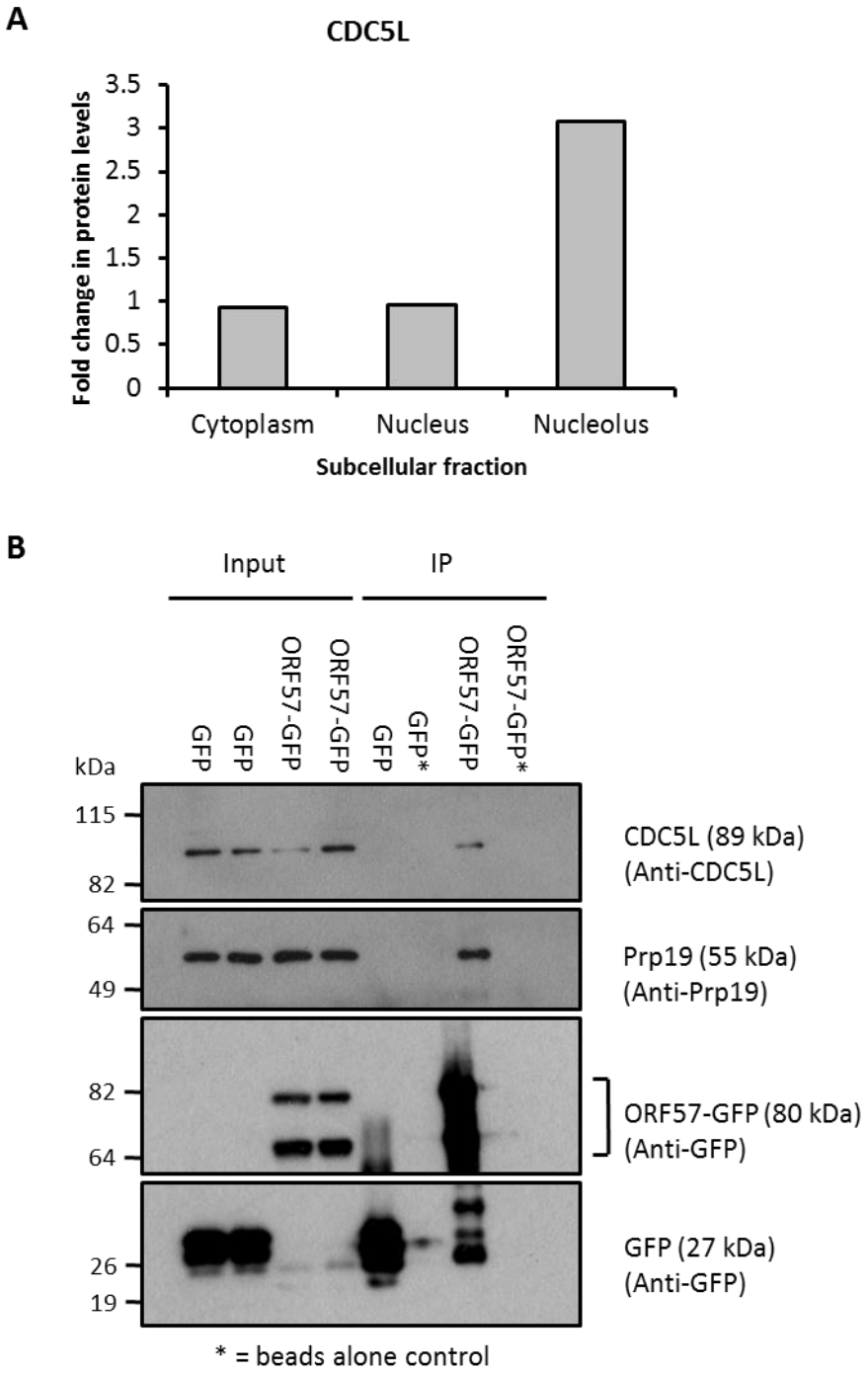

Figure 3.13: ORF57 interacts with CDC5L.
(a) Fold change increase in CDC5L levels in subcellular fractions of HEK 293T expressing an inducible ORF57 protein compared to uninduced cells. (b) HEK 293T cells were transfected with pEGFP-N1 or pORF57-EGFP. After 24 hours lysates were harvested, treated with RNase A and immunoprecipitation with GFP-trap beads was performed. Input and IP samples were separated by SDS-PAGE and immunoblots were performed using antibodies specific for CDC5L, Prp19 and GFP. Samples used for this immunoblot analysis came from the same experiment as shown in Figure 3.5.

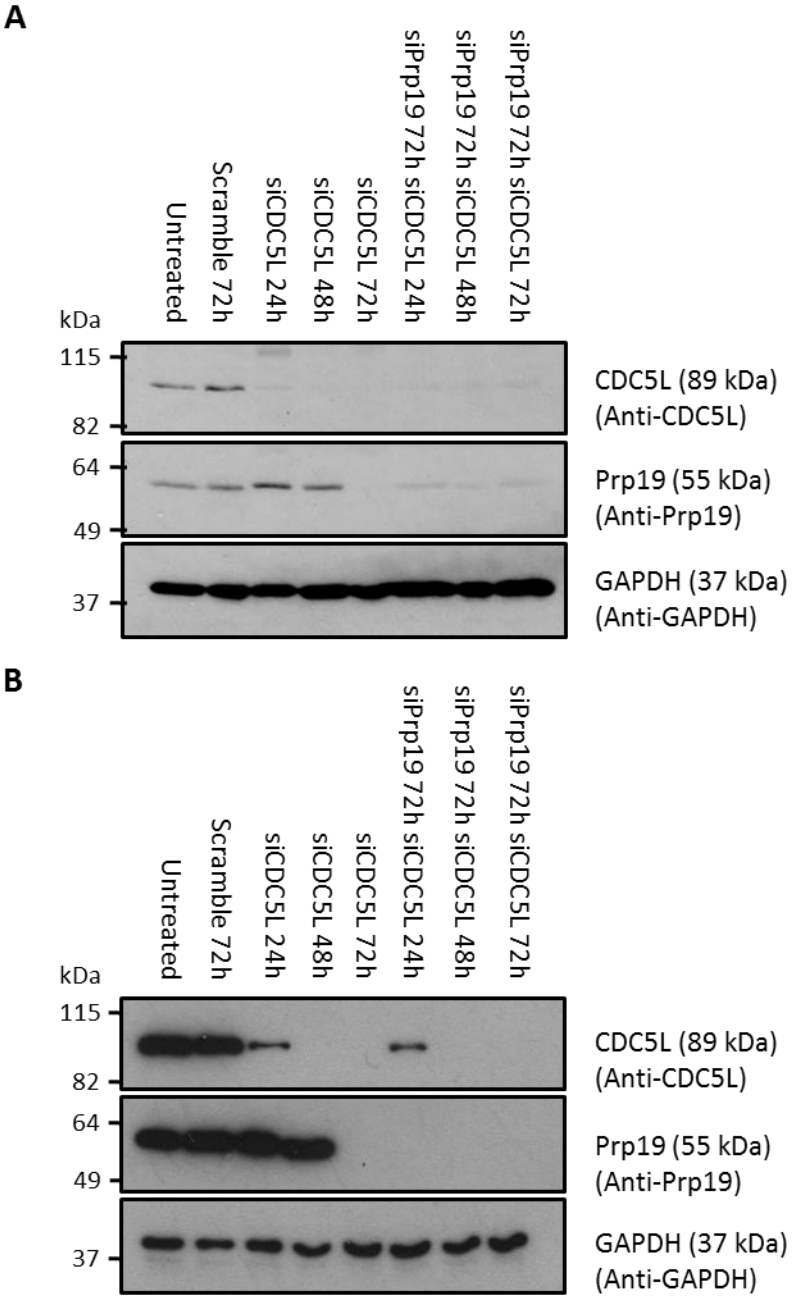

Figure 3.14: CDC5L and Prp19 are efficiently knocked down by siRNAs in HEK 293T and 293T rKSHV.219 cells.
(a) HEK 293T cells or (b) 293T rKSHV.219 cells were transfected with siRNA specific to CDC5L or both Prp19 and CDC5L or scramble siRNA. Lysates were harvested at 24, 48 and 72 hours post transfection. Samples were separated by SDS-PAGE and immunoblots were performed using antibodies specific to CDC5L, Prp19 and GAPDH. GAPDH specific antibody was used to control for equal loading.

In order to examine a possible role of CDC5L in the KSHV lytic cycle, siRNAs targeted specifically to CDC5L were used, and the efficiency of CDC5L knockdown was examined in HEK 293T and 293T rKSHV.219 cells **(Fig. 3.14)**. Cells were transfected with either scramble control siRNA, or siRNA directed against CDC5L in the absence or presence of

siRNA directed against Prp19 for 24, 48 or 72 hours. Following incubation with siRNAs, cells were harvested and protein samples were then separated by SDS PAGE and analysed by immunoblot using antibodies directed against Prp19, CDC5L and GAPDH. Results showed that siRNAs targeted against CDC5L were highly effective at reducing CDC5L protein levels at 24 hours post transfection, with increased efficiency at 48 and 72 hours. In addition, they were also efficient when cells were simultaneously treated with siRNA directed against Prp19. Interestingly, Prp19 protein levels were observed to decrease after 72 hours incubation with siRNA directed against CDC5L. This may be due to the inability of the Prp19/CDC5L complex to splice Prp19 mRNA efficiently without the CDC5L protein present, or decreased complex stability.

3.8 Depletion of Prp19, CDC5L or both simultaneously has little effect on the nuclear export or stability of KSHV intronless mRNAs, or the splicing of KSHV intron containing mRNAs

Previous attempts to examine the effects of the Prp19/CDC5L complex on the nuclear export and stability of viral intronless mRNAs only focussed on Prp19 and did not include CDC5L depletion. Therefore, the same previously described set of experiments were repeated upon CDC5L depletion or in combination with Prp19 depletion. Cells were transfected with GFP or ORF57-GFP, as well as either scramble siRNA, siRNA directed against Prp19, siRNA directed against CDC5L or a combination of siRNAs directed against both Prp19 and CDC5L simultaneously. Cells were then split into cytoplasmic and nuclear fractions, and immunoblots were performed to analyse the levels of GAPDH, LaminB, Prp19, CDC5L, GFP and ORF57-GFP present in the fractions **(Fig. 3.15A)**. Fractionation was shown to be efficient by the presence of GAPDH only in the cytoplasmic fractions, and LaminB only in the nuclear fractions. Levels of extracted ORF47 and GAPDH mRNA were analysed using qRT-PCR, and the relative changes in ORF47 mRNA levels were determined **(Fig. 3.15B)**. Results showed that depletion of Prp19, CDC5L or both simultaneously did not appear to have an effect on the nuclear export or stability of ORF47 mRNA. This data suggests that the Prp19/CDC5L complex is not involved in the nuclear export or stability of KSHV intronless mRNAs.

To examine a possible role of CDC5L on the splicing of viral intron-containing mRNA, the K8 splicing assay was also repeated in the presence of CDC5L specific siRNAs. Cells were transfected with either scramble siRNA, siRNA directed against Prp19, siRNA directed against CDC5L or a combination of siRNAs directed against both Prp19 and CDC5L simultaneously. Cells were subsequently exposed to KSHV lytic replication for 24 hours, or remained untreated as a latent control, before total RNA was harvested and levels of partially and fully spliced K8 mRNA were analysed using RT-PCR. GAPDH was used as a loading control. Results showed that depletion of Prp19, CDC5L or both simultaneously had no noticeable effect on the levels of partially or fully spliced K8 mRNA after 24 hours of virus lytic cycle reactivation in 293T rKSHV.219 cells. This data suggests the Prp19/CDC5L complex is not involved in the splicing of KSHV encoded intron containing mRNAs.

3.9 Depletion of both CDC5L and Prp19 results in a minor reduction in KSHV minor capsid protein levels

Previous attempts to examine the effects of Prp19 on the levels of KSHV encoded late protein production failed to show any effect. Therefore the experiment was repeated using cells that were also depleted of CDC5L. Cells were transfected with either scramble siRNA, siRNA directed against Prp19, siRNA directed against CDC5L, a combination of siRNAs directed against both Prp19 and CDC5L simultaneously, or untransfected (control). Cells were subsequently exposed to KSHV lytic cycle for 72 hours, or untreated as a latent control, before cells were lysed with modified RIPA buffer. Protein samples were separated by SDS PAGE and levels of CDC5L, Prp19, GAPDH and KSHV minor capsid protein were analysed by immunoblot **(Fig. 3.17A)**. Results showed that depletion of CDC5L failed to reduce the amount of KSHV mCP, however, depletion of both CDC5L and Prp19 resulted in a minor reduction of ~34% in KSHV mCP levels present in the sample when analysed by densitometry **(Fig. 3.17B)**. This suggests that inhibition of Prp19/CDC5L complex formation and function may have a minor inhibitory effect on KSHV mRNA or protein levels during the lytic cycle.

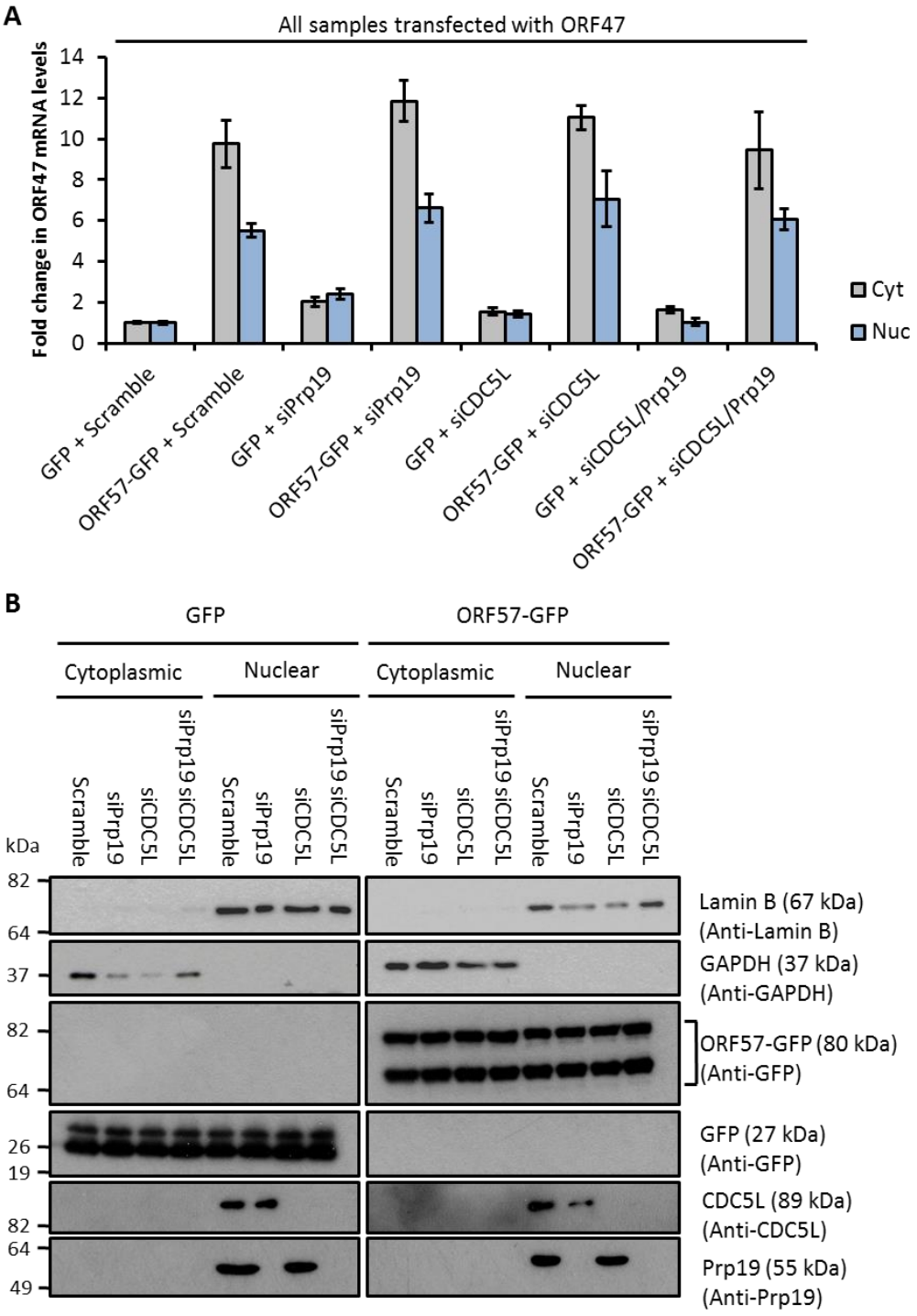

Figure 3.15: CDC5L and Prp19 double knockdown does not affect nuclear stability or ORF57 mediated export of intronless KSHV mRNAs.

(a) HEK 293T cells were transfected with scramble siRNA (control), Prp19 specific siRNA, CDC5L specific siRNA or a combination of both for 48 hours, then transfected with either pORF47 and either pEGFP-N1 or pORF57-EGFP. 24 hours later cells were separated into cytoplasmic and nuclear fractions. RNA was then extracted from each fraction and subjected to DNase treatment. RNA was then reverse transcribed into cDNA and qRT-PCR was performed using primers specific to ORF47. 3 biological replicates were combined, the relative values were displayed on a graph and the standard deviation was calculated. Error bars = SD, $p<0.01$ = **, $p<0.05$ = * compared with same fraction from GFP/ORF57-GFP + scramble control samples. (b) Fractionation samples were separated by SDS-PAGE and immunoblots were performed using antibodies specific for LaminB, GAPDH, Prp19, CDC5L and GFP.

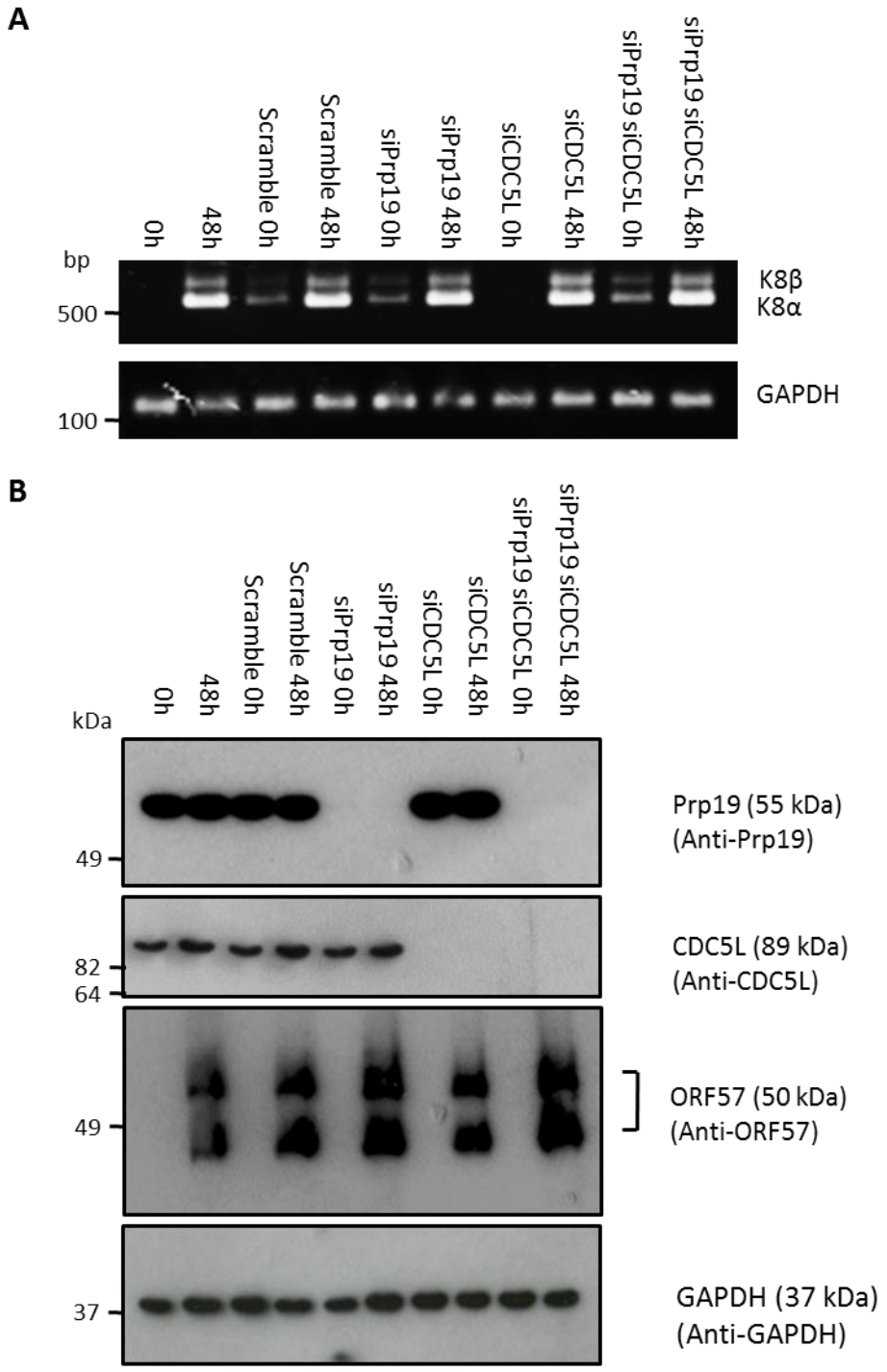

Figure 3.16: Prp19 and CDC5L double knockdown does not affect ORF57 mediated splicing of KSHV K8 mRNA.

293T rKSHV.219 cells were transfected with Prp19 or CDC5L specific siRNA, a combination of both or scramble siRNA. 48 hours after transfection cells were either reactivated with NaBu and TPA for 24 hours (lytic infection) or left unreactivated (latent - control). (a) RNA was then extracted from cells, samples were treated with DNase and reverse transcription was performed. PCR was then performed on the resulting cDNA using primers specific for KSHV K8. PCR products were run on a 1% Agarose gel and visualised with a UV scanner. GAPDH was used as a loading control. (b) Lysates were harvested at 0 and 48 hours post viral reactivation. Samples were separated by SDS-PAGE and immunoblots were performed using antibodies specific to Prp19, CDC5L, ORF57 and GAPDH.

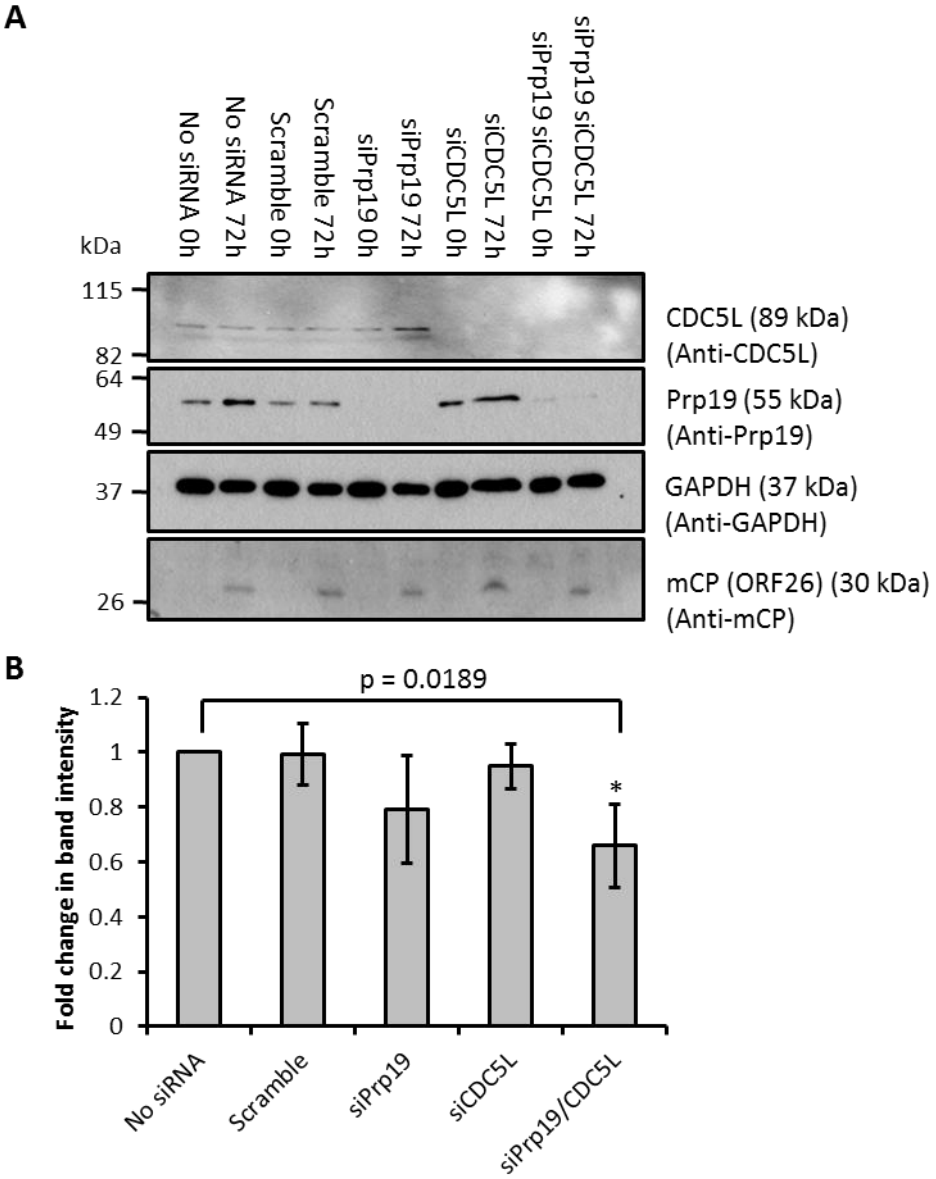

Figure 3.17: Depletion of both Prp19 and CDC5L causes minor reduction in KSHV minor capsid protein production.

(a) 293T rKSHV.219 cells were transfected without DNA (mock), pPrp19-HA, Prp19 specific siRNA or scramble siRNA. 48 hours after transfection cells were either reactivated with NaBu and TPA for 72 hours (lytic infection) or left unreactivated (latent - control). Lysates were then harvested and proteins were separated by SDS-PAGE. Immunoblots were performed with antibodies specific to KSHV ORF57, GAPDH, Prp19 and KSHV mCP ORF26. GAPDH specific antibody was used to control for equal loading. (b) The fold change in mCP levels was calculated for each reactivated sample when compared with mock transfected reactivated 293T rKSHV.219 cells. Immunoblots were analysed using ImageJ software. Values are average of 3 independent immunoblots. Error bars = SD, $p<0.01$ = **, $p<0.05$ = * compared with No siRNA control sample.

3.10 ORF57 limits activation of the DNA damage response signalling cascade caused by Prp19 overexpression

Prp19 has been demonstrated to play a role in the early stages of the DNA damage signalling pathway, sensing sites of RPA bound single stranded DNA, ubiquitylating RPA through its E3 ubiquitin ligase function and facilitating the recruitment of ATRIP and ATR to these sites (Maréchal et al., 2014). These interactions support the well characterised ATR-Chk1 DNA damage response pathway, ultimately leading to one of two potential outcomes: DNA damage repair or apoptosis (Shiloh, 2001).

Previous work has shown that ORF57 induces DNA damage, primarily through the recruitment of the human TREX complex, in a process that is necessary for intronless viral mRNA nuclear stability, export and efficient translation (Jackson et al., 2014). The DNA damage occurs due to the inhibition of events during cellular transcription, when a short 8bp RNA:DNA duplex forms in the transcription bubble (Westover, 2004). hTREX usually binds newly synthesised mRNA, increasing stability and efficiency of nuclear export, but also reducing the potential of the newly synthesised mRNA to "thread back" and bind to an extended region of its complementary DNA sequence before the DNA duplex can reanneal. Inhibition of this process leads to the formation of an RNA:DNA hybrid known as an R-Loop (Köhler and Hurt, 2007; Masuda et al., 2005; Aguilera and García-Muse, 2012). R-loops have previously been characterised as agents of DNA damage (Gan et al., 2011). During KSHV lytic replication, ORF57-mediated recruitment of hTREX onto viral mRNAs also leads to R-loop formation and subsequent DNA damage (Jackson et al., 2014). This coupled with the involvement of Prp19 in the DNA damage response, led to the hypothesis that ORF57 and Prp19 may prevent a DDR at sites of R-Loop formation and, therefore, also prevent cell cycle arrest/apoptosis which would limit the replication potential of KSHV.

To explore a possible link between ORF57 and Prp19 in the DNA damage response, a positive control was required, and the compound camptothecin was elected for this purpose. Camptothecin binds and stabilises topoisomerase I bound DNA, preventing the ligation of DNA by topoisomerase I, thus initiating a DNA damage response and, ultimately, apoptosis (Liu et al., 2000). Camptothecin has been shown to cause DNA

strand breaks in cells, eventually leading to apoptosis, and therefore mimics the predicted effects of widespread R-loop formation and a subsequent lack of a productive DNA damage response (Yamauchi et al., 2011). The effect of camptothecin on HEK 293T cells was examined by incubating cells with increasing amounts of camptothecin for 4 hours, compared with DMSO control. Protein lysates were harvested following treatment, and samples were analysed by immunoblotting, using antibodies directed against S15 phosphorylated p53, T21 phosphorylated RPA, RPA32 and GAPDH (loading control) **(Fig. 3.18)**. Camptothecin treatment, but not DMSO treatment, caused the phosphorylation of both RPA and p53 at all tested concentrations.

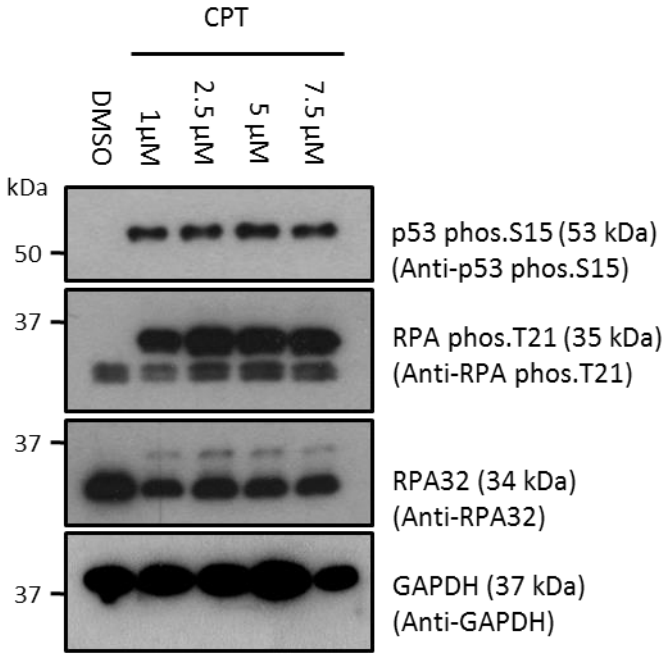

Figure 3.18: Camptothecin induces DNA damage response in HEK 293T cells.
(a) HEK 293T cells were treated with 0.75% DMSO in DMEM (control) or 1, 2.5, 5 or 7.5μM camptothecin (CPT) in DMEM for 4 hours. Lysates were harvested, samples were separated by SDS-PAGE and immunoblots were performed with antibodies specific to p53 (phosphorylated at S15), RPA (phosphorylated at T21), RPA, and GAPDH. GAPDH specific antibody was used to control for equal loading.

In order to investigate the effect of the Prp19-mediated DNA damage response during ORF57 expression, HEK 293T cells were transfected with either ORF57-GFP or a GFP control plasmid, in the presence or absence of overexpressed Prp19-HA. 24 hours post transfection, cells were treated with either 5 μM camptothecin or DMSO (control) for 4 hours. Protein lysates were subsequently harvested and the levels of GAPDH, Prp19,

Prp19-HA, ORF57-GFP, GFP, T21 phosphorylated RPA and S15 phosphorylated p53 were examined by immunoblot, using GAPDH as a loading control **(Fig. 3.19)**. GFP control cells expressing Prp19-HA exhibited a dramatic increase in phosphorylated RPA and p53. This effect has not been previously reported, however, the ubiquitylated form of Prp19 is known to be significantly increased upon Prp19 overexpression, and this form is also increased during the activation of the ATR-Chk1 DDR pathway (Lu and Legerski, 2007). This may suggest that Prp19 overexpression is enough to trigger the phosphorylation and activation of certain proteins in this pathway. Interestingly, ORF57-GFP expressing cells did not exhibit this significant increase in p53 and RPA phosphorylation following Prp19-HA overexpression. ORF57-GFP expressing cells did exhibit a slightly higher background level of RPA and p53 phosphorylation to negative controls, but these levels were significantly lower than those in the Prp19-HA expressing GFP cells. This suggests that the interaction between ORF57 and Prp19 may act to inhibit some functions of Prp19 in the ATR-Chk1 DNA damage response pathway, ultimately limiting the phosphorylation of p53 and RPA. Importantly, camptothecin treated cells all exhibited similar levels of RPA and p53 phosphorylation, irrespective of ORF57-GFP, GFP or Prp19-HA expression, suggesting that ORF57 expression is unable to override these phosphorylation events following camptothecin induced DNA damage. This suggests some redundancy in this pathway, and indeed other agents are known to be able to phosphorylate p53 and RPA following activation of the ATR-Chk1 DNA damage response pathway.

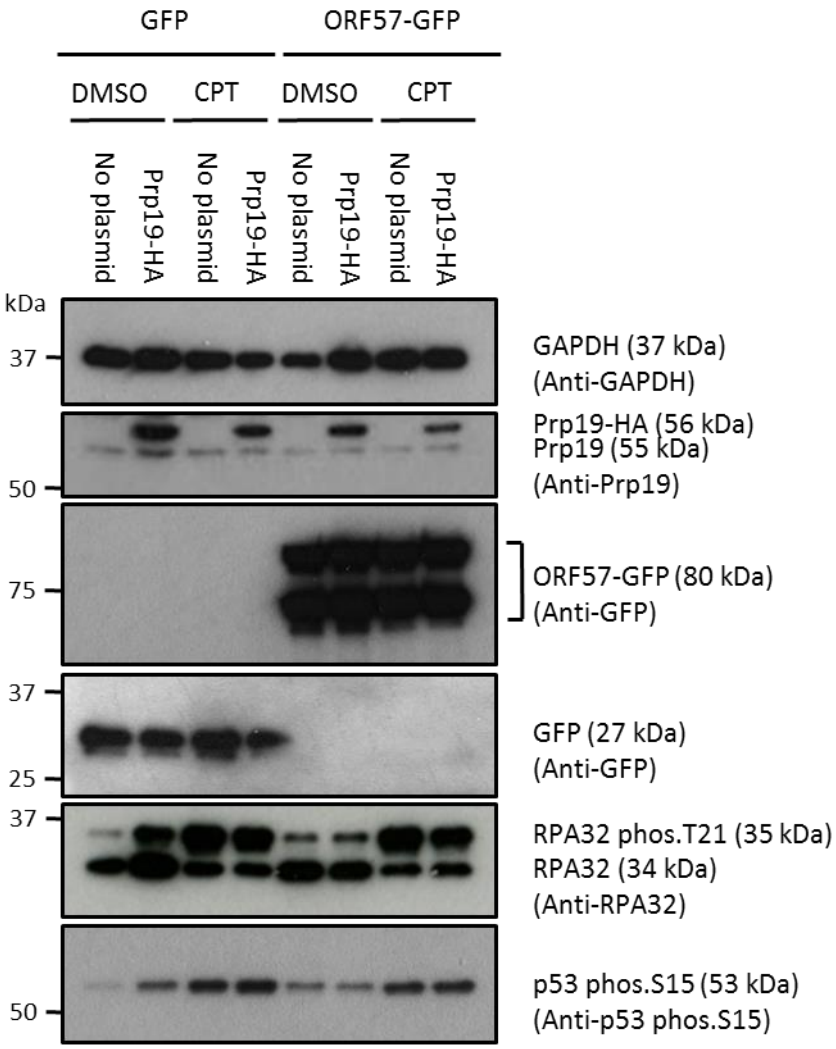

Figure 3.19: ORF57 expression limits DNA damage response caused by Prp19-HA overexpression in HEK 293T cells.

(a) HEK 293T cells transfected with pEGFP-N1/pORF57-EGFP and no DNA (mock) or pPrp19-HA were treated with 0.5% DMSO in DMEM or 5 µM camptothecin in DMEM. 4 hours after treatment lysates were harvested and separated by SDS-PAGE. Immunoblots were performed using antibodies specific for GAPDH, Prp19, GFP, RPA (phosphorylated at T21) and p53 (phosphorylated at S15). GAPDH specific antibody was used to control for equal loading.

3.11 ORF57 ablates RPA speckle formation and relocalises to discrete subnuclear puncta with Prp19 during Camptothecin induced DNA damage

The canonical DNA strand break response begins with RPA binding to single stranded DNA, before becoming hyperphosphorylated (Wu et al., 2005). RPA coated ssDNA is sensed and bound by various components of the DDR, including Prp19, ATR and ATRIP (Maréchal et al., 2014 p. 19). Prp19 recruits more ATRIP and ATR to the damaged site,

and also ubiquitinates RPA, and both of these processes lead to the subsequent phosphorylation of ATR substrates. p53 is then phosphorylated by ATR, and this process leads to the activation of the p53-mediated signalling cascade, ultimately triggering apoptosis **(Fig. 3.20)**. In order to further investigate the putative ORF57-mediated inhibition of Prp19 during the ATR-Chk1 DNA damage response pathway, the localisation of the closest (temporal and spatial) known proteins involved in the signalling cascade were examined upon ORF57-GFP expression. To this end, the subcellular localisation of Prp19 and RPA was examined in control vs ORF57 expressing cells in the absence or presence of DNA damage **(Fig. 3.21)**. Prp19 specifically localised to nucleoli upon ORF57 expression, as had been previously been observed **(Fig. 3.4)**. During DMSO treatment, RPA showed diffuse nuclear staining in both ORF57-GFP and GFP expressing cells **(Fig. 3.21A)**. However, during camptothecin treatment, GFP expressing cells displayed a speckled nuclear distribution of RPA. RPA foci have previously been observed, and it has been suggested that they represent sites of RPA bound ssDNA. Surprisingly, Prp19 was not observed to localise to these foci, suggesting either that the involvement of RPA or Prp19 in this process is transient, or that the observed foci are not sites of ssDNA. RPA subnuclear puncta were not seen in ORF57-GFP expressing cells **(Fig. 3.21B)**, suggesting that ORF57 is able to block an as yet uncharacterised function of RPA. Furthermore, upon camptothecin treatment, ORF57-GFP and Prp19 were seen to localise to discrete nuclear foci, particularly evident at the nuclear periphery, and somewhat reminiscent of the previously described RPA speckles. This localisation of ORF57-GFP has not been previously reported, and further indicates an effect of ORF57 on the roles of Prp19 during the ATR-Chk1 DDR. Prp19 and ORF57-GFP still appeared to colocalise in the nucleoli of camptothecin treated cells, but this effect was partially masked by the large numbers of other nuclear foci.

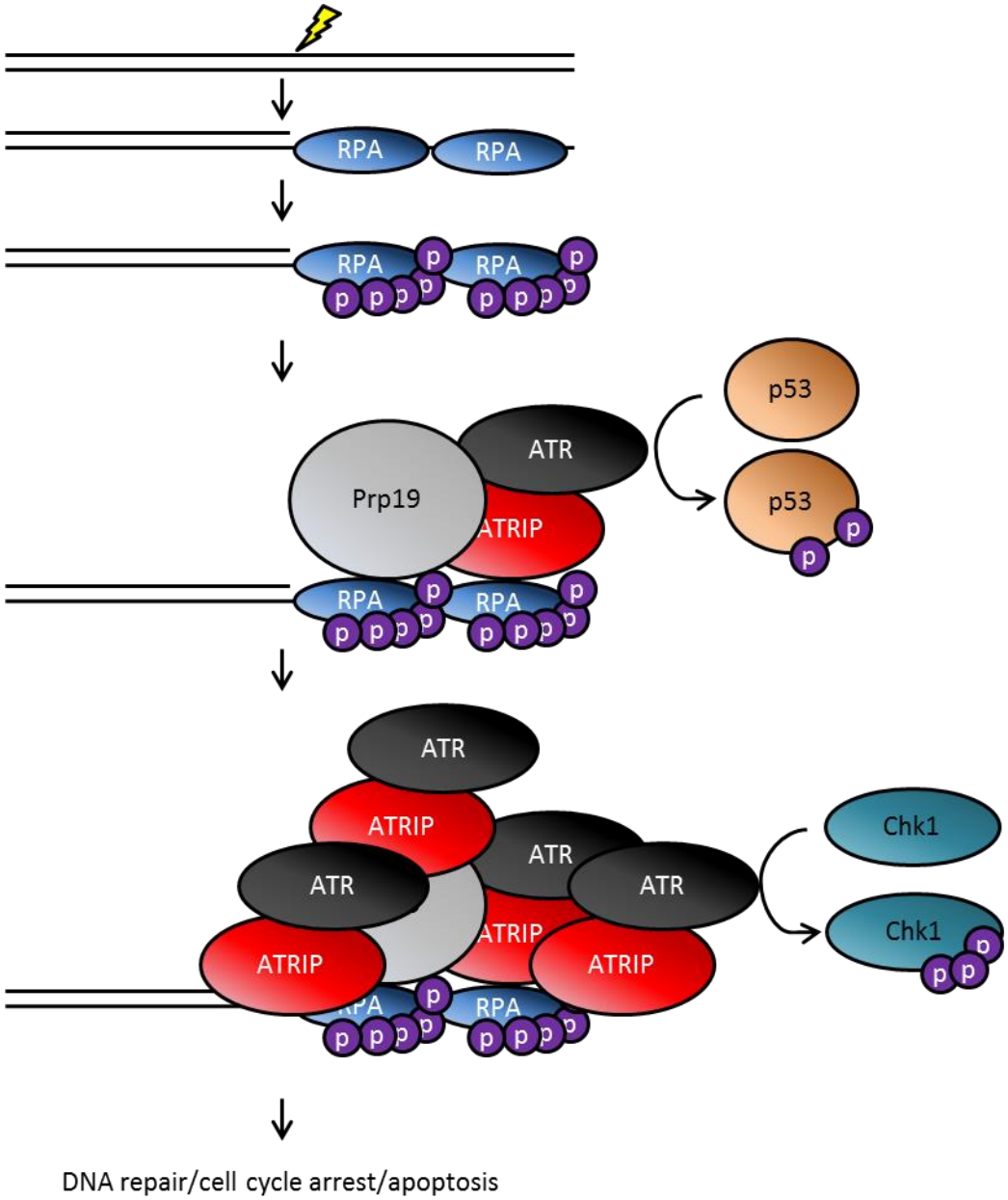

Figure 3.20: Involvement of RPA, ATRIP, ATR, p53 and Prp19 in the DNA single strand break response. Following the generation of a DNA single strand break, RPA binds to the exposed strand and is subsequently phosphorylated. Phosphorylated RPA is able to recruit ATR, the ATR cofactor ATRIP and Prp19. ATR is able to phosphorylate p53 and Prp19 is then able to recruit more ATR/ATRIP complexes to the site. ATR then phosphorylates Chk1, and this begins a signalling cascade designed to bring more DNA damage response proteins to the damaged site, resulting in strand break repair.

Prp19-HA overexpression was previously demonstrated to cause a relocalisation of ORF57 to nuclear speckles, suggesting ORF57 is able to exert control over the lower endogenous levels of Prp19, but not overexpressed Prp19 **(Fig. 3.4)**. It was therefore hypothesised that overexpression of Prp19-HA may be able to overcome the proposed block of function attributed to ORF57. Therefore, a similar experiment was performed to examine the effect of overexpression of Prp19-HA during camptothecin induced

DNA damage. Prp19-HA was shown to relocalise to the nuclear periphery, but not specifically to ORF57-GFP peripheral speckles **(Fig 3.22)**. Prp19-HA overexpression failed to rescue the RPA speckle phenotype in ORF57-GFP expressing cells in the presence of camptothecin.

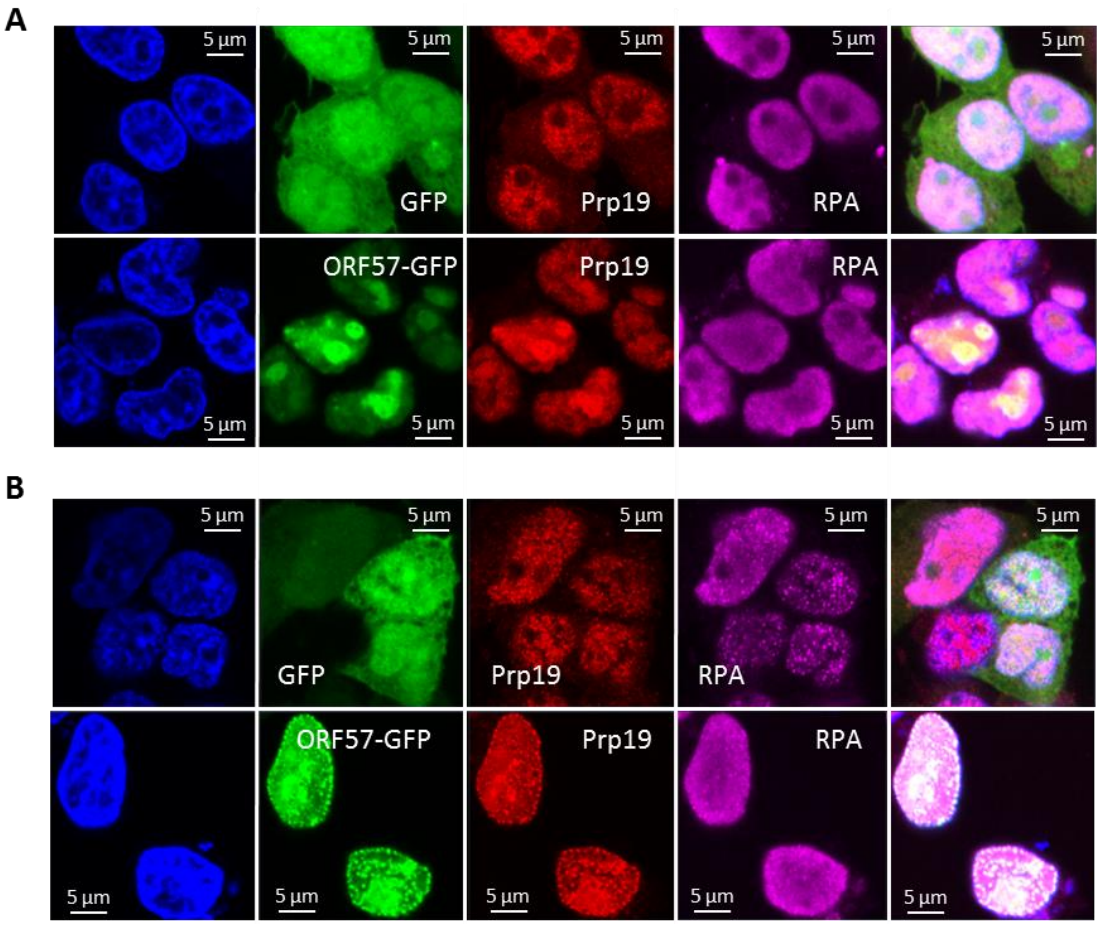

Figure 3.21: Aberrantly localised ORF57-Prp19 complex inhibits relocalisation of RPA to discrete nuclear puncta during Camptothecin treatment in HEK 293T cells.
(a) HEK 293T cells transfected with pEGFP-N1 or pORF57-EGFP were treated with 0.5% DMSO and (b) 5 µM CPT for 2 hours before being fixed and stained with antibodies specific to Prp19 and RPA. Slides were analysed using a Zeiss LSM510 confocal laser scanning microscope.

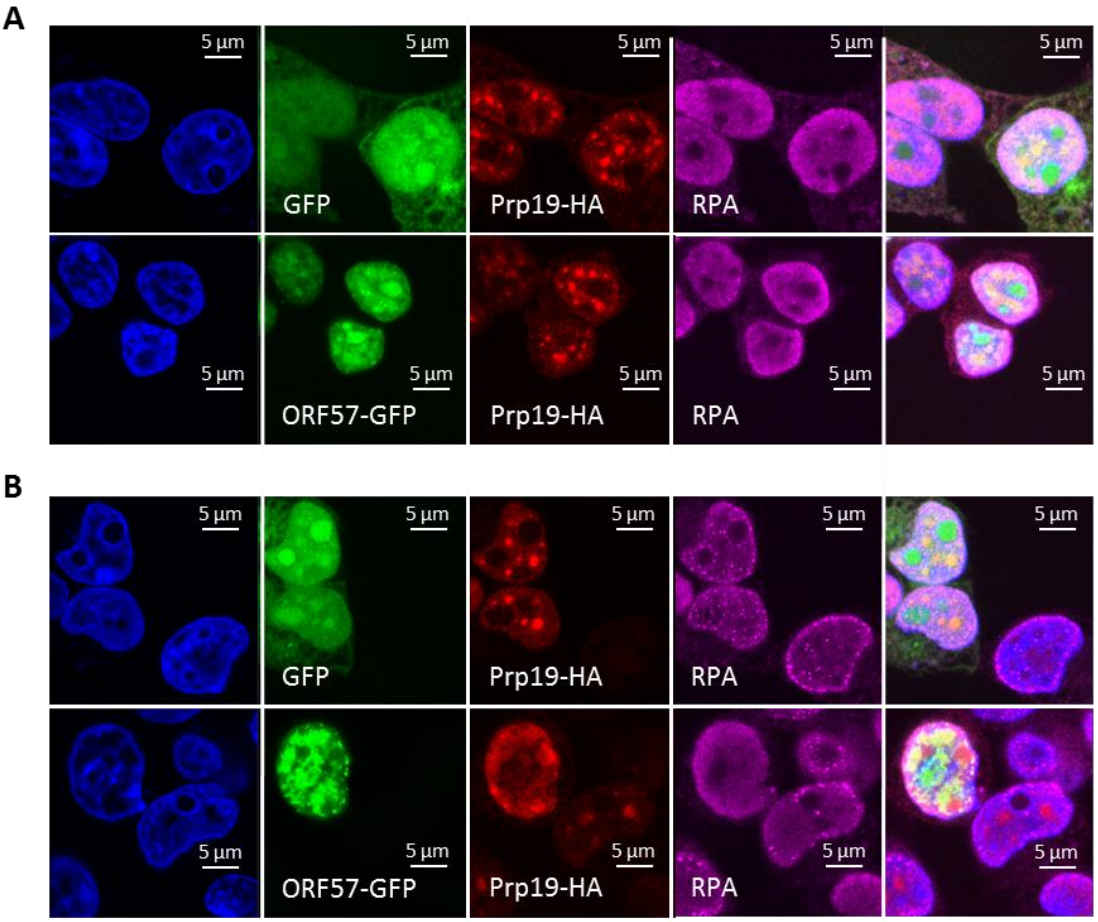

Figure 3.22: Prp19-HA overexpression does not rescue RPA defect or affect speckled rearrangement of ORF57-GFP and Prp19.
(a) HEK 293T cells transfected with pPrp19-HA as well as pEGFP-N1 or pORF57-EGFP were treated with 0.5% DMSO and (b) 5 µM CPT for 2 hours before being fixed and stained with antibodies specific to Prp19 and RPA. Slides were analysed using a Zeiss LSM510 confocal laser scanning microscope.

3.12 ATRIP colocalises with ORF57-Prp19 puncta during Camptothecin induced DNA damage

A second protein which has a close temporal and spatial involvement to Prp19 in the ATR-Chk1 DDR pathway is the ATR cofactor ATRIP. In order to further characterise the ORF57-Prp19 subnuclear puncta that form in the presence of DNA damage, ATRIP localisation was examined in the presence of ORF57-GFP/GFP and in cells treated with either camptothecin/DMSO using confocal microscopy **(Fig. 3.23)**. ATRIP displayed diffuse cellular staining in GFP control cells treated with DMSO and camptothecin, however, surprisingly, ATRIP localised to nucleoli in ORF57-GFP expressing cells treated with DMSO, and displayed a similar distribution to Prp19 in ORF57-GFP expressing cells treated with camptothecin. These results indicate that Prp19 and ATRIP are still able to

interact at ORF57 nuclear foci as well as nucleoli. The association at the nuclear foci may indicate that Prp19 is not inhibited from its role in recruiting ATRIP following DNA damage, however the presence of ATRIP at nucleoli may suggest that the interaction between ORF57 and Prp19 leads to the recruitment of ATRIP, even in the absence of DNA damage, via an unknown mechanism.

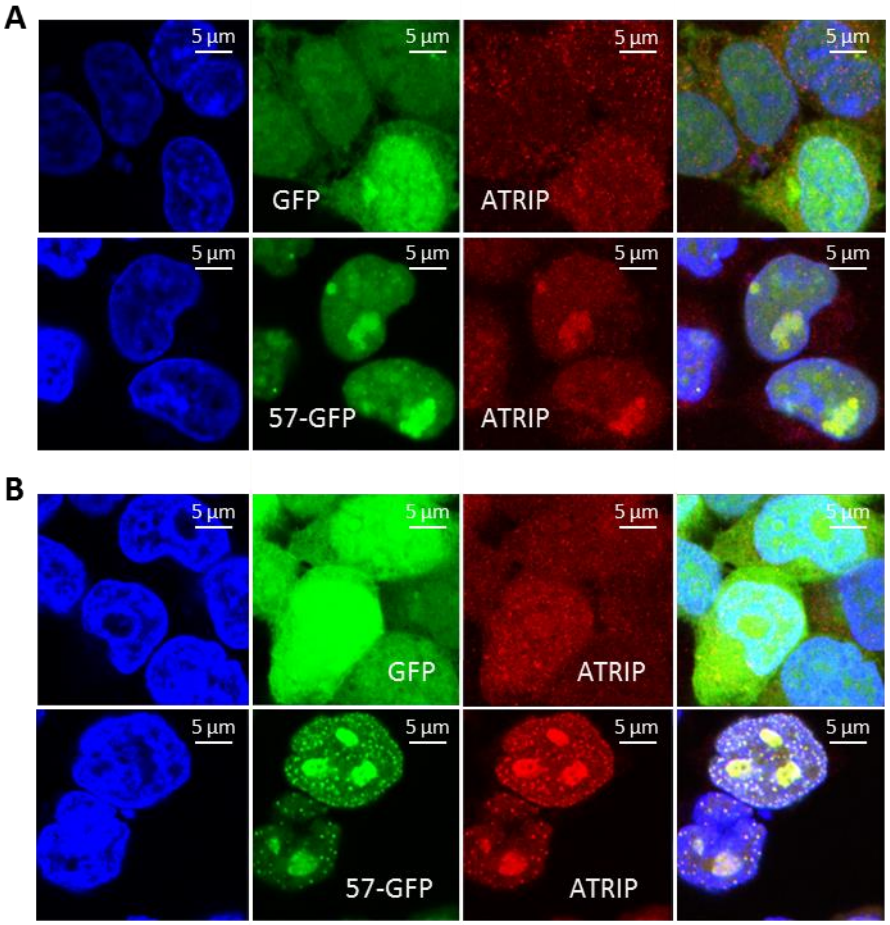

Figure 3.23: ATRIP colocalises with ORF57-Prp19 complex in discrete subnuclear puncta during Camptothecin treatment in HEK 293T cells.
(a) HEK 293T cells transfected with pEGFP-N1 or pORF57-EGFP were treated with 0.5% DMSO and (b) 5 µM CPT for 2 hours before being fixed and stained with antibodies specific to ATRIP. Slides were analysed using a Zeiss LSM510 confocal laser scanning microscope.

The ablation of RPA speckles in the presence of ORF57-GFP, combined with the relocalisation of ORF57-GFP, Prp19 and ATRIP to distinct nuclear foci led to the hypothesis that ORF57-GFP, Prp19 and ATRIP localise to sites of DNA damage, but ORF57 is able to block one or more functions of Prp19, ultimately preventing an unknown modification of RPA and causing a partial block on the ATR-Chk1 pathway **(Fig. 3.24)**. This is also believed to apply to cells undergoing DNA damage by ORF57-mediated R-loops, however, this effect is likely to be less obvious than in cells

subjected to camptothecin induced DNA damage. Indeed, a few small ORF57 speckles can be observed in many of the ORF57-GFP expressing DMSO control cells examined by confocal microscopy, possibly indicating sites of R-loop induced DNA damage. This would suggest that ORF57 recruits Prp19 and ATRIP to sites of DNA damage, and that the recruitment of these proteins to nucleoli is a side effect of this process, brought about by the high levels of ORF57 present in nucleoli.

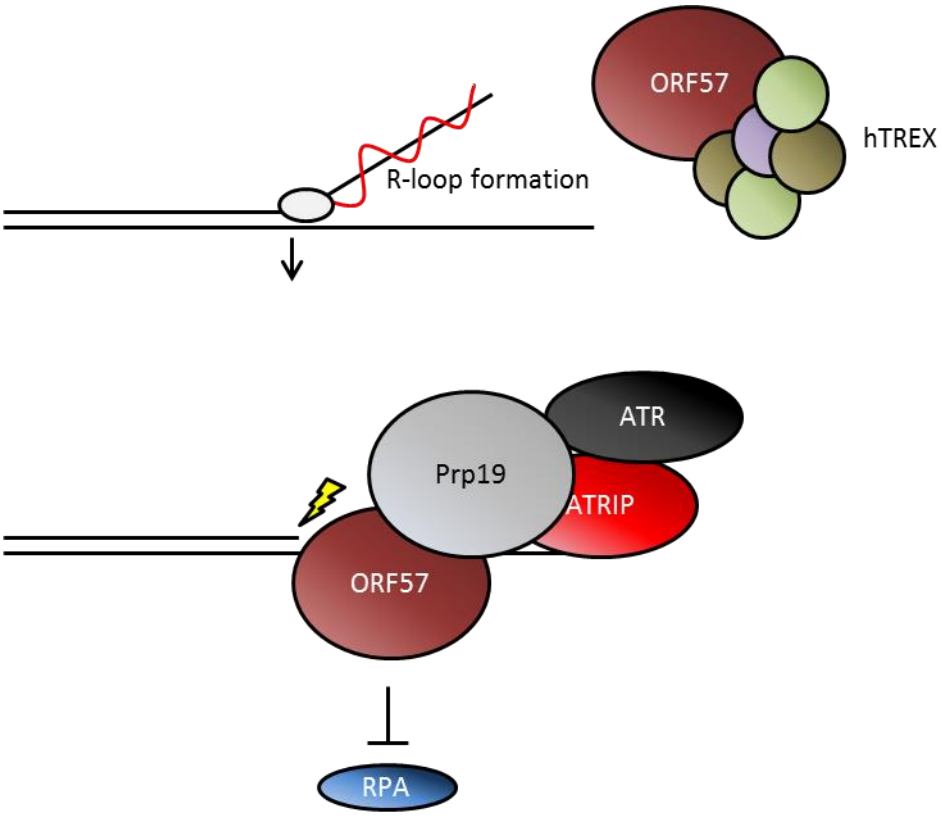

Figure 3.24: Formation of R-loops and inhibition of DNA damage response by ORF57.
ORF57 recruitment of hTREX complex prevents hTREX binding to newly synthesised mRNAs, allowing mRNAs to bind to complementary DNA strand, forming R-loops. Prp19, ATRIP and ORF57 are recruited to sites of DNA damage, but normal RPA function is inhibited by an unknown mechanism, preventing the formation of RPA speckles.

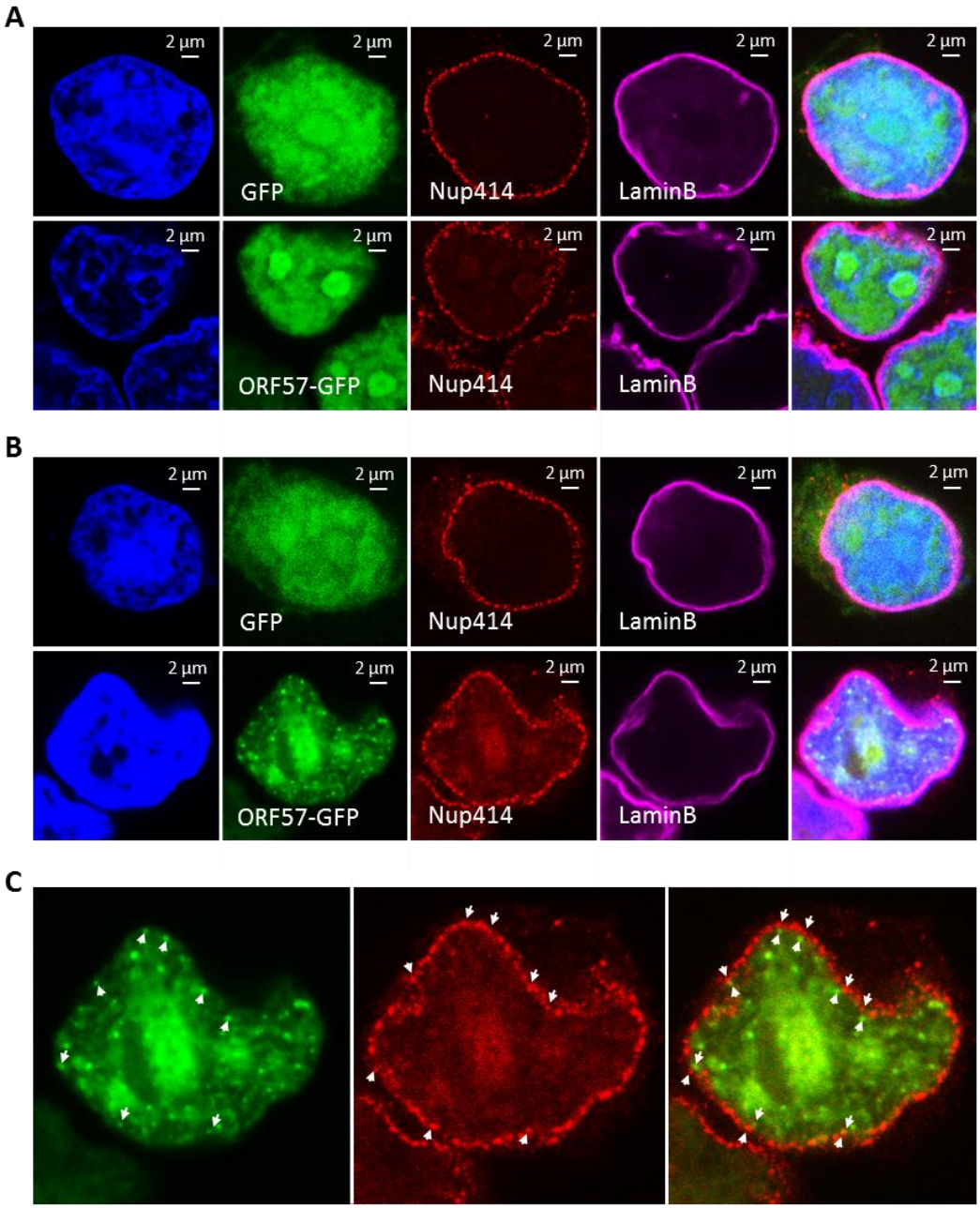

Figure 3.25: ORF57 nuclear foci localise within close proximity of the nuclear pore complex.
(a) HEK 293T cells transfected with pEGFP-N1 or pORF57-EGFP were treated with 0.5% DMSO and (b) 5 µM CPT for 2 hours before being fixed and stained with antibodies specific to Nup414 and LaminB. (c) Enhanced image demonstrating close proximity between ORF57-GFP (green) and Nup414 (red), indicated by white arrows. Slides were analysed using a Zeiss LSM510 confocal laser scanning microscope.

The observed ORF57/Prp19/ATRIP speckles appeared to line the nuclear periphery in a discontinuous manner, and their appearance by confocal microscopy was suggestive of close proximity to nuclear pore complexes. Heterochromatin/euchromatin barriers are often found close to nuclear pores, allowing for efficient export of newly transcribed mRNAs. Moreover, euchromatin is believed to be more susceptible to DNA damaging

agents such as camptothecin, as the DNA is more accessible in this arrangement. Therefore, in order to further investigate the hypothesis that ORF57, Prp19 and ATRIP localise to sites of DNA damage, the localisation of Nucleoporin 414 and LaminB was examined in the presence of ORF57-GFP/GFP and in cells treated with either camptothecin/DMSO using confocal microscopy **(Fig. 3.25)**. ORF57 nuclear foci were observed to localise in close proximity to the discontinuous Nup414 foci **(Fig. 3.25C)**. This ORF57 staining is indicative of localisation to euchromatin, and likely sites of DNA damage.

3.12 Discussion

The Prp19/CDC5L complex has previously been thought to be necessary for the splicing of mRNAs (Makarova et al., 2004)), however it does not appear to be necessary for the splicing of KSHV encoded intron containing transcripts. Furthermore, the depletion of two key members of this protein complex, Prp19 and CDC5L, failed to reduce the nuclear export or stability of KSHV encoded intronless mRNAs. This is surprising, as both of these processes have previously been attributed to hTREX activity, and it has previously been suggested that the Prp19/CDC5L complex is necessary for hTREX recruitment to both intron-containing and intronless genes, both of which are encoded by KSHV (Lei et al., 2011; Chanarat et al., 2011). This phenomenon, however, can be explained by the direct interaction between ORF57 and members of the hTREX complex, particularly Aly, which allows ORF57 to directly recruit the hTREX complex to KSHV encoded mRNAs, bypassing the need for the Prp19/CDC5L complex in this mechanism.

In addition to its role in splicing, Prp19 has recently been identified as an important protein in the early stages of the ATR-Chk1 DNA damage response pathway (Maréchal et al., 2014). Upon the induction of DNA strand breaks by either replication stress or exposure to DNA damage inducing agents, Replication Protein A (RPA) binds to and coats single stranded DNA, forming a structure known as RPA-ssDNA. RPA-ssDNA is bound by ATRIP, facilitating the activation of the ATR kinase, leading to the

phosphorylation of RPA and Chk1, resulting in a productive DNA damage response (Zou and Elledge, 2003; Maréchal et al., 2014 p. 19)

. It has been demonstrated that Prp19 acts as a sensor of RPA-ssDNA, and is necessary for the recruitment of higher levels of the ATR kinase and its cofactor ATRIP to these sites in order to amplify the ATR-Chk1-dependent DNA damage response (Maréchal et al., 2014 p. 19).

ORF57 has previously been implicated as a DNA damage factor, causing R-Loops which lead to genome instability (Aguilera and García-Muse, 2012; Jackson et al., 2014). R-loop formation is believed to occur due to the sequestration of the hTREX complex by ORF57, as hTREX would normally bind to newly transcribed mRNAs, stabilising them and preventing the binding of these mRNAs to the complementary DNA strand that they were transcribed from. Herein, it is hypothesised that the widespread formation of R-loops would ultimately culminate in apoptosis via a DNA damage response. Therefore, the role that Prp19 may play in the DNA damage response during ORF57 induced DNA damage was investigated. Surprisingly, both Prp19 and ATRIP are recruited to nucleoli in the presence of ORF57-GFP. However, both also dramatically relocalise to subnuclear speckles in cells that have been subjected to camptothecin induced DNA damage, and this coincides with an ablation of RPA speckle formation, normally observed during DNA damage. Therefore, it is hypothesised that upon the induction of DNA damage, ORF57 is recruited to sites of strand breaks, where it is able to block one or more functions of Prp19, ultimately preventing the formation of RPA speckles. Although ORF57-GFP expression was able to limit the phosphorylation of RPA at the T21 residue during Prp19-HA overexpression, this is unlikely to contribute to the RPA speckle phenotype observed during camptothecin treatment, as levels of T21 phosphorylated RPA were comparable between both GFP and ORF57-GFP expressing cells undergoing camptothecin induced DNA damage. As Prp19 is able to ubiquitinate RPA, it is possible that the relocalisation of RPA to these subnuclear speckles is dependent on its ubiquitination, and that this is prevented by the interaction between ORF57 and Prp19.

Small foci containing ORF57, Prp19 and ATRIP were also observed in DMSO control cells, albeit at a much lower level than in camptothecin treated cells. It is hypothesised that these speckles also represent sites of DNA damage, following ORF57-mediated R-loop induced DNA damage, and that a similar process occurs at these sites. These foci occupied sites near the nuclear periphery, similarly to many of the observed camptothecin induced ORF57/Prp19/ATRIP foci, attributed to DNA damage at euchromatin. As R-loops form at sites of transcription, which in turn occurs at euchromatin, this localisation is to be expected if this hypothesis is correct.

Interestingly, the ATM and DNA-PK DNA damage response pathways have both been shown to respond to KSHV lytic infection (Hollingworth et al., 2015). Activation of the ATM pathway, in particular, appears to be required, as the treatment of lytically infected cells with an ATM inhibitor reduces levels of viral replication. Furthermore, it was demonstrated that Chk1 phosphorylation is inhibited during lytic infection, while RPA is recruited to sites of viral DNA replication. It remains to be seen whether the formation of RPA speckles, possibly formed via Prp19-mediated ubiquitination of RPA, could inhibit the recruitment of RPA to viral replication centres. This would represent further explanation of the unusual interactions between ORF57 and the machinery of the early ATR-Chk1 response, where inhibition of modified RPA speckles both restricts the DNA damage response and subsequent apoptosis, while also allowing unmodified RPA to be recruited to viral replication centres.

These hypotheses have led to the formation of a model in which ORF57, Prp19 and ATRIP associate with sites of R-loop mediated DNA damage at euchromatin. An interaction between ORF57 and Prp19 then prevents an unknown modification of RPA, presumed to be ubiquitination. In turn, this inhibits the formation of RPA speckles, preventing the full activation of the ATR-Chk1 DDR pathway and allowing recruitment of unmodified RPA to KSHV replication centres **(Fig. 3.26)**.

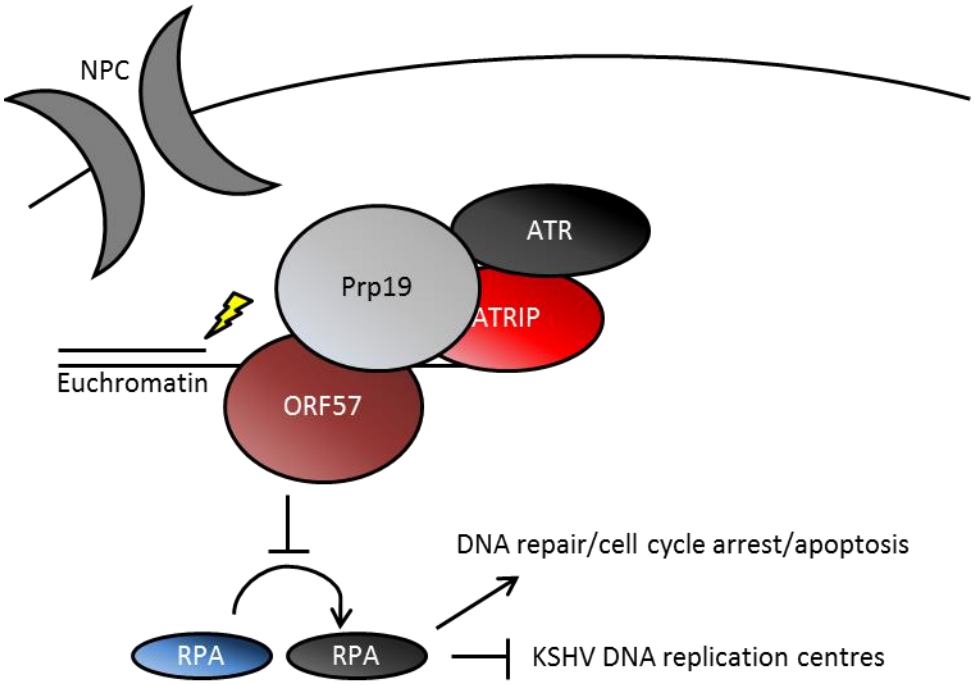

Figure 3.26: Model of ORF57 inhibition of Prp19 functions during the ATR-Chk1 DDR pathway.
ORF57 interacts with Prp19 at sites of DNA damage, blocking one or more functions of Prp19 and ultimately preventing a modification of RPA, preventing the speckled localisation of RPA. Blue and black RPA represent unmodified and modified forms respectively.

CHAPTER 4

~

Host cell microRNAs 151a-5p and 365a-3p are dysregulated during KSHV lytic infection

4 Host cell microRNAs 151a-5p and 365a-3p are dysregulated during KSHV lytic infection

4.1 Introduction

The discovery of microRNAs represents a relatively recent addition to the general understanding of gene expression, adding an extra layer of complexity in the form of post transcriptional regulation (Cannell et al., 2008). These short, 17-25 nucleotide RNA fragments are used to target complementary mRNAs for degradation or translational repression, in a process very closely related to the RNA interference mechanism first discovered in plants (Gurtan and Sharp, 2013; Agrawal et al., 2003; Napoli, 1990). The biogenesis of miRNAs usually begins with the transcription of a pri-miRNA, a 5' capped and 3' polyadenylated RNA sequence, containing one or more ~80 nucleotide hairpin structures (Ha and Kim, 2014). Drosha, a ribonuclease enzyme, then releases ~60 nucleotides of the hairpin from the surrounding sequence by a cleaving mechanism involving the Drosha cofactor DGCR8, generating a pre-miRNA (Han, 2004). The pre-miRNA is subsequently exported from the nucleus through the nuclear pore complex, mediated by Exportin-5 (Yi et al., 2003) **(Fig. 4.1)**. Once in the cytoplasm, the tip of the pre-miRNA stem loop is cleaved, generating a double stranded miRNA/miRNA* duplex, which is subsequently loaded onto Argonaute (Ago), a component of the RNA Induced Silencing Complex (RISC) (Boland et al., 2011). The miRNA:miRNA* duplex is then separated into single strands, the passenger strand is ejected while the guide strand remains bound to Ago and is used to target complementary mRNAs for degradation or translational repression (Ha and Kim, 2014).

Virally-encoded miRNAs possess great utility as they are non-immunogenic and require much less space to encode than viral proteins, and so it is no surprise that there are numerous viruses that encode their own miRNAs, including many of the herpesviruses (Skalsky and Cullen, 2010). Epstein-Barr virus encodes 25 pre-miRNAs, 22 of which are expressed during latency II, and 3 in latency III (Barth et al., 2011). Cytomegalovirus encodes 15 miRNAs that are, surprisingly, expressed during the lytic cycle. It is currently unknown whether HCMV encoded miRNAs play a role in latency, as with other herpesviruses (Shen et al., 2014). Other examples from outside the herpesvirus

family include Adenovirus, which produces 2 dsRNAs known as virus associated (VA) RNAs that act to limit miRNA action through the inhibition of Dicer, but which are, themselves, processed into RISC associating miRNAs (Andersson et al., 2005; Aparicio et al., 2006). Moreover, *Heliothis virescens* ascovirus encodes a miRNA that depletes the levels of viral DNA polymerase transcripts during late stages of infection, oddly acting to reduce viral replication (Hussain et al., 2008). Furthermore, polyomaviruses such as SV40, Merkel cell polyomavirus, human BK virus and JC virus all express a miRNA known as miR-S1, and its temporal expression, sequence and spatial organisation in the genome are all highly conserved (Cantalupo et al., 2005; Seo et al., 2008). There are also many examples of viruses altering host miRNA expression to enhance viral replication. Again the majority of these examples have been discovered during herpesvirus infection. EBV is able to induce the expression of both miR-146a and miR-155 in B cells, leading to the degradation of a number of interferon responsive genes (Cameron et al., 2008)(Lu et al., 2008), while HCMV downregulates miR-100 and miR-101, both of which regulate mTOR pathway dynamics (F.-Z. Wang et al., 2008). In a complete reversal of the usual miRNA mechanism, Hepatitis C virus utilises miR-122 in a mechanism that is necessary for viral replication, binding to the 5' UTR of the viral RNA to protect it from degradation by the host exonuclease Xrn1 (Y. Li et al., 2013).

The introduction and rapid increase in the utility of RNA sequencing technologies means that it is now possible to size select and sequence miRNAs (Buermans et al., 2010; Lee et al., 2010; Pritchard et al., 2012). Furthermore, algorithms have now been developed to allow greater quantitation of RNA sequencing data, allowing for the investigation of global changes in miRNA levels over multiple samples (Li et al., 2012; Metpally et al., 2013). This powerful technology is proving extremely useful in unravelling the additional layer of complexity associated with miRNAs in the dynamics of gene regulation, particularly in the context of virus infection (Huang et al., 2012; Szeto et al., 2014; Shrinet et al., 2014).

Herein it is demonstrated that KSHV is able to dysregulate a number of host miRNAs during lytic infection, including miR-151a-5p and miR-365a-3p. Furthermore, inhibition of the function of these miRNAs during KSHV infection increases viral load but

decreases viral reinfection, suggesting that these miRNAs play important roles in the egress of mature KSHV virions.

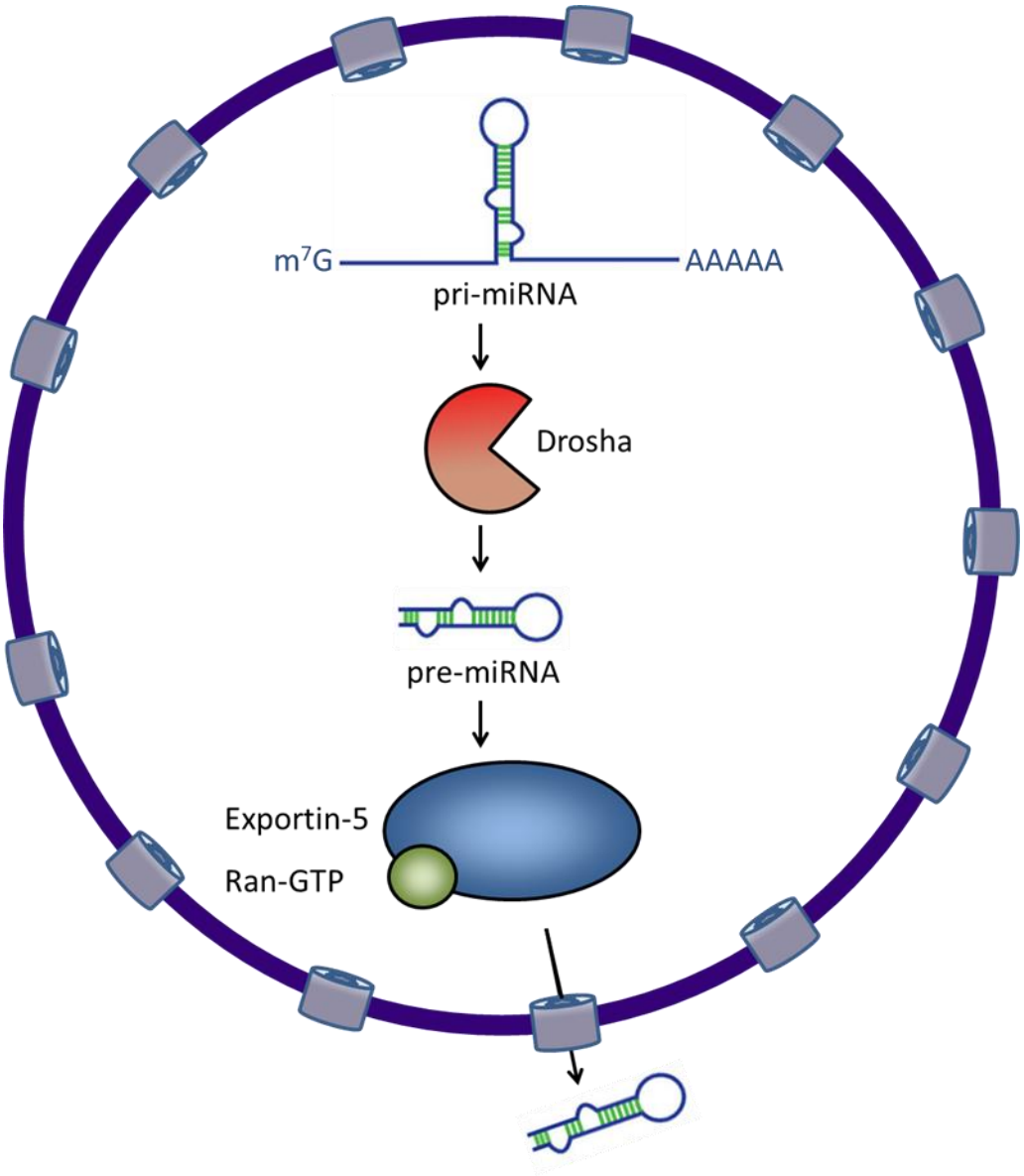

Figure 4.1: The role of Exportin-5 in miRNA nuclear export.
The biogenesis of miRNAs begins in the nucleus with the transcription of pri-miRNAs, capped and polyadenylated transcripts containing one or more hairpin structures. The hairpin is cleaved out of the surrounding sequence by Drosha, and this newly generated pre-miRNA is subsequently exported into the cytoplasm by Exportin-5 in a Ran-GTP dependent mechanism.

4.2 Exportin-5 and SMARCA4 proteins are found at increased levels in ORF57 SILAC datasets

KSHV expresses 18 mature viral miRNAs, all encoded by the latency associated region of the viral genome (Qin et al., 2012). They are associated with a number of latent

processes, including inhibition of the lytic switch protein, RTA (Bellare and Ganem, 2009; Lu et al., 2010). It was, therefore, striking when Exportin-5 and the telomerase interacting SWI/SNF protein SMARCA4, 2 essential factors in miRNA biogenesis, were observed at increased levels in the nucleolus in ORF57 SILAC datasets **(Fig. 4.2)** (Yi et al., 2003**;** Lassmann et al., 2015). This observation suggests that ORF57 may be able to modulate the processing of miRNAs, as well as mRNAs. Due to the lytic expression of ORF57 and the latent expression of the KSHV encoded miRNAs, it would appear that this alteration is likely to affect the biogenesis or functioning of host miRNAs. Based on this hypothesis, the expression of cellular miRNAs was investigated during the course of a KSHV lytic replication cycle. To this end, miRNA-seq was performed, where small RNA libraries were generated and analysed using next generation sequencing. To perform these experiments RNA samples were initially harvested from KSHV infected B cells at three different stages of infection, 0h (latent control), 8h (lytic) and 18h (lytic). These times allowed for the investigation of early and late stages of infection, as well as the observation of general trends in host miRNA levels over the course of the viral lytic cycle. The levels of the viral lytic gene ORF57 were examined in the generated RNA samples, in order to ensure a progression of the lytic cycle over the chosen times **(Fig. 4.3)**. These RNA samples were also subjected to analysis by an Agilent Bioanalyzer to ensure the high integrity required for reliable analysis by next generation RNA sequencing.

4.3 Generation of miRNA sequencing libraries

Following confirmation that the generated total RNA samples were suitable for analysis, an Illumina RiboZero kit was employed, which uses magnetic rRNA probes and magnetic beads to remove ribosomes from the RNA sample, and the samples were assessed by bioanalyzer **(Fig. 4.4a)**. Following this, miRNA sequencing libraries were prepared using a NEBNext Small RNA Library Preparation kit. In short, adaptor oligos were hybridised to the 3’ end of the RNA, and a complementary primer was also added to bind to this adaptor. A 5’ adaptor was also added to the RNA, and the RNA was reverse transcribed into cDNA. PCR was then performed to enrich the sample for correctly amplified cDNA, and then a clean-up and gel-electrophoresis based size

selection protocol was employed to ensure good library quality prior to sequencing. Following this, samples were again examined by bioanalyzer **(Fig. 4.4b)**. Following the addition of adaptor sequences, the miRNAs were ~160bp in length, and the bioanalyzer trace showed a large spike at the corresponding point, with little other material present in the sample, suggesting that the libraries were highly enriched for miRNAs. The libraries were pooled and sequenced on an Illumina HiSeq at the Leeds Institute of Biomedical and Clinical Sciences (LIBACS) by Dr. Sally Harrison.

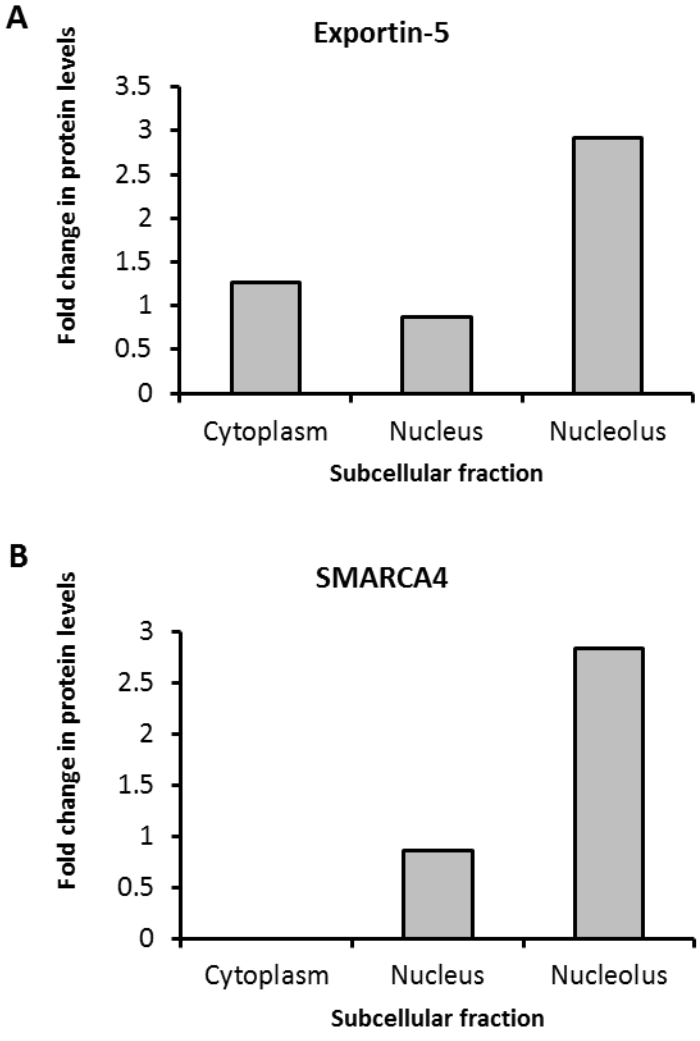

Figure 4.2: Exportin-5 and SMARCA4 levels increase in nucleolar fraction of KSHV ORF57 expressing cells.
(a) Fold change increase in Exportin-5 and (b) SMARCA4 levels in subcellular fractions of HEK 293T expressing an inducible ORF57 protein compared to uninduced cells.

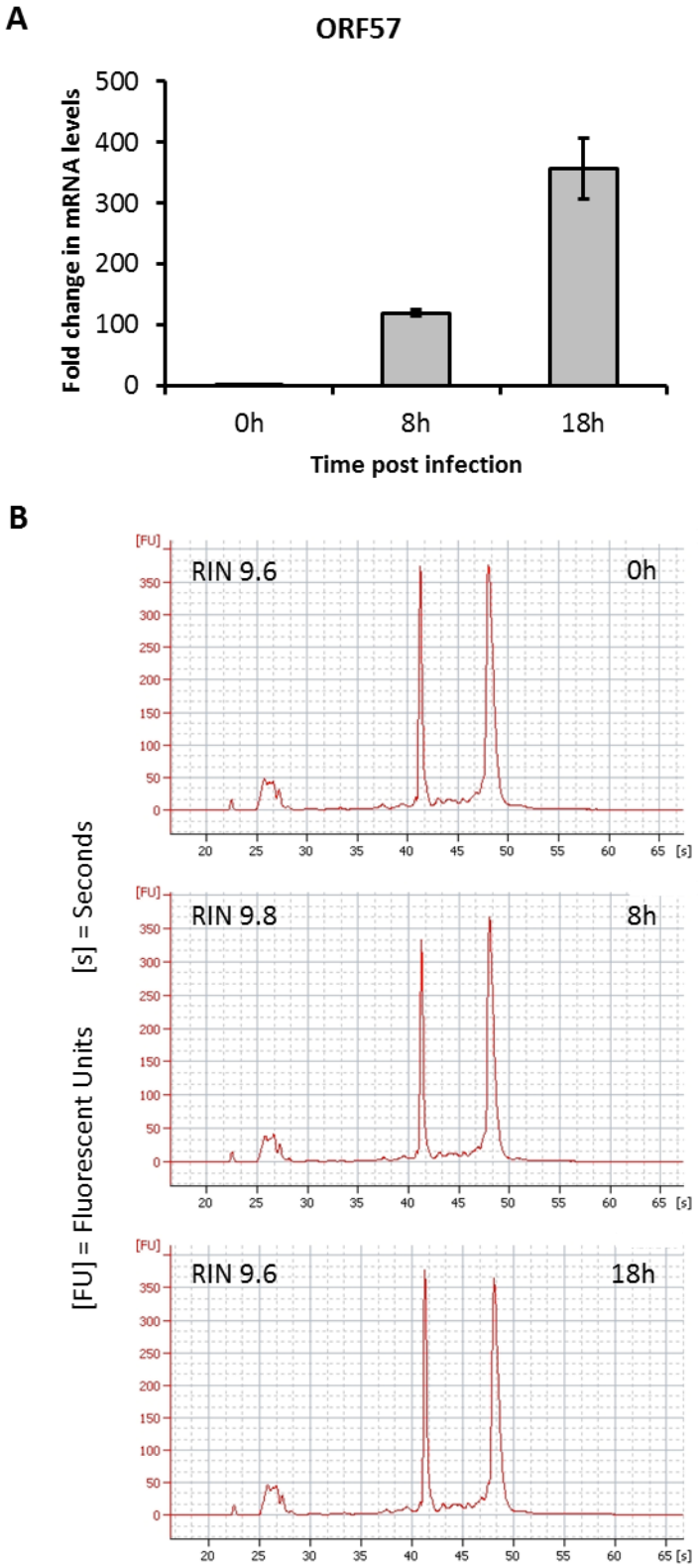

Figure 4.3: Extraction of high integrity RNA from TREx BCBL1-Rta cells at 0, 8 and 18 hours post lytic reactivation.

(a) TREx BCBL1-Rta cells were unreactivated (latent control) or reactivated (lytic infection) for 8 or 18 hours with doxycycline hyclate before total RNA was isolated. This RNA was used to generate cDNA and ORF57 specific primers were used to analyse ORF57 mRNA levels in each sample by qRT-PCR. (b) Extracted RNA samples were analysed using an Agilent Bioanalyzer and an RNA Integrity Number (RIN) was calculated for each sample.

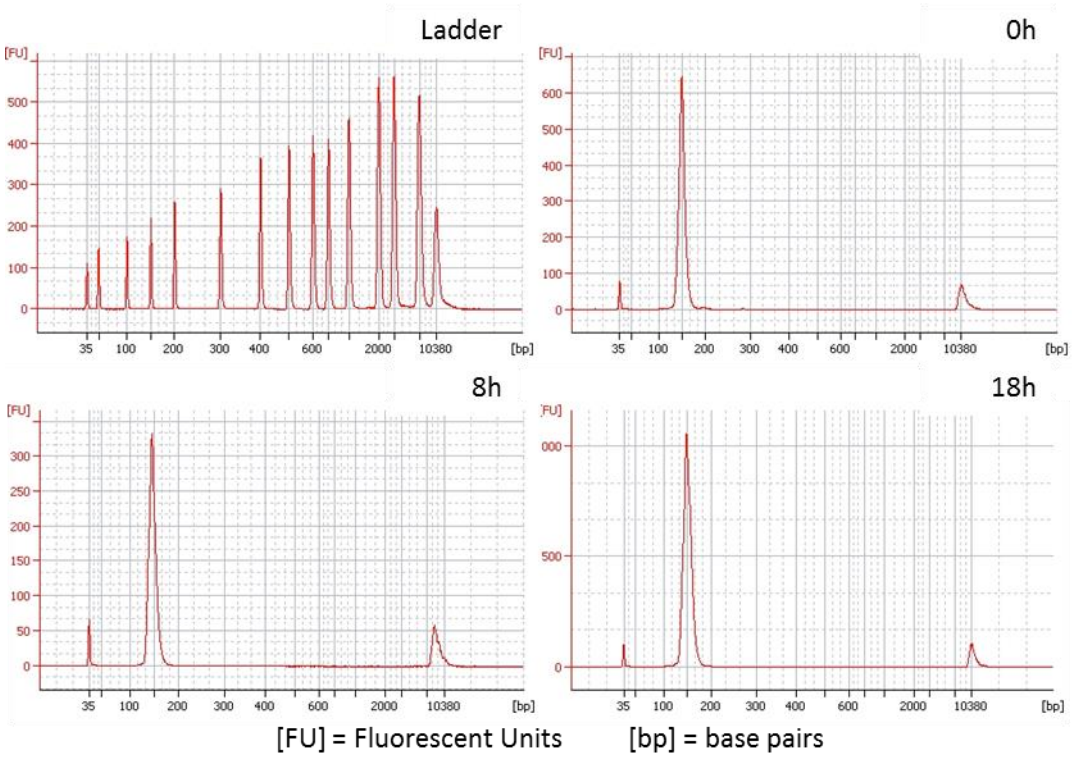

Figure 4.4: Preparation of small RNA sequencing libraries from TREx BCBL1-Rta cells at 0, 8 and 18 hours post lytic reactivation.
Total RNA samples extracted from TREx BCBL1-Rta cells were processed into small RNA libraries using a NEBNext Small RNA Library Prep kit for Illumina. Final libraries were analysed using an Agilent Bioanalyzer.

4.4 KSHV lytic infection affects the expression levels of 19 mature host miRNAs

The reads generated by miRNA-seq were aligned to a database of all known *Homo sapiens* miRNAs (miRBase version 19). Reads that aligned at more than one location were assigned to the most probable location of origin using SeqEM (Martin et al., 2010). Read counts were normalised using edgeR (Robinson et al., 2010). Bioinformatics analysis using SeqEM and edgeR was performed by Dr. Alastair Droop and Dr. Lucy Stead at the Leeds Biomedical Health Research Centre. Over 3 million reads mapped to canonical miRNAs across the 3 samples. miRNAs displaying the greatest fold change between latent and lytic stages were identified and grouped by their expression trend over the 3 stages of infection **(Fig. 4.5)**. Most of these miRNAs had not previously been identified as altered during KSHV infection, however, both miR-221-5p and miR-222-5p have been identified as targets of the KSHV latent nuclear antigen (LANA) and Kaposin B, and are, therefore, depleted during latent KSHV

infection in endothelial cells (Wu et al., 2011). These miRNAs are believed to play roles in reducing endothelial cell migration, and therefore their depletion by LANA and Kaposin B is thought to contribute to the increased migration of endothelial cells during KSHV infection (Wu et al., 2011). It is not surprising, therefore, that the miRNA sequencing data generated from TREx cells shows a large increase in the levels of both miR-221-5p and miR-222-5p over the course of KSHV lytic infection.

It is also interesting to note that many of these miRNAs, including miR-221-5p and miR-222-5p, have previously been identified in B cell cancer samples (Lim et al., 2015). Many miRNAs exhibit cell type specificity, and may even present utility in characterising different forms of cancer and cells of origin and may ultimately be used as prognostic indicators (Sood et al., 2006; Lim et al., 2015).

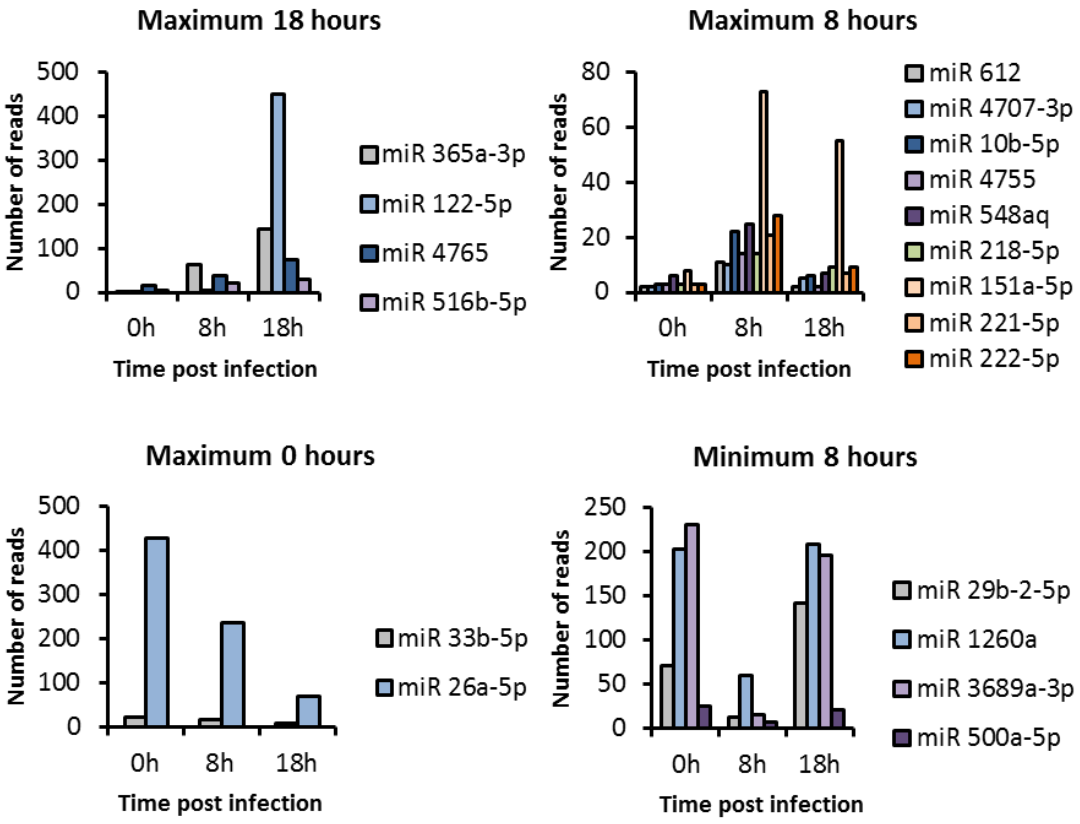

Figure 4.5: Identification of 19 mature miRNAs with altered expression levels during KSHV lytic infection.

Small RNA libraries generated from TREx BCBL1-Rta cells at 0 (latent control) 8 and 18 (lytic infection) hours post infection were sequenced using an Illumina HiSeq. Sequence reads were analysed by SeqEM and aligned to known *Homo sapiens* miRNA sequences (this work was performed by Dr. Lucy Stead and Dr. Alastair Droop – BHRC, Leeds). Read numbers of miRNAs that were significantly altered during the course of KSHV lytic infection were plotted on 4 bar charts using MS Excel according to their general trend.

In order to validate the trends observed in the miRNA-seq data, a highly specific, quantitative approach to identify levels of mature miRNAs was required. The stem loop qRT-PCR method meets all of these needs, and represents a relatively quick and affordable way to verify miRNA sequencing data (Chen, 2005) **(Fig. 4.6)**. The assay involves the reverse transcription of a mature miRNA, where specificity is achieved using a reverse transcription primer containing a hairpin structure with only ~6 nucleotides to bind to a target. Despite this relatively short binding sequence, the hairpin structure prevents non-specific binding by acting as a barrier. A universal probe library (UPL) probe #21 binding site is present in the hairpin sequence, and therefore UPL #21 can only bind following denaturation of the reverse transcribed mature miRNA. UPL #21 is a short oligo attached to a fluorophore and quencher at each end. During *Taq* Polymerase amplification of the target strand, the quencher and fluorophore are released from the oligos, producing a quantifiable signal.

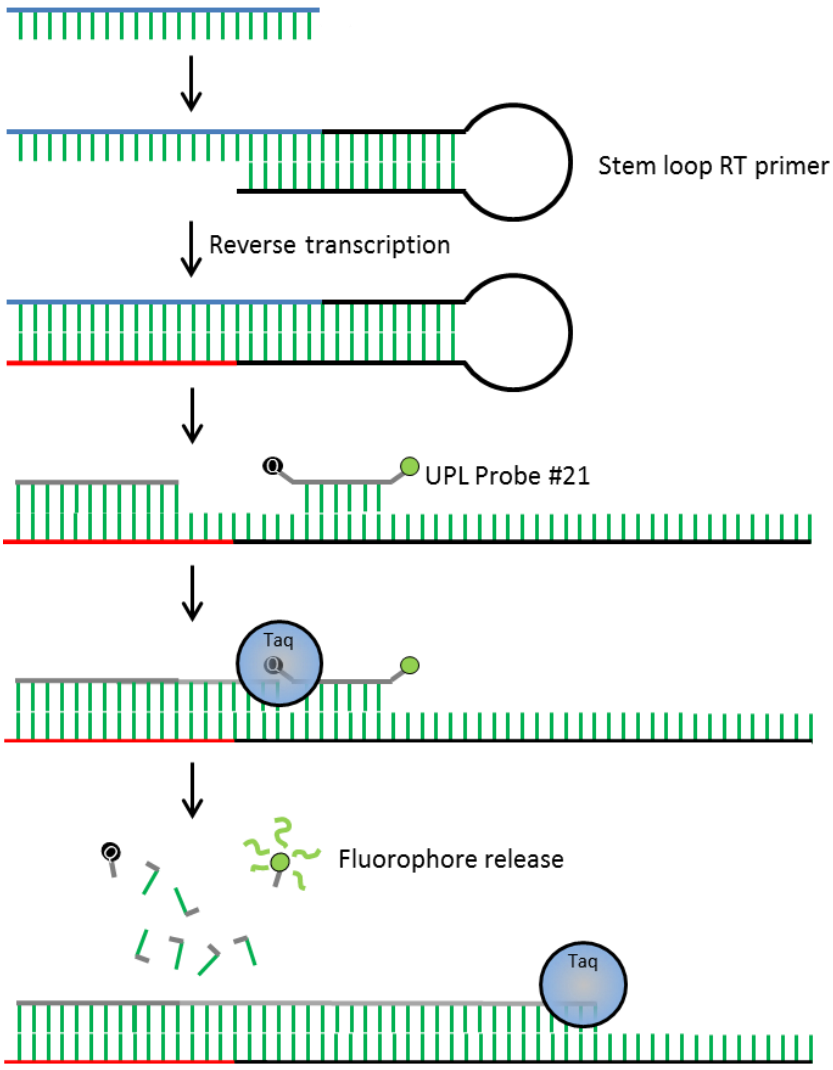

Figure 4.6: Stem loop qRT-PCR specifically amplifies mature miRNAs.
Stem loop qRT-PCR begins with the extraction of total RNA and the subsequent reverse transcription of a miRNA of interest using a primer specific to the final 6 nucleotides of the miRNA, containing a hairpin loop structure to prevent the binding of non-specific targets. Following reverse transcription, quantitative PCR is performed using a Universal Probe Library probe specific to a sequence present in the hairpin structure, which is only accessible following the denaturation step. The DNA polymerase used in the assay has exonuclease function and is therefore able to release both the fluorophore and quencher attached to the probe, producing signal specifically when the target is amplified.

The KSHV lytic cycle occurs in both B cells and endothelial cells of patients afflicted by all KSHV-related malignancies (Ganem, 2007). Therefore, miRNAs that are dysregulated by KSHV in multiple cell types would represent the best potential as novel drug targets. For this reason, stem loop qRT-PCR was used to investigate the expression levels of these miRNAs across 3 different cell lines harbouring a latent KSHV genome that could be reactivated (Nakamura et al., 2003; Vieira and O'Hearn, 2004; Myoung and Ganem, 2011). Levels of both miR-151a-5p and miR-365a-3p followed

similar trends to those seen in the miRNA-seq data across all 3 cell lines **(Fig. 4.7)**. Importantly, both of these miRNAs were present at a relative abundance greater than 0.01% (100 reads per million) in at least one of the samples analysed by miRNA-seq (of those that aligned to the known Homo sapiens miRNAs annotated in miRDB). Neither of the miRNA trends validated in TREx BCBL1-Rta cells displayed the same levels of change as identified in the miRNA-seq expression data. This may be due to biases in the miRNA-seq library preparation stages, such as concentration of miRNA levels during gel purification.

As the reads generated by miRNA-seq had only been aligned to the known miRNAs in miRDB, it was important to verify that both validated KSHV dysregulated miRNAs were not viral in origin. To this end, pairwise alignments were performed between both validated miRNAs and all known KSHV encoded mature miRNAs, using the Sequence Manipulation Suite Pairwise Align DNA program **(Fig. 4.8)**. Maximum scores were generated by aligning each validated miRNA with itself, and scores for KSHV encoded miRNAs were then compared to this maximum score, and a percentage calculated. The closest similarity between the validated miRNAs and KSHV encoded miRNAs was between miR-151a-5p and KSHV miR-K3-5p, at 33%. This result indicates that neither of the validated KSHV dysregulated miRNAs are viral in origin, and suggests that they have both been correctly identified as cellular miRNAs.

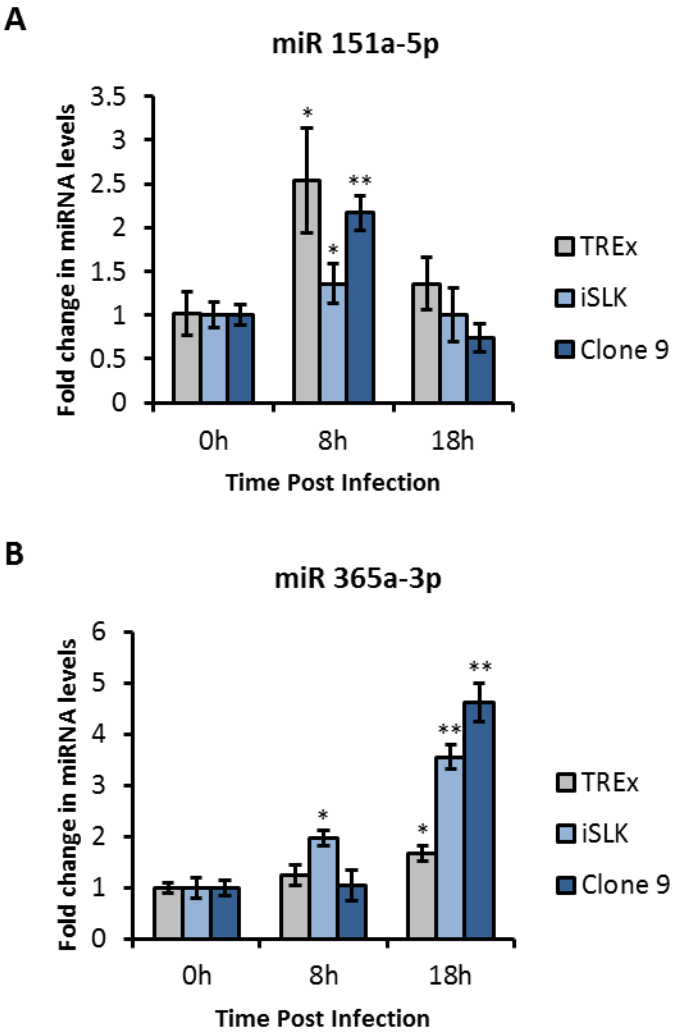

Figure 4.7: Validation of changes to miR-151a-5p and miR-365a-3p expression levels over KSHV lytic infection in TREx BCBL1-Rta, 293T rKSHV.219 and iSLK.219 cells.

(a) miR-151a-5p and (b) miR-365a-3p levels over the course of KSHV lytic infection in 3 KSHV-positive cell lines. RNA was extracted from TREx BCBL1-Rta, iSLK.219 and 293T rKSHV.219 cells at 0 (latent control), 8 and 18 (lytic infection) hours post infection and extracted RNA was subjected to DNase treatment. RNA was then reverse transcribed into cDNA using a miRNA specific stem loop RT primer and qPCR was performed using primers specific to the mature miRNAs and the stem loop sequence. 3 biological replicates were combined, the relative values were displayed on a graph and the standard deviation was calculated. Error bars = SD, $p<0.01$ = **, $p<0.05$ = *compared with 0 h sample from same cell line.

A

KSHV	
miR K1-5p	AUUACAGGAAACUGGGUGUAAGCUG
miR K2-5p	AACUGUAGUCCGGGUCGAUCUGA
miR K3-5p	UCACAUUCUGAGGACGGCAGCGACG
miR K4-3p	UAGAAUACUGAGGCCUAGCUGA
miR K4-5p	AGCUAAACCGCAGUACUCUAGG
miR K5-3p	UAGGAUGCCUGGAACUUGCCGGU
miR K6-3p	UGAUGGUUUUCGGGCUGUUGAGC
miR K6-5p	CCAGCAGCACCUAAUCCAUCGG
miR K7-3p	UGAUCCCAUGUUGCUGGCGCUCA
miR K7-5p	AGCGCCACCGGACGGGGAUUUAUG
miR K8-3p	CUAGGCGCGACUGAGAGAGCAC
miR K8-5p	ACUCCCUCACUAACGCCCCGCU
miR K9-3p	CUGGGUAUACGCAGCUGCGUAA
miR K9-5p	ACCCAGCUGCGUAAACCCCGCU
miR K10-3p	UAGUGUUGUCCCCCCGAGUGGC
miR K11-3p	UUAAUGCUUAGCCUGUGUCCGAU
miR K12-3p	UGGGGGAGGGUGCCCUGGUUGA
miR K12-5p	AACCAGGCCACCAUUCCUCUCCG
Homo sapiens	
miR 151a-5p	UCGAGGAGCUCACAGUCUAGU
miR 365a-3p	UAAUGCCCCUAAAAAUCCUUAU

B

miR 151a 5p	KSHV miRNA	Score	% Max	miR 365a 3p	KSHV miRNA	Score	% Max
(Max score = 42)	miR K1-5p	8	19	(Max score = 44)	miR K1-5p	6	14
	miR K2-5p	8	19		miR K2-5p	6	14
	miR K3-5p	14	33		miR K3-5p	6	14
	miR K4-3p	10	24		miR K4-3p	6	14
	miR K4-5p	12	29		miR K4-5p	4	9
	miR K5-3p	6	14		miR K5-3p	6	14
	miR K6-3p	6	14		miR K6-3p	4	9
	miR K6-5p	10	24		miR K6-5p	8	18
	miR K7-3p	10	24		miR K7-3p	4	9
	miR K7-5p	2	5		miR K7-5p	6	14
	miR K8-3p	12	29		miR K8-3p	4	9
	miR K8-5p	6	14		miR K8-5p	12	27
	miR K9-3p	8	19		miR K9-3p	6	14
	miR K9-5p	8	19		miR K9-5p	10	23
	miR K10-3p	8	19		miR K10-3p	4	9
	miR K11-3p	4	10		miR K11-3p	6	14
	miR K12-3p	6	14		miR K12-3p	2	5
	miR K12-5p	6	14		miR K12-5p	4	9

Figure 4.8: Alignment based rejection of KSHV origins of identified miRNAs.
(a) List of all 18 known mature miRNAs encoded by KSHV and their nucleotide sequences, as well as those of hsa-mir-151a-5p and hsa-mir-365a-3p. (b) Scores were generated for each KSHV encoded miRNA to determine their similarity with hsa-mir-151a-5p and has-mir-365a-3p using Sequence Manipulation Suite Pairwise Align DNA program.

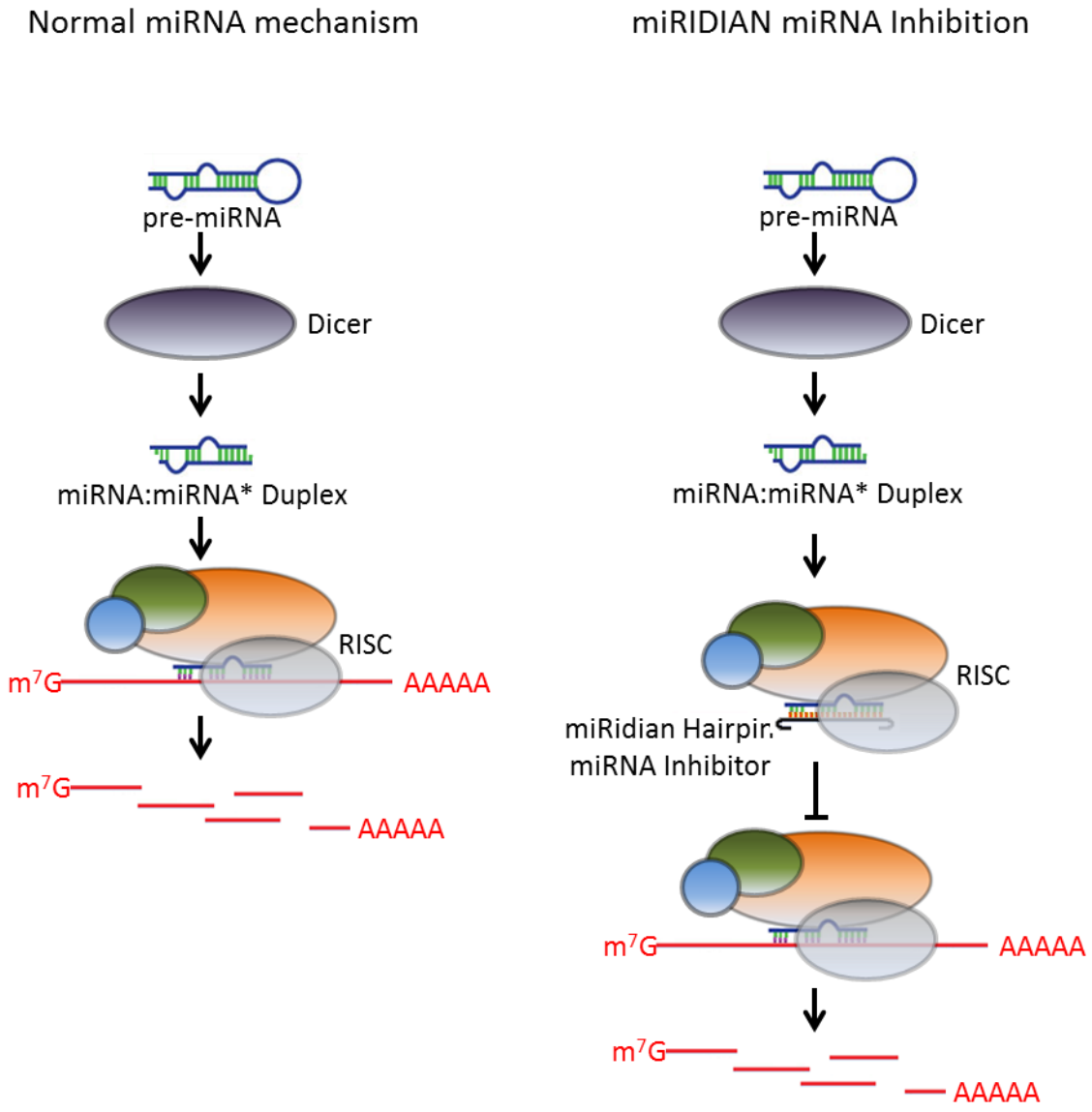

Figure 4.9: The role of miRIDIANs in the inhibition of miRNA action.
Following nuclear export, pre-miRNAs are cleaved at the tip of the stem loop by Dicer, producing a double stranded RNA molecule known as a miRNA:miRNA* duplex. A single strand of this duplex is selected by the RISC complex, and separated from its counterpart strand. The selected strand, now bound by RISC, is used to target complementary mRNAs for degradation. This process can theoretically be ablated by miRIDIAN miRNA inhibitors, which bind to the guide strand and prevent miRNA directed mRNA degradation.

4.5 miRIDIAN miRNA inhibitors specifically prevent action of targeted miRNAs

In order to assess the possible effects of miR-151a-5p and miR-365a-3p during KSHV lytic infection, attempts were made to inactivate their functions. This was achieved using miRIDIAN miRNA inhibitors: oligos complementary to miRNAs, consisting of a complementary sequence to the targeted miRNA, flanked by hairpin structures on either side (Thermo Scientific, 2009; Robertson et al., 2010). These molecules also

contain modifications to increase their binding affinity (proprietary information – modifications not disclosed). They then function by binding to the targeted mature miRNAs that have been selected as guide strands by the RISC complex, miRIDIANs are predicted to prevent the use of the guide strand to bind complementary mRNAs, and therefore ablate their degradative effects on these mRNAs **(Fig. 4.9)**.

The effects of targeted miRIDIAN miRNA inhibitors on the validated KSHV dysregulated miRNAs were therefore examined. To this end, 293T rKSHV.219 cells were transfected with miRIDIANs and 72 hours following transfection, cells were treated to induce the KSHV lytic cycle for 0 (control), 8 or 18 hours. Scramble siRNA was used as a control, and both miRIDIANs were also used as controls against each other. Total RNA was then extracted and subjected to stem loop qRT-PCR as described previously. miRIDIAN miRNA inhibitors were shown to specifically decrease detection of their targeted miRNA, though miRIDIAN 365a-3p treatment appeared to result in a ~50% reduction in the detectable levels of miR-151a-5p at all examined stages of infection, suggesting miRIDIAN 365a-3p may exhibit some off target binding **(Fig. 4.10)**. miRIDIAN miRNA inhibitors are not predicted to deplete levels of targeted miRNAs, and this result may instead indicate that miRIDIAN miRNA inhibitors bind to their target miRNA at higher temperatures and with greater efficiency than the stem loop RT primer used during the stem loop miRNA qRT-PCR reaction. Alternatively, miRIDIAN miRNA inhibitors may inhibit the amplification of reverse transcribed miRNAs during the qPCR stage of the technique. Regardless, this data suggests that miRIDIAN miRNA inhibitors can be used to interfere with miRNA-target binding to further investigate the roles of miR-151a-5p and miR-365a-3p during the KSHV lytic cycle.

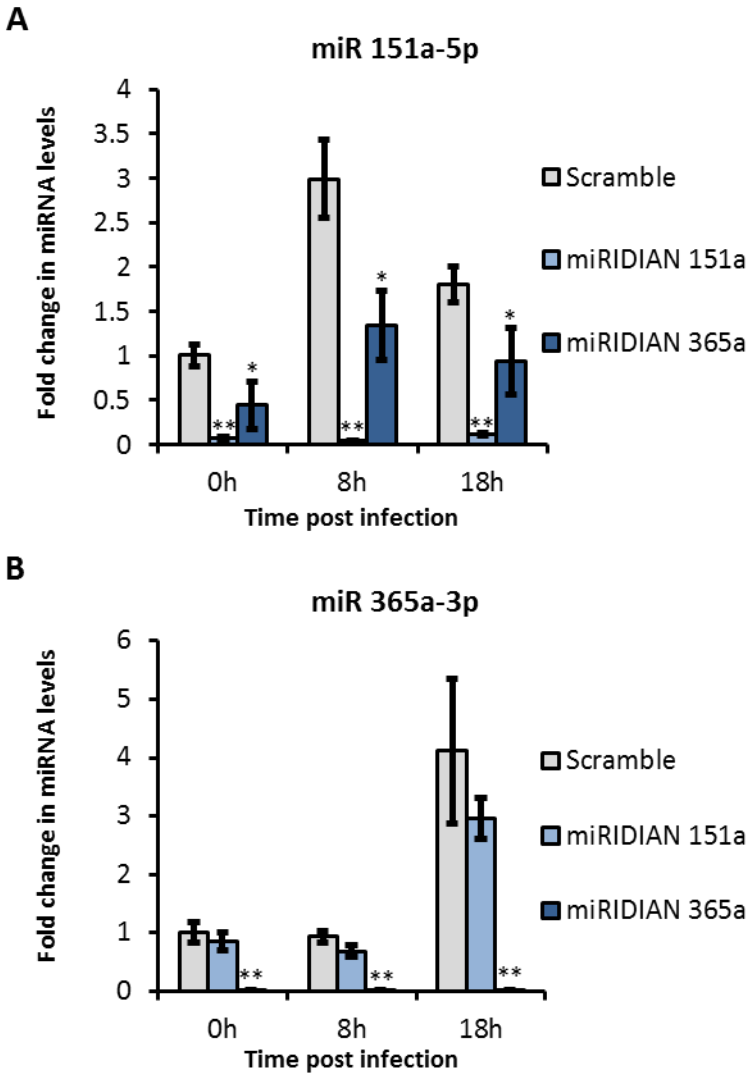

Figure 4.10: miRidian inhibitors efficiently inhibit target miRNAs from being amplified by stem loop miRNA qRT-PCR.
(a) miR-151a-5p and (b) miR-365a-3p levels following miRIDIAN antagomiR treatment over the course of KSHV lytic infection in 293T rKSHV.219 cells. Cells were transfected with scramble siRNA (control) or miRidian inhibitor specific to hsa-mir-151a-5p or hsa-mir-365a-3p. 72 hours after transfection lytic infection was induced for 0 (latent control) 8 or 18 (lytic infection) hours using NaBu and TPA. Total RNA was then harvested and subjected to DNase treatment. RNA was then reverse transcribed into cDNA using a stem loop hsa-mir-151a-5p or hsa-mir-365a-3p RT primer and qPCR was performed using primers specific to hsa-mir-151a-5p or hsa-mir-365a-3p and the stem loop sequence. 3 biological replicates were combined, the relative values were displayed on a graph and the standard deviation was calculated. Error bars = SD, $p<0.01$ = **, $p<0.05$ = * compared with scramble control for the same time point.

4.6 Inhibition of miR-365a-3p, but not miR-151a-5p, has a minor effect on viral RNA expression but no effect on late viral protein expression

As miRNAs function at a post-transcriptional level, the levels of a panel of KSHV encoded mRNAs were examined by qRT-PCR in the presence of both miRIDIANs, as

well as scramble siRNA control. The levels of all 5 examined mRNAs were partially depleted upon miRIDIAN 365a-3p treatment, while miRIDIAN 151a-5p treatment produced discontinuous results, with some KSHV mRNAs becoming depleted, while others increased in expression. Interestingly, miRIDIAN 365a-3p caused a dramatic reduction in the level of PAN RNA, a long noncoding RNA that is retained in the nucleus (Sun et al., 1996; Zhong et al., 1996). During HCV infection, miR-122 has been shown to protect viral RNA from degradation (Y. Li et al., 2013), however, miRNAs mature in the cytoplasm, and in order for miR-365a-3p to protect PAN in a similar manner, it would need to be transported back into the nucleus.

In order to further investigate whether the slight reduction in viral gene expression observed caused a reduction in viral protein production, the effects of miRIDIAN miRNA inhibitors on the expression of a late viral protein, the minor capsid protein, were examined. Minor capsid protein levels were not affected in the presence of miRIDIAN 151a-5p and 365a-3p, according to densitometry. This suggests that the lytic gene cascade remains relatively unaffected during miRIDIAN treatment.

4.7 Inhibition of miR-151a-5p or miR-365a-3p increases viral load following lytic replication

In order to investigate the effect of inhibition of miR-151a-5p and miR-365a-3p on the process of viral DNA replication, cells were treated to induce lytic infection for 7 days, or left untreated as a latent control, total DNA was subsequently extracted and qPCR was performed to assess the levels of KSHV ORF47 present, using GAPDH as a normalisation control. Inhibition of miR-151a-5p caused a ~23% increase in viral load, while inhibition of miR-365a-3p exhibited a more dramatic effect, increasing viral load by ~70%.

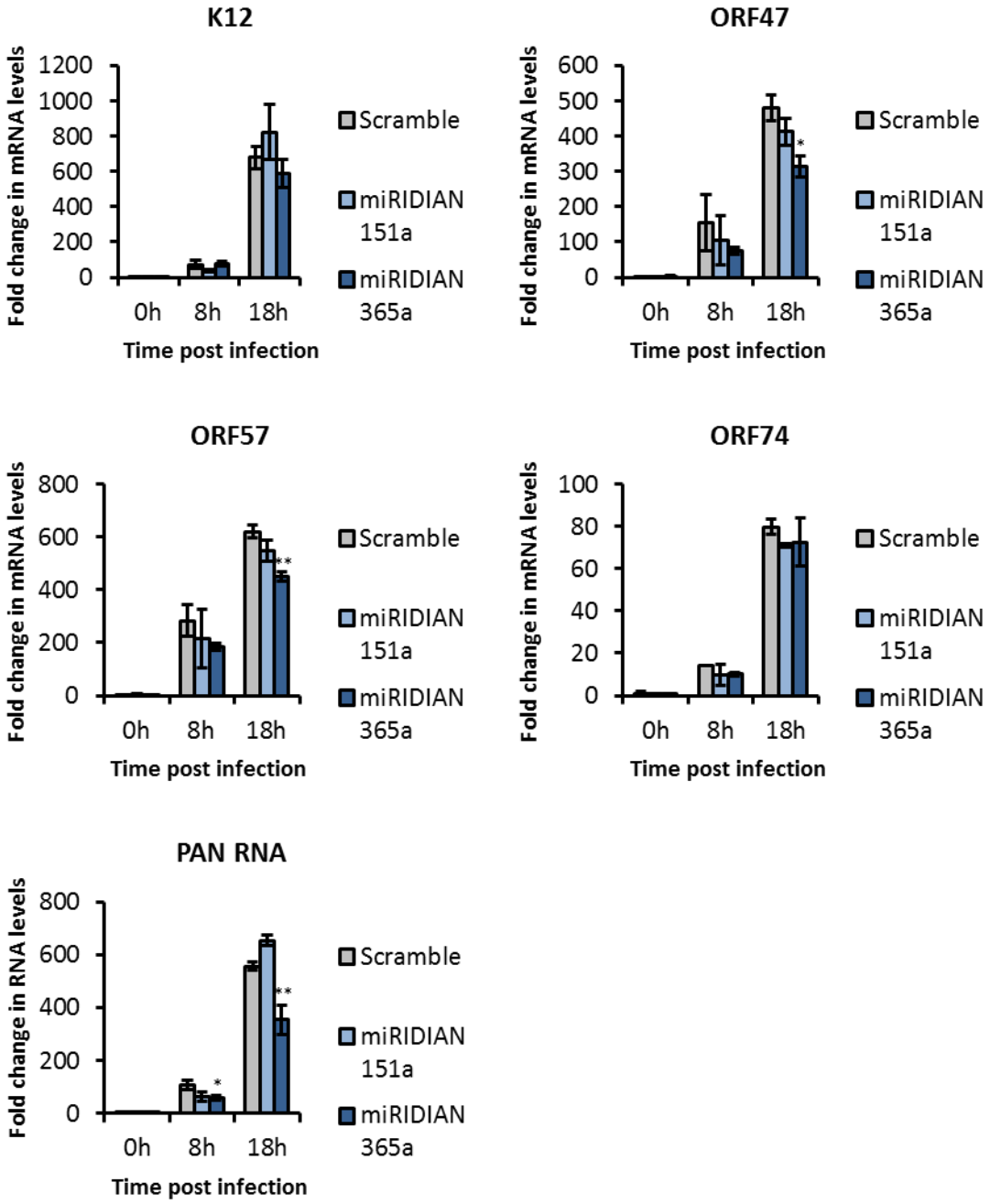

Figure 4.11: Minor reduction of early KSHV mRNA levels caused by miRidian inhibitors.
293T rKSHV.219 cells were transfected with scramble siRNA (control), miRidian inhibitor specific to hsa-mir-151a-5p or miRidian inhibitor specific to hsa-mir-365a-3p . 72 hours after transfection lytic infection was induced for 0 (latent control) 8 or 18 (lytic infection) hours using NaBu and TPA. Total RNA was then harvested and subjected to DNase treatment. RNA was then reverse transcribed into cDNA using an oligo dT primer and qPCR was performed using primers specific to K12, ORF47, ORF57, ORF74 and PAN RNA. 3 biological replicates were combined, the relative values were displayed on a graph and the standard deviation was calculated. Error bars = SD, $p<0.01$ = **, $p<0.05$ = * compared with scramble control from the same time point.

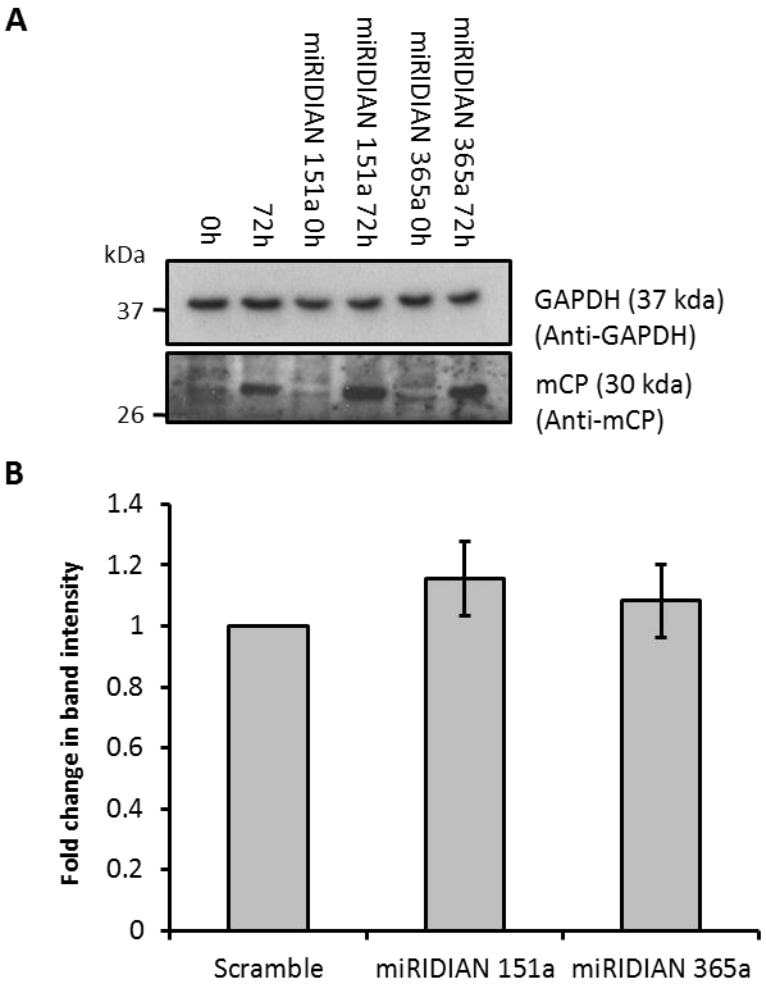

Figure 4.12: miRIDIANs do not affect levels of late KSHV proteins.
(a) 293T rKSHV.219 cells transfected with scramble siRNA (control) or miRIDIAN miRNA inhibitors targeting either miR-151a-5p or miR-365a-3p were left untreated (latent control) or treated to induce lytic replication for 72 hours before protein lysates were harvested and analysed by immunoblot to observe the levels of KSHV minor capsid protein, using GAPDH as a loading control. (b) Densitometry analysis was performed on the minor capsid protein immunoblot to assess the levels of protein present in each reactivated sample. Error bars = SD, $p<0.01$ = **, $p<0.05$ = * compared with scramble control.

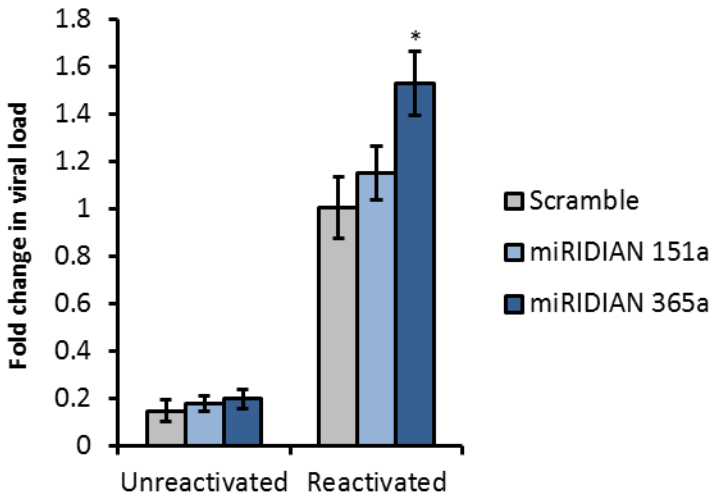

Figure 4.13: miRIDIANs increase viral load following KSHV lytic infection.
293T rKSHV.219 cells were transfected with scramble siRNA (control) or miRIDIAN miRNA inhibitors directed against miR-151a-5p or miR-365a-3p. 72 hours after transfection, cells were treated to induce KSHV lytic replication, or left untreated as a latent control. After 7 days, DNA was harvested and viral load was assessed using qPCR against ORF47 using GAPDH as a normalisation control. Fold change was calculated and graphs were plotted using Microsoft Excel. Error bars = SD, $p<0.01$ = **, $p<0.05$ = * compared with scramble control from the same time point.

4.8 Inhibition of miR-151a-5p in KSHV positive cells reduces reinfection of naïve cells

In order to investigate whether the increase in viral load observed during miR-151a-5p and miR-365a-3p inhibition was due to increased viral replication or decreased viral egress, a viral reinfection assay was performed. 293T rKSHV.219 cells were transfected with miRIDIANs or scramble siRNA (control) and reactivated for 7 days before the virus containing supernatant was used to infect naïve HEK 293T cells. Viral load was then assessed in HEK 293T cells by qPCR **(Fig. 4.14)**. Reinfection using supernatant from miRIDIAN 151a-5p treated cells produced a ~19% reduction in viral load in naïve HEK 293T cells, while miRIDIAN 365a-3p caused a slightly increased reduction of ~23%. This data, taken together with data from the viral load assay **(Fig. 4.13)** suggest that inhibition of miR-151a-5p and miR-365a-3p causes a reduction in viral egress, with a stronger effect produced by inhibition of miR-365a-3p.

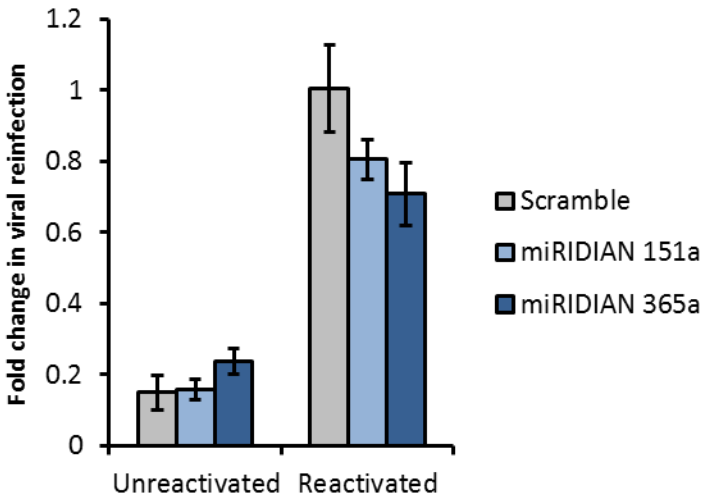

Figure 4.14: miRIDIAN 151a-5p and miRIDIAN 365a-3p decrease the ability of newly generated KSHV virions to infect naïve cells.
293T rKSHV.219 cells were transfected with scramble siRNA (control) or miRIDIAN miRNA inhibitors directed against miR-151a-5p or miR-365a-3p. 72 hours after transfection, cells were treated to induce KSHV lytic replication, or left untreated as a latent control. After 7 days, supernatant was used to infect naïve HEK 293T cells. 24 hours post reinfection, DNA was harvested and viral load was assessed using qPCR against ORF47 using GAPDH as a normalisation control. Fold change was calculated and graphs were plotted using Microsoft Excel. Error bars = SD, $p<0.01$ = **, $p<0.05$ = * compared with scramble control from the same time point.

4.9 Discussion

The utilisation of host miRNAs by viruses represents a relatively new field of biological study, and may be of great use in the near future as an area to exploit in the development of new antiviral drugs. KSHV, as with many other viruses, particularly the Herpesviridae, encodes its own miRNAs but is also able to alter host miRNA dynamics to increase the efficiency of mature virion synthesis. Herein, inhibition of miR-365a-3p has been demonstrated to increase viral load and decrease reinfection of naïve cells, leading to the hypothesis that miR-365a-3p is able to increase the efficiency of viral egress. miRNAs are believed to act at a post-transcriptional level and, therefore, it is likely that this effect is due to the targeting of specific cellular mRNAs, either for degradation or translation repression, by miR-365a-3p.

miRNA sequencing represents a valuable and high resolution approach for identifying dysregulation of global miRNA levels in an unbiased manner. The identification of the upregulation of the miR-221/222 cluster during KSHV lytic infection confirms previous reports that miR-221 and miR-222 are downregulated by latent KSHV gene products,

and also validates the miRNA-seq approach used in this study. 19 mature cellular miRNAs were identified as dysregulated during KSHV lytic infection at some point between 8 and 18 hours. The validation approaches used in this study confirmed that at least 2 of these miRNAs; miR-151a-5p and miR-365a-3p, are dysregulated due to KSHV infection, as their levels follow similar trends in 3 different lytically infected cell types. This approach did, however, limit the possibility of identifying B cell specific miRNA dysregulation during KSHV lytic infection. This means that any future therapeutics designed to target miR-151a-5p or miR-365a-3p will have a better chance of working in multiple KSHV positive cell types, and therefore is likely to make these therapeutics better at treating KS, rather than acting as a preventative measure.

The use of miRIDIAN antagomiRs has been demonstrated, both here and in other studies, to reduce the detection of targeted mature miRNAs by miRNA specific stem loop qRT-PCR. It is not predicted that these miRIDIANs will lead to the degradation of the mature miRNAs, therefore, this effect is believed to be due to highly efficient binding of miRIDIANs to their target miRNA. miRNA sponges also represent a viable means of ablating miRNA function, however, as each miRNA sponge is targeted against multiple miRNAs, often miRNA families, the use of miRIDIAN antagomiRs is more appropriate in this study as well as other studies investigating the roles of specific individual miRNAs.

Exportin-5 and SMARCA4 were observed to localise to the nucleolus of ORF57 expressing cells by subcellular fractionation and SILAC analysis. Both of these proteins play important roles in the biogenesis of mature host miRNAs, and were observed at higher levels in nucleolar fractions during ORF57 expression, suggesting a similar effect may occur during KSHV lytic infection. As KSHV encoded miRNAs are believed to be expressed solely during latent infection, an investigation into the effect of KSHV lytic infection on the levels of host encoded miRNAs was undertaken. However, the relocalisation of Exportin-5 and SMARCA4 was not further characterised. ORF57 localises predominantly to the nucleolus of infected cells, and has been shown to interact with many RNA interacting proteins, particularly those involved in mRNA biogenesis and maturation. It remains to be seen whether ORF57 is also able to exert its influence on miRNA related processes, as indicated by the aforementioned

relocalisation of Exportin-5 and SMARCA4, and so a further investigation into this phenomenon is certainly warranted.

CHAPTER 5

~

KSHV dysregulated microRNA miR-365a-3p depletes levels of DOCK5 mRNA during late infection, and DOCK5 overexpression reduces viral shedding

5 KSHV dysregulated microRNA miR-365a-3p depletes levels of DOCK5 mRNA during late infection, and DOCK5 overexpression reduces viral shedding

5.1 Introduction

The sequencing of mRNAs is rapidly replacing microarray technology for transcriptional profiling experiments (Ozsolak and Milos, 2011; Law et al., 2013). The advantages of these next generation sequencing technologies are manifold, allowing the discovery of novel mRNAs, as well as the detection of RNAs containing sequence polymorphisms, alternative isoforms and edited molecules, whilst also reducing background noise associated with fluorescence-based quantification methods and removing the possibility for non-specific signal detection (Wang et al., 2009; Malone and Oliver, 2011; Zhao et al., 2014).

The regulation of mRNA abundance is a key aspect of gene regulation, and can be affected by a number of different mechanisms (Valencia-Sanchez, 2006; Garneau et al., 2007; Wu and Brewer, 2012; Fu et al., 2014). These include mRNA degradation, through well characterised processes such as exo/endonuclease activity, as seen with KSHV ORF37 encoded protein SOX, which is able to cleave host mRNAs, allowing the cellular exonuclease Xrn1 to bring about large scale degradation of host mRNA molecules (Covarrubias et al., 2011). Furthermore, SOX exerts control over numerous other cellular mRNA maturation/degradation factors, whilst also appearing to affect mRNA trafficking pathways (Sokoloski et al., 2009; Lee and Glaunsinger, 2009; Arias et al., 2009). This demonstrates the importance of regulating host mRNA abundance during lytic viral infection. Conversely, the actions of many miRNAs have also been shown to negatively affect the abundance of target mRNAs (Fabian et al., 2010; Valinezhad Orang et al., 2014). Indeed, this is now believed to be the major role of miRNAs, and hundreds of host miRNA-host mRNA interactions have now been observed. Interestingly, many viruses have been shown to encode miRNAs to target host pathways, and have also developed ways to alter the levels of host miRNAs to dysregulate host gene regulation (Skalsky and Cullen, 2010). Moreover, multiple viral proteins appear to target host miRNA transcription factors in order to further exploit

the cell and increase replication efficacy (Z. Li et al., 2013). Furthermore, some viruses utilise host miRNAs in non-canonical mechanisms, such as HCV, which is able to protect its viral genomic RNA, using miR-122 as a shield, preventing the activity of Xrn1 at the 5' end of the genome (Y. Li et al., 2013).

In this chapter, mRNA sequencing has been employed to examine the expression levels of predicted cellular mRNA targets of miR-151a-5p and miR-365a-3p at multiple points during KSHV lytic infection. Results highlight an interaction between miR-365a-3p and at least two cellular mRNAs, leading to degradation of these mRNAs during late KSHV lytic infection. Importantly, this effect is much more pronounced than the effect caused by the SOX induced host shutoff alone.

5.2 Generation of mRNA sequencing libraries

In order to further understand the effects of miR-151a-5p and miR-365a-3p dysregulation during KSHV lytic replication, mRNA sequencing was utilised in an attempt to find target mRNAs affected by these miRNAs. To this end, total RNA was extracted from TREx BCBL1-Rta cells at 0h (latent control), 8h and 18h post KSHV lytic infection, and examined using an Agilent Bioanalyzer **(Figure 5.1A)**. Samples were of high integrity, and suitable for mRNA-sequencing. mRNA sequencing libraries were then generated using an Illumina TruSeq Stranded mRNA Library Prep Kit and libraries were examined using an Agilent Bioanalyzer **(Figure 5.1B)**. Loss of ribosomal RNA was observed, along with an increase in abundance of RNAs between 25 and 500 base pairs, believed to be total mRNA following fragmentation. Libraries were pooled at a 1:1:1 ratio and sequenced using an Illumina HiSeq by Dr. Sally Harrison and Dr. Catherine Daly (LIBACS). Reads were aligned to the *Homo sapiens* genome and gene expression analysis was performed by Dr. Ian Carr (LIBACS).

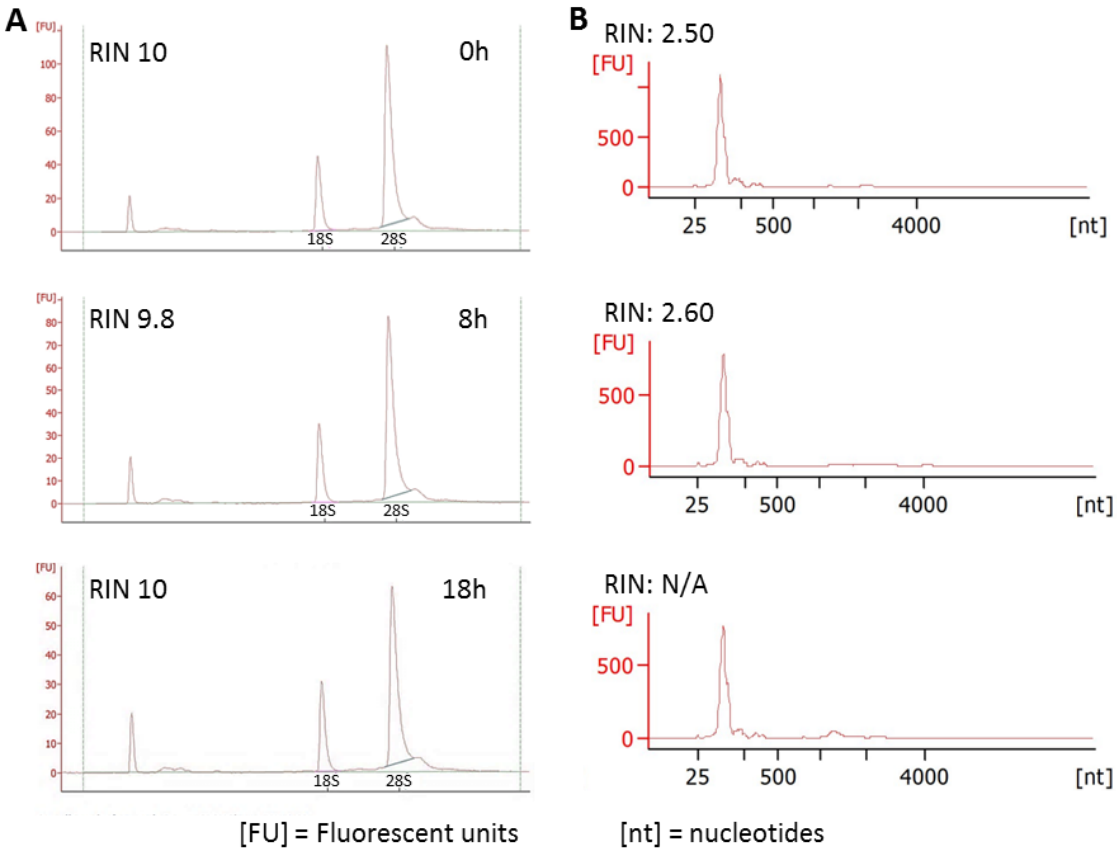

Figure 5.1: Preparation of mRNA sequencing libraries from TREx BCBL1-Rta cells at 0, 8 and 18 hours post lytic reactivation.
(a) Total RNA samples extracted from TREx BCBL1-Rta cells and (b) mRNA sequencing libraries. Samples were analysed using an Agilent Bioanalyzer and RNA integrity values were calculated.

5.3 KSHV dysregulation of miR-365a-3p does not affect abundance of IL-6 or vIL-6 transcripts

An interaction between miR-365a-3p and the cellular IL-6 transcript has previously been reported, resulting in the degradation of IL-6 transcripts (Xu et al., 2011). In order to examine whether this interaction plays a role during KSHV lytic infection, IL-6 read counts over the course of KSHV lytic infection were plotted on a bar chart (read counts were used instead of quantified expression data due to issues with normalisation caused by the KSHV host shutoff phenomenon as well as the increasing complement of viral mRNA in samples from later timepoints) **(Fig. 5.2A)**. IL-6 transcript levels appeared to increase over the course of infection, as previously reported (Aoki et al., 1999; Polson et al., 2002). This suggests miR-365a-3p does not deplete the abundance of IL-6 mRNA during KSHV infection in TREx BCBL1-Rta cells. To further investigate this, 293T rKSHV.219 cells were transfected with scramble siRNA control or miRIDIANs

directed against miR-151a-5p or miR-365a-3p and levels of cellular IL-6 mRNA, as well as the viral homolog vIL-6 mRNAs were quantified by qRT-PCR at 0h (latent control), 8h and 18h post lytic infection **(Fig. 5.2B)**. Abundance of both cellular and viral IL-6 mRNAs were observed to increase over the course of infection, in agreement with the mRNA sequencing data from TREx BCBL1-Rta cells. Taken together, these data suggest that KSHV does not upregulate miR-365a-3p in order to regulate IL-6 or vIL-6 mRNA levels.

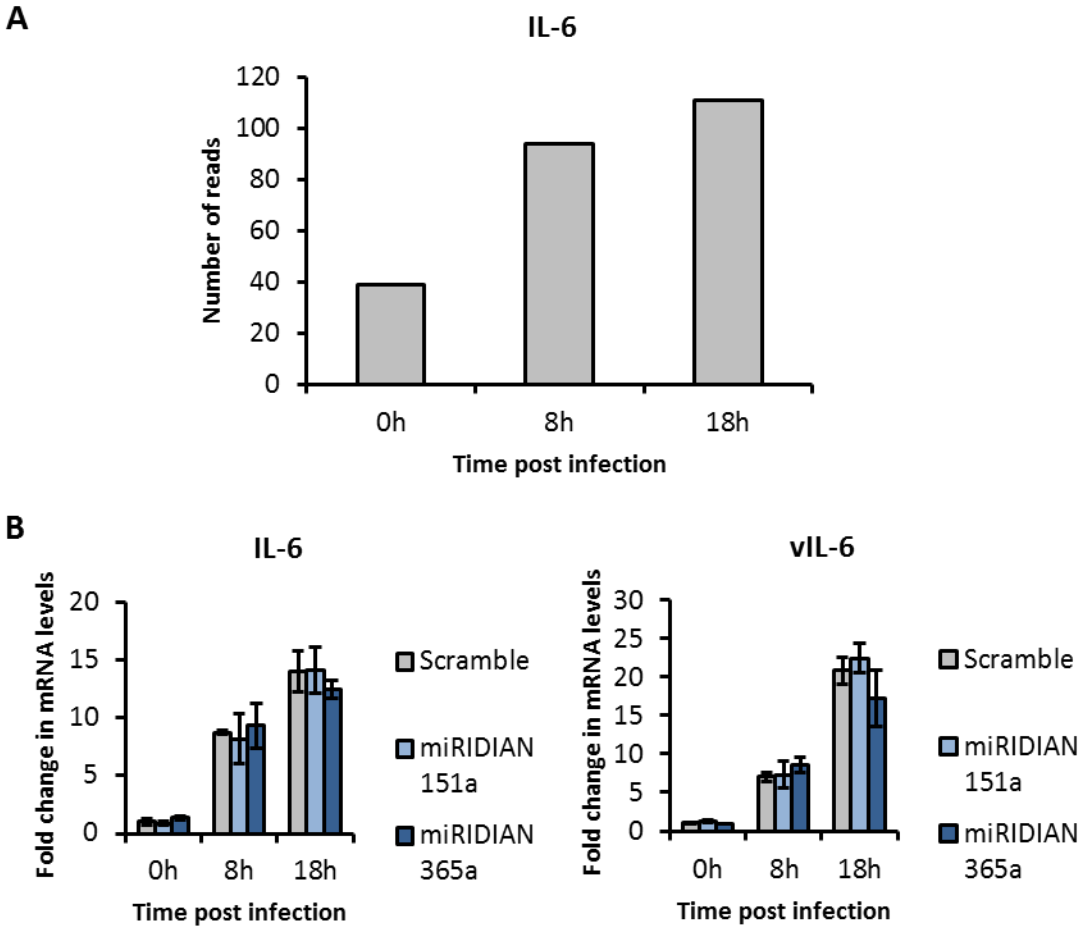

Figure 5.2: Interleukin-6 mRNA levels are not depleted during KSHV lytic infection in TREx BCBL1-Rta cells.

(a) Read counts from mRNA sequencing of TREx BCBL1-Rta cells corresponding to Interleukin 6 over the course of KSHV lytic infection. (b) 293T rKSHV.219 cells were transfected with scramble siRNA (control), or miRidian inhibitors specific to hsa-mir-151a-5p or hsa-mir-365a-3p. 72 hours after transfection lytic infection was induced for 0 (latent control) 8 or 18 (lytic infection) hours. Total RNA was then harvested and extracted RNA was subjected to DNase treatment. RNA was then reverse transcribed into cDNA using an oligo dT primer and qRT-PCR was performed using primers specific to IL-6 and vIL-6. GAPDH was used as a normalisation control. 3 biological replicates were combined, the relative values were displayed on a graph and the standard deviation was calculated. Error bars = SD, $p<0.01$ = **, $p<0.05$ = * compared with scramble control from the same time point.

5.4 Prediction and validation of cellular mRNAs targeted by miR-151a-5p and miR-365a-3p

In order to determine potential mRNA targets of miR-151a-5p and miR-365a-3p, open source miRNA target prediction programs, miRDB.org and microRNA.org, were employed (Betel et al., 2007; Wong and Wang, 2015). Genes identified in these analyses were then cross referenced with the mRNA sequencing data in order to examine their read counts. The trends of the predicted mRNA targets of miR-151a-5p and miR-365a-3p were then plotted on a scatter graph after normalising the read counts so that each mRNA started at a value of 1 in the 0h sample **(Fig. 5.3)**. The vast majority of mRNAs appeared to decrease in abundance by 8 hours, and this effect was more dramatic by 18 hours. This phenomenon has previously been reported during KSHV and is known as the host shutoff response, mainly caused by the interaction between the viral protein SOX (shutoff and exonuclease) and the cellular exoribonuclease Xrn1 (Covarrubias et al., 2011). In order to compensate for this effect, the 4 mRNAs that were depleted to the largest extent were selected for each miRNA (solid lines, **Fig. 5.3**). It was hypothesised that the more rapid and enhanced depletion of these mRNAs may demonstrate an additional degradative effect due to the action of the identified miRNAs. HOXA3 was selected as the fourth predicted target of miR-151a-5p, as its expression trend inversely correlated with that of the miRNA during KSHV lytic infection. Therefore, these mRNAs were taken forward for further analysis.

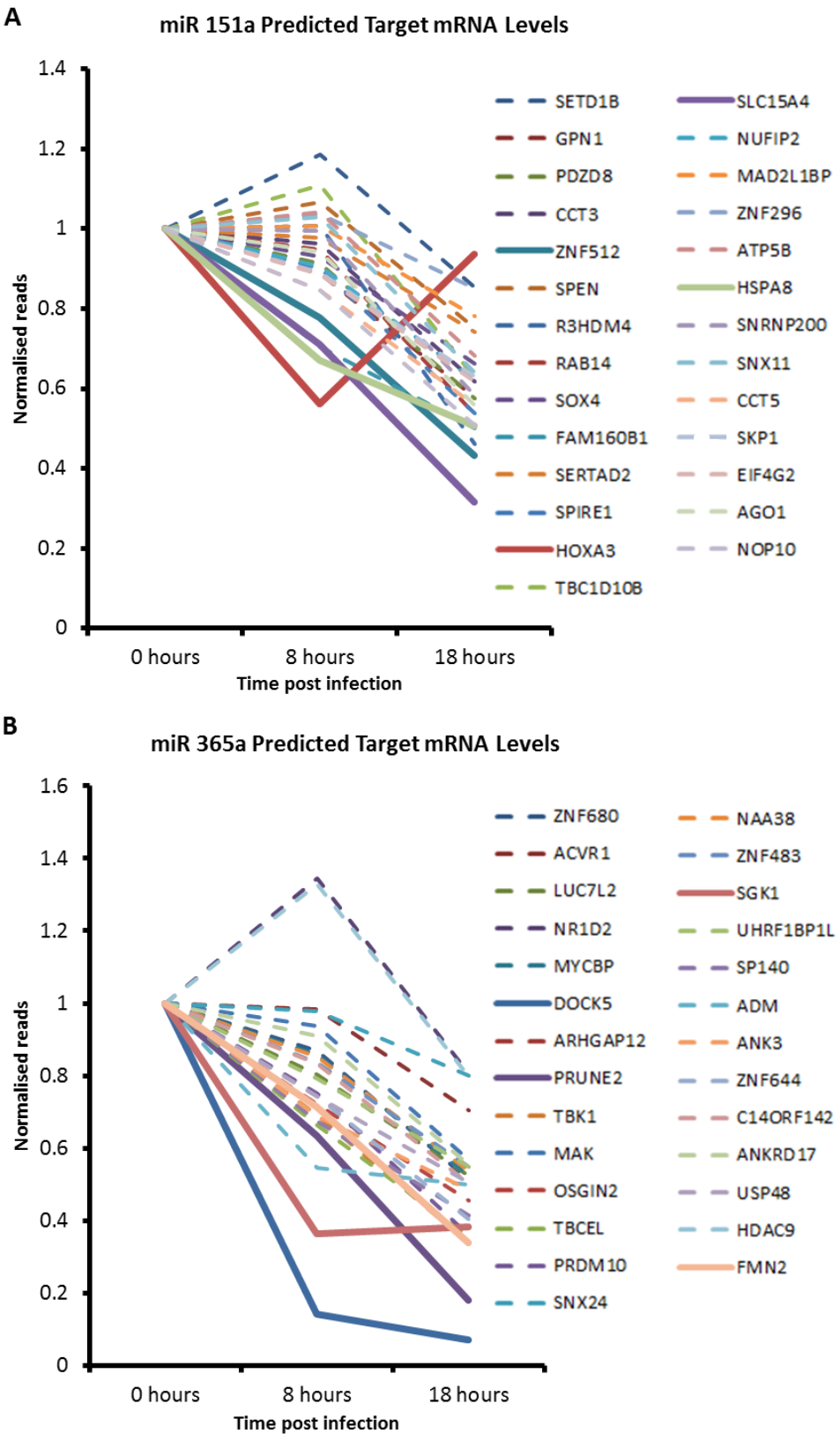

Figure 5.3: mRNA-seq expression data for predicted miR-151a-5p and miR-365a-3p target genes.
(a) miRNA target prediction software was used to identify mRNAs predicted to be bound by miR-151a-5p and (b) miR-365a-3p. Predicted mRNAs were cross referenced with mRNA sequencing data from KSHV infected TREx BCBL1-Rta cells. Read counts for identified mRNAs were all normalised to give a value of 1 in the 0h sample. Trends were then plotted on scattergraphs. Solid lines indicate 4 mRNAs that are most depleted over the course of KSHV infection.

In order to assess the validity of the predicted miRNA-mRNA interactions, the abundance of the mRNAs were investigated during KSHV lytic infection in the presence of scramble siRNA as well as miRIDIANs directed against miR-151a-5p and miR-365a-3p. However, a suitable reference gene was required in order to normalise the data. The criteria set for this reference gene were that it should remain at the same abundance over the course of the KSHV infection (i.e. should not be subjected to the host shutoff response) and that its abundance should not be affected by either miRIDIAN or scramble siRNA. A number of candidate RNAs were chosen for investigation: 5s and 18s ribosomal RNA should remain stable over a range of cellular stresses; ABI3, DSP, FAM9C and SPINK2 all remained at relatively stable levels in the mRNA sequencing data, and GAPDH was also examined as this gene is commonly used as a normalisation control in many laboratories across the world. The host shutoff response was visualised by counting up the total number of reads that aligned to the *Homo sapiens* genome in each sample analysed by mRNA sequencing and a scatter graph was plotted **(Fig. 5.4)**. The levels of candidate genes were then assessed at 0h, 8h and 18h post KSHV lytic infection in the presence of scramble siRNA, and miRIDIANs directed against miR-151a-5p and miR-365a-3p. The levels were then displayed in bar charts (Fig. 5.4). Surprisingly, levels of both 5s and 18s rRNA were dramatically altered between different samples, appearing to be depleted by KSHV infection, and stabilised at the 8h time point by either miRIDIAN. Levels of ABI3 and FAM9C transcripts displayed an increase at 0h in the presence of miRIDIAN 365a-3p, whilst levels of SPINK2 appeared to increase at 18h in the presence of scramble siRNA. DSP and GAPDH appeared to be the most appropriate reference genes for qRT-PCR involving miRIDIANs and KSHV infection. GAPDH was eventually chosen because although transcript levels drop over the course of KSHV lytic infection, the error between samples at individual timepoints was less than that of DSP.

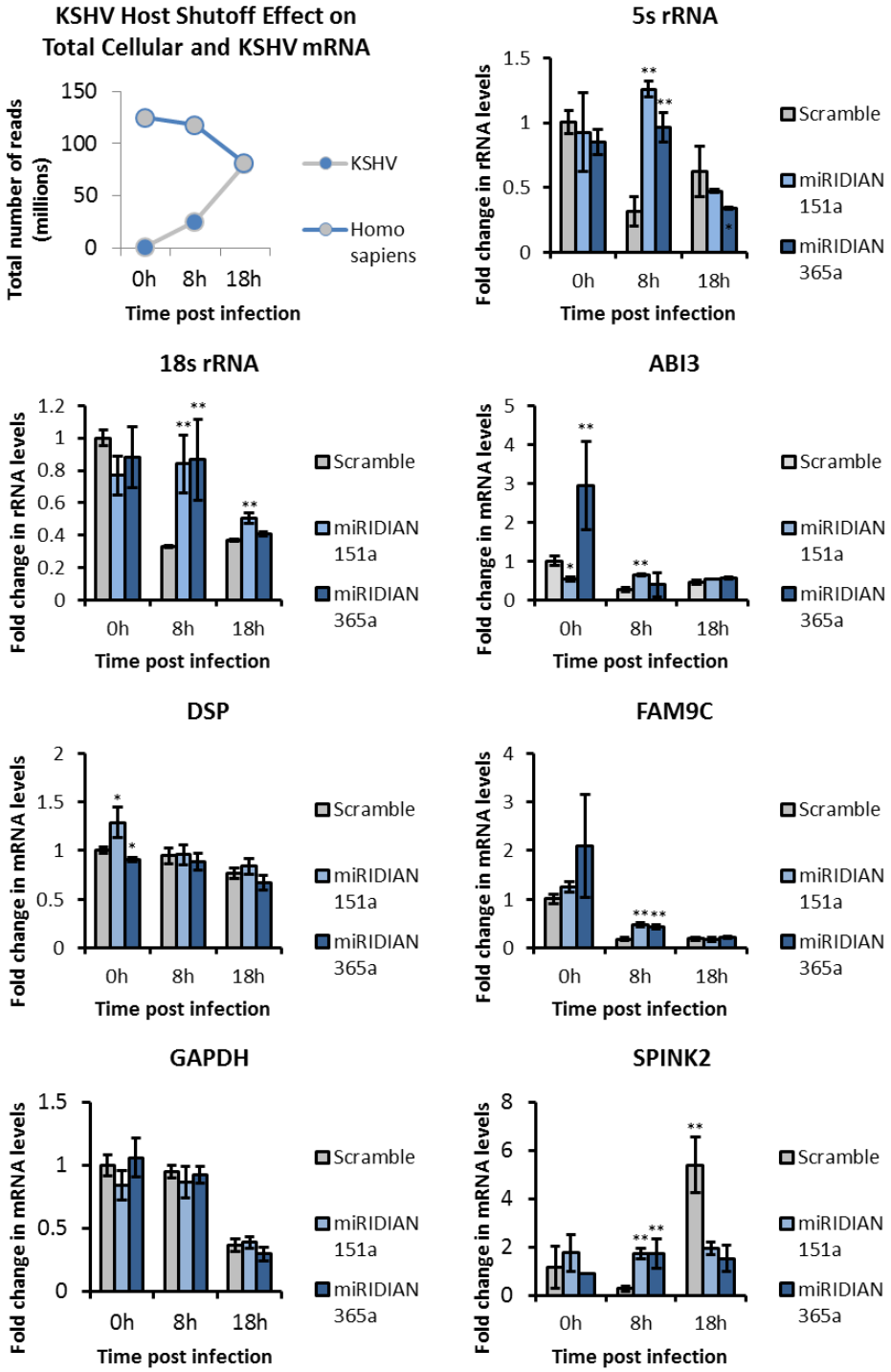

Figure 5.4: Determination of GAPDH as a suitable qRT-PCR reference gene during KSHV lytic reactivation in 293T rKSHV.219 cells.

293T rKSHV.219 cells were transfected with scramble siRNA (control), or miRidian inhibitors specific to hsa-mir-151a-5p or hsa-mir-365a-3p. 72 hours after transfection lytic infection was induced for 0 (latent control) 8 or 18 (lytic infection) hours. Total RNA was then harvested and subjected to DNase treatment. RNA was then diluted to 50ng μl^{-1} and reverse transcribed into cDNA using random hexamers (for 5s and 18s rRNA) or oligo dT primers and qRT-PCR was performed using primers specific to 5s rRNA, 18srRNA, ABI3, DSP, FAM9C, GAPDH and SPINK2. 3 biological replicates were combined, the relative values were displayed on a graph and the standard deviation was calculated. Error bars = SD, $p<0.01$ = **, $p<0.05$ = * compared with scramble control of the same time point.

The levels of 4 predicted mRNA targets of miR-151a-5p; HOXA3, HSPA8, SLC15A4 and ZNF512 were then assessed using qRT-PCR in the presence of scramble siRNA or miRIDIANs directed against miR-151a-5p or miR-365a-3p **(Fig. 5.5)**. miRIDIAN 151a-5p did not appear to produce a stabilising effect on any of the mRNAs tested, suggesting that miR-151a-5p does not cause an enhanced degradation of these predicted target mRNAs during KSHV host shutoff. This therefore, suggests that the viral host shutoff response alone degrades these mRNAs more rapidly than many of the other mRNAs predicted to interact with miR-151a-5p. Interestingly, in 293T rKSHV.219 cells, the levels of both HOXA3 and HSPA8 appeared stable when compared with GAPDH, suggesting they are depleted at the same rate, differing from the trend observed in the TREx BCBL1-Rta mRNA sequencing data. Furthermore, levels of SLC15A4 appeared to increase in scramble control samples when normalised to GAPDH, suggesting this gene is depleted at a slower rate than GAPDH, again differing from the trend seen in the mRNA sequencing data. ZNF512 was seen to decrease over the course of the experiment when normalised to GAPDH, following the trend observed in the mRNA sequencing data. This highlights the differences between the dynamics of mRNA expression in different cell lines.

The levels of 4 predicted mRNA targets of miR-365a-3p; DOCK5, PRUNE2, FMN2 and SGK1 were assessed using qRT-PCR in the presence of scramble siRNA or miRIDIANs directed against miR-151a-5p or miR-365a-3p **(Fig. 5.6)**. miRIDIAN 365a-3p did not appear to produce a stabilising effect on FMN2 or SGK1, suggesting that miR-365a-3p does not cause an enhanced degradation of these mRNAs during KSHV host shutoff. Both of these mRNAs were degraded at a higher rate than GAPDH, in agreement with the mRNA sequencing data. Interestingly, both DOCK5 and PRUNE2 mRNA levels were stabilised by miRIDIAN 365a-3p at 18h post KSHV lytic infection, meaning that without the action of miR-365a-3p these mRNAs are degraded at the same rate as GAPDH. This suggests that KSHV is able to utilise host miRNAs to degrade specific host mRNAs at a much greater rate than by the SOX induced host shutoff response alone. This effect is clearly most pronounced after 8 hours, as the lytic cycle moves from the immediate early into the early stage – coinciding with the expression of a large number of viral genes, including ORF37 (SOX).

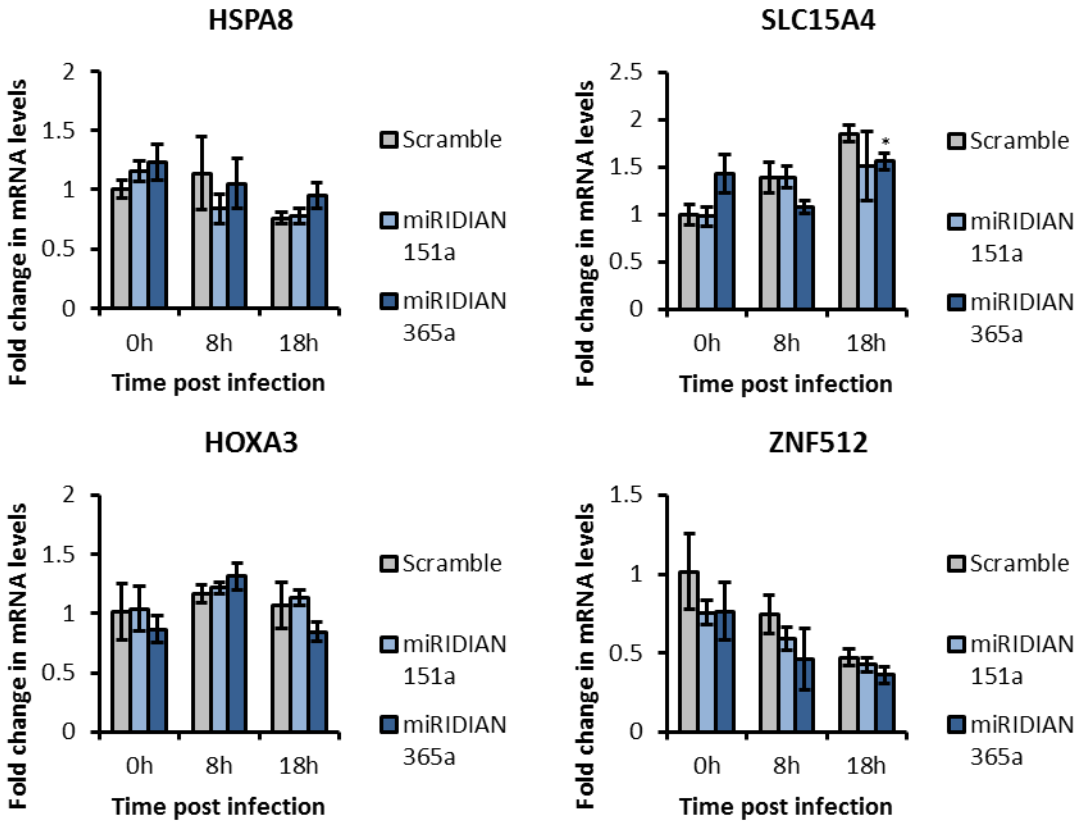

Figure 5.5: Predicted miR-151a-5p target gene levels are not affected by inhibition of miR-151a-5p action using miRidian inhibitor.
293T rKSHV.219 cells were transfected with scramble siRNA (control), or miRidian inhibitors specific to hsa-mir-151a-5p or hsa-mir-365a-3p. 72 hours after transfection lytic infection was induced for 0 (latent control) 8 or 18 (lytic infection) hours. Total RNA was then harvested and subjected to DNase treatment. RNA was then reverse transcribed into cDNA using an oligo dT primer and qRT-PCR was performed using primers specific to HSPA8, SLC15A4, HOXA3 and ZNF512. GAPDH was used as a normalisation control. 3 biological replicates were combined, the relative values were displayed on a graph and the standard deviation was calculated. Error bars = SD, $p<0.01$ = **, $p<0.05$ = * compared with scramble control of the same time point.

5.5 DOCK5 overexpression does not affect KSHV RNA or late protein expression

As miR-365a-3p inhibition appeared to affect KSHV RNA and protein expression levels, it was hypothesised that DOCK5 overexpression may also cause a similar effect. In order to investigate this, 293T rKSHV.219 were transfected with DOCK5-GFP or GFP (control) and either induced for 0 (latent control) 8 or 18 hours lytic infection. The expression levels of a panel of KSHV encoded RNAs were then examined by qRT-PCR **(Fig. 5.7)**. DOCK5-GFP overexpression did not appear to affect the levels of any KSHV RNAs tested at various times post infection. This indicates that the reduction in KSHV

RNA levels observed in the presence of miRIDIAN 365a-3p is likely due to the inhibition of interactions between miR-365a-3p and other mRNA targets.

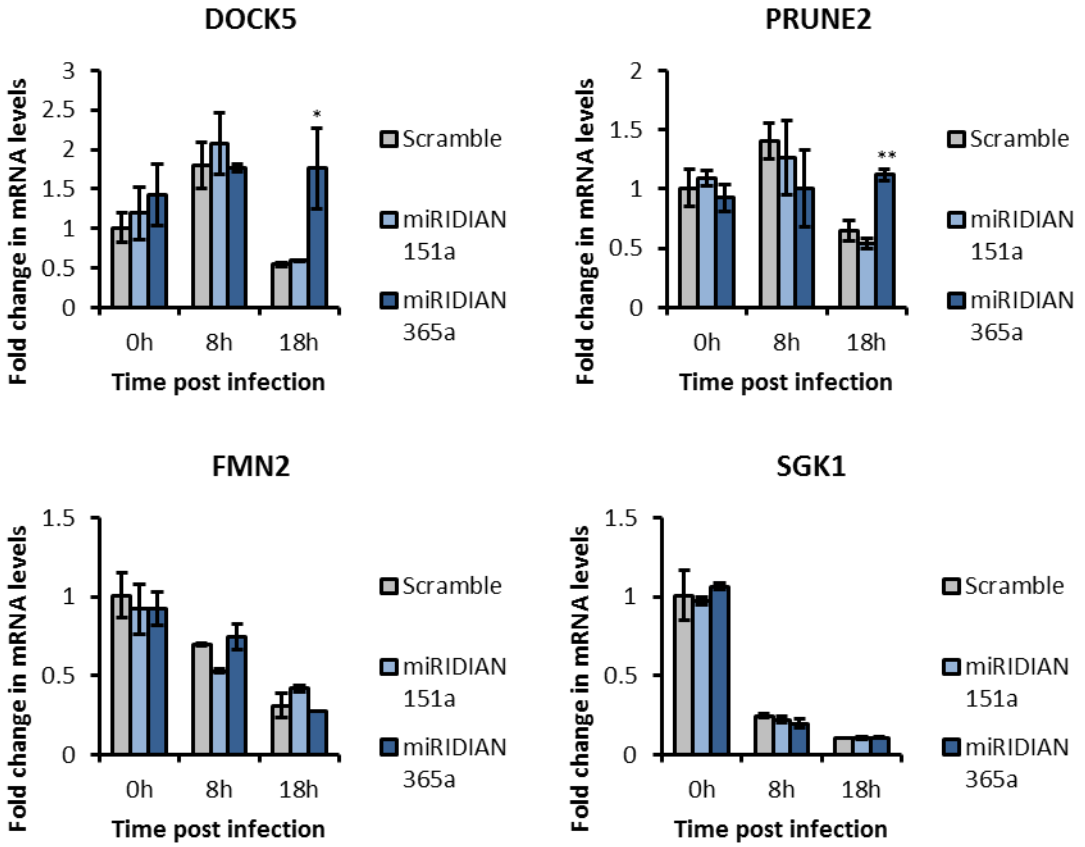

Figure 5.6: Expression levels of predicted miR-365a-3p target genes DOCK5 and PRUNE2 are stabilised by inhibition of miR-365a-3p action using miRidian inhibitor.
293T rKSHV.219 cells were transfected with scramble siRNA (control), or miRidian inhibitors specific to hsa-mir-151a-5p or hsa-mir-365a-3p. 72 hours after transfection lytic infection was induced for 0 (latent control) 8 or 18 (lytic infection) hours. Total RNA was then harvested and subjected to DNase treatment. RNA was then reverse transcribed into cDNA using an oligo dT primer and qRT-PCR was performed using primers specific to DOCK5, PRUNE2, FMN2 and SGK1. GAPDH was used as a normalisation control. 3 biological replicates were combined, the relative values were displayed on a graph and the standard deviation was calculated. Error bars = SD, $p<0.01$ = **, $p<0.05$ = * compared with scramble control of the same time point.

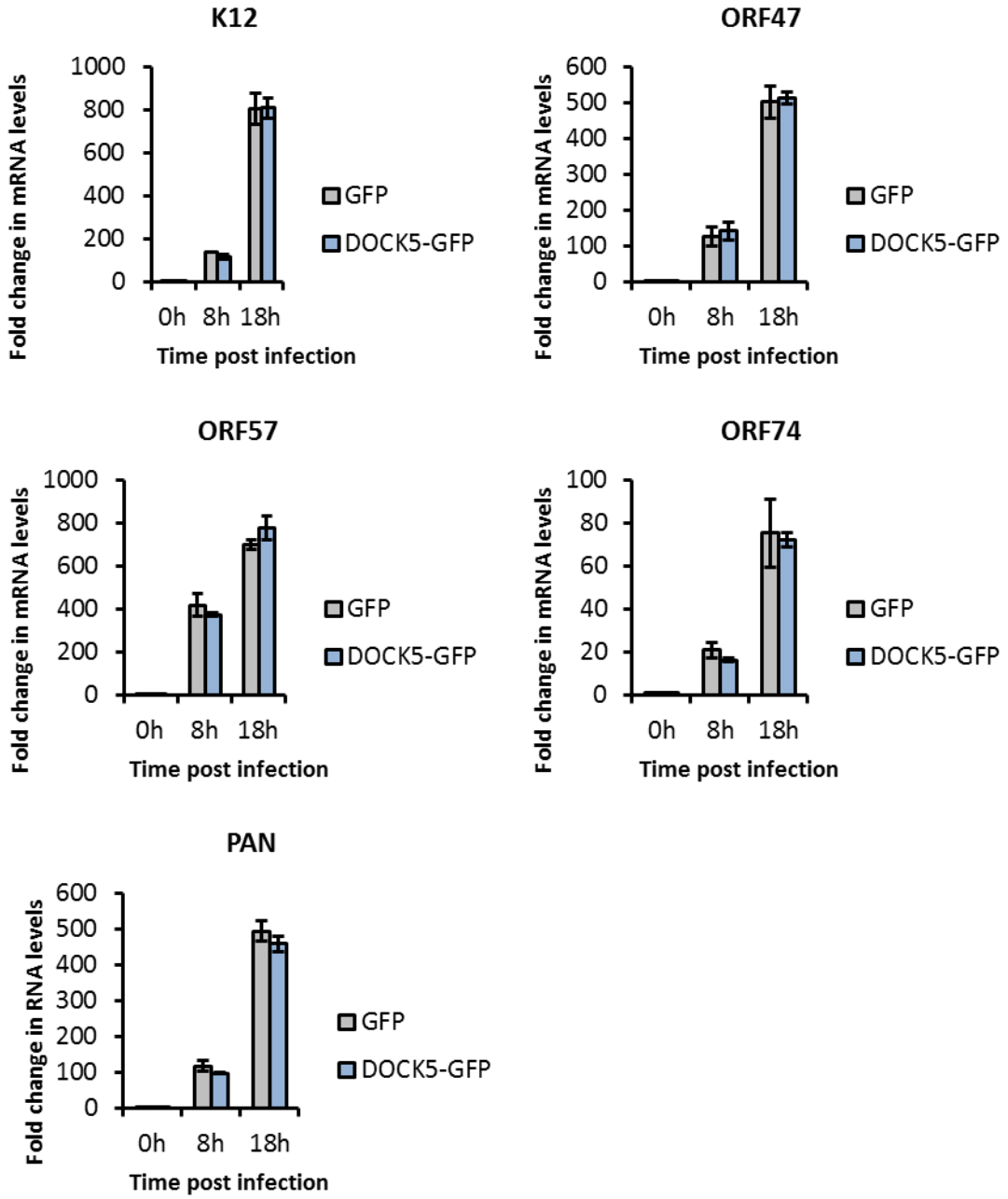

Figure 5.7: DOCK5-GFP overexpression has no effect on expression levels of KSHV RNAs.
293T rKSHV.219 cells were transfected with DOCK5-GFP or GFP (control). 24 hours after transfection lytic infection was induced for 0 (latent control) 8 or 18 (lytic infection) hours. Total RNA was then harvested and subjected to DNase treatment. RNA was then reverse transcribed into cDNA using an oligo dT primer and qRT-PCR was performed using primers specific to K12, ORF47, ORF57, ORF74 and PAN. GAPDH was used as a normalisation control. 3 biological replicates were combined, the relative values were displayed on a graph and the standard deviation was calculated. Error bars = SD, $p<0.01$ = **, $p<0.05$ = * compared with GFP control of the same time point.

The effects of DOCK5-GFP overexpression on late viral protein expression was also examined. 293T rKSHV.219 cells transfected with DOCK5-GFP, GFP (control) or untransfected (control) were induced for 0 (control) or 72 hours lytic infection. Lysates were harvested and immunoblotting was performed to examine the levels of DOCK5-

GFP, GFP and minor capsid protein, using GAPDH as a loading control **(Fig. 5.8)**. Overexpression of DOCK5-GFP was not observed to significantly affect the levels of minor capsid protein produced by densitometry analysis. This suggests that overexpression of DOCK5-GFP does not significantly affect the efficiency of the viral lytic gene cascade.

5.6 DOCK5 overexpression reduces rate of viral shedding

DOCK5 is a member of the DOCK-A family of proteins, which are believed to act as guanine nucleotide exchange factors (GEFs) with the ultimate goal of activating small G proteins (Sanders et al., 2009; Ogawa et al., 2014). DOCK5, specifically, mediates Rac activity, and therefore may play an important regulatory role in a diverse range of Rac-related cellular processes (Cote, 2002; Brugnera et al., 2002; Meller et al., 2002). Interestingly, other members of the DOCK family have been shown to influence cytoskeletal change through activation of Rac (Sanui, 2003; Xu and Jin, 2012). The host cell cytoskeleton plays important roles during many viral infections, and can act in both pro- and anti-viral mechanisms (Johnson and Huber, 2002; Mothes et al., 2010; Fletcher and Mullins, 2010; Delorme-Axford and Coyne, 2011; Taylor et al., 2011; Xu et al., 2014; Knight et al., 2015). Herpesviruses in particular have been shown to use actin networks during ingress in certain cell types (Clement et al., 2006). Furthermore, it has been demonstrated that some herpesviruses use an ATP-dependent mechanism in order to translocate nucleocapsids inside the nucleus of an infected cell, with actin standing out as a prime candidate for the mediation of this process (Forest et al., 2005). Conversely, the cortical actin network can act as an inhibitor to viral egress, as it has evolved to function as a barrier that must be overcome prior to the secretion of granules and other small biological structures (Ward, 2011). Myosin Va (myoVa) is a key protein in this mechanism, and allows such secretory structures to pass through the cortical actin network, and this has also been implicated in HSV-1 egress (Roberts and Baines, 2010). Furthermore, myoVa expression is important for the correct localisation of the HSV-1 encoded gD, gB and gM glycoproteins (Roberts and Baines, 2010).

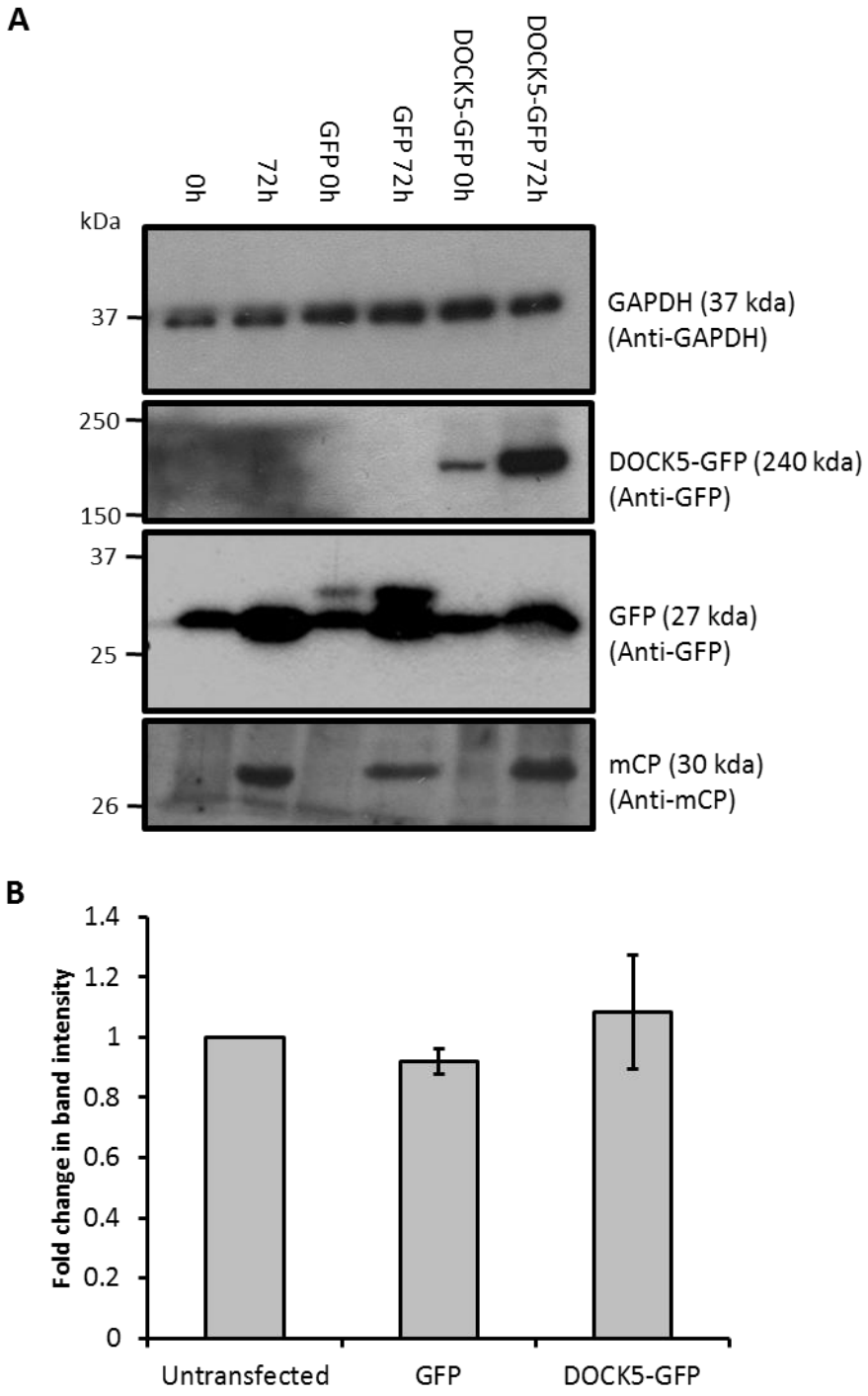

Figure 5.8: Overexpression of DOCK5-GFP does not affect KSHV mCP expression in 293T rKSHV.219 cells.

(a) 293T rKSHV.219 cells were transfected without DNA (mock), pEGFP-N1 or pDOCK5-GFP. 48 hours after transfection cells were either reactivated with NaBu and TPA for 72 hours (lytic infection) or left unreactivated (latent - control). Lysates were then harvested and immunoblot analysis was performed with antibodies specific to GFP, GAPDH and KSHV mCP ORF26. GAPDH specific antibody was used to control for equal loading. (b) The fold change in mCP levels was calculated for each reactivated sample when compared with scramble siRNA control. Immunoblots were analysed using ImageJ software. Values are average of 3 independent immunoblots. Error bars = SD, $p<0.01$ = **, $p<0.05$ = * compared with Untransfected control.

Therefore, it was hypothesised that by stimulating the overexpression of miR-365a-3p, KSHV may deplete levels of DOCK5 in order to overcome the cortical actin barrier. As such, it was also hypothesised that DOCK5-GFP overexpression would limit viral egress. In order to investigate these hypotheses, 293T rKSHV.219 cells were transfected with DOCK5-GFP or GFP (control). 24 hours post transfection, cells were induced for lytic reactivation, or left uninduced (latent control). 7 days post lytic infection, cells were collected by centrifugation, DNA was harvested and viral load was measured by qPCR **(Fig. 5.9)**. DOCK5-GFP overexpression was observed to increase viral load by 50% after 7 days, which may suggest one of two possibilities. Firstly, that DOCK5-GFP overexpression promotes viral replication, or secondly, limits viral egress.

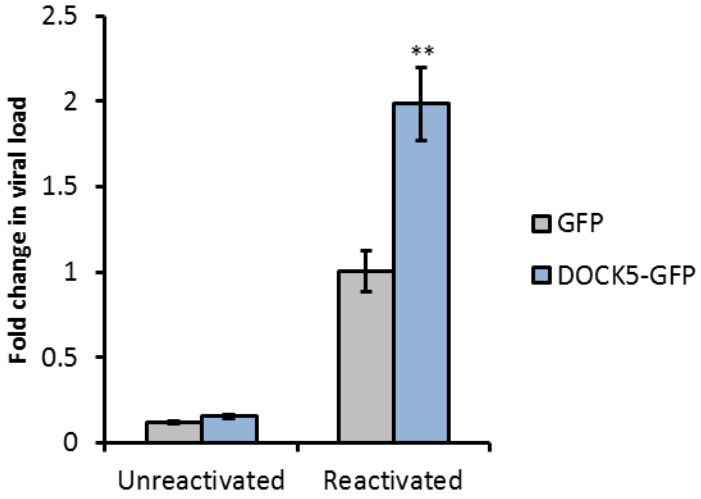

Figure 5.9: DOCK5-GFP overexpression increases viral load following lytic replication in 293T rKSHV.219 cells.
293T rKSHV.219 cells were transfected with DOCK5-GFP or GFP (control). 24 hours after transfection lytic infection was induced for 0 (latent control) or 7 days (lytic infection). Total DNA was then harvested and qPCR was performed using primers specific to ORF47. GAPDH was used as a normalisation control. 3 biological replicates were combined, the relative values were displayed on a graph and the standard deviation was calculated. Error bars = SD, $p<0.01$ = **, $p<0.05$ = * compared with GFP control of the same reactivation state.

In order to determine whether DOCK5-GFP overexpression caused enhanced viral expression or reduced viral egress, a reinfection assay was performed using KSHV naïve cells. 293T rKSHV.219 cells were transfected with DOCK5-GFP or GFP (control). 24 hours post transfection, cells were induced for lytic reactivation, or left uninduced (latent control). 7 days post lytic infection, cells were pelleted by centrifugation and supernatant was used to infect KSHV naïve HEK 293T cells. 1 day post infection, DNA was harvested and viral load was measured by qPCR **(Fig. 5.10)**. Reinfection was

impaired using supernatant from DOCK5-GFP expressing cells when compared with GFP expressing cells. Taken together in combination with the results from the viral load assay in 293T rKSHV.219 cells **(Fig. 5.9)**, these data suggest that DOCK5-GFP overexpression is able to reduce KSHV egress. Furthermore, this suggests that KSHV upregulates miR-365a-3p levels in order to deplete levels of DOCK5 overcoming this inhibitory effect of DOCK5 and increasing viral egress.

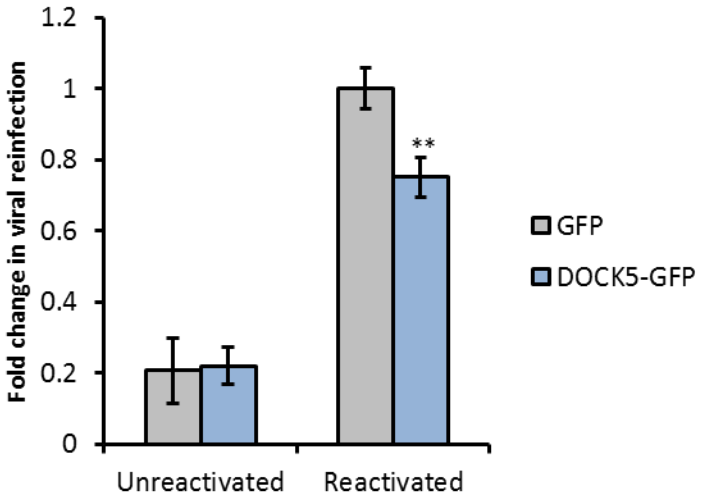

Figure 5.10: DOCK5-GFP overexpression reduces the ability of newly generated KSHV virions to infect naïve cells.
293T rKSHV.219 cells were transfected with DOCK5-GFP or GFP (control). 24 hours after transfection lytic infection was induced for 0 (latent control) or 7 days (lytic infection). Total DNA was then harvested and qPCR was performed using primers specific to ORF47. GAPDH was used as a normalisation control. 3 biological replicates were combined, the relative values were displayed on a graph and the standard deviation was calculated. Error bars = SD, $p<0.01$ = **, $p<0.05$ = * compared with GFP control of the same reactivation state.

5.7 Discussion

It is becoming evident that by combining multiple high throughput, high resolution approaches, further insight can be gained into biological phenomena than by the application of any individual approach. Herein, it is demonstrated that by combining miRNA-seq, open source miRNA target prediction and mRNA-seq during viral infection, it is possible to identify dysregulated miRNAs, as well as their downstream targets. These approaches have variable false positive rates, and in this particular study of 8 predicted target mRNAs examined, only 2 were found to be associated with real biological effects, representing a 25% success rate, albeit with a very small sample size.

This emphasises the requirement for validation of results attained through these approaches in a wet laboratory setting. It has also previously been demonstrated that by repeating the initial analyses, the data obtained tend to exhibit an increased percentage of positive hits. Nevertheless, in this study 2 previously unreported mRNA targets of miR-365a-3p have been identified, and DOCK5 has been demonstrated to have an inhibitory effect on a lytic viral process prior to the release of a mature infectious virion, hypothesised to be viral egress.

DOCK5 belongs to the DOCK family of proteins, which are believed to contribute towards cytoskeleton organisation, particularly through the polymerization of actin (Li et al., 2001; Kaipa et al., 2013). Many viruses have been shown to interact with the host cytoskeleton in order to mediate viral ingress, movement of viral material to various subcellular structures, viral egress, cell to cell spread as well as cell motility and metastatic potential (Johnson and Huber, 2002; Mothes et al., 2010; Taylor et al., 2011; Knight et al., 2015). This demonstrates the importance of the host cytoskeleton, both as a functional highway for the movement of various molecules around the intracellular environment, and also as a barrier to molecules attempting to gain access to or escape from the cell (Fletcher and Mullins, 2010; Delorme-Axford and Coyne, 2011). Furthermore, the involvement of the cytoskeleton in cell to cell spread and virally induced metastasis demonstrates that these intracellular dynamics can affect intercellular processes, particularly during viral infection (Radtke et al., 2006; Taylor et al., 2011; Xu et al., 2014; Knight et al., 2015). It is not surprising, therefore, that many viruses exert considerable control over the host cytoskeleton at multiple levels and times during infection. Expression of the hypothesised actin regulator protein DOCK5, or inhibition of miR-365a-3p, which is herein shown to also increase DOCK5 during KSHV lytic infection, increases the viral load of treated cells, whilst reducing the release of infectious mature virions for reinfection in naïve cells. It is therefore hypothesised that DOCK5 expression inhibits viral egress. Furthermore, it is hypothesised that this effect is, at least in part, associated with actin dynamics, possibly involved in capsid movement following the assembly and partial maturation of a new virion. Alternatively, actin may interfere with egress at the point of viral release from the cell, as actin forms a network near the cellular periphery known as the cortical actin

network. Indeed, the cortical actin network has been shown to act as a barrier to HSV-1 egress (Roberts and Baines, 2010). HSV-1 is able to overcome this effect via an interaction with the molecular motor protein Myosin Va, which is able to mediate the movement of HSV-1 virions through the cortical actin network, ultimately leading to the efficient egress of infectious mature virions.

The effects of PRUNE2 overexpression on the KSHV lytic cycle have not been explored. PRUNE2 is a 340 kDa protein that has been characterised as a proapoptotic factor, associated with a favourable prognosis in neuroblastoma and epithelial-derived cancers (Machida et al., 2006; Tatsumi et al., 2015). PRUNE2 expression produces downstream effects on a number of proteins associated with the DNA damage response, including AKT, forkhead box protein O3 (FOXO3a) and ATM, via an interaction with apoptosis regulator Bcl-2 (Bcl-2) (Tatsumi et al., 2015). It has yet to be determined whether the downregulation of PRUNE2 mRNA produces an effect at the protein level, however this may correlate with a decrease in apoptosis of KSHV infected cells, which has already been discussed in chapter 3 of this work. Furthermore, low expression of PRUNE2 is associated with poor prognosis in a number of cancers, and therefore may also be of research interest with respect to Kaposi's sarcoma and the development of novel therapeutics against this important disease.

CHAPTER 6

~

Discussion

6 Discussion and future perspectives

Since the discovery of KSHV in 1994, the virus has been extensively studied and important many virus-host interactions have been identified (Chang et al., 1994). Despite this, a significant number of interactions remain uncharacterised, and many more are yet to be discovered. High throughput, high resolution “omics” approaches represent powerful technologies to aid our understanding of these interactions and processes. Herein, three of these approaches, SILAC-based quantitative proteomics, miRNA sequencing and mRNA sequencing, have been utilised to identify and characterise novel interactions between KSHV and the host cell.

In chapter 3, it is observed that KSHV lytic infection leads to the increased abundance of a number of splicing factors, including Prp19 (Chanarat and Sträßer, 2013), in subnuclear bodies such as the nucleolus and nuclear speckles. Prp19 was observed to interact with the KSHV encoded ORF57 protein, which plays an important role in all stages of the maturation and nuclear export of KSHV encoded mRNAs (Schumann et al., 2013). KSHV encodes both intron-containing and intronless transcripts (Arias et al., 2014 p. 0), and therefore the interactions between Prp19 and both of these types of viral mRNAs were examined, using both overexpression and depletion of Prp19, as well as its cofactor, CDC5L (Grote et al., 2010). Unexpectedly, depletion of either or both of these proteins did not appear to affect KSHV transcript maturation or protein production, despite previous suggestions that Prp19/CDC5L complex recruitment is essential for hTREX occupancy at both inton-containing and intronless transcripts (Chanarat et al., 2011). While this effect can be explained by the ORF57 dependent direct recruitment of hTREX to viral intronless transcripts (Boyne et al., 2008), it is particularly striking that KSHV encoded intron-containing transcript maturation and export is not affected by Prp19 and CDC5L depletion. Although it is possible that a small pool of both of these proteins remains in the cell following depletion by siRNA treatment, it seems unlikely that this greatly reduced pool would achieve the same efficiency of mRNA maturation and export. This may suggest that ORF57 is able to exert considerable influence on the splicing of viral intron-containing transcripts, allowing them to bypass the requirement for Prp19/CDC5L complex activity in this

process. Indeed, in support of this, ORF57 is necessary for the complete splicing of the alternatively spliced viral K8 transcript (Majerciak et al., 2008).

Prp19 overexpression was observed to contribute to a minor activation of several DNA damage response pathway proteins. Although this effect has not been previously described, Prp19 ubiquitylation is known to increase during overexpression (Lu and Legerski, 2007 p. 19), and this modification is also observed during the involvement of Prp19 in the ATR-Chk1 DNA damage signalling pathway, which may partially explain this unexpected effect. Interestingly, ORF57 overexpression limits this phenomenon, suggesting that the interaction between ORF57 and Prp19 may be a pro-viral response to prevent activation of the ATR-Chk1 dependent DNA damage response. Indeed, it has been previously observed that while the ATM-Chk2 and DNA-PK dependent DNA damage response pathways are both activated during KSHV lytic infection, downstream signalling of the ATR-Chk1 dependent pathway remains inactive (Hollingworth et al., 2015). It was subsequently demonstrated that, upon DNA damage induction, ORF57, Prp19 and ATRIP all localise to subnuclear puncta, often observed near the nuclear pore, possibly indicating sites of euchromatin (Jerabek and Heermann, 2014). Euchromatin is more susceptible to both camptothecin induced DNA damage (Bassi et al., 1998), as well as the R-loop induced DNA damage that is known to occur during KSHV infection (Jackson et al., 2014). It is therefore hypothesised that ORF57 blocks a role of Prp19 in the ATR-Chk1 DNA damage signalling pathway, limiting downstream pathway activation, presumably to prevent apoptosis or cell cycle arrest which would likely be detrimental to viral replication.

Further investigation is necessary in order to demonstrate that ORF57 is, indeed, able to specifically block Prp19 function in this pathway, and that this interaction is not a side effect of ORF57 inhibition of ATRIP function, or the function of any other ATR-Chk1 DNA damage response pathway proteins that may be associated with these foci. This could initially be investigated by analysing post translational modifications of RPA, which is ubiquitylated by Prp19 during early stages of the ATR-Chk1 pathway. Furthermore, additional studies are necessary to demonstrate that inhibition of the ATR-Chk1 DNA damage response pathway is beneficial to the virus, particularly as the ATM-Chk2 and DNA-PK pathways do not appear to be affected, and are all believed to

contribute to similar downstream effects (Hollingworth et al., 2015; Branzei and Foiani, 2008). Constitutively active Chk1 mutants have been identified, and could be expressed to characterise the effect of pathway activation on KSHV lytic replication (Wang et al., 2012). Finally, additional SILAC-based quantitative proteomic analysis of the nucleolus of lytically infected cells, as well as ORF57 SILAC immunoprecipitation experiments suggest that ORF57 interacts with multiple splicing components, including other members of the Prp19/CDC5L complex. Further work is, therefore, required to assess whether these other factors play a role in the maturation of KSHV intron-containing or intronless transcripts, or indeed whether any of these factors are involved in the ATR-Chk1 DNA damage response, which may explain their association with ORF57.

The SILAC data analysed in chapter 3 also revealed the increased abundance of proteins associated with miRNA biogenesis in subnuclear bodies during KSHV lytic infection. KSHV encoded miRNAs are expressed during latency (Qin et al., 2012), and therefore, work presented in chapter 4 describes the utilisation of miRNA sequencing, and the subsequent identification of 19 mature host miRNAs that display altered expression levels during lytic KSHV infection in TREx BCBL1-Rta cells. Cell type specificity is commonly observed for different miRNAs, however, the strategy described herein was able to identify two host miRNAs, miR-151a-5p and miR-365a-3p, that display similar expression trends in three different cell lines undergoing KSHV lytic infection. This is hypothesised to allow for greater therapeutic potential if the interactions between these host miRNAs and the KSHV lytic cycle become viable targets for therapeutic intervention, particularly as KSHV infects both B cells and endothelial cells in infected individuals (Chen and Lagunoff, 2005). Interestingly, these miRNAs exhibit different expression trends during the course of KSHV lytic infection, with miR-151a-5p displaying maximum levels at 8 hours, while miR-365a-3p was most upregulated at 18 hours. These two miRNAs have different genomic contexts, with miR-151a-5p found in an intronic sequence, while miR-365a-3p is an intergenic miRNA. These genomic contexts may have some involvement in the different trends observed for these miRNAs during the KSHV lytic cycle, and it would be interesting to further characterise the specific mechanisms leading to their biogenesis and dysregulation.

This would first require an investigation into the precise genomic context of each dysregulated miRNA, as parent transcript expression, alternative splicing and proximity of pri-miRNAs to splice junctions have been shown to contribute to the regulation of intronic miRNA expression (Melamed et al., 2013). Conversely, intergenic miRNAs are transcribed by RNA polymerase II using their own promoters, and likely requiring the activities of cellular transcription factors (Lee et al., 2004). A detailed analysis of transcript biogenesis and regulation could, therefore, be attempted by first using DNA-affinity purification followed by mass spectrometry-based identification of associated transcription and splicing factors (Y. Wang et al., 2008).

Interestingly, inhibition of either miRNA using miRIDIAN antagomiRs does not appear to have serious implications for viral RNA or protein expression levels, suggesting that dysregulation of either miR-151a-5p or miR-365a-3p does not represent an anti-viral response directed against the virus by the host cell. Subsequently, it was hypothesised that the increased expression of these miRNAs at different times during KSHV lytic infection, contributed to a pro-viral process, and that the miRNAs were likely to target cellular transcripts. To investigate this, mRNA sequencing was employed to observe changes in host transcript expression levels over the course of the KSHV lytic cycle. Open source miRNA target prediction software was used to predict likely target host cell mRNAs of miR-151a-5p and miR-365a-3p, and the predicted target transcript levels were analysed by cross referencing this list with the mRNA sequencing data. The data displayed the effects of both the KSHV-mediated host-shutoff response and an increasing viral mRNA component present in the sample, resulting in the vast majority of host transcripts decreasing in abundance over the course of the lytic cycle. Therefore, predicted target transcripts that appeared to be most severely depleted were examined in the presence of the two miRIDIANs at different times during lytic infection. The four predicted targets of miR-151a-5p did not appear to be stabilised in the presence of the miR-151a-5p miRIDIAN at any time during infection, suggesting that these transcripts do not interact with miR-151a-5p. In contrast, however, two predicted mRNA targets of miR-365a-3p, DOCK5 and PRUNE2, were stabilised specifically in the presence of a miRIDIAN directed against miR-365a-3p at 18 hours post induction of the KSHV lytic cycle. The levels of miR-365a-3p gradually increase

over the course of lytic infection, with maximum expression at 18 hours post induction. However, it is surprising that treatment with the miRIDIAN directed against miR-365a-3p does not appear to stabilise either DOCK5 or PRUNE2 transcripts at 8 hours, when there is also an increased abundance of the miRNA. It is possible that the miR-365a-3p is only functional at certain levels, and this may reflect a stoichiometric effect between a miRNA and its target transcript.

A plasmid encoding a DOCK5-GFP fusion protein was acquired in order to investigate the effects of DOCK5 overexpression, as this was predicted to overcome miR-365a-3p activity. DOCK5-GFP overexpression could not account for the minor reduction in KSHV RNA levels observed when cells were treated with a miRIDIAN directed against miR-365a-3p, suggesting that this effect is due to another gene or possibly represents an off target effect of the antagomiR. DOCK5-GFP overexpression did, however, result in a reduced reinfection rate when supernatant harvested from transfected cells undergoing lytic infection for 7 days was used to infect naïve cells. This correlated with an increased viral load in the initial cells after this time, and therefore suggests that DOCK5 expression inhibits a viral process following DNA replication, but prior to egress. Similar data were obtained when cells were treated with miRIDIANs, with a miRIDIAN directed against miR-365a-3p showing similar viral load in both cell types to DOCK5-GFP overexpression, and a miRIDIAN directed against miR-151a-5p exhibiting an intermediate effect. The overexpression of DOCK5-GFP is unlikely to produce the same levels of DOCK5 protein, or DOCK5 activity, as miR-365a-3p inhibition. Therefore, it remains to be seen whether other targets of miR-365a-3p also contribute to this effect.

Other members of the DOCK family, sharing considerable homology to DOCK5, activate Rac1 and Cdc42, influencing actin dynamics, specifically polymerisation (Laurin and Cote, 2014; Ruiz-Lafuente et al., 2015). Herpesviruses interact with components of the host cell cytoskeleton at multiple stages during infection (Lyman and Enquist, 2009), however, intracellular capsid movement studies with herpesviruses suggest that microtubules are primarily used for viral translocation (Sodeik et al., 1997; Douglas et al., 2004; Lee et al., 2006). It is hypothesised, therefore, that DOCK5 mediates the polymerisation of actin in the cortical actin network, and that this acts as a barrier to

KSHV egress. HSV-1 has been shown to require Myosin Va activity for egress, and it is believed that this interaction allows the capsid to traffic through the cortical actin network prior to egress (Roberts and Baines, 2010). This suggests that cortical actin can act as an anti-viral factor that must be overcome, and it is therefore hypothesised that KSHV upregulates miR-365a-3p, targeting DOCK5 mRNA for degradation or translational repression, ultimately reorganising the cortical actin network to increase the efficiency of viral egress. Further work will now be conducted to characterise changes in cortical actin morphology during KSHV lytic replication in the absence or presence of DOCK5 overexpression or miRIDIAN 365a. In addition, an intracellular infectivity assay will be performed to further confirm that viral egress is the specific mechanism being inhibited.

To date, PRUNE2 overexpression and its effect on the KSHV lytic cycle has not been investigated. PRUNE2 is an endosomal protein, associated with the AP-2 cargo adaptor complex, and is associated with positive prognosis in neuroblastoma (Harris et al., 2013; Machida et al., 2006). Endosomes are believed to play an important role during herpesvirus secondary envelopment prior to egress (Johnson and Baines, 2011). It is interesting to note that the downregulation of both DOCK5 and PRUNE2 via the activity of a single miRNA during KSHV lytic infection may contribute to increased efficiency of viral egress. As miR-365a-3p is a cellular miRNA, the identification of these targeted processes may suggest it plays a role in exocytosis. Interestingly, miR-365a-3p is intergenic, and so its expression is not directly coupled to the transcription of an mRNA. In addition, it has been identified in multiple tissues including cerebellum, kidney and heart, suggesting involvement in a general cellular process rather than a tissue specific mechanism. Further investigations into the requirements for miR-365a-3p expression may shed more light on its function in uninfected cells. An investigation into the effects of PRUNE2 overexpression, similar to work already undertaken using DOCK5-GFP, may help to further characterise miR-365a-3p and its role in KSHV lytic replication.

Taken together, the work described in this thesis will broaden our understanding of the interactions that occur during KSHV lytic infection. This work may have implications for KSHV pathology, as well as potentially increasing general

understanding of factors involved in both cellular and cancer biology. Finally, interactions identified in this work, such as the interactions between ORF57 and Prp19, or miR-365a and DOCK5 may represent novel targets for therapeutic intervention against KSHV-associated malignancies.

References

Abraham, G., Rhodes, D.P. and Banerjee, A.K. 1975. The 5' terminal structure of the methylated mRNA synthesized in vitro by vesicular stomatitis virus. *Cell*. **5**(1),pp.51–58.

Adams, M.D., Kelley, J.M., Gocayne, J.D., Dubnick, M., Polymeropoulos, M.H., Xiao, H., Merril, C.R., Wu, A., Olde, B. and Moreno, R.F. 1991. Complementary DNA sequencing: expressed sequence tags and human genome project. *Science (New York, N.Y.)*. **252**(5013),pp.1651–1656.

Agrawal, N., Dasaradhi, P.V.N., Mohmmed, A., Malhotra, P., Bhatnagar, R.K. and Mukherjee, S.K. 2003. RNA interference: biology, mechanism, and applications. *Microbiology and Molecular Biology Reviews*. **67**(4),pp.657–685.

Aguilera, A. and García-Muse, T. 2012. R loops: from transcription byproducts to threats to genome stability. *Molecular Cell*. **46**(2),pp.115–124.

Ahn, J.-Y., Li, X., Davis, H.L. and Canman, C.E. 2002. Phosphorylation of threonine 68 promotes oligomerization and autophosphorylation of the Chk2 protein kinase via the forkhead-associated domain. *The Journal of Biological Chemistry*. **277**(22),pp.19389–19395.

Akhtar, J. and Shukla, D. 2009. Viral entry mechanisms: cellular and viral mediators of herpes simplex virus entry: Cellular and viral mediators of HSV entry. *FEBS Journal*. **276**(24),pp.7228–7236.

Amen, M.A. and Griffiths, A. 2011. Packaging of non-coding RNAs into herpesvirus virions: comparisons to coding RNAs. *Frontiers in Genetics*. [Online]. **2**. [Accessed 25 June 2015]. Available from: http://journal.frontiersin.org/article/10.3389/fgene.2011.00081/abstract.

Anastasiadou, E., Boccellato, F., Vincenti, S., Rosato, P., Bozzoni, I., Frati, L., Faggioni, A., Presutti, C. and Trivedi, P. 2010. Epstein-Barr virus encoded LMP1 downregulates TCL1 oncogene through miR-29b. *Oncogene*. **29**(9),pp.1316–1328.

Andersen, J.S., Lyon, C.E., Fox, A.H., Leung, A.K.L., Lam, Y.W., Steen, H., Mann, M. and Lamond, A.I. 2002. Directed proteomic analysis of the human nucleolus. *Current biology: CB*. **12**(1),pp.1–11.

Andersson, M.G., Haasnoot, P.C.J., Xu, N., Berenjian, S., Berkhout, B. and Akusjärvi, G. 2005. Suppression of RNA interference by adenovirus virus-associated RNA. *Journal of Virology*. **79**(15),pp.9556–9565.

An, J. 2004. Transcriptional coactivation of c-Jun by the KSHV-encoded LANA. *Blood*. **103**(1),pp.222–228.

Aoki, Y., Jaffe, E.S., Chang, Y., Jones, K., Teruya-Feldstein, J., Moore, P.S. and Tosato, G. 1999. Angiogenesis and hematopoiesis induced by Kaposi's sarcoma-associated herpesvirus-encoded interleukin-6. *Blood*. **93**(12),pp.4034–4043.

Aparicio, O., Razquin, N., Zaratiegui, M., Narvaiza, I. and Fortes, P. 2006. Adenovirus virus-associated RNA is processed to functional interfering RNAs involved in virus production. *Journal of Virology*. **80**(3),pp.1376–1384.

Aravind, L. 1999. Conserved domains in DNA repair proteins and evolution of repair systems. *Nucleic Acids Research*. **27**(5),pp.1223–1242.

Arias, C., Walsh, D., Harbell, J., Wilson, A.C. and Mohr, I. 2009. Activation of host translational control pathways by a viral developmental switch B. Sugden, ed. *PLoS Pathogens*. **5**(3),p.e1000334.

Arias, C., Weisburd, B., Stern-Ginossar, N., Mercier, A., Madrid, A.S., Bellare, P., Holdorf, M., Weissman, J.S. and Ganem, D. 2014. KSHV 2.0: a comprehensive annotation of the Kaposi's sarcoma-associated herpesvirus genome using next-generation sequencing reveals novel genomic and functional features D. P. Dittmer, ed. *PLoS Pathogens*. **10**(1),p.e1003847.

Arvin, A.M. (ed.). 2007. *Human herpesviruses: biology, therapy, and immunoprophylaxis*. Cambridge ; New York: Cambridge University Press.

Bainbridge, M.N., Warren, R.L., Hirst, M., Romanuik, T., Zeng, T., Go, A., Delaney, A., Griffith, M., Hickenbotham, M., Magrini, V., Mardis, E.R., Sadar, M.D., Siddiqui, A.S., Marra, M.A. and Jones, S.J.M. 2006. Analysis of the prostate cancer cell line LNCaP transcriptome using a sequencing-by-synthesis approach. *BMC genomics*. **7**,p.246.

Ballestas, M.E. and Kaye, K.M. 2011. The latency-associated nuclear antigen, a multifunctional protein central to Kaposi's sarcoma-associated herpesvirus latency. *Future Microbiology*. **6**(12),pp.1399–1413.

Banerji, J., Rusconi, S. and Schaffner, W. 1981. Expression of a beta-globin gene is enhanced by remote SV40 DNA sequences. *Cell*. **27**(2 Pt 1),pp.299–308.

Bartek, J., Falck, J. and Lukas, J. 2001. CHK2 kinase--a busy messenger. *Nature Reviews. Molecular Cell Biology*. **2**(12),pp.877–886.

Barth, S., Meister, G. and Grässer, F.A. 2011. EBV-encoded miRNAs. *Biochimica et Biophysica Acta (BBA) - Gene Regulatory Mechanisms*. **1809**(11-12),pp.631–640.

Bassi, L., Palitti, F., Mosesso, P. and Natarajan, A.T. 1998. Distribution of camptothecin-induced break points in Chinese hamster cells treated in late S and G2 phases of the cell cycle. *Mutagenesis*. **13**(3),pp.257–261.

Batushansky, A., Kirma, M., Grillich, N., Toubiana, D., Pham, P.A., Balbo, I., Fromm, H., Galili, G., Fernie, A.R. and Fait, A. 2014. Combined transcriptomics and metabolomics of Arabidopsis thaliana seedlings exposed to exogenous GABA suggest its role in plants is predominantly metabolic. *Molecular Plant*. **7**(6),pp.1065–1068.

Belgnaoui, S.M., Fryrear, K.A., Nyalwidhe, J.O., Guo, X. and Semmes, O.J. 2010. The viral oncoprotein Tax sequesters DNA damage response factors by tethering MDC1 to chromatin. *Journal of Biological Chemistry*. **285**(43),pp.32897–32905.

Bellare, P. and Ganem, D. 2009. Regulation of KSHV lytic switch protein expression by a virus-encoded microRNA: an evolutionary adaptation that fine-tunes lytic reactivation. *Cell Host & Microbe*. **6**(6),pp.570–575.

Benoist, C. and Chambon, P. 1981. In vivo sequence requirements of the SV40 early promotor region. *Nature*. **290**(5804),pp.304–310.

Beral, V., Peterman, T.A., Berkelman, R.L. and Jaffe, H.W. 1990. Kaposi's sarcoma among persons with AIDS: a sexually transmitted infection? *Lancet (London, England)*. **335**(8682),pp.123–128.

Berget, S.M., Moore, C. and Sharp, P.A. 1977. Spliced segments at the 5' terminus of adenovirus 2 late mRNA. *Proceedings of the National Academy of Sciences of the United States of America*. **74**(8),pp.3171–3175.

Betel, D., Wilson, M., Gabow, A., Marks, D.S. and Sander, C. 2007. The microRNA.org resource: targets and expression. *Nucleic Acids Research*. **36**(Database),pp.D149–D153.

Bienroth, S., Keller, W. and Wahle, E. 1993. Assembly of a processive messenger RNA polyadenylation complex. *The EMBO journal*. **12**(2),pp.585–594.

Bohnsack, M.T., Czaplinski, K. and Gorlich, D. 2004. Exportin 5 is a RanGTP-dependent dsRNA-binding protein that mediates nuclear export of pre-miRNAs. *RNA (New York, N.Y.)*. **10**(2),pp.185–191.

Boisvert, F.-M., van Koningsbruggen, S., Navascués, J. and Lamond, A.I. 2007. The multifunctional nucleolus. *Nature Reviews. Molecular Cell Biology*. **8**(7),pp.574–585.

Boland, A., Huntzinger, E., Schmidt, S., Izaurralde, E. and Weichenrieder, O. 2011. Crystal structure of the MID-PIWI lobe of a eukaryotic Argonaute protein. *Proceedings of the National Academy of Sciences*. **108**(26),pp.10466–10471.

Bollard, C.M., Rooney, C.M. and Heslop, H.E. 2012. T-cell therapy in the treatment of post-transplant lymphoproliferative disease. *Nature Reviews Clinical Oncology*. **9**(9),pp.510–519.

Bondarenko, P.V., Chelius, D. and Shaler, T.A. 2002. Identification and relative quantitation of protein mixtures by enzymatic digestion followed by capillary reversed-phase liquid chromatography-tandem mass spectrometry. *Analytical Chemistry*. **74**(18),pp.4741–4749.

Boshoff, C. and Weiss, R.A. 2001. Epidemiology and pathogenesis of Kaposi's sarcoma-associated herpesvirus. *Philosophical Transactions of the Royal Society B: Biological Sciences*. **356**(1408),pp.517–534.

Bottero, V., Sharma-Walia, N., Kerur, N., Paul, A.G., Sadagopan, S., Cannon, M. and Chandran, B. 2009. Kaposi Sarcoma-associated herpes virus (KSHV) G protein-coupled receptor (vGPCR) activates the ORF50 lytic switch promoter: A potential positive feedback loop for sustained ORF50 gene expression. *Virology*. **392**(1),pp.34–51.

Boyne, J.R., Colgan, K.J. and Whitehouse, A. 2008. Recruitment of the complete hTREX complex is required for Kaposi's sarcoma-associated herpesvirus intronless mRNA nuclear export and virus replication. *PLoS pathogens*. **4**(10),p.e1000194.

Boyne, J.R., Jackson, B.R., Taylor, A., Macnab, S.A. and Whitehouse, A. 2010. Kaposi's sarcoma-associated herpesvirus ORF57 protein interacts with PYM to enhance translation of viral intronless mRNAs. *The EMBO journal*. **29**(11),pp.1851–1864.

Boyne, J.R. and Whitehouse, A. 2009. Nucleolar disruption impairs Kaposi's sarcoma-associated herpesvirus ORF57-mediated nuclear export of intronless viral mRNAs. *FEBS letters*. **583**(22),pp.3549–3556.

Boyne, J.R. and Whitehouse, A. 2006. Nucleolar trafficking is essential for nuclear export of intronless herpesvirus mRNA. *Proceedings of the National Academy of Sciences of the United States of America*. **103**(41),pp.15190–15195.

Branzei, D. and Foiani, M. 2008. Regulation of DNA repair throughout the cell cycle. *Nature Reviews. Molecular Cell Biology*. **9**(4),pp.297–308.

Brennecke, J., Stark, A., Russell, R.B. and Cohen, S.M. 2005. Principles of microRNA–target recognition. *PLoS Biology*. **3**(3),p.e85.

Brigneti, G. 1998. Viral pathogenicity determinants are suppressors of transgene silencing in Nicotiana benthamiana. *The EMBO Journal*. **17**(22),pp.6739–6746.

Brugnera, E., Haney, L., Grimsley, C., Lu, M., Walk, S.F., Tosello-Trampont, A.-C., Macara, I.G., Madhani, H., Fink, G.R. and Ravichandran, K.S. 2002. Unconventional Rac-GEF activity is mediated through the Dock180–ELMO complex. *Nature Cell Biology*. [Online]. [Accessed 15 June 2015]. Available from: http://www.nature.com/doifinder/10.1038/ncb824.

Buermans, H.P., Ariyurek, Y., van Ommen, G., Dunnen, J.T. den and Hoen, P.A. 't 2010. New methods for next generation sequencing based microRNA expression profiling. *BMC Genomics*. **11**(1),p.716.

Caesar, R., Manieri, M., Kelder, T., Boekschoten, M., Evelo, C., Müller, M., Kooistra, T., Cinti, S., Kleemann, R. and Drevon, C.A. 2010. A combined transcriptomics and lipidomics analysis of subcutaneous, epididymal and mesenteric adipose tissue reveals marked functional differences A. Bartolomucci, ed. *PLoS ONE*. **5**(7),p.e11525.

Cai, Q., Banerjee, S., Cervini, A., Lu, J., Hislop, A.D., Dzeng, R. and Robertson, E.S. 2013. IRF-4-Mediated CIITA Transcription Is Blocked by KSHV Encoded LANA to Inhibit MHC II Presentation S.-J. Gao, ed. *PLoS Pathogens*. **9**(10),p.e1003751.

Cai, Q., Lan, K., Verma, S.C., Si, H., Lin, D. and Robertson, E.S. 2006. Kaposi's sarcoma-associated herpesvirus latent protein LANA interacts with HIF-1 to upregulate Rta expression during hypoxia: latency control under low oxygen conditions. *Journal of Virology*. **80**(16),pp.7965–7975.

Cameron, J.E., Yin, Q., Fewell, C., Lacey, M., McBride, J., Wang, X., Lin, Z., Schaefer, B.C. and Flemington, E.K. 2008. Epstein-Barr Virus Latent Membrane Protein 1 Induces Cellular MicroRNA miR-146a, a Modulator of Lymphocyte Signaling Pathways. *Journal of Virology*. **82**(4),pp.1946–1958.

Cannell, I.G., Kong, Y.W. and Bushell, M. 2008. How do microRNAs regulate gene expression? *Biochemical Society Transactions*. **36**(Pt 6),pp.1224–1231.

Cantalupo, P., Doering, A., Sullivan, C.S., Pal, A., Peden, K.W.C., Lewis, A.M. and Pipas, J.M. 2005. Complete nucleotide sequence of polyomavirus SA12. *Journal of Virology*. **79**(20),pp.13094–13104.

Caputi, M. and Zahler, A.M. 2002. SR proteins and hnRNP H regulate the splicing of the HIV-1 tev-specific exon 6D. *The EMBO journal*. **21**(4),pp.845–855.

Cardone, G., Winkler, D.C., Trus, B.L., Cheng, N., Heuser, J.E., Newcomb, W.W., Brown, J.C. and Steven, A.C. 2007. Visualization of the herpes simplex virus portal in situ by cryo-electron tomography. *Virology*. **361**(2),pp.426–434.

Carmody, S.R. and Wente, S.R. 2009. mRNA nuclear export at a glance. *Journal of Cell Science*. **122**(12),pp.1933–1937.

Cazalla, D., Yario, T. and Steitz, J.A. 2010. Down-Regulation of a Host MicroRNA by a Herpesvirus saimiri Noncoding RNA. *Science*. **328**(5985),pp.1563–1566.

Cesarman, E., Chang, Y., Moore, P.S., Said, J.W. and Knowles, D.M. 1995. Kaposi's sarcoma-associated herpesvirus-like DNA sequences in AIDS-related body-cavity-based lymphomas. *The New England Journal of Medicine*. **332**(18),pp.1186–1191.

Chakraborty, S., Veettil, M.V. and Chandran, B. 2012. Kaposi's Sarcoma Associated Herpesvirus Entry into Target Cells. *Frontiers in Microbiology*. [Online]. **3**. [Accessed 26 June 2015]. Available from: http://journal.frontiersin.org/article/10.3389/fmicb.2012.00006/abstract.

Challberg, M.D. and Kelly, T.J. 1979. Adenovirus DNA replication in vitro. *Proceedings of the National Academy of Sciences of the United States of America*. **76**(2),pp.655–659.

Chanarat, S., Seizl, M. and Strässer, K. 2011. The Prp19 complex is a novel transcription elongation factor required for TREX occupancy at transcribed genes. *Genes & Development*. **25**(11),pp.1147–1158.

Chanarat, S. and Sträßer, K. 2013. Splicing and beyond: The many faces of the Prp19 complex. *Biochimica et Biophysica Acta (BBA) - Molecular Cell Research*. **1833**(10),pp.2126–2134.

Chandhasin, C., Ducu, R.I., Berkovich, E., Kastan, M.B. and Marriott, S.J. 2008. Human T-Cell Leukemia Virus Type 1 Tax Attenuates the ATM-Mediated Cellular DNA Damage Response. *Journal of Virology*. **82**(14),pp.6952–6961.

Chang, P.-J., Shedd, D., Gradoville, L., Cho, M.-S., Chen, L.-W., Chang, J. and Miller, G. 2002. Open reading frame 50 protein of Kaposi's sarcoma-associated herpesvirus directly activates the viral PAN and K12 genes by binding to related response elements. *Journal of Virology*. **76**(7),pp.3168–3178.

Chang, P.-J., Shedd, D. and Miller, G. 2005. Two subclasses of Kaposi's sarcoma-associated herpesvirus lytic cycle promoters distinguished by open reading frame 50 mutant proteins that are deficient in binding to DNA. *Journal of Virology*. **79**(14),pp.8750–8763.

Chang, T.-W. 1984. Herpesvirus diseases of veterinary importance. *Clinics in Dermatology*. **2**(2),pp.147–151.

Chang, Y., Cesarman, E., Pessin, M.S., Lee, F., Culpepper, J., Knowles, D.M. and Moore, P.S. 1994. Identification of herpesvirus-like DNA sequences in AIDS-associated Kaposi's sarcoma. *Science (New York, N.Y.)*. **266**(5192),pp.1865–1869.

Chelius, D. and Bondarenko, P.V. 2002. Quantitative profiling of proteins in complex mixtures using liquid chromatography and mass spectrometry. *Journal of Proteome Research*. **1**(4),pp.317–323.

Chen, B.P.C., Uematsu, N., Kobayashi, J., Lerenthal, Y., Krempler, A., Yajima, H., Löbrich, M., Shiloh, Y. and Chen, D.J. 2007. Ataxia telangiectasia mutated (ATM) is essential for DNA-PKcs phosphorylations at the Thr-2609 cluster upon DNA double strand break. *The Journal of Biological Chemistry*. **282**(9),pp.6582–6587.

Chen, C. 2005. Real-time quantification of microRNAs by stem-loop RT-PCR. *Nucleic Acids Research*. **33**(20),pp.e179–e179.

Cheng, H., Dufu, K., Lee, C.-S., Hsu, J.L., Dias, A. and Reed, R. 2006. Human mRNA export machinery recruited to the 5' end of mRNA. *Cell*. **127**(7),pp.1389–1400.

Chen, L. and Lagunoff, M. 2005. Establishment and Maintenance of Kaposi's Sarcoma-Associated Herpesvirus Latency in B Cells. *Journal of Virology*. **79**(22),pp.14383–14391.

Chentoufi, A.A., Kritzer, E., Tran, M.V., Dasgupta, G., Lim, C.H., Yu, D.C., Afifi, R.E., Jiang, X., Carpenter, D., Osorio, N., Hsiang, C., Nesburn, A.B., Wechsler, S.L. and BenMohamed, L. 2011. The Herpes Simplex Virus 1 Latency-Associated Transcript Promotes Functional Exhaustion of Virus-Specific CD8+ T Cells in Latently Infected Trigeminal Ganglia: a Novel Immune Evasion Mechanism. *Journal of Virology*. **85**(17),pp.9127–9138.

Chen, W., Hilton, I.B., Staudt, M.R., Burd, C.E. and Dittmer, D.P. 2010. Distinct p53, p53:LANA, and LANA Complexes in Kaposi's Sarcoma-Associated Herpesvirus Lymphomas. *Journal of Virology*. **84**(8),pp.3898–3908.

Chen, Y.-B., Rahemtullah, A. and Hochberg, E. 2007. Primary effusion lymphoma. *The Oncologist*. **12**(5),pp.569–576.

Chiang, H.R., Schoenfeld, L.W., Ruby, J.G., Auyeung, V.C., Spies, N., Baek, D., Johnston, W.K., Russ, C., Luo, S., Babiarz, J.E., Blelloch, R., Schroth, G.P., Nusbaum, C. and Bartel, D.P. 2010. Mammalian microRNAs: experimental evaluation of novel and previously annotated genes. *Genes & Development*. **24**(10),pp.992–1009.

Chi, B., Wang, Q., Wu, G., Tan, M., Wang, L., Shi, M., Chang, X. and Cheng, H. 2013. Aly and THO are required for assembly of the human TREX complex and association of TREX components with the spliced mRNA. *Nucleic Acids Research*. **41**(2),pp.1294–1306.

Cho, E.J., Kobor, M.S., Kim, M., Greenblatt, J. and Buratowski, S. 2001. Opposing effects of Ctk1 kinase and Fcp1 phosphatase at Ser 2 of the RNA polymerase II C-terminal domain. *Genes & Development*. **15**(24),pp.3319–3329.

Chow, L.T., Gelinas, R.E., Broker, T.R. and Roberts, R.J. 1977. An amazing sequence arrangement at the 5' ends of adenovirus 2 messenger RNA. *Cell*. **12**(1),pp.1–8.

Choy, E.Y.-W., Siu, K.-L., Kok, K.-H., Lung, R.W.-M., Tsang, C.M., To, K.-F., Kwong, D.L.-W., Tsao, S.W. and Jin, D.-Y. 2008. An Epstein-Barr virus-encoded microRNA targets PUMA to promote host cell survival. *The Journal of Experimental Medicine*. **205**(11),pp.2551–2560.

Chua, M.A., Schmid, S., Perez, J.T., Langlois, R.A. and Tenoever, B.R. 2013. Influenza A virus utilizes suboptimal splicing to coordinate the timing of infection. *Cell Reports*. **3**(1),pp.23–29.

Cimprich, K.A. and Cortez, D. 2008. ATR: an essential regulator of genome integrity. *Nature Reviews. Molecular Cell Biology*. **9**(8),pp.616–627.

Clauson, C., Scharer, O.D. and Niedernhofer, L. 2013. Advances in Understanding the Complex Mechanisms of DNA Interstrand Cross-Link Repair. *Cold Spring Harbor Perspectives in Biology*. **5**(10),pp.a012732–a012732.

Clement, C., Tiwari, V., Scanlan, P.M., Valyi-Nagy, T., Yue, B.Y.J.T. and Shukla, D. 2006. A novel role for phagocytosis-like uptake in herpes simplex virus entry. *The Journal of Cell Biology*. **174**(7),pp.1009–1021.

Cliffe, A.R., Garber, D.A. and Knipe, D.M. 2009. Transcription of the Herpes Simplex Virus Latency-Associated Transcript Promotes the Formation of Facultative Heterochromatin on Lytic Promoters. *Journal of Virology*. **83**(16),pp.8182–8190.

Cohrs, R.J. and Gilden, D.H. 2001. Human herpesvirus latency. *Brain Pathology (Zurich, Switzerland)*. **11**(4),pp.465–474.

Coppola, J.A., Field, A.S. and Luse, D.S. 1983. Promoter-proximal pausing by RNA polymerase II in vitro: transcripts shorter than 20 nucleotides are not capped. *Proceedings of the National Academy of Sciences of the United States of America*. **80**(5),pp.1251–1255.

Coscoy, L. 2007. Immune evasion by Kaposi's sarcoma-associated herpesvirus. *Nature Reviews Immunology*. **7**(5),pp.391–401.

Cote, J.-F. 2002. Identification of an evolutionarily conserved superfamily of DOCK180-related proteins with guanine nucleotide exchange activity. *Journal of Cell Science*. **115**(24),pp.4901–4913.

Cotter, M.A. and Robertson, E.S. 1999. The latency-associated nuclear antigen tethers the Kaposi's sarcoma-associated herpesvirus genome to host chromosomes in body cavity-based lymphoma cells. *Virology*. **264**(2),pp.254–264.

Covarrubias, S., Gaglia, M.M., Kumar, G.R., Wong, W., Jackson, A.O. and Glaunsinger, B.A. 2011. Coordinated Destruction of Cellular Messages in Translation Complexes by the Gammaherpesvirus Host Shutoff Factor and the Mammalian Exonuclease Xrn1 R. Renne, ed. *PLoS Pathogens*. **7**(10),p.e1002339.

Damania, B. 2004. Oncogenic gamma-herpesviruses: comparison of viral proteins involved in tumorigenesis. *Nature Reviews. Microbiology*. **2**(8),pp.656–668.

Damania, B. and Pipas, J.M. (eds.). 2009. *DNA Tumor Viruses* [Online]. New York, NY: Springer US. [Accessed 25 June 2015]. Available from: http://link.springer.com/10.1007/978-0-387-68945-6.

Davis, A.J. and Chen, D.J. 2013. DNA double strand break repair via non-homologous end-joining. *Translational Cancer Research*. **2**(3),pp.130–143.

Davis, D.A. 2001. Hypoxia induces lytic replication of Kaposi sarcoma-associated herpesvirus. *Blood*. **97**(10),pp.3244–3250.

Davison, A.J. 2007a. Comparative analysis of the genomes *In*: A. Arvin, G. Campadelli-Fiume, E. Mocarski, P. S. Moore, B. Roizman, R. Whitley and K. Yamanishi, eds. *Human Herpesviruses: Biology, Therapy, and Immunoprophylaxis* [Online]. Cambridge: Cambridge University Press. [Accessed 25 June 2015]. Available from: http://www.ncbi.nlm.nih.gov/books/NBK47439/.

Davison, A.J. 2010. Herpesvirus systematics. *Veterinary Microbiology*. **143**(1),pp.52–69.

Davison, A.J. 2007b. Overview of classification *In*: A. Arvin, G. Campadelli-Fiume, E. Mocarski, P. S. Moore, B. Roizman, R. Whitley and K. Yamanishi, eds. *Human Herpesviruses: Biology, Therapy, and Immunoprophylaxis* [Online]. Cambridge: Cambridge University Press. [Accessed 25 June 2015]. Available from: http://www.ncbi.nlm.nih.gov/books/NBK47406/.

Davison, A.J., Eberle, R., Ehlers, B., Hayward, G.S., McGeoch, D.J., Minson, A.C., Pellett, P.E., Roizman, B., Studdert, M.J. and Thiry, E. 2009. The order Herpesvirales. *Archives of Virology*. **154**(1),pp.171–177.

Davison, A.J., Trus, B.L., Cheng, N., Steven, A.C., Watson, M.S., Cunningham, C., Le Deuff, R.-M. and Renault, T. 2005. A novel class of herpesvirus with bivalve hosts. *The Journal of General Virology*. **86**(Pt 1),pp.41–53.

DeCaprio, J.A., Ludlow, J.W., Figge, J., Shew, J.Y., Huang, C.M., Lee, W.H., Marsilio, E., Paucha, E. and Livingston, D.M. 1988. SV40 large tumor antigen forms a specific complex with the product of the retinoblastoma susceptibility gene. *Cell*. **54**(2),pp.275–283.

Decroly, E., Ferron, F., Lescar, J. and Canard, B. 2011. Conventional and unconventional mechanisms for capping viral mRNA. *Nature Reviews Microbiology*. [Online]. [Accessed 13 July 2015]. Available from: http://www.nature.com/doifinder/10.1038/nrmicro2675.

Delorme-Axford, E. and Coyne, C.B. 2011. The Actin Cytoskeleton as a Barrier to Virus Infection of Polarized Epithelial Cells. *Viruses*. **3**(12),pp.2462–2477.

Denli, A.M., Tops, B.B.J., Plasterk, R.H.A., Ketting, R.F. and Hannon, G.J. 2004. Processing of primary microRNAs by the Microprocessor complex. *Nature*. **432**(7014),pp.231–235.

Desselberger, U., Racaniello, V.R., Zazra, J.J. and Palese, P. 1980. The 3’ and 5’-terminal sequences of influenza A, B and C virus RNA segments are highly conserved and show partial inverted complementarity. *Gene*. **8**(3),pp.315–328.

Dictor, M. and Andersson, C. 1988. Lymphaticovenous differentiation in Kaposi’s sarcoma. Cellular phenotypes by stage. *The American Journal of Pathology*. **130**(2),pp.411–417.

Direkze, S. and Laman, H. 2004. Regulation of growth signalling and cell cycle by Kaposi’s sarcoma-associated herpesvirus genes: KSHV regulation of growth

signalling and cell cycle. *International Journal of Experimental Pathology*. **85**(6),pp.305–319.

Domingo, E., Parrish, C. and Holland, J.J. (eds.). 2008. *Origin and evolution of viruses* 2nd ed. Amsterdam: Elsevier, Acad. Press.

Douglas, M.W., Diefenbach, R.J., Homa, F.L., Miranda-Saksena, M., Rixon, F.J., Vittone, V., Byth, K. and Cunningham, A.L. 2004. Herpes Simplex Virus Type 1 Capsid Protein VP26 Interacts with Dynein Light Chains RP3 and Tctex1 and Plays a Role in Retrograde Cellular Transport. *Journal of Biological Chemistry*. **279**(27),pp.28522–28530.

Dourmishev, L.A., Dourmishev, A.L., Palmeri, D., Schwartz, R.A. and Lukac, D.M. 2003. Molecular Genetics of Kaposi's Sarcoma-Associated Herpesvirus (Human Herpesvirus 8) Epidemiology and Pathogenesis. *Microbiology and Molecular Biology Reviews*. **67**(2),pp.175–212.

Dubois, J., Terrier, O. and Rosa-Calatrava, M. 2014. Influenza Viruses and mRNA Splicing: Doing More with Less. *mBio*. **5**(3),pp.e00070–14–e00070–14.

Duman, S., Töz, H., Aşçi, G., Alper, S., Ozkahya, M., Unal, I., Celik, A., Ok, E. and Başçi, A. 2002. Successful treatment of post-transplant Kaposi's sarcoma by reduction of immunosuppression. *Nephrology, Dialysis, Transplantation: Official Publication of the European Dialysis and Transplant Association - European Renal Association*. **17**(5),pp.892–896.

Durocher, D. and Jackson, S.P. 2001. DNA-PK, ATM and ATR as sensors of DNA damage: variations on a theme? *Current Opinion in Cell Biology*. **13**(2),pp.225–231.

Dynan, W.S. and Tjian, R. 1983. The promoter-specific transcription factor Sp1 binds to upstream sequences in the SV40 early promoter. *Cell*. **35**(1),pp.79–87.

Edmonds, M., Vaughan, M.H. and Nakazato, H. 1971. Polyadenylic acid sequences in the heterogeneous nuclear RNA and rapidly-labeled polyribosomal RNA of HeLa cells: possible evidence for a precursor relationship. *Proceedings of the National Academy of Sciences of the United States of America*. **68**(6),pp.1336–1340.

Eiring, A.M., Harb, J.G., Neviani, P., Garton, C., Oaks, J.J., Spizzo, R., Liu, S., Schwind, S., Santhanam, R., Hickey, C.J., Becker, H., Chandler, J.C., Andino, R., Cortes, J., Hokland, P., Huettner, C.S., Bhatia, R., Roy, D.C., Liebhaber, S.A., Caligiuri, M.A., Marcucci, G., Garzon, R., Croce, C.M., Calin, G.A. and Perrotti, D. 2010. miR-328 functions as an RNA decoy to modulate hnRNP E2 regulation of mRNA translation in leukemic blasts. *Cell*. **140**(5),pp.652–665.

Emmott, E., Dove, B.K., Howell, G., Chappell, L.A., Reed, M.L., Boyne, J.R., You, J.-H., Brooks, G., Whitehouse, A. and Hiscox, J.A. 2008. Viral nucleolar localisation signals determine dynamic trafficking within the nucleolus. *Virology*. **380**(2),pp.191–202.

Epstein, M.A., Achong, B.G. and Barr, Y.M. 1964. Virus particles in cultured lymphoblasts from Burkitt's lymphoma. *Lancet (London, England)*. **1**(7335),pp.702–703.

Evans, V.C., Barker, G., Heesom, K.J., Fan, J., Bessant, C. and Matthews, D.A. 2012. De novo derivation of proteomes from transcriptomes for transcript and protein identification. *Nature Methods*. **9**(12),pp.1207–1211.

Everett, R.D. 2006. Interactions between DNA viruses, ND10 and the DNA damage response. *Cellular Microbiology*. **8**(3),pp.365–374.

Everett, R.D., Rechter, S., Papior, P., Tavalai, N., Stamminger, T. and Orr, A. 2006. PML contributes to a cellular mechanism of repression of herpes simplex virus type 1 infection that is inactivated by ICP0. *Journal of Virology*. **80**(16),pp.7995–8005.

E, X., Pickering, M.T., Debatis, M., Castillo, J., Lagadinos, A., Wang, S., Lu, S. and Kowalik, T.F. 2011. An E2F1-mediated DNA damage response contributes to the replication of human cytomegalovirus. *PLoS pathogens*. **7**(5),p.e1001342.

Fabian, M.R., Sonenberg, N. and Filipowicz, W. 2010. Regulation of mRNA Translation and Stability by microRNAs. *Annual Review of Biochemistry*. **79**(1),pp.351–379.

Fakhari, F.D. and Dittmer, D.P. 2002. Charting latency transcripts in Kaposi's sarcoma-associated herpesvirus by whole-genome real-time quantitative PCR. *Journal of Virology*. **76**(12),pp.6213–6223.

Faraoni, I., Antonetti, F.R., Cardone, J. and Bonmassar, E. 2009. miR-155 gene: A typical multifunctional microRNA. *Biochimica et Biophysica Acta (BBA) - Molecular Basis of Disease*. **1792**(6),pp.497–505.

Fire, A., Xu, S., Montgomery, M.K., Kostas, S.A., Driver, S.E. and Mello, C.C. 1998. Potent and specific genetic interference by double-stranded RNA in Caenorhabditis elegans. *Nature*. **391**(6669),pp.806–811.

Fletcher, D.A. and Mullins, R.D. 2010. Cell mechanics and the cytoskeleton. *Nature*. **463**(7280),pp.485–492.

Forest, T., Barnard, S. and Baines, J.D. 2005. Active intranuclear movement of herpesvirus capsids. *Nature Cell Biology*. **7**(4),pp.429–431.

Fromm, M. and Berg, P. 1983. Simian virus 40 early- and late-region promoter functions are enhanced by the 72-base-pair repeat inserted at distant locations and inverted orientations. *Molecular and Cellular Biology*. **3**(6),pp.991–999.

Fu, Y., Dominissini, D., Rechavi, G. and He, C. 2014. Gene expression regulation mediated through reversible m6A RNA methylation. *Nature Reviews Genetics*. **15**(5),pp.293–306.

Ganem, D. 2007. Kaposi's sarcoma-associated herpesvirus *In*: *Fields Virology*. Philadelphia, PA: Lippincott, Williams & Wilkins, pp. 2487–2888.

Ganem, D. 2010. KSHV and the pathogenesis of Kaposi sarcoma: listening to human biology and medicine. *The Journal of Clinical Investigation*. **120**(4),pp.939–949.

Gan, W., Guan, Z., Liu, J., Gui, T., Shen, K., Manley, J.L. and Li, X. 2011. R-loop-mediated genomic instability is caused by impairment of replication fork progression. *Genes & Development*. **25**(19),pp.2041–2056.

Gao, L. and Qi, J. 2007. Whole genome molecular phylogeny of large dsDNA viruses using composition vector method. *BMC Evolutionary Biology*. **7**(1),p.41.

Garber, A.C., Hu, J. and Renne, R. 2002. Latency-associated nuclear antigen (LANA) cooperatively binds to two sites within the terminal repeat, and both sites contribute to the ability of LANA to suppress transcription and to facilitate DNA replication. *The Journal of Biological Chemistry*. **277**(30),pp.27401–27411.

Garneau, N.L., Wilusz, J. and Wilusz, C.J. 2007. The highways and byways of mRNA decay. *Nature Reviews Molecular Cell Biology*. **8**(2),pp.113–126.

Garriga, J. and Graña, X. 2004. Cellular control of gene expression by T-type cyclin/CDK9 complexes. *Gene*. **337**,pp.15–23.

Gershburg, E. and Pagano, J.S. 2008. Conserved herpesvirus protein kinases. *Biochimica et Biophysica Acta (BBA) - Proteins and Proteomics*. **1784**(1),pp.203–212.

Giacinti, C. and Giordano, A. 2006. RB and cell cycle progression. *Oncogene*. **25**(38),pp.5220–5227.

Gilmartin, G.M. and Nevins, J.R. 1989. An ordered pathway of assembly of components required for polyadenylation site recognition and processing. *Genes & Development*. **3**(12B),pp.2180–2190.

Glass, M. and Everett, R.D. 2013. Components of promyelocytic leukemia nuclear bodies (ND10) act cooperatively to repress herpesvirus infection. *Journal of Virology*. **87**(4),pp.2174–2185.

Goodsell, D.S. 2001. The Molecular Perspective: Ultraviolet Light and Pyrimidine Dimers. *The Oncologist*. **6**(3),pp.298–299.

Görg, A., Weiss, W. and Dunn, M.J. 2004. Current two-dimensional electrophoresis technology for proteomics. *Proteomics*. **4**(12),pp.3665–3685.

Gottlieb, T.M. and Jackson, S.P. 1993. The DNA-dependent protein kinase: requirement for DNA ends and association with Ku antigen. *Cell*. **72**(1),pp.131–142.

Gottwein, E., Corcoran, D.L., Mukherjee, N., Skalsky, R.L., Hafner, M., Nusbaum, J.D., Shamulailatpam, P., Love, C.L., Dave, S.S., Tuschl, T., Ohler, U. and Cullen, B.R.

2011. Viral MicroRNA Targetome of KSHV-Infected Primary Effusion Lymphoma Cell Lines. *Cell Host & Microbe*. **10**(5),pp.515–526.

Gottwein, E., Mukherjee, N., Sachse, C., Frenzel, C., Majoros, W.H., Chi, J.-T.A., Braich, R., Manoharan, M., Soutschek, J., Ohler, U. and Cullen, B.R. 2007. A viral microRNA functions as an orthologue of cellular miR-155. *Nature*. **450**(7172),pp.1096–1099.

Gradoville, L., Gerlach, J., Grogan, E., Shedd, D., Nikiforow, S., Metroka, C. and Miller, G. 2000. Kaposi's Sarcoma-Associated Herpesvirus Open Reading Frame 50/Rta Protein Activates the Entire Viral Lytic Cycle in the HH-B2 Primary Effusion Lymphoma Cell Line. *Journal of Virology*. **74**(13),pp.6207–6212.

Granzow, H., Klupp, B.G., Fuchs, W., Veits, J., Osterrieder, N. and Mettenleiter, T.C. 2001. Egress of alphaherpesviruses: comparative ultrastructural study. *Journal of Virology*. **75**(8),pp.3675–3684.

Greninger, A.L., Naccache, S.N., Federman, S., Yu, G., Mbala, P., Bres, V., Bouquet, J., Stryke, D., Somasekar, S., Linnen, J., Dodd, R., Mulembakani, P., Schneider, B., Muyembe, J.-J., Stramer, S. and Chiu, C.Y. 2015. *Rapid metagenomic identification of viral pathogens in clinical samples by real-time nanopore sequencing analysis* [Online]. [Accessed 6 July 2015]. Available from: http://biorxiv.org/lookup/doi/10.1101/020420.

Griffin, N.M., Yu, J., Long, F., Oh, P., Shore, S., Li, Y., Koziol, J.A. and Schnitzer, J.E. 2010. Label-free, normalized quantification of complex mass spectrometry data for proteomic analysis. *Nature Biotechnology*. **28**(1),pp.83–89.

Grote, M., Wolf, E., Will, C.L., Lemm, I., Agafonov, D.E., Schomburg, A., Fischle, W., Urlaub, H. and Lührmann, R. 2010. Molecular architecture of the human Prp19/CDC5L complex. *Molecular and Cellular Biology*. **30**(9),pp.2105–2119.

Grundhoff, A. and Ganem, D. 2004. Inefficient establishment of KSHV latency suggests an additional role for continued lytic replication in Kaposi sarcoma pathogenesis. *Journal of Clinical Investigation*. **113**(1),pp.124–136.

Guasparri, I. 2004. KSHV vFLIP Is Essential for the Survival of Infected Lymphoma Cells. *Journal of Experimental Medicine*. **199**(7),pp.993–1003.

Guilligay, D., Kadlec, J., Crépin, T., Lunardi, T., Bouvier, D., Kochs, G., Ruigrok, R.W.H. and Cusack, S. 2014. Comparative Structural and Functional Analysis of Orthomyxovirus Polymerase Cap-Snatching Domains P. Digard, ed. *PLoS ONE*. **9**(1),p.e84973.

Guo, Y.E., Riley, K.J., Iwasaki, A. and Steitz, J.A. 2014. Alternative Capture of Noncoding RNAs or Protein-Coding Genes by Herpesviruses to Alter Host T Cell Function. *Molecular Cell*. **54**(1),pp.67–79.

Gurtan, A.M. and Sharp, P.A. 2013. The Role of miRNAs in Regulating Gene Expression Networks. *Journal of Molecular Biology*. **425**(19),pp.3582–3600.

Gwack, Y., Baek, H.J., Nakamura, H., Lee, S.H., Meisterernst, M., Roeder, R.G. and Jung, J.U. 2003. Principal Role of TRAP/Mediator and SWI/SNF Complexes in Kaposi's Sarcoma-Associated Herpesvirus RTA-Mediated Lytic Reactivation. *Molecular and Cellular Biology*. **23**(6),pp.2055–2067.

Gygi, S.P., Rist, B., Gerber, S.A., Turecek, F., Gelb, M.H. and Aebersold, R. 1999. Quantitative analysis of complex protein mixtures using isotope-coded affinity tags. *Nature Biotechnology*. **17**(10),pp.994–999.

Ha, M. and Kim, V.N. 2014. Regulation of microRNA biogenesis. *Nature Reviews Molecular Cell Biology*. **15**(8),pp.509–524.

Han, J. 2004. The Drosha-DGCR8 complex in primary microRNA processing. *Genes & Development*. **18**(24),pp.3016–3027.

Harris, J.L., Richards, R.S., Chow, C.W.K., Lee, S., Kim, M., Buck, M., Teng, L., Clarke, R., Gardiner, R.A. and Lavin, M.F. 2013. BMCC1 is an AP-2 associated endosomal protein in prostate cancer cells. *PloS One*. **8**(9),p.e73880.

Helleday, T., Eshtad, S. and Nik-Zainal, S. 2014. Mechanisms underlying mutational signatures in human cancers. *Nature Reviews Genetics*. **15**(9),pp.585–598.

Henle, W., Diehl, V., Kohn, G., Hausen, H. Zur and Henle, G. 1967. Herpes-type virus and chromosome marker in normal leukocytes after growth with irradiated Burkitt cells. *Science (New York, N.Y.)*. **157**(3792),pp.1064–1065.

Le Hir, H. 2001. The exon-exon junction complex provides a binding platform for factors involved in mRNA export and nonsense-mediated mRNA decay. *The EMBO Journal*. **20**(17),pp.4987–4997.

Hiscox, J.A. 2007. RNA viruses: hijacking the dynamic nucleolus. *Nature Reviews. Microbiology*. **5**(2),pp.119–127.

Hiscox, J.A. 2002. The nucleolus--a gateway to viral infection? *Archives of Virology*. **147**(6),pp.1077–1089.

Ho, B.-C., Yu, S.-L., Chen, J.J.W., Chang, S.-Y., Yan, B.-S., Hong, Q.-S., Singh, S., Kao, C.-L., Chen, H.-Y., Su, K.-Y., Li, K.-C., Cheng, C.-L., Cheng, H.-W., Lee, J.-Y., Lee, C.-N. and Yang, P.-C. 2011. Enterovirus-induced miR-141 contributes to shutoff of host protein translation by targeting the translation initiation factor eIF4E. *Cell Host & Microbe*. **9**(1),pp.58–69.

Hofmann, T.G., Glas, C. and Bitomsky, N. 2013. HIPK2: A tumour suppressor that controls DNA damage-induced cell fate and cytokinesis. *BioEssays*. **35**(1),pp.55–64.

Hollingworth, R., Skalka, G., Stewart, G., Hislop, A., Blackbourn, D. and Grand, R. 2015. Activation of DNA Damage Response Pathways during Lytic Replication of KSHV. *Viruses*. **7**(6),pp.2908–2927.

Hollinshead, M., Johns, H.L., Sayers, C.L., Gonzalez-Lopez, C., Smith, G.L. and Elliott, G. 2012. Endocytic tubules regulated by Rab GTPases 5 and 11 are used for envelopment of herpes simplex virus: HSV1 envelopment by endocytic membranes. *The EMBO Journal*. **31**(21),pp.4204–4220.

Holmes, E.C. 2010. The comparative genomics of viral emergence. *Proceedings of the National Academy of Sciences*. **107**(suppl_1),pp.1742–1746.

Hricová, M. and Mistríková, J. 2007. Murine gammaherpesvirus 68 serum antibodies in general human population. *Acta Virologica*. **51**(4),pp.283–287.

Hsu, M.T., Parvin, J.D., Gupta, S., Krystal, M. and Palese, P. 1987. Genomic RNAs of influenza viruses are held in a circular conformation in virions and in infected cells by a terminal panhandle. *Proceedings of the National Academy of Sciences of the United States of America*. **84**(22),pp.8140–8144.

Huang, D.W., Sherman, B.T., Tan, Q., Kir, J., Liu, D., Bryant, D., Guo, Y., Stephens, R., Baseler, M.W., Lane, H.C. and Lempicki, R.A. 2007. DAVID Bioinformatics Resources: expanded annotation database and novel algorithms to better extract biology from large gene lists. *Nucleic Acids Research*. **35**(Web Server),pp.W169–W175.

Huang, T., Xu, D. and Zhang, X. 2012. Characterization of host microRNAs that respond to DNA virus infection in a crustacean. *BMC Genomics*. **13**(1),p.159.

Huang, Y. and Carmichael, G.G. 1996. Role of polyadenylation in nucleocytoplasmic transport of mRNA. *Molecular and Cellular Biology*. **16**(4),pp.1534–1542.

Huff, J.L. and Barry, P.A. 2003. B-Virus (*Cercopithecine herpesvirus* 1) Infection in Humans and Macaques: Potential for Zoonotic Disease. *Emerging Infectious Diseases*. **9**(2),pp.246–250.

Hu, J., Garber, A.C. and Renne, R. 2002. The latency-associated nuclear antigen of Kaposi's sarcoma-associated herpesvirus supports latent DNA replication in dividing cells. *Journal of Virology*. **76**(22),pp.11677–11687.

Hussain, M., Taft, R.J. and Asgari, S. 2008. An insect virus-encoded microRNA regulates viral replication. *Journal of Virology*. **82**(18),pp.9164–9170.

Hwang, L.N., Englund, N. and Pattnaik, A.K. 1998. Polyadenylation of vesicular stomatitis virus mRNA dictates efficient transcription termination at the intercistronic gene junctions. *Journal of Virology*. **72**(3),pp.1805–1813.

Ikeda, J.E., Longiaru, M., Horwitz, M.S. and Hurwitz, J. 1980. Elongation of primed DNA templates by eukaryotic DNA polymerases. *Proceedings of the National Academy of Sciences of the United States of America*. **77**(10),pp.5827–5831.

Ikeda, M.A. and Nevins, J.R. 1993. Identification of distinct roles for separate E1A domains in disruption of E2F complexes. *Molecular and Cellular Biology*. **13**(11),pp.7029–7035.

Jackson, B.R., Boyne, J.R., Noerenberg, M., Taylor, A., Hautbergue, G.M., Walsh, M.J., Wheat, R., Blackbourn, D.J., Wilson, S.A. and Whitehouse, A. 2011. An Interaction between KSHV ORF57 and UIF Provides mRNA-Adaptor Redundancy in Herpesvirus Intronless mRNA Export B. A. Glaunsinger, ed. *PLoS Pathogens*. **7**(7),p.e1002138.

Jackson, B.R., Noerenberg, M. and Whitehouse, A. 2014. A novel mechanism inducing genome instability in Kaposi's sarcoma-associated herpesvirus infected cells. *PLoS pathogens*. **10**(5),p.e1004098.

Jackson, B.R., Noerenberg, M. and Whitehouse, A. 2012. The Kaposi's Sarcoma-Associated Herpesvirus ORF57 Protein and Its Multiple Roles in mRNA Biogenesis. *Frontiers in Microbiology*. **3**,p.59.

Jacquenet, S., Méreau, A., Bilodeau, P.S., Damier, L., Stoltzfus, C.M. and Branlant, C. 2001. A second exon splicing silencer within human immunodeficiency virus type 1 tat exon 2 represses splicing of Tat mRNA and binds protein hnRNP H. *The Journal of Biological Chemistry*. **276**(44),pp.40464–40475.

Jerabek, H. and Heermann, D.W. 2014. How chromatin looping and nuclear envelope attachment affect genome organization in eukaryotic cell nuclei. *International Review of Cell and Molecular Biology*. **307**,pp.351–381.

Jiricny, J. 2013. Postreplicative Mismatch Repair. *Cold Spring Harbor Perspectives in Biology*. **5**(4),pp.a012633–a012633.

Joaquin, A. and Fernandez-Capetillo, O. 2012. Signalling DNA Damage *In*: C. Huang, ed. *Protein Phosphorylation in Human Health* [Online]. InTech. [Accessed 23 June 2015]. Available from: http://www.intechopen.com/books/protein-phosphorylation-in-human-health/signalling-dna-damage.

Johns, H.L., Gonzalez-Lopez, C., Sayers, C.L., Hollinshead, M. and Elliott, G. 2014. Rab6 Dependent Post-Golgi Trafficking of HSV1 Envelope Proteins to Sites of Virus Envelopment: Rab6 Specific Exocytosis of Virus Glycoproteins. *Traffic*. **15**(2),pp.157–178.

Johnson, A.S., Maronian, N. and Vieira, J. 2005. Activation of Kaposi's Sarcoma-Associated Herpesvirus Lytic Gene Expression during Epithelial Differentiation. *Journal of Virology*. **79**(21),pp.13769–13777.

Johnson, D.C. and Baines, J.D. 2011. Herpesviruses remodel host membranes for virus egress. *Nature Reviews Microbiology*. **9**(5),pp.382–394.

Johnson, D.C. and Huber, M.T. 2002. Directed Egress of Animal Viruses Promotes Cell-to-Cell Spread. *Journal of Virology*. **76**(1),pp.1–8.

Jones, J.F., Shurin, S., Abramowsky, C., Tubbs, R.R., Sciotto, C.G., Wahl, R., Sands, J., Gottman, D., Katz, B.Z. and Sklar, J. 1988. T-Cell Lymphomas Containing Epstein–Barr Viral DNA in Patients with Chronic Epstein–Barr Virus Infections. *New England Journal of Medicine*. **318**(12),pp.733–741.

Jopling, C.L., Yi, M., Lancaster, A.M., Lemon, S.M. and Sarnow, P. 2005. Modulation of hepatitis C virus RNA abundance by a liver-specific MicroRNA. *Science (New York, N.Y.)*. **309**(5740),pp.1577–1581.

Jurica, M.S. and Moore, M.J. 2003. Pre-mRNA splicing: awash in a sea of proteins. *Molecular Cell*. **12**(1),pp.5–14.

Kaipa, B.R., Shao, H., Schäfer, G., Trinkewitz, T., Groth, V., Liu, J., Beck, L., Bogdan, S., Abmayr, S.M. and Önel, S.-F. 2013. Dock mediates Scar- and WASp-dependent actin polymerization through interaction with cell adhesion molecules in founder cells and fusion-competent myoblasts. *Journal of Cell Science*. **126**(Pt 1),pp.360–372.

Kaposi 1872. Idiopathisches multiples Pigmentsarkom der Haut. *Archiv für Dermatologie und Syphilis*. **4**(2),pp.265–273.

Kaschka-Dierich, C., Werner, F.J., Bauer, I. and Fleckenstein, B. 1982. Structure of nonintegrated, circular Herpesvirus saimiri and Herpesvirus ateles genomes in tumor cell lines and in vitro-transformed cells. *Journal of Virology*. **44**(1),pp.295–310.

Katahira, J. 2012. mRNA export and the TREX complex. *Biochimica Et Biophysica Acta*. **1819**(6),pp.507–513.

Katahira, J., Inoue, H., Hurt, E. and Yoneda, Y. 2009. Adaptor Aly and co-adaptor Thoc5 function in the Tap-p15-mediated nuclear export of HSP70 mRNA. *The EMBO Journal*. **28**(5),pp.556–567.

Kati, S., Tsao, E.H., Gunther, T., Weidner-Glunde, M., Rothamel, T., Grundhoff, A., Kellam, P. and Schulz, T.F. 2013. Activation of the B Cell Antigen Receptor Triggers Reactivation of Latent Kaposi's Sarcoma-Associated Herpesvirus in B Cells. *Journal of Virology*. **87**(14),pp.8004–8016.

Kawaji, H. and Hayashizaki, Y. 2008. Exploration of small RNAs. *PLoS genetics*. **4**(1),p.e22.

Kawamata, T. and Tomari, Y. 2010. Making RISC. *Trends in Biochemical Sciences*. **35**(7),pp.368–376.

Keller, S.A., Schattner, E.J. and Cesarman, E. 2000. Inhibition of NF-kappaB induces apoptosis of KSHV-infected primary effusion lymphoma cells. *Blood*. **96**(7),pp.2537–2542.

Kelly, B.J., Fraefel, C., Cunningham, A.L. and Diefenbach, R.J. 2009. Functional roles of the tegument proteins of herpes simplex virus type 1. *Virus Research*. **145**(2),pp.173–186.

Khvorova, A., Reynolds, A. and Jayasena, S.D. 2003. Functional siRNAs and miRNAs exhibit strand bias. *Cell*. **115**(2),pp.209–216.

Klose, J. and Kobalz, U. 1995. Two-dimensional electrophoresis of proteins: an updated protocol and implications for a functional analysis of the genome. *Electrophoresis*. **16**(6),pp.1034–1059.

Knight, L.M., Stakaityte, G., Wood, J., J., Abdul-Sada, H., Griffiths, D.A., Howell, G.J., Wheat, R., Blair, G.E., Steven, N.M., Macdonald, A., Blackbourn, D.J. and Whitehouse, A. 2015. Merkel Cell Polyomavirus Small T Antigen Mediates Microtubule Destabilization To Promote Cell Motility and Migration M. J. Imperiale, ed. *Journal of Virology*. **89**(1),pp.35–47.

Köhler, A. and Hurt, E. 2007. Exporting RNA from the nucleus to the cytoplasm. *Nature Reviews. Molecular Cell Biology*. **8**(10),pp.761–773.

Komarnitsky, P., Cho, E.J. and Buratowski, S. 2000. Different phosphorylated forms of RNA polymerase II and associated mRNA processing factors during transcription. *Genes & Development*. **14**(19),pp.2452–2460.

Koretzky, G.A. 2007. The legacy of the Philadelphia chromosome. *Journal of Clinical Investigation*. **117**(8),pp.2030–2032.

Kornberg, R.D. 2001. The eukaryotic gene transcription machinery. *Biological Chemistry*. **382**(8),pp.1103–1107.

Kosior, K., Lewandowska-Grygiel, M. and Giannopoulos, K. 2011. Tyrosine kinase inhibitors in hematological malignancies. *Postępy Higieny I Medycyny Doświadczalnej (Online)*. **65**,pp.819–828.

Krijgsveld, J., Ketting, R.F., Mahmoudi, T., Johansen, J., Artal-Sanz, M., Verrijzer, C.P., Plasterk, R.H.A. and Heck, A.J.R. 2003. Metabolic labeling of C. elegans and D. melanogaster for quantitative proteomics. *Nature Biotechnology*. **21**(8),pp.927–931.

Krokan, H.E., Drabløs, F. and Slupphaug, G. 2002. Uracil in DNA – occurrence, consequences and repair. *Oncogene*. **21**(58),pp.8935–8948.

Krokan, H.E., Standal, R. and Slupphaug, G. 1997. DNA glycosylases in the base excision repair of DNA. *The Biochemical Journal*. **325 (Pt 1)**,pp.1–16.

Krüger, M., Moser, M., Ussar, S., Thievessen, I., Luber, C.A., Forner, F., Schmidt, S., Zanivan, S., Fässler, R. and Mann, M. 2008. SILAC mouse for quantitative proteomics uncovers kindlin-3 as an essential factor for red blood cell function. *Cell*. **134**(2),pp.353–364.

Kusumoto-Matsuo, R., Ghosh, D., Karmakar, P., May, A., Ramsden, D. and Bohr, V.A. 2014. Serines 440 and 467 in the Werner syndrome protein are phosphorylated by DNA-PK and affects its dynamics in response to DNA double strand breaks. *Aging*. **6**(1),pp.70–81.

Labokha, A. and Fassati, A. 2013. Viruses Challenge Selectivity Barrier of Nuclear Pores. *Viruses*. **5**(10),pp.2410–2423.

Laemmli, U.K. 1970. Cleavage of structural proteins during the assembly of the head of bacteriophage T4. *Nature*. **227**(5259),pp.680–685.

Lakin, N.D. and Jackson, S.P. 1999. Regulation of p53 in response to DNA damage. *Oncogene*. **18**(53),pp.7644–7655.

Lam, Y.W., Evans, V.C., Heesom, K.J., Lamond, A.I. and Matthews, D.A. 2010. Proteomics Analysis of the Nucleolus in Adenovirus-infected Cells. *Molecular & Cellular Proteomics*. **9**(1),pp.117–130.

Lander, E.S., Linton, L.M., Birren, B., Nusbaum, C., Zody, M.C., Baldwin, J., Devon, K., Dewar, K., Doyle, M., FitzHugh, W., Funke, R., Gage, D., Harris, K., Heaford, A., Howland, J., Kann, L., Lehoczky, J., LeVine, R., McEwan, P., McKernan, K., Meldrim, J., Mesirov, J.P., Miranda, C., Morris, W., Naylor, J., Raymond, C., Rosetti, M., Santos, R., Sheridan, A., Sougnez, C., Stange-Thomann, N., Stojanovic, N., Subramanian, A., Wyman, D., Rogers, J., Sulston, J., Ainscough, R., Beck, S., Bentley, D., Burton, J., Clee, C., Carter, N., Coulson, A., Deadman, R., Deloukas, P., Dunham, A., Dunham, I., Durbin, R., French, L., Grafham, D., Gregory, S., Hubbard, T., Humphray, S., Hunt, A., Jones, M., Lloyd, C., McMurray, A., Matthews, L., Mercer, S., Milne, S., Mullikin, J.C., Mungall, A., Plumb, R., Ross, M., Shownkeen, R., Sims, S., Waterston, R.H., Wilson, R.K., Hillier, L.W., McPherson, J.D., Marra, M.A., Mardis, E.R., Fulton, L.A., Chinwalla, A.T., Pepin, K.H., Gish, W.R., Chissoe, S.L., Wendl, M.C., Delehaunty, K.D., Miner, T.L., Delehaunty, A., Kramer, J.B., Cook, L.L., Fulton, R.S., Johnson, D.L., Minx, P.J., Clifton, S.W., Hawkins, T., Branscomb, E., Predki, P., Richardson, P., Wenning, S., Slezak, T., Doggett, N., Cheng, J.F., Olsen, A., Lucas, S., Elkin, C., Uberbacher, E., Frazier, M., Gibbs, R.A., Muzny, D.M., Scherer, S.E., Bouck, J.B., Sodergren, E.J., Worley, K.C., Rives, C.M., Gorrell, J.H., Metzker, M.L., Naylor, S.L., Kucherlapati, R.S., Nelson, D.L., Weinstock, G.M., Sakaki, Y., Fujiyama, A., Hattori, M., Yada, T., Toyoda, A., Itoh, T., Kawagoe, C., Watanabe, H., Totoki, Y., Taylor, T., Weissenbach, J., Heilig, R., Saurin, W., Artiguenave, F., Brottier, P., Bruls, T., Pelletier, E., Robert, C., Wincker, P., Smith, D.R., Doucette-Stamm, L., Rubenfield, M., Weinstock, K., Lee, H.M., Dubois, J., Rosenthal, A., Platzer, M., Nyakatura, G., Taudien, S., Rump, A., Yang, H., Yu, J., Wang, J., Huang, G., Gu, J., Hood, L., Rowen, L., Madan, A., Qin, S., Davis, R.W., Federspiel, N.A., Abola,

A.P., Proctor, M.J., Myers, R.M., Schmutz, J., Dickson, M., Grimwood, J., Cox, D.R., Olson, M.V., Kaul, R., Raymond, C., Shimizu, N., Kawasaki, K., Minoshima, S., Evans, G.A., Athanasiou, M., Schultz, R., Roe, B.A., Chen, F., Pan, H., Ramser, J., Lehrach, H., Reinhardt, R., McCombie, W.R., de la Bastide, M., Dedhia, N., Blöcker, H., Hornischer, K., Nordsiek, G., Agarwala, R., Aravind, L., Bailey, J.A., Bateman, A., Batzoglou, S., Birney, E., Bork, P., Brown, D.G., Burge, C.B., Cerutti, L., Chen, H.C., Church, D., Clamp, M., Copley, R.R., Doerks, T., Eddy, S.R., Eichler, E.E., Furey, T.S., Galagan, J., Gilbert, J.G., Harmon, C., Hayashizaki, Y., Haussler, D., Hermjakob, H., Hokamp, K., Jang, W., Johnson, L.S., Jones, T.A., Kasif, S., Kaspryzk, A., Kennedy, S., Kent, W.J., Kitts, P., Koonin, E.V., Korf, I., Kulp, D., Lancet, D., Lowe, T.M., McLysaght, A., Mikkelsen, T., Moran, J.V., Mulder, N., Pollara, V.J., Ponting, C.P., Schuler, G., Schultz, J., Slater, G., Smit, A.F., Stupka, E., Szustakowski, J., Thierry-Mieg, D., Thierry-Mieg, J., Wagner, L., Wallis, J., Wheeler, R., Williams, A., Wolf, Y.I., Wolfe, K.H., Yang, S.P., Yeh, R.F., Collins, F., Guyer, M.S., Peterson, J., Felsenfeld, A., Wetterstrand, K.A., Patrinos, A., Morgan, M.J., de Jong, P., Catanese, J.J., Osoegawa, K., Shizuya, H., Choi, S., Chen, Y.J., Szustakowki, J. and International Human Genome Sequencing Consortium 2001. Initial sequencing and analysis of the human genome. *Nature*. **409**(6822),pp.860–921.

Lane, D.P. and Crawford, L.V. 1979. T antigen is bound to a host protein in SV40-transformed cells. *Nature*. **278**(5701),pp.261–263.

Lassmann, T., Maida, Y., Tomaru, Y., Yasukawa, M., Ando, Y., Kojima, M., Kasim, V., Simon, C., Daub, C., Carninci, P., Hayashizaki, Y. and Masutomi, K. 2015. Telomerase Reverse Transcriptase Regulates microRNAs. *International Journal of Molecular Sciences*. **16**(1),pp.1192–1208.

Laurin, M. and Cote, J.-F. 2014. Insights into the biological functions of Dock family guanine nucleotide exchange factors. *Genes & Development*. **28**(6),pp.533–547.

Law, G.L., Korth, M.J., Benecke, A.G. and Katze, M.G. 2013. Systems virology: host-directed approaches to viral pathogenesis and drug targeting. *Nature Reviews Microbiology*. **11**(7),pp.455–466.

Lee, G.E., Murray, J.W., Wolkoff, A.W. and Wilson, D.W. 2006. Reconstitution of herpes simplex virus microtubule-dependent trafficking in vitro. *Journal of Virology*. **80**(9),pp.4264–4275.

Lee, L.W., Zhang, S., Etheridge, A., Ma, L., Martin, D., Galas, D. and Wang, K. 2010. Complexity of the microRNA repertoire revealed by next-generation sequencing. *RNA*. **16**(11),pp.2170–2180.

Lee, Y., Jeon, K., Lee, J.-T., Kim, S. and Kim, V.N. 2002. MicroRNA maturation: stepwise processing and subcellular localization. *The EMBO journal*. **21**(17),pp.4663–4670.

Lee, Y.J. and Glaunsinger, B.A. 2009. Aberrant Herpesvirus-Induced Polyadenylation Correlates With Cellular Messenger RNA Destruction B. Sugden, ed. *PLoS Biology*. **7**(5),p.e1000107.

Lee, Y., Kim, M., Han, J., Yeom, K.-H., Lee, S., Baek, S.H. and Kim, V.N. 2004. MicroRNA genes are transcribed by RNA polymerase II. *The EMBO Journal*. **23**(20),pp.4051–4060.

Lei, H., Dias, A.P. and Reed, R. 2011. Export and stability of naturally intronless mRNAs require specific coding region sequences and the TREX mRNA export complex. *Proceedings of the National Academy of Sciences*. **108**(44),pp.17985–17990.

Lei, X., Bai, Z., Ye, F., Xie, J., Kim, C.-G., Huang, Y. and Gao, S.-J. 2010. Regulation of NF-kappaB inhibitor IkappaBalpha and viral replication by a KSHV microRNA. *Nature Cell Biology*. **12**(2),pp.193–199.

Lei, X., Ye, F., Bai, Z., Huang, Y. and Gao, S.-J. 2010. Regulation of herpes virus lifecycle by viral microRNAs. *Virulence*. **1**(5),pp.433–435.

Levine, P.H., Ablashi, D.V., Berard, C.W., Carbone, P.P., Waggoner, D.E. and Malan, L. 1971. Elevated antibody titers to epstein-barr virus in Hodgkin's disease. *Cancer*. **27**(2),pp.416–421.

Lewis, B.P., Burge, C.B. and Bartel, D.P. 2005. Conserved seed pairing, often flanked by adenosines, indicates that thousands of human genes are microRNA targets. *Cell*. **120**(1),pp.15–20.

Lewis, B.P., Shih, I. -hun., Jones-Rhoades, M.W., Bartel, D.P. and Burge, C.B. 2003. Prediction of mammalian microRNA targets. *Cell*. **115**(7),pp.787–798.

Lewis, J.D., Gunderson, S.I. and Mattaj, I.W. 1995. The influence of 5' and 3' end structures on pre-mRNA metabolism. *Journal of Cell Science*. **1995**(Supplement 19),pp.13–19.

Liang, X., Pickering, M.T., Cho, N.-H., Chang, H., Volkert, M.R., Kowalik, T.F. and Jung, J.U. 2006. Deregulation of DNA damage signal transduction by herpesvirus latency-associated M2. *Journal of Virology*. **80**(12),pp.5862–5874.

Liang, Y. 2002. The lytic switch protein of KSHV activates gene expression via functional interaction with RBP-Jkappa (CSL), the target of the Notch signaling pathway. *Genes & Development*. **16**(15),pp.1977–1989.

Lieberman, P.M., Hu, J. and Renne, R. 2007. Maintenance and replication during latency *In*: A. Arvin, G. Campadelli-Fiume, E. Mocarski, P. S. Moore, B. Roizman, R. Whitley and K. Yamanishi, eds. *Human Herpesviruses: Biology, Therapy, and Immunoprophylaxis* [Online]. Cambridge: Cambridge University Press. [Accessed 25 June 2015]. Available from: http://www.ncbi.nlm.nih.gov/books/NBK47400/.

Li, J.Z., Chapman, B., Charlebois, P., Hofmann, O., Weiner, B., Porter, A.J., Samuel, R., Vardhanabhuti, S., Zheng, L., Eron, J., Taiwo, B., Zody, M.C., Henn, M.R., Kuritzkes, D.R. and Hide, W. 2014. Comparison of Illumina and 454 Deep Sequencing in Participants Failing Raltegravir-Based Antiretroviral Therapy L. Kaderali, ed. *PLoS ONE*. **9**(3),p.e90485.

Lim, E.L., Trinh, D.L., Scott, D.W., Chu, A., Krzywinski, M., Zhao, Y., Robertson, A.G., Mungall, A.J., Schein, J., Boyle, M., Mottok, A., Ennishi, D., Johnson, N.A., Steidl, C., Connors, J.M., Morin, R.D., Gascoyne, R.D. and Marra, M.A. 2015. Comprehensive miRNA sequence analysis reveals survival differences in diffuse large B-cell lymphoma patients. *Genome Biology*. [Online]. **16**(1). [Accessed 29 April 2015]. Available from: http://genomebiology.com/2015/16/1/18.

Li, M., Lee, H., Yoon, D.W., Albrecht, J.C., Fleckenstein, B., Neipel, F. and Jung, J.U. 1997. Kaposi's sarcoma-associated herpesvirus encodes a functional cyclin. *Journal of Virology*. **71**(3),pp.1984–1991.

Ling, H., Fabbri, M. and Calin, G.A. 2013. MicroRNAs and other non-coding RNAs as targets for anticancer drug development. *Nature Reviews Drug Discovery*. **12**(11),pp.847–865.

Linsen, S.E.V., de Wit, E., Janssens, G., Heater, S., Chapman, L., Parkin, R.K., Fritz, B., Wyman, S.K., de Bruijn, E., Voest, E.E., Kuersten, S., Tewari, M. and Cuppen, E. 2009. Limitations and possibilities of small RNA digital gene expression profiling. *Nature Methods*. **6**(7),pp.474–476.

Lin, X., Liang, D., He, Z., Deng, Q., Robertson, E.S. and Lan, K. 2011. miR-K12-7-5p Encoded by Kaposi's Sarcoma-Associated Herpesvirus Stabilizes the Latent State by Targeting Viral ORF50/RTA T. F. Schulz, ed. *PLoS ONE*. **6**(1),p.e16224.

Linzer, D.I. and Levine, A.J. 1979. Characterization of a 54K dalton cellular SV40 tumor antigen present in SV40-transformed cells and uninfected embryonal carcinoma cells. *Cell*. **17**(1),pp.43–52.

Li, R., Zhu, J., Xie, Z., Liao, G., Liu, J., Chen, M.-R., Hu, S., Woodard, C., Lin, J., Taverna, S.D., Desai, P., Ambinder, R.F., Hayward, G.S., Qian, J., Zhu, H. and Hayward, S.D. 2011. Conserved Herpesvirus Kinases Target the DNA Damage Response Pathway and TIP60 Histone Acetyltransferase to Promote Virus Replication. *Cell Host & Microbe*. **10**(4),pp.390–400.

Liu, H., Sadygov, R.G. and Yates, J.R. 2004. A model for random sampling and estimation of relative protein abundance in shotgun proteomics. *Analytical Chemistry*. **76**(14),pp.4193–4201.

Liu, L.F., Desai, S.D., Li, T.K., Mao, Y., Sun, M. and Sim, S.P. 2000. Mechanism of action of camptothecin. *Annals of the New York Academy of Sciences*. **922**,pp.1–10.

Liu, S., Shiotani, B., Lahiri, M., Maréchal, A., Tse, A., Leung, C.C.Y., Glover, J.N.M., Yang, X.H. and Zou, L. 2011. ATR Autophosphorylation as a Molecular Switch for Checkpoint Activation. *Molecular Cell*. **43**(2),pp.192–202.

Li, W., Fan, J. and Woodley, D.T. 2001. Nck/Dock: an adapter between cell surface receptors and the actin cytoskeleton. *Oncogene*. **20**(44),pp.6403–6417.

Li, X. and Heyer, W.-D. 2008. Homologous recombination in DNA repair and DNA damage tolerance. *Cell Research*. **18**(1),pp.99–113.

Li, Y., Masaki, T., Yamane, D., McGivern, D.R. and Lemon, S.M. 2013. Competing and noncompeting activities of miR-122 and the 5' exonuclease Xrn1 in regulation of hepatitis C virus replication. *Proceedings of the National Academy of Sciences of the United States of America*. **110**(5),pp.1881–1886.

Li, Y., Zhang, Z., Liu, F., Vongsangnak, W., Jing, Q. and Shen, B. 2012. Performance comparison and evaluation of software tools for microRNA deep-sequencing data analysis. *Nucleic Acids Research*. **40**(10),pp.4298–4305.

Li, Z., Cui, X., Li, F., Li, P., Ni, M., Wang, S. and Bo, X. 2013. Exploring the role of human miRNAs in virus-host interactions using systematic overlap analysis. *Bioinformatics*. **29**(19),pp.2375–2379.

Lodish, H.F. (ed.). 2000. *Molecular cell biology* 4th ed. New York: W.H. Freeman.

Loeb, L.A. and Preston, B.D. 1986. Mutagenesis by apurinic/apyrimidinic sites. *Annual Review of Genetics*. **20**,pp.201–230.

Longnecker, R. and Neipel, F. 2007. Introduction to the human γ-herpesviruses *In*: A. Arvin, G. Campadelli-Fiume, E. Mocarski, P. S. Moore, B. Roizman, R. Whitley and K. Yamanishi, eds. *Human Herpesviruses: Biology, Therapy, and Immunoprophylaxis* [Online]. Cambridge: Cambridge University Press. [Accessed 25 June 2015]. Available from: http://www.ncbi.nlm.nih.gov/books/NBK47397/.

Lu, F., Stedman, W., Yousef, M., Renne, R. and Lieberman, P.M. 2010. Epigenetic Regulation of Kaposi's Sarcoma-Associated Herpesvirus Latency by Virus-Encoded MicroRNAs That Target Rta and the Cellular Rbl2-DNMT Pathway. *Journal of Virology*. **84**(6),pp.2697–2706.

Luftig, M.A. 2014. Viruses and the DNA Damage Response: Activation and Antagonism. *Annual Review of Virology*. **1**(1),pp.605–625.

Lu, F., Weidmer, A., Liu, C.-G., Volinia, S., Croce, C.M. and Lieberman, P.M. 2008. Epstein-Barr Virus-Induced miR-155 Attenuates NF- B Signaling and Stabilizes Latent Virus Persistence. *Journal of Virology*. **82**(21),pp.10436–10443.

Luitweiler, E.M., Henson, B.W., Pryce, E.N., Patel, V., Coombs, G., McCaffery, J.M., Desai, P.J. 2013. Interactions of the Kaposi's Sarcoma-associated herpesvirus

nuclear egress complex: ORF69 is a potent factor for remodeling cellular membranes. *Journal of Virology*. **87**(7), pp.3915-3929.

Lukac, D.M., Renne, R., Kirshner, J.R. and Ganem, D. 1998. Reactivation of Kaposi's sarcoma-associated herpesvirus infection from latency by expression of the ORF 50 transactivator, a homolog of the EBV R protein. *Virology*. **252**(2),pp.304–312.

Luna, J.M., Scheel, T.K.H., Danino, T., Shaw, K.S., Mele, A., Fak, J.J., Nishiuchi, E., Takacs, C.N., Catanese, M.T., de Jong, Y.P., Jacobson, I.M., Rice, C.M. and Darnell, R.B. 2015. Hepatitis C Virus RNA Functionally Sequesters miR-122. *Cell*. **160**(6),pp.1099–1110.

Luo, C., Tsementzi, D., Kyrpides, N., Read, T. and Konstantinidis, K.T. 2012. Direct Comparisons of Illumina vs. Roche 454 Sequencing Technologies on the Same Microbial Community DNA Sample F. Rodriguez-Valera, ed. *PLoS ONE*. **7**(2),p.e30087.

Lu, X. and Legerski, R.J. 2007. The Prp19/Pso4 core complex undergoes ubiquitylation and structural alterations in response to DNA damage. *Biochemical and Biophysical Research Communications*. **354**(4),pp.968–974.

Lyman, M.G. and Enquist, L.W. 2009. Herpesvirus interactions with the host cytoskeleton. *Journal of Virology*. **83**(5),pp.2058–2066.

Lytle, J.R., Yario, T.A. and Steitz, J.A. 2007. Target mRNAs are repressed as efficiently by microRNA-binding sites in the 5' UTR as in the 3' UTR. *Proceedings of the National Academy of Sciences of the United States of America*. **104**(23),pp.9667–9672.

Mabit, H., Nakano, M.Y., Prank, U., Saam, B., Dohner, K., Sodeik, B. and Greber, U.F. 2002. Intact Microtubules Support Adenovirus and Herpes Simplex Virus Infections. *Journal of Virology*. **76**(19),pp.9962–9971.

Machida, T., Fujita, T., Ooo, M.L., Ohira, M., Isogai, E., Mihara, M., Hirato, J., Tomotsune, D., Hirata, T., Fujimori, M., Adachi, W. and Nakagawara, A. 2006. Increased expression of proapoptotic BMCC1, a novel gene with the BNIP2 and Cdc42GAP homology (BCH) domain, is associated with favorable prognosis in human neuroblastomas. *Oncogene*. **25**(13),pp.1931–1942.

Majerciak, V., Ni, T., Yang, W., Meng, B., Zhu, J. and Zheng, Z.-M. 2013. A Viral Genome Landscape of RNA Polyadenylation from KSHV Latent to Lytic Infection B. A. Glaunsinger, ed. *PLoS Pathogens*. **9**(11),p.e1003749.

Majerciak, V., Yamanegi, K., Allemand, E., Kruhlak, M., Krainer, A.R. and Zheng, Z.-M. 2008. Kaposi's sarcoma-associated herpesvirus ORF57 functions as a viral splicing factor and promotes expression of intron-containing viral lytic genes in spliceosome-mediated RNA splicing. *Journal of Virology*. **82**(6),pp.2792–2801.

Majerciak, V. and Zheng, Z.-M. 2015. KSHV ORF57, a protein of many faces. *Viruses*. **7**(2),pp.604–633.

Makarova, O.V., Makarov, E.M., Urlaub, H., Will, C.L., Gentzel, M., Wilm, M. and Lührmann, R. 2004. A subset of human 35S U5 proteins, including Prp19, function prior to catalytic step 1 of splicing. *The EMBO journal*. **23**(12),pp.2381–2391.

Malik, P., Blackbourn, D.J. and Clements, J.B. 2004. The evolutionarily conserved Kaposi's sarcoma-associated herpesvirus ORF57 protein interacts with REF protein and acts as an RNA export factor. *The Journal of Biological Chemistry*. **279**(31),pp.33001–33011.

Malone, J.H. and Oliver, B. 2011. Microarrays, deep sequencing and the true measure of the transcriptome. *BMC Biology*. **9**(1),p.34.

Manley, J.L. 1995. A complex protein assembly catalyzes polyadenylation of mRNA precursors. *Current Opinion in Genetics & Development*. **5**(2),pp.222–228.

Mardis, E.R. 2008. Next-Generation DNA Sequencing Methods. *Annual Review of Genomics and Human Genetics*. **9**(1),pp.387–402.

Maréchal, A., Li, J.-M., Ji, X.Y., Wu, C.-S., Yazinski, S.A., Nguyen, H.D., Liu, S., Jiménez, A.E., Jin, J. and Zou, L. 2014. PRP19 transforms into a sensor of RPA-ssDNA after DNA damage and drives ATR activation via a ubiquitin-mediated circuitry. *Molecular Cell*. **53**(2),pp.235–246.

Marquitz, A.R., Mathur, A., Nam, C.S. and Raab-Traub, N. 2011. The Epstein-Barr Virus BART microRNAs target the pro-apoptotic protein Bim. *Virology*. **412**(2),pp.392–400.

Marteijn, J.A., Lans, H., Vermeulen, W. and Hoeijmakers, J.H.J. 2014. Understanding nucleotide excision repair and its roles in cancer and ageing. *Nature Reviews Molecular Cell Biology*. **15**(7),pp.465–481.

Martin, E.R., Kinnamon, D.D., Schmidt, M.A., Powell, E.H., Zuchner, S. and Morris, R.W. 2010. SeqEM: an adaptive genotype-calling approach for next-generation sequencing studies. *Bioinformatics*. **26**(22),pp.2803–2810.

Masuda, S., Das, R., Cheng, H., Hurt, E., Dorman, N. and Reed, R. 2005. Recruitment of the human TREX complex to mRNA during splicing. *Genes & Development*. **19**(13),pp.1512–1517.

Matthews, R.E. 1979. Third report of the International Committee on Taxonomy of Viruses. Classification and nomenclature of viruses. *Intervirology*. **12**(3-5),pp.129–296.

McCracken, S., Fong, N., Yankulov, K., Ballantyne, S., Pan, G., Greenblatt, J., Patterson, S.D., Wickens, M. and Bentley, D.L. 1997. The C-terminal domain of RNA

polymerase II couples mRNA processing to transcription. *Nature*. **385**(6614),pp.357–361.

McGeoch, D.J., Rixon, F.J. and Davison, A.J. 2006. Topics in herpesvirus genomics and evolution. *Virus Research*. **117**(1),pp.90–104.

McKendrick, L., Thompson, E., Ferreira, J., Morley, S.J. and Lewis, J.D. 2001. Interaction of Eukaryotic Translation Initiation Factor 4G with the Nuclear Cap-Binding Complex Provides a Link between Nuclear and Cytoplasmic Functions of the m7 Guanosine Cap. *Molecular and Cellular Biology*. **21**(11),pp.3632–3641.

Megger, D.A., Bracht, T., Meyer, H.E. and Sitek, B. 2013. Label-free quantification in clinical proteomics. *Biochimica et Biophysica Acta (BBA) - Proteins and Proteomics*. **1834**(8),pp.1581–1590.

Melamed, Z., Levy, A., Ashwal-Fluss, R., Lev-Maor, G., Mekahel, K., Atias, N., Gilad, S., Sharan, R., Levy, C., Kadener, S. and Ast, G. 2013. Alternative Splicing Regulates Biogenesis of miRNAs Located across Exon-Intron Junctions. *Molecular Cell*. **50**(6),pp.869–881.

Meller, N., Irani-Tehrani, M., Kiosses, W.B., Del Pozo, M.A. and Schwartz, M.A. 2002. Zizimin1, a novel Cdc42 activator, reveals a new GEF domain for Rho proteins. *Nature Cell Biology*. **4**(9),pp.639–647.

Menon, V. and Povirk, L. 2014. Involvement of p53 in the Repair of DNA Double Strand Breaks: Multifaceted Roles of p53 in Homologous Recombination Repair (HRR) and Non-Homologous End Joining (NHEJ) *In*: S. P. Deb and S. Deb, eds. *Mutant p53 and MDM2 in Cancer* [Online]. Dordrecht: Springer Netherlands, pp. 321–336. [Accessed 29 June 2015]. Available from: http://link.springer.com/10.1007/978-94-017-9211-0_17.

Mercader, M., Taddeo, B., Panella, J.R., Chandran, B., Nickoloff, B.J. and Foreman, K.E. 2000. Induction of HHV-8 lytic cycle replication by inflammatory cytokines produced by HIV-1-infected T cells. *The American Journal of Pathology*. **156**(6),pp.1961–1971.

Mesri, E.A., Cesarman, E. and Boshoff, C. 2010. Kaposi's sarcoma and its associated herpesvirus. *Nature Reviews Cancer*. **10**(10),pp.707–719.

Metpally, R.P.R., Nasser, S., Malenica, I., Courtright, A., Carlson, E., Ghaffari, L., Villa, S., Tembe, W. and Van Keuren-Jensen, K. 2013. Comparison of Analysis Tools for miRNA High Throughput Sequencing Using Nerve Crush as a Model. *Frontiers in Genetics*. [Online]. **4**. [Accessed 29 April 2015]. Available from: http://journal.frontiersin.org/article/10.3389/fgene.2013.00020/abstract.

Mettenleiter, T.C. 2004. Budding events in herpesvirus morphogenesis. *Virus Research*. **106**(2),pp.167–180.

Mettenleiter, T.C., Klupp, B.G. and Granzow, H. 2009. Herpesvirus assembly: An update. *Virus Research*. **143**(2),pp.222–234.

Michalski, A., Cox, J. and Mann, M. 2011. More than 100,000 detectable peptide species elute in single shotgun proteomics runs but the majority is inaccessible to data-dependent LC-MS/MS. *Journal of Proteome Research*. **10**(4),pp.1785–1793.

Mizumoto, K. and Kaziro, Y. 1987. Messenger RNA capping enzymes from eukaryotic cells. *Progress in Nucleic Acid Research and Molecular Biology*. **34**,pp.1–28.

Mocarski Jr., E.S. 2007. Comparative analysis of herpesvirus-common proteins *In*: A. Arvin, G. Campadelli-Fiume, E. Mocarski, P. S. Moore, B. Roizman, R. Whitley and K. Yamanishi, eds. *Human Herpesviruses: Biology, Therapy, and Immunoprophylaxis* [Online]. Cambridge: Cambridge University Press. [Accessed 25 June 2015]. Available from: http://www.ncbi.nlm.nih.gov/books/NBK47403/.

Mochan, T.A., Venere, M., DiTullio, R.A. and Halazonetis, T.D. 2003. 53BP1 and NFBD1/MDC1-Nbs1 function in parallel interacting pathways activating ataxia-telangiectasia mutated (ATM) in response to DNA damage. *Cancer Research*. **63**(24),pp.8586–8591.

Monteys, A.M., Spengler, R.M., Dufour, B.D., Wilson, M.S., Oakley, C.K., Sowada, M.J., McBride, J.L. and Davidson, B.L. 2014. Single nucleotide seed modification restores in vivo tolerability of a toxic artificial miRNA sequence in the mouse brain. *Nucleic Acids Research*. **42**(21),pp.13315–13327.

Moody, C.A. and Laimins, L.A. 2009. Human Papillomaviruses Activate the ATM DNA Damage Pathway for Viral Genome Amplification upon Differentiation D. Galloway, ed. *PLoS Pathogens*. **5**(10),p.e1000605.

Moore, P.S. 2007. KSHV manipulation of the cell cycle and apoptosis *In*: A. Arvin, G. Campadelli-Fiume, E. Mocarski, P. S. Moore, B. Roizman, R. Whitley and K. Yamanishi, eds. *Human Herpesviruses: Biology, Therapy, and Immunoprophylaxis* [Online]. Cambridge: Cambridge University Press. [Accessed 26 June 2015]. Available from: http://www.ncbi.nlm.nih.gov/books/NBK47432/.

Mortazavi, A., Williams, B.A., McCue, K., Schaeffer, L. and Wold, B. 2008. Mapping and quantifying mammalian transcriptomes by RNA-Seq. *Nature Methods*. **5**(7),pp.621–628.

Moteki, S. and Price, D. 2002. Functional coupling of capping and transcription of mRNA. *Molecular Cell*. **10**(3),pp.599–609.

Mothes, W., Sherer, N.M., Jin, J. and Zhong, P. 2010. Virus Cell-to-Cell Transmission. *Journal of Virology*. **84**(17),pp.8360–8368.

Münger, K., Werness, B.A., Dyson, N., Phelps, W.C., Harlow, E. and Howley, P.M. 1989. Complex formation of human papillomavirus E7 proteins with the retinoblastoma tumor suppressor gene product. *The EMBO journal*. **8**(13),pp.4099–4105.

Muthukrishnan, S., Both, G.W., Furuichi, Y. and Shatkin, A.J. 1975. 5'-Terminal 7-methylguanosine in eukaryotic mRNA is required for translation. *Nature*. **255**(5503),pp.33–37.

Myoung, J. and Ganem, D. 2011. Generation of a doxycycline-inducible KSHV producer cell line of endothelial origin: Maintenance of tight latency with efficient reactivation upon induction. *Journal of Virological Methods*. **174**(1-2),pp.12–21.

Nakamura, H., Lu, M., Gwack, Y., Souvlis, J., Zeichner, S.L. and Jung, J.U. 2003. Global Changes in Kaposi's Sarcoma-Associated Virus Gene Expression Patterns following Expression of a Tetracycline-Inducible Rta Transactivator. *Journal of Virology*. **77**(7),pp.4205–4220.

Napoli, C. 1990. Introduction of a Chimeric Chalcone Synthase Gene into Petunia Results in Reversible Co-Suppression of Homologous Genes in trans. *THE PLANT CELL ONLINE*. **2**(4),pp.279–289.

Naranatt, P.P., Krishnan, H.H., Smith, M.S. and Chandran, B. 2005. Kaposi's sarcoma-associated herpesvirus modulates microtubule dynamics via RhoA-GTP-diaphanous 2 signaling and utilizes the dynein motors to deliver its DNA to the nucleus. *Journal of Virology*. **79**(2),pp.1191–1206.

Odumade, O.A., Hogquist, K.A. and Balfour, H.H. 2011. Progress and Problems in Understanding and Managing Primary Epstein-Barr Virus Infections. *Clinical Microbiology Reviews*. **24**(1),pp.193–209.

O'Farrell, P.H. 1975. High resolution two-dimensional electrophoresis of proteins. *The Journal of Biological Chemistry*. **250**(10),pp.4007–4021.

Ogawa, K., Tanaka, Y., Uruno, T., Duan, X., Harada, Y., Sanematsu, F., Yamamura, K., Terasawa, M., Nishikimi, A., Cote, J.-F. and Fukui, Y. 2014. DOCK5 functions as a key signaling adaptor that links Fc RI signals to microtubule dynamics during mast cell degranulation. *Journal of Experimental Medicine*. **211**(7),pp.1407–1419.

Ong, S.-E., Blagoev, B., Kratchmarova, I., Kristensen, D.B., Steen, H., Pandey, A. and Mann, M. 2002. Stable isotope labeling by amino acids in cell culture, SILAC, as a simple and accurate approach to expression proteomics. *Molecular & cellular proteomics: MCP*. **1**(5),pp.376–386.

Ong, S.-E. and Mann, M. 2007. A practical recipe for stable isotope labeling by amino acids in cell culture (SILAC). *Nature Protocols*. **1**(6),pp.2650–2660.

O'Reilly, M.M., McNally, M.T. and Beemon, K.L. 1995. Two strong 5' splice sites and competing, suboptimal 3' splice sites involved in alternative splicing of human immunodeficiency virus type 1 RNA. *Virology*. **213**(2),pp.373–385.

Owen, C., Hughes, D., Baquero-Perez, B., Berndt, A., Schumann, S., Jackson, B. and Whitehouse, A. 2014. Utilising proteomic approaches to understand oncogenic human herpesviruses (Review). *Molecular and Clinical Oncology*. [Online]. [Accessed 24 April 2015]. Available from: http://www.spandidos-publications.com/10.3892/mco.2014.341.

Ozsolak, F. and Milos, P.M. 2011. RNA sequencing: advances, challenges and opportunities. *Nature Reviews Genetics*. **12**(2),pp.87–98.

Paludan, S.R., Bowie, A.G., Horan, K.A. and Fitzgerald, K.A. 2011. Recognition of herpesviruses by the innate immune system. *Nature Reviews Immunology*. **11**(2),pp.143–154.

Paniagua, R., Nistal, M., Amat, P. and Rodríguez, M.C. 1986. Ultrastructural observations on nucleoli and related structures during human spermatogenesis. *Anatomy and Embryology*. **174**(3),pp.301–306.

Parkin, D.M., Sitas, F., Chirenje, M., Stein, L., Abratt, R. and Wabinga, H. 2008. Part I: Cancer in Indigenous Africans--burden, distribution, and trends. *The Lancet. Oncology*. **9**(7),pp.683–692.

Park, J.-E., Heo, I., Tian, Y., Simanshu, D.K., Chang, H., Jee, D., Patel, D.J. and Kim, V.N. 2011. Dicer recognizes the 5' end of RNA for efficient and accurate processing. *Nature*. **475**(7355),pp.201–205.

Pathmanathan, R., Prasad, U., Sadler, R., Flynn, K. and Raab-Traub, N. 1995. Clonal proliferations of cells infected with Epstein-Barr virus in preinvasive lesions related to nasopharyngeal carcinoma. *The New England Journal of Medicine*. **333**(11),pp.693–698.

Patton, W.F. 2002. Detection technologies in proteome analysis. *Journal of Chromatography. B, Analytical Technologies in the Biomedical and Life Sciences*. **771**(1-2),pp.3–31.

Payvar, F., DeFranco, D., Firestone, G.L., Edgar, B., Wrange, O., Okret, S., Gustafsson, J.A. and Yamamoto, K.R. 1983. Sequence-specific binding of glucocorticoid receptor to MTV DNA at sites within and upstream of the transcribed region. *Cell*. **35**(2 Pt 1),pp.381–392.

Pedro Simas, J. and Efstathiou, S. 1998. Murine gammaherpesvirus 68: a model for the study of gammaherpesvirus pathogenesis. *Trends in Microbiology*. **6**(7),pp.276–282.

Penkert, R.R. and Kalejta, R.F. 2011. Tegument protein control of latent herpesvirus establishment and animation. *Herpesviridae*. **2**(1),p.3.

Pfeffer, S., Zavolan, M., Grässer, F.A., Chien, M., Russo, J.J., Ju, J., John, B., Enright, A.J., Marks, D., Sander, C. and Tuschl, T. 2004. Identification of virus-encoded microRNAs. *Science (New York, N.Y.)*. **304**(5671),pp.734–736.

Plotch, S.J., Bouloy, M., Ulmanen, I. and Krug, R.M. 1981. A unique cap(m7GpppXm)-dependent influenza virion endonuclease cleaves capped RNAs to generate the primers that initiate viral RNA transcription. *Cell*. **23**(3),pp.847–858.

Plotch, S.J. and Krug, R.M. 1977. Influenza virion transcriptase: synthesis in vitro of large, polyadenylic acid-containing complementary RNA. *Journal of Virology*. **21**(1),pp.24–34.

Podhorecka, M., Skladanowski, A. and Bozko, P. 2010. H2AX Phosphorylation: Its Role in DNA Damage Response and Cancer Therapy. *Journal of Nucleic Acids*. **2010**,pp.1–9.

Poirier, M.C. 2012. Chemical-induced DNA damage and human cancer risk. *Discovery Medicine*. **14**(77),pp.283–288.

Polizzotto, M.N., Uldrick, T.S. and Yarchoan, R. 2013. Multicentric Castleman Disease *In*: T. J. Hope, M. Stevenson and D. Richman, eds. *Encyclopedia of AIDS* [Online]. New York, NY: Springer New York, pp. 1–11. [Accessed 26 June 2015]. Available from: http://link.springer.com/10.1007/978-1-4614-9610-6_6-1.

Polson, A.G., Wang, D., DeRisi, J. and Ganem, D. 2002. Modulation of host gene expression by the constitutively active G protein-coupled receptor of Kaposi's sarcoma-associated herpesvirus. *Cancer Research*. **62**(15),pp.4525–4530.

Pratt, Z.L., Kuzembayeva, M., Sengupta, S. and Sugden, B. 2009. The microRNAs of Epstein–Barr Virus are expressed at dramatically differing levels among cell lines. *Virology*. **386**(2),pp.387–397.

Pritchard, C.C., Cheng, H.H. and Tewari, M. 2012. MicroRNA profiling: approaches and considerations. *Nature Reviews Genetics*. **13**(5),pp.358–369.

Pritlove, D.C., Poon, L.L., Fodor, E., Sharps, J. and Brownlee, G.G. 1998. Polyadenylation of influenza virus mRNA transcribed in vitro from model virion RNA templates: requirement for 5' conserved sequences. *Journal of Virology*. **72**(2),pp.1280–1286.

Proudfoot, N. 1991. Poly(A) signals. *Cell*. **64**(4),pp.671–674.

Punj, V., Matta, H., Schamus, S., Tamewitz, A., Anyang, B. and Chaudhary, P.M. 2010. Kaposi's sarcoma-associated herpesvirus-encoded viral FLICE inhibitory protein (vFLIP) K13 suppresses CXCR4 expression by upregulating miR-146a. *Oncogene*. **29**(12),pp.1835–1844.

Purcell, D.F. and Martin, M.A. 1993. Alternative splicing of human immunodeficiency virus type 1 mRNA modulates viral protein expression, replication, and infectivity. *Journal of Virology*. **67**(11),pp.6365–6378.

Qin, Z., Jakymiw, A., Findlay, V. and Parsons, C. 2012. KSHV-Encoded MicroRNAs: Lessons for Viral Cancer Pathogenesis and Emerging Concepts. *International Journal of Cell Biology*. **2012**,pp.1–9.

Quinlan, M.P., Chen, L.B. and Knipe, D.M. 1984. The intranuclear location of a herpes simplex virus DNA-binding protein is determined by the status of viral DNA replication. *Cell*. **36**(4),pp.857–868.

Qunibi, W., Al-Furayh, O., Almeshari, K., Lin, S.F., Sun, R., Heston, L., Ross, D., Rigsby, M. and Miller, G. 1998. Serologic association of human herpesvirus eight with posttransplant Kaposi's sarcoma in Saudi Arabia. *Transplantation*. **65**(4),pp.583–585.

Radtke, K., Dohner, K. and Sodeik, B. 2006. Viral interactions with the cytoskeleton: a hitchhiker's guide to the cell. *Cellular Microbiology*. **8**(3),pp.387–400.

Rajagopalan, R., Vaucheret, H., Trejo, J. and Bartel, D.P. 2006. A diverse and evolutionarily fluid set of microRNAs in Arabidopsis thaliana. *Genes & Development*. **20**(24),pp.3407–3425.

Rass, U., Compton, S.A., Matos, J., Singleton, M.R., Ip, S.C.Y., Blanco, M.G., Griffith, J.D. and West, S.C. 2010. Mechanism of Holliday junction resolution by the human GEN1 protein. *Genes & Development*. **24**(14),pp.1559–1569.

Reed, R. and Maniatis, T. 1985. Intron sequences involved in lariat formation during pre-mRNA splicing. *Cell*. **41**(1),pp.95–105.

Rivera-Calzada, A., Spagnolo, L., Pearl, L.H. and Llorca, O. 2007. Structural model of full-length human Ku70–Ku80 heterodimer and its recognition of DNA and DNA-PKcs. *EMBO reports*. **8**(1),pp.56–62.

Roberts, K.L. and Baines, J.D. 2010. Myosin Va Enhances Secretion of Herpes Simplex Virus 1 Virions and Cell Surface Expression of Viral Glycoproteins. *Journal of Virology*. **84**(19),pp.9889–9896.

Robertson, B., Dalby, A.B., Karpilow, J., Khvorova, A., Leake, D. and Vermeulen, A. 2010. Specificity and functionality of microRNA inhibitors. *Silence*. **1**(1),p.10.

Robey, R.C., Mletzko, S. and Gotch, F.M. 2010. The T-Cell Immune Response against Kaposi's Sarcoma-Associated Herpesvirus. *Advances in Virology*. **2010**,pp.1–9.

Robinson, M.D., McCarthy, D.J. and Smyth, G.K. 2010. edgeR: a Bioconductor package for differential expression analysis of digital gene expression data. *Bioinformatics*. **26**(1),pp.139–140.

Rochat, R.H., Liu, X., Murata, K., Nagayama, K., Rixon, F.J. and Chiu, W. 2011. Seeing the Portal in Herpes Simplex Virus Type 1 B Capsids. *Journal of Virology*. **85**(4),pp.1871–1874.

Rode, K., Dohner, K., Binz, A., Glass, M., Strive, T., Bauerfeind, R. and Sodeik, B. 2011. Uncoupling Uncoating of Herpes Simplex Virus Genomes from Their Nuclear Import and Gene Expression. *Journal of Virology*. **85**(9),pp.4271–4283.

Rodríguez-Navarro, S. and Hurt, E. 2011. Linking gene regulation to mRNA production and export. *Current Opinion in Cell Biology*. **23**(3),pp.302–309.

Roizmann, B., Desrosiers, R.C., Fleckenstein, B., Lopez, C., Minson, A.C. and Studdert, M.J. 1992. The family Herpesviridae: an update. The Herpesvirus Study Group of the International Committee on Taxonomy of Viruses. *Archives of Virology*. **123**(3-4),pp.425–449.

Roos, W.P. and Kaina, B. 2006. DNA damage-induced cell death by apoptosis. *Trends in Molecular Medicine*. **12**(9),pp.440–450.

Ross, P.L., Huang, Y.N., Marchese, J.N., Williamson, B., Parker, K., Hattan, S., Khainovski, N., Pillai, S., Dey, S., Daniels, S., Purkayastha, S., Juhasz, P., Martin, S., Bartlet-Jones, M., He, F., Jacobson, A. and Pappin, D.J. 2004. Multiplexed protein quantitation in Saccharomyces cerevisiae using amine-reactive isobaric tagging reagents. *Molecular & cellular proteomics: MCP*. **3**(12),pp.1154–1169.

Roukos, V. and Misteli, T. 2014. The biogenesis of chromosome translocations. *Nature Cell Biology*. **16**(4),pp.293–300.

Ruby, J.G., Jan, C., Player, C., Axtell, M.J., Lee, W., Nusbaum, C., Ge, H. and Bartel, D.P. 2006. Large-Scale Sequencing Reveals 21U-RNAs and Additional MicroRNAs and Endogenous siRNAs in C. elegans. *Cell*. **127**(6),pp.1193–1207.

Ruiz-Lafuente, N., Alcaraz-Garcia, M.-J., Garcia-Serna, A.-M., Sebastian-Ruiz, S., Moya-Quiles, M.-R., Garcia-Alonso, A.-M. and Parrado, A. 2015. Dock10, a Cdc42 and Rac1 GEF, induces loss of elongation, filopodia, and ruffles in cervical cancer epithelial HeLa cells. *Biology Open*. **4**(5),pp.627–635.

Russo, J.J., Bohenzky, R.A., Chien, M.C., Chen, J., Yan, M., Maddalena, D., Parry, J.P., Peruzzi, D., Edelman, I.S., Chang, Y. and Moore, P.S. 1996. Nucleotide sequence of the Kaposi sarcoma-associated herpesvirus (HHV8). *Proceedings of the National Academy of Sciences of the United States of America*. **93**(25),pp.14862–14867.

Ryu, S., Gallis, B., Goo, Y.A., Shaffer, S.A., Radulovic, D. and Goodlett, D.R. 2008. Comparison of a label-free quantitative proteomic method based on peptide ion current area to the isotope coded affinity tag method. *Cancer Informatics*. **6**,pp.243–255.

Sahin, B.B., Patel, D. and Conrad, N.K. 2010. Kaposi's sarcoma-associated herpesvirus ORF57 protein binds and protects a nuclear noncoding RNA from cellular RNA decay pathways. *PLoS pathogens*. **6**(3),p.e1000799.

Salvetti, A. and Greco, A. 2014. Viruses and the nucleolus: the fatal attraction. *Biochimica Et Biophysica Acta*. **1842**(6),pp.840–847.

Sanders, M.A., Ampasala, D. and Basson, M.D. 2009. DOCK5 and DOCK1 Regulate Caco-2 Intestinal Epithelial Cell Spreading and Migration on Collagen IV. *Journal of Biological Chemistry*. **284**(1),pp.27–35.

Sanford, J.R. 2004. Pre-mRNA splicing: life at the centre of the central dogma. *Journal of Cell Science*. **117**(26),pp.6261–6263.

Sanui, T. 2003. DOCK2 regulates Rac activation and cytoskeletal reorganization through interaction with ELMO1. *Blood*. **102**(8),pp.2948–2950.

Savin, K.W., Cocks, B.G., Wong, F., Sawbridge, T., Cogan, N., Savage, D. and Warner, S. 2010. A neurotropic herpesvirus infecting the gastropod, abalone, shares ancestry with oyster herpesvirus and a herpesvirus associated with the amphioxus genome. *Virology Journal*. **7**(1),p.308.

Schena, M., Shalon, D., Davis, R.W. and Brown, P.O. 1995. Quantitative monitoring of gene expression patterns with a complementary DNA microarray. *Science (New York, N.Y.)*. **270**(5235),pp.467–470.

Schmidt, A., Kellermann, J. and Lottspeich, F. 2005. A novel strategy for quantitative proteomics using isotope-coded protein labels. *Proteomics*. **5**(1),pp.4–15.

Schroeder, S.C., Schwer, B., Shuman, S. and Bentley, D. 2000. Dynamic association of capping enzymes with transcribing RNA polymerase II. *Genes & Development*. **14**(19),pp.2435–2440.

Schubert, M., Keene, J.D., Herman, R.C. and Lazzarini, R.A. 1980. Site on the vesicular stomatitis virus genome specifying polyadenylation and the end of the L gene mRNA. *Journal of Virology*. **34**(2),pp.550–559.

Schulz, T.F. and Chang, Y. 2007. KSHV gene expression and regulation *In*: A. Arvin, G. Campadelli-Fiume, E. Mocarski, P. S. Moore, B. Roizman, R. Whitley and K. Yamanishi, eds. *Human Herpesviruses: Biology, Therapy, and Immunoprophylaxis* [Online]. Cambridge: Cambridge University Press. [Accessed 26 June 2015]. Available from: http://www.ncbi.nlm.nih.gov/books/NBK47415/.

Schumann, S., Jackson, B., Baquero-Perez, B. and Whitehouse, A. 2013. Kaposi's Sarcoma-Associated Herpesvirus ORF57 Protein: Exploiting All Stages of Viral mRNA Processing. *Viruses*. **5**(8),pp.1901–1923.

Seo, G.J., Fink, L.H.L., O'Hara, B., Atwood, W.J. and Sullivan, C.S. 2008. Evolutionarily Conserved Function of a Viral MicroRNA. *Journal of Virology*. **82**(20),pp.9823–9828.

Shahin, V. 2006. The genome of HSV-1 translocates through the nuclear pore as a condensed rod-like structure. *Journal of Cell Science*. **119**(1),pp.23–30.

Shatkin, A.J. 1976. Capping of eucaryotic mRNAs. *Cell*. **9**(4 PT 2),pp.645–653.

Shen, Z.-Z., Pan, X., Miao, L.-F., Ye, H.-Q., Chavanas, S., Davrinche, C., McVoy, M. and Luo, M.-H. 2014. Comprehensive Analysis of Human Cytomegalovirus MicroRNA Expression during Lytic and Quiescent Infection W. Ho, ed. *PLoS ONE*. **9**(2),p.e88531.

Shih, S.R. and Krug, R.M. 1996. Novel exploitation of a nuclear function by influenza virus: the cellular SF2/ASF splicing factor controls the amount of the essential viral M2 ion channel protein in infected cells. *The EMBO journal*. **15**(19),pp.5415–5427.

Shih, S.R., Nemeroff, M.E. and Krug, R.M. 1995. The choice of alternative 5' splice sites in influenza virus M1 mRNA is regulated by the viral polymerase complex. *Proceedings of the National Academy of Sciences of the United States of America*. **92**(14),pp.6324–6328.

Shiio, Y. and Aebersold, R. 2006. Quantitative proteome analysis using isotope-coded affinity tags and mass spectrometry. *Nature Protocols*. **1**(1),pp.139–145.

Shiloh, Y. 2001. ATM and ATR: networking cellular responses to DNA damage. *Current Opinion in Genetics & Development*. **11**(1),pp.71–77.

Shiloh, Y. and Ziv, Y. 2013. The ATM protein kinase: regulating the cellular response to genotoxic stress, and more. *Nature Reviews Molecular Cell Biology*. **14**(4),pp.197–210.

Shrinet, J., Jain, S., Jain, J., Bhatnagar, R.K. and Sunil, S. 2014. Next Generation Sequencing Reveals Regulation of Distinct Aedes microRNAs during Chikungunya Virus Development J. M. C. Ribeiro, ed. *PLoS Neglected Tropical Diseases*. **8**(1),p.e2616.

da Silva, L.F. and Jones, C. 2013. Small non-coding RNAs encoded within the herpes simplex virus type 1 latency associated transcript (LAT) cooperate with the retinoic acid inducible gene I (RIG-I) to induce beta-interferon promoter activity and promote cell survival. *Virus Research*. **175**(2),pp.101–109.

Skalsky, R.L. and Cullen, B.R. 2010. Viruses, microRNAs, and host interactions. *Annual Review of Microbiology*. **64**,pp.123–141.

Smith, G.L. and McFadden, G. 2002. Science and society: Smallpox: anything to declare? *Nature Reviews Immunology*. **2**(7),pp.521–527.

Smith, J., Tho, L.M., Xu, N. and Gillespie, D.A. 2010. The ATM-Chk2 and ATR-Chk1 pathways in DNA damage signaling and cancer. *Advances in Cancer Research*. **108**,pp.73–112.

Sodeik, B., Ebersold, M.W. and Helenius, A. 1997. Microtubule-mediated transport of incoming herpes simplex virus 1 capsids to the nucleus. *The Journal of Cell Biology*. **136**(5),pp.1007–1021.

Sokoloski, K.J., Chaskey, E.L. and Wilusz, J. 2009. Virus-mediated mRNA decay by hyperadenylation. *Genome Biology*. **10**(8),p.234.

Song, M.J., Li, X., Brown, H.J. and Sun, R. 2002. Characterization of interactions between RTA and the promoter of polyadenylated nuclear RNA in Kaposi's sarcoma-associated herpesvirus/human herpesvirus 8. *Journal of Virology*. **76**(10),pp.5000–5013.

Sood, P., Krek, A., Zavolan, M., Macino, G. and Rajewsky, N. 2006. Cell-type-specific signatures of microRNAs on target mRNA expression. *Proceedings of the National Academy of Sciences*. **103**(8),pp.2746–2751.

Soulier, J., Grollet, L., Oksenhendler, E., Cacoub, P., Cazals-Hatem, D., Babinet, P., d'Agay, M.F., Clauvel, J.P., Raphael, M. and Degos, L. 1995. Kaposi's sarcoma-associated herpesvirus-like DNA sequences in multicentric Castleman's disease. *Blood*. **86**(4),pp.1276–1280.

Spear, P.G. and Longnecker, R. 2003. Herpesvirus entry: an update. *Journal of Virology*. **77**(19),pp.10179–10185.

Speck, S.H. and Ganem, D. 2010. Viral Latency and Its Regulation: Lessons from the γ-Herpesviruses. *Cell Host & Microbe*. **8**(1),pp.100–115.

Squatrito, M., Gorrini, C. and Amati, B. 2006. Tip60 in DNA damage response and growth control: many tricks in one HAT. *Trends in Cell Biology*. **16**(9),pp.433–442.

Staffa, A. and Cochrane, A. 1994. The tat/rev intron of human immunodeficiency virus type 1 is inefficiently spliced because of suboptimal signals in the 3' splice site. *Journal of Virology*. **68**(5),pp.3071–3079.

Stoltzfus, C.M. and Madsen, J.M. 2006. Role of viral splicing elements and cellular RNA binding proteins in regulation of HIV-1 alternative RNA splicing. *Current HIV research*. **4**(1),pp.43–55.

Sultan, M., Schulz, M.H., Richard, H., Magen, A., Klingenhoff, A., Scherf, M., Seifert, M., Borodina, T., Soldatov, A., Parkhomchuk, D., Schmidt, D., O'Keeffe, S., Haas, S., Vingron, M., Lehrach, H. and Yaspo, M.-L. 2008. A Global View of Gene Activity and Alternative Splicing by Deep Sequencing of the Human Transcriptome. *Science*. **321**(5891),pp.956–960.

Sun, R., Lin, S.F., Gradoville, L. and Miller, G. 1996. Polyadenylylated nuclear RNA encoded by Kaposi sarcoma-associated herpesvirus. *Proceedings of the National Academy of Sciences of the United States of America*. **93**(21),pp.11883–11888.

Sun, R., Lin, S.-F., Gradoville, L., Yuan, Y., Zhu, F. and Miller, G. 1998. A viral gene that activates lytic cycle expression of Kaposi's sarcoma-associated herpesvirus. *Proceedings of the National Academy of Sciences*. **95**(18),pp.10866–10871.

Sun, R., Lin, S.-F., Staskus, K., Gradoville, L., Grogan, E., Haase, A. and Miller, G. 1999. Kinetics of Kaposi's Sarcoma-Associated Herpesvirus Gene Expression. *Journal of Virology*. **73**(3),pp.2232–2242.

Szeto, C.Y.-Y., Lin, C.H., Choi, S.C., Yip, T.T.C., Ngan, R.K.-C., Tsao, G.S.-W. and Lung, M. 2014. Integrated mRNA and microRNA transcriptome sequencing characterizes sequence variants and mRNA–microRNA regulatory network in nasopharyngeal carcinoma model systems. *FEBS Open Bio*. **4**,pp.128–140.

Tang, S., Bertke, A.S., Patel, A., Margolis, T.P. and Krause, P.R. 2011. Herpes Simplex Virus 2 MicroRNA miR-H6 Is a Novel Latency-Associated Transcript-Associated MicroRNA, but Reduction of Its Expression Does Not Influence the Establishment of Viral Latency or the Recurrence Phenotype. *Journal of Virology*. **85**(9),pp.4501–4509.

Tatsumi, Y., Takano, R., Islam, M.S., Yokochi, T., Itami, M., Nakamura, Y. and Nakagawara, A. 2015. BMCC1, which is an interacting partner of BCL2, attenuates AKT activity, accompanied by apoptosis. *Cell Death and Disease*. **6**(1),p.e1607.

Taylor, M.P., Koyuncu, O.O. and Enquist, L.W. 2011. Subversion of the actin cytoskeleton during viral infection. *Nature Reviews Microbiology*. **9**(6),pp.427–439.

Tay, Y., Zhang, J., Thomson, A.M., Lim, B. and Rigoutsos, I. 2008. MicroRNAs to Nanog, Oct4 and Sox2 coding regions modulate embryonic stem cell differentiation. *Nature*. **455**(7216),pp.1124–1128.

Thermo Scientific 2009. Thermo Scientific Dharmacon miRIDIAN microRNA Mimics & Hairpin Inhibitors. [Accessed 30 April 2015]. Available from: http://www.thermo.com.cn/Resources/200907/1711741370.pdf.

Thompson, A., Schäfer, J., Kuhn, K., Kienle, S., Schwarz, J., Schmidt, G., Neumann, T., Johnstone, R., Mohammed, A.K.A. and Hamon, C. 2003. Tandem mass tags: a novel quantification strategy for comparative analysis of complex protein mixtures by MS/MS. *Analytical Chemistry*. **75**(8),pp.1895–1904.

Thompson, S.R. and Sarnow, P. 2003. Enterovirus 71 contains a type I IRES element that functions when eukaryotic initiation factor eIF4G is cleaved. *Virology*. **315**(1),pp.259–266.

Tischer, B.K. and Osterrieder, N. 2010. Herpesviruses—A zoonotic threat? *Veterinary Microbiology*. **140**(3-4),pp.266–270.

Tortora, G.J., Funke, B.R. and Case, C.L. 2013. *Microbiology: an introduction* 11th ed. Boston: Pearson.

Trigon, S., Serizawa, H., Conaway, J.W., Conaway, R.C., Jackson, S.P. and Morange, M. 1998. Characterization of the residues phosphorylated in vitro by different C-terminal domain kinases. *The Journal of Biological Chemistry*. **273**(12),pp.6769–6775.

Tsai, P.-L., Chiou, N.-T., Kuss, S., García-Sastre, A., Lynch, K.W. and Fontoura, B.M.A. 2013. Cellular RNA binding proteins NS1-BP and hnRNP K regulate influenza A virus RNA splicing. *PLoS pathogens*. **9**(6),p.e1003460.

Tsai, Y.-H., Wu, M.-F., Wu, Y.-H., Chang, S.-J., Lin, S.-F., Sharp, T.V. and Wang, H.-W. 2009. The M type K15 protein of Kaposi's sarcoma-associated herpesvirus regulates microRNA expression via its SH2-binding motif to induce cell migration and invasion. *Journal of Virology*. **83**(2),pp.622–632.

Uldrick, T.S. and Whitby, D. 2011. Update on KSHV epidemiology, Kaposi Sarcoma pathogenesis, and treatment of Kaposi Sarcoma. *Cancer Letters*. **305**(2),pp.150–162.

Umbach, J.L., Kramer, M.F., Jurak, I., Karnowski, H.W., Coen, D.M. and Cullen, B.R. 2008. MicroRNAs expressed by herpes simplex virus 1 during latent infection regulate viral mRNAs. *Nature*. [Online]. [Accessed 25 June 2015]. Available from: http://www.nature.com/doifinder/10.1038/nature07103.

Uziel, T. 2003. Requirement of the MRN complex for ATM activation by DNA damage. *The EMBO Journal*. **22**(20),pp.5612–5621.

Valencia-Sanchez, M.A. 2006. Control of translation and mRNA degradation by miRNAs and siRNAs. *Genes & Development*. **20**(5),pp.515–524.

Valinezhad Orang, A., Safaralizadeh, R. and Kazemzadeh-Bavili, M. 2014. Mechanisms of miRNA-Mediated Gene Regulation from Common Downregulation to mRNA-Specific Upregulation. *International Journal of Genomics*. **2014**,pp.1–15.

Varthakavi, V., Browning, P.J. and Spearman, P. 1999. Human immunodeficiency virus replication in a primary effusion lymphoma cell line stimulates lytic-phase replication of Kaposi's sarcoma-associated herpesvirus. *Journal of Virology*. **73**(12),pp.10329–10338.

Vassalli, J.D., Huarte, J., Belin, D., Gubler, P., Vassalli, A., O'Connell, M.L., Parton, L.A., Rickles, R.J. and Strickland, S. 1989. Regulated polyadenylation controls mRNA translation during meiotic maturation of mouse oocytes. *Genes & Development*. **3**(12B),pp.2163–2171.

Vasudevan, S., Tong, Y. and Steitz, J.A. 2007. Switching from repression to activation: microRNAs can up-regulate translation. *Science (New York, N.Y.)*. **318**(5858),pp.1931–1934.

Verma, S.C., Borah, S. and Robertson, E.S. 2004. Latency-Associated Nuclear Antigen of Kaposi's Sarcoma-Associated Herpesvirus Up-Regulates Transcription of Human Telomerase Reverse Transcriptase Promoter through Interaction with Transcription Factor Sp1. *Journal of Virology*. **78**(19),pp.10348–10359.

Verma, S.C., Lan, K. and Robertson, E. 2007. Structure and function of latency-associated nuclear antigen. *Current Topics in Microbiology and Immunology*. **312**,pp.101–136.

Verschuren, E.W. 2004. The cell cycle and how it is steered by Kaposi's sarcoma-associated herpesvirus cyclin. *Journal of General Virology*. **85**(6),pp.1347–1361.

Vieira, J. and O'Hearn, P.M. 2004. Use of the red fluorescent protein as a marker of Kaposi's sarcoma-associated herpesvirus lytic gene expression. *Virology*. **325**(2),pp.225–240.

Vousden, K.H. and Prives, C. 2009. Blinded by the Light: The Growing Complexity of p53. *Cell*. **137**(3),pp.413–431.

Wachtler, F., Hopman, A.H., Wiegant, J. and Schwarzacher, H.G. 1986. On the position of nucleolus organizer regions (NORs) in interphase nuclei. Studies with a new, non-autoradiographic in situ hybridization method. *Experimental Cell Research*. **167**(1),pp.227–240.

Wahle, E., Lustig, A., Jenö, P. and Maurer, P. 1993. Mammalian poly(A)-binding protein II. Physical properties and binding to polynucleotides. *The Journal of Biological Chemistry*. **268**(4),pp.2937–2945.

Wang, F.-Z., Weber, F., Croce, C., Liu, C.-G., Liao, X. and Pellett, P.E. 2008. Human cytomegalovirus infection alters the expression of cellular microRNA species that affect its replication. *Journal of Virology*. **82**(18),pp.9065–9074.

Wang, J., Han, X. and Zhang, Y. 2012. Autoregulatory Mechanisms of Phosphorylation of Checkpoint Kinase 1. *Cancer Research*. **72**(15),pp.3786–3794.

Wang, Q.-Y., Zhou, C., Johnson, K.E., Colgrove, R.C., Coen, D.M. and Knipe, D.M. 2005. Herpesviral latency-associated transcript gene promotes assembly of heterochromatin on viral lytic-gene promoters in latent infection. *Proceedings of the National Academy of Sciences of the United States of America*. **102**(44),pp.16055–16059.

Wang, S.E., Wu, F.Y., Chen, H., Shamay, M., Zheng, Q. and Hayward, G.S. 2004. Early activation of the Kaposi's sarcoma-associated herpesvirus RTA, RAP, and MTA promoters by the tetradecanoyl phorbol acetate-induced AP1 pathway. *Journal of Virology*. **78**(8),pp.4248–4267.

Wang, S.E., Wu, F.Y., Fujimuro, M., Zong, J., Hayward, S.D. and Hayward, G.S. 2003. Role of CCAAT/enhancer-binding protein alpha (C/EBPalpha) in activation of the Kaposi's sarcoma-associated herpesvirus (KSHV) lytic-cycle replication-associated protein (RAP) promoter in cooperation with the KSHV replication and transcription activator (RTA) and RAP. *Journal of Virology*. **77**(1),pp.600–623.

Wang, Y., Li, H., Tang, Q., Maul, G.G. and Yuan, Y. 2008. Kaposi's Sarcoma-Associated Herpesvirus ori-Lyt-Dependent DNA Replication: Involvement of Host Cellular Factors. *Journal of Virology*. **82**(6),pp.2867–2882.

Wang, Z., Gerstein, M. and Snyder, M. 2009. RNA-Seq: a revolutionary tool for transcriptomics. *Nature Reviews Genetics*. **10**(1),pp.57–63.

Ward, B.M. 2011. The taking of the cytoskeleton one two three: How viruses utilize the cytoskeleton during egress. *Virology*. **411**(2),pp.244–250.

Washburn, M.P., Wolters, D. and Yates, J.R. 2001. Large-scale analysis of the yeast proteome by multidimensional protein identification technology. *Nature Biotechnology*. **19**(3),pp.242–247.

Wei, C.M. and Moss, B. 1975. Methylated nucleotides block 5'-terminus of vaccinia virus messenger RNA. *Proceedings of the National Academy of Sciences of the United States of America*. **72**(1),pp.318–322.

Wells, S.E., Hillner, P.E., Vale, R.D. and Sachs, A.B. 1998. Circularization of mRNA by eukaryotic translation initiation factors. *Molecular Cell*. **2**(1),pp.135–140.

Wen, H.-J., Minhas, V. and Wood, C. 2009. Identification and characterization of a new Kaposi's sarcoma-associated herpesvirus replication and transcription activator (RTA)-responsive element involved in RTA-mediated transactivation. *Journal of General Virology*. **90**(4),pp.944–953.

Werner, F.J., Bornkamm, G.W., Fleckenstein, B. and Mulder, C. 1978. Episomal viral DNA in herpesvirus saimiri-transformed lymphoid cell lines. *IARC scientific publications*. (24 Pt 1),pp.125–130.

Westover, K.D. 2004. Structural Basis of Transcription: Separation of RNA from DNA by RNA Polymerase II. *Science*. **303**(5660),pp.1014–1016.

White, C.A., Stow, N.D., Patel, A.H., Hughes, M. and Preston, V.G. 2003. Herpes simplex virus type 1 portal protein UL6 interacts with the putative terminase subunits UL15 and UL28. *Journal of Virology*. **77**(11),pp.6351–6358.

Wiese, S., Reidegeld, K.A., Meyer, H.E. and Warscheid, B. 2007. Protein labeling by iTRAQ: a new tool for quantitative mass spectrometry in proteome research. *Proteomics*. **7**(3),pp.340–350.

Wilhelm, B.T., Marguerat, S., Watt, S., Schubert, F., Wood, V., Goodhead, I., Penkett, C.J., Rogers, J. and Bähler, J. 2008. Dynamic repertoire of a eukaryotic transcriptome surveyed at single-nucleotide resolution. *Nature*. **453**(7199),pp.1239–1243.

Wilson, D.M., Takeshita, M. and Demple, B. 1997. Abasic Site Binding by the Human Apurinic Endonuclease, Ape, and Determination of the DNA Contact Sites. *Nucleic Acids Research*. **25**(5),pp.933–939.

Wong, J.W.H. and Cagney, G. 2010. An Overview of Label-Free Quantitation Methods in Proteomics by Mass Spectrometry *In*: S. J. Hubbard and A. R. Jones, eds. *Proteome Bioinformatics* [Online]. Totowa, NJ: Humana Press, pp. 273–283. [Accessed 8 July 2015]. Available from: http://link.springer.com/10.1007/978-1-60761-444-9_18.

Wong, N. and Wang, X. 2015. miRDB: an online resource for microRNA target prediction and functional annotations. *Nucleic Acids Research*. **43**(D1),pp.D146–D152.

Wu, R. 1972. Nucleotide Sequence Analysis of DNA. *Nature New Biology*. **236**(68),pp.198–200.

Wu, X. and Brewer, G. 2012. The regulation of mRNA stability in mammalian cells: 2.0. *Gene*. **500**(1),pp.10–21.

Wu, X., Yang, Z., Liu, Y. and Zou, Y. 2005. Preferential localization of hyperphosphorylated replication protein A to double-strand break repair and checkpoint complexes upon DNA damage. *The Biochemical Journal*. **391**(Pt 3),pp.473–480.

Wu, Y.-H., Hu, T.-F., Chen, Y.-C., Tsai, Y.-N., Tsai, Y.-H., Cheng, C.-C. and Wang, H.-W. 2011. The manipulation of miRNA-gene regulatory networks by KSHV induces endothelial cell motility. *Blood*. **118**(10),pp.2896–2905.

Xiao, C. and Rajewsky, K. 2009. MicroRNA control in the immune system: basic principles. *Cell*. **136**(1),pp.26–36.

Xie, A. and Scully, R. 2007. Hijacking the DNA Damage Response to Enhance Viral Replication: γ-Herpesvirus 68 orf36 Phosphorylates Histone H2AX. *Molecular Cell*. **27**(2),pp.178–179.

Xu, N., Lao, Y., Zhang, Y. and Gillespie, D.A. 2012. Akt: a double-edged sword in cell proliferation and genome stability. *Journal of Oncology*. **2012**,p.951724.

Xu, N., Wang, J., Zhang, Z.-F., Pang, D.-W., Wang, H.-Z. and Zhang, Z.-L. 2014. Anisotropic cell-to-cell spread of vaccinia virus on microgrooved substrate. *Biomaterials*. **35**(19),pp.5049–5055.

Xu, X. and Jin, T. 2012. A shortcut from GPCR signaling to Rac-mediated actin cytoskeleton through an ELMO/DOCK complex. *Small GTPases*. **3**(3),pp.183–185.

Xu, Z., Xiao, S.-B., Xu, P., Xie, Q., Cao, L., Wang, D., Luo, R., Zhong, Y., Chen, H.-C. and Fang, L.-R. 2011. miR-365, a Novel Negative Regulator of Interleukin-6 Gene Expression, Is Cooperatively Regulated by Sp1 and NF- B. *Journal of Biological Chemistry*. **286**(24),pp.21401–21412.

Yamauchi, T., Yoshida, A. and Ueda, T. 2011. Camptothecin induces DNA strand breaks and is cytotoxic in stimulated normal lymphocytes. *Oncology Reports*. **25**(2),pp.347–352.

Yang, J. 2003. ATM, ATR and DNA-PK: initiators of the cellular genotoxic stress responses. *Carcinogenesis*. **24**(10),pp.1571–1580.

Yang, J.-S. and Lai, E.C. 2011. Alternative miRNA biogenesis pathways and the interpretation of core miRNA pathway mutants. *Molecular Cell*. **43**(6),pp.892–903.

Yang, J., Yu, Y. and Duerksen-Hughes, P.J. 2003. Protein kinases and their involvement in the cellular responses to genotoxic stress. *Mutation Research*. **543**(1),pp.31–58.

Yates, J.R., Eng, J.K., McCormack, A.L. and Schieltz, D. 1995. Method to correlate tandem mass spectra of modified peptides to amino acid sequences in the protein database. *Analytical Chemistry*. **67**(8),pp.1426–1436.

Yi, R., Qin, Y., Macara, I.G. and Cullen, B.R. 2003. Exportin-5 mediates the nuclear export of pre-microRNAs and short hairpin RNAs. *Genes & Development*. **17**(24),pp.3011–3016.

Yoo, S. 1999. Geometry of a complex formed by double strand break repair proteins at a single DNA end: recruitment of DNA-PKcs induces inward translocation of Ku protein. *Nucleic Acids Research*. **27**(24),pp.4679–4686.

Yoshizaki, K., Matsuda, T., Nishimoto, N., Kuritani, T., Taeho, L., Aozasa, K., Nakahata, T., Kawai, H., Tagoh, H. and Komori, T. 1989. Pathogenic significance of interleukin-6 (IL-6/BSF-2) in Castleman's disease. *Blood*. **74**(4),pp.1360–1367.

Young, L.S., Arrand, J.R. and Murray, P.G. 2007. EBV gene expression and regulation *In*: A. Arvin, G. Campadelli-Fiume, E. Mocarski, P. S. Moore, B. Roizman, R. Whitley and K. Yamanishi, eds. *Human Herpesviruses: Biology, Therapy, and Immunoprophylaxis* [Online]. Cambridge: Cambridge University Press. [Accessed 25 June 2015]. Available from: http://www.ncbi.nlm.nih.gov/books/NBK47431/.

Young, L.S. and Rickinson, A.B. 2004. Epstein–Barr virus: 40 years on. *Nature Reviews Cancer*. **4**(10),pp.757–768.

Yu, F., Feng, J., Harada, J.N., Chanda, S.K., Kenney, S.C. and Sun, R. 2007. B cell terminal differentiation factor XBP-1 induces reactivation of Kaposi's sarcoma-associated herpesvirus. *FEBS letters*. **581**(18),pp.3485–3488.

Yu, M.C. and Yuan, J.-M. 2002. Epidemiology of nasopharyngeal carcinoma. *Seminars in Cancer Biology*. **12**(6),pp.421–429.

Zahler, A.M., Damgaard, C.K., Kjems, J. and Caputi, M. 2004. SC35 and heterogeneous nuclear ribonucleoprotein A/B proteins bind to a juxtaposed exonic splicing enhancer/exonic splicing silencer element to regulate HIV-1 tat exon 2 splicing. *The Journal of Biological Chemistry*. **279**(11),pp.10077–10084.

Zeng, Y., Yi, R. and Cullen, B.R. 2005. Recognition and cleavage of primary microRNA precursors by the nuclear processing enzyme Drosha. *The EMBO journal*. **24**(1),pp.138–148.

Zhao, S., Fung-Leung, W.-P., Bittner, A., Ngo, K. and Liu, X. 2014. Comparison of RNA-Seq and Microarray in Transcriptome Profiling of Activated T Cells S.-D. Zhang, ed. *PLoS ONE*. **9**(1),p.e78644.

Zhong, W., Wang, H., Herndier, B. and Ganem, D. 1996. Restricted expression of Kaposi sarcoma-associated herpesvirus (human herpesvirus 8) genes in Kaposi sarcoma. *Proceedings of the National Academy of Sciences of the United States of America*. **93**(13),pp.6641–6646.

Zhou, Z., Luo, M.J., Straesser, K., Katahira, J., Hurt, E. and Reed, R. 2000. The protein Aly links pre-messenger-RNA splicing to nuclear export in metazoans. *Nature*. **407**(6802),pp.401–405.

Ziegler, J.L. and Katongole-Mbidde, E. 1996. Kaposi's sarcoma in childhood: an analysis of 100 cases from Uganda and relationship to HIV infection. *International Journal of Cancer. Journal International Du Cancer*. **65**(2),pp.200–203.

Zisoulis, D.G., Lovci, M.T., Wilbert, M.L., Hutt, K.R., Liang, T.Y., Pasquinelli, A.E. and Yeo, G.W. 2010. Comprehensive discovery of endogenous Argonaute binding sites in Caenorhabditis elegans. *Nature Structural & Molecular Biology*. **17**(2),pp.173–179.

Zorio, D. 2004. The link between mRNA processing and transcription: communication works both ways. *Experimental Cell Research*. **296**(1),pp.91–97.

Zou, L. 2007. Single- and double-stranded DNA: building a trigger of ATR-mediated DNA damage response. *Genes & Development*. **21**(8),pp.879–885.

Zou, L. and Elledge, S.J. 2003. Sensing DNA damage through ATRIP recognition of RPA-ssDNA complexes. *Science (New York, N.Y.)*. **300**(5625),pp.1542–1548.